THE ADSORPTIVE SEPARATION
OF
AROMATIC HYDROCARBON MIXTURES

By
KHAIRYA ALI AL-ZAID
Doctor of Philosophy

THE UNIVERSITY OF ASTON
IN BIRMINGHAM

APRIL 1987

The University of Aston in Birmingham

THE ADSORPTIVE SEPARATION OF AROMATIC HYDROCARBON MIXTURES

Khairya Ali Al-Zaid

Doctor of Philosophy   1987

SUMMARY

A detailed study has been made of the feasibility of adsorptive purification of slack waxes from traces of aromatic compounds using type 13X molecular sieves to achieve $\leq$ 0.01% aromatics in the product.

The limited literature relating to the adsorption of high molecular weight aromatic compounds by zeolites were reviewed. Equilibrium isotherms were determined for typical individual aromatic compounds. Lower molecular weight, or more compact, molecules were preferentially adsorbed and the number of molecules captured by one unit cell decreased with increasing molecular weight of the adsorbate. An increase in adsorption temperature resulted in a decrease in the adsorption value.

The isosteric heat of adsorption of different types of aromatic compounds were determined from pairs of isotherms at 303 K to 343 K at specific coverages. The lowest heats of adsorption were for dodecylbenzene and phenanthrene.

Kinetics of adsorption were studied for different aromatic compounds. The diffusivity decreased significantly when a long alkyl chain was attached to the benzene ring e.g. in dodecylbenzene; molecules with small cross-sectional diameter e.g. cumene were adsorbed most rapidly. The sorption rate increased with temperature. Apparent activation energies increased with increasing polarity.

In a study of the dynamic adsorption of selected aromatic compounds from binary solutions in isooctane or n-alkanes, naphthalene exhibited the best dynamic properties followed by dibenzothiophene and finally dodecylbenzene. The dynamic adsorption of naphthalene from different n-alkane solvents increased with a decrease in solvent molecular weight. A tentative mathematical approach is proposed for the prediction of dynamic breakthrough curves from equilibrium isotherms and kinetic data.

The dynamic properties of liquid phase adsorption of aromatics from slack waxes were studied at different temperatures and concentrations. The optimum operating temperature was 543K. The best dynamic performance was achieved with feeds of low aromatic content.

The studies with individual aromatic compounds demonstrated the affinity of type NaX molecular sieves to adsorb aromatics in the concentration range 3% - 5%. Wax purification by adsorption was considered promising and extension of the experimental programme was recommended.

Key words: Adsorption of Aromatic Compounds
             Molecular Sieve Type 13X
             Dearomatization of Waxes

TO MY BELOVED COUNTRY, KUWAIT

MY HUSBAND

AND

MY CHILDREN

ACKNOWLEDGEMENTS

CONTENTS

LIST OF TABLES

LIST OF FIGURES

1.0 INTRODUCTION

Petroleum hydrocarbons are valuable feedstocks for manufacturing a variety of petrochemical products, for example liquid paraffin and waxes which are major raw materials for the pharmaceutical, detergents and protein industries.

The purities of the liquid paraffin and waxes are the most important factors determining the type of application, particularly the aromatic content which should not exceed 0.1% by wt for the above applications. Purification of liquid paraffins and waxes from aromatic hydrocarbons can be achieved by using oleum treatment, hydrotreating, hydrocracking or different types of adsorbent such as activated charcoal, silica gel or alumina silicate.

Using oleum for purification presents many difficulties such as corrosion problems and difficulties in acid tar neutralization and utilization. The hydrotreating process is expensive since high temperature, high pressure and catalysts are required. Use of adsorbents also has some drawbacks due to their inability to remove some alkylbenzene. This study was therefore initiated to investigate the potential use of molecular sieves for purification of slack waxes, i.e. high molecular weight paraffins, from aromatic compounds. Molecular sieves type X, and model aromatic compounds were used. Equilibrium isotherms and the kinetics of adsorption were studied.

The main objectives of this work were to investigate the use of molecular sieves type X for dearomatization of high molecular weight waxes, and to fractionate the aromatic compounds according to their chemical structure and molecular dimensions. Molecular sieves type NaX was used for adsorption of standard models of individual aromatic compounds from binary solutions with iso-octane.

1.1 Structure and Properties of Zeolite

Zeolites are crystalline chemically and structurally complex materials. They are composed mainly of hydrated alumino silicates of group I and group II elements in particular Na, K, Mg, Ca, Sr, and Ba. The framework contains channels and interconnected voids which are occupied by the

cation and water molecules. The structural formula of a zeolite is best expressed for the crystallographic cell as

$$M^n_{x/y} \left((AlO_2)_x \ (SiO_2)_y \right) w \ H_2O$$
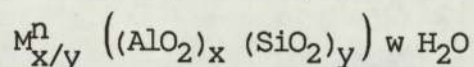
Where M is the cation of valence n

w is the number of water molecules, and the ratio

x/y usually has values of 1-5 depending upon the structure.

$\Big(\ \Big)$ represents the framework composition

Since a high degree of reproducibility is required in an industrial separation process, uniformity in composition and purity are necessary. Thus any synthetic zeolite must be characterized by the following information.

1. The basic crystal structure, by X-ray;

2. Chemical composition;

3. Chemical and physical properties such as stability, dehydration behaviour, cation exchange, adsorption behaviour of gases and vapours.

Most of the synthetic zeolites are monocationic or dicationic, and have one or two different species. Zeolites in general have the power of selectivity, i.e., they adsorb or reject different molecules. Molecular sieve action may be total or partial. If it is total the diffusion of one species into the solid may be wholly prevented, whilst the diffusion of a second species occurs. If the action is partial, the components of a binary mixture diffuse into the solid at different rates depending upon the conditions eg. pressure, temperature, the nature of the mixture and the type of zeolite.

When a solid dehydrated zeolite is exposed to gas or liquid the intracrystalline voids and channels fill with the molecular species concerned, and when filling is complete no more adsorption occurs. If the temperature is maintained constant, this results in an equilibrium isotherm.

1.2 Porosity Structure of Zeolite NaX.

The pore volume of zeolite X has been determined from the adsorption of different types of molecules including water, gases, and hydrocarbons. The water pore volume is equivalent to 7908 A^3 per unit cell. With most molecules, with the possible exception of water, only the larger super cages are occupied.

The total calculated void volume of zeolite X is 7832 A^3 per unit cell. The total calculated void volume for the large voids is 0.296 cm^3/g. At any temperature the void fraction of zeolite X which can be filled is nearly 50% of the total crystal volume. Based on the structure of the zeolites the calculated surface areas are 1400 m^2/g for NaX. There are three types of zeolite A, X, and Y. In these there are voids of two types:

1.   The small spherical voids comprised of the β cage with a diameter of 6.6 A° and

2.   Larger voids such as the α cage (supercages 26 hedron) in zeolite X and Y. The diameter of the spherical unit in zeolite A is 11.4 A° and in X and Y is = 11.8 A°.

1.3 Purification of Paraffin Waxes

The purity of paraffin waxes is an important aspect in their grading. The degree of purity required, obviously depends on the type of application. Paraffins applied in food conservation and packaging must be odorless and free from compounds, particularly polycyclic aromatic substances, which are toxic to the human organism. Even stricter specifications are applied to paraffin products to be used for medical purposes.

The complete purification of paraffin waxes and paraffin liquid involves the removal of impurities usually present in small concentrations like unsaturated compounds, mono, bi and polycyclic aromatic hydrocarbons, hydrocarbon derivatives containing S, N and O atoms, and heterocyclic compounds. The n-alkane, branched alkane and naphthene compounds should remain intact as far as possible.

Owing to the widespread applications of paraffin waxes, a large number of purification processes have been developed. These can be classified essentially into 3 groups:

1.   Treatment with chemicals

2.   Adsorption

3.   Hydrogenation

1.3.1 Treatment with Chemicals

The most important agent is concentrated sulphuric acid. In this process oxidation, condensation, polymerization, sulfonation and resin-formation takes place. The final degree of the purification depends on the composition of the initial product, concentration of H_2SO_4, temperature of operation, contact time and manner of execution.

Aromatics are sulfonated, unsaturated hydrocarbons yield polymerized products, and resinous compounds are converted via polymerization and oxidation reactions into asphaltenes.

Final purification with H_2SO_4 is sometimes used in the manufacture of n-alkanes by urea adduct formation if the specified aromatic content must not exceed 0.01 wt%. It could be reduced to zero, if necessary.

1.3.2 Adsorption

The simplest process, essentially purification by adsorption, is by mixing with bleaching earth. After equilibrium has been established, the paraffin wax is separated by filtration. Various types of fuller's earth, activated carbon, silica gel, bauxites, or natural and synthetic aluminosilicates are suitable adsorbents.

One of the most important methods for paraffin waxes purification is the percolation process. Two alternative methods are known: the stationary bed method and the moving bed method. The former is more widespread on a commercial scale, especially in the petroleum industry.

1.3.3 Hydrogenation

Hydrogenation processes have recently been developed for purification. The most common is the ferro-refining process. A typical catalyst comprises molybdenum oxide, cobalt oxide and iron oxide on an alumina support. This process is considered satisfactory for the manufacture of macro and micro-crystalline paraffin waxes for food and pharmaceutical industries.

Purification by hydrogenation brings about both chemical and physical changes of the product. It reduces S, O and N content, the diolefins are hydrogenated into alkanes and the polycyclic aromatics into asphaltenes. It requires a high temperature, from 533 K, to > 703 K, since otherwise undesirable side reactions occur, e.g. hydrocracking and increased carbon

deposit-formation. The process is expensive since high temperature, pressure and catalysts are required.

The aromatic content for the final liquid paraffin product using a hydrogenation process is below 0.01 wt%, compared with 1.2 wt% before treatment.

1.4 Application of Paraffin Waxes and Liquid Paraffins

The potential uses of liquid paraffins and paraffin waxes are large and very diverse. Essentially they can be classified into 3 main groups:

1. Utilization without any chemical transformation.

    Direct applications of liquid paraffins and paraffin waxes arise in the paper industry, in household chemicals (polishes, creams, candles, etc.) in cosmetics, in the food industry, and in food preservation etc. They are utilized in matches, textiles, the electrical industry, pencil manufacture etc.

2. Utilization as feedstock for the chemical industry.

    n-paraffin can be used as feed stock for manufacturing alcohols, fatty acids and dicarboxylic acids by oxidation processes.

3. Manufacture of proteins and other products by the biological transformation of paraffins.

    Certain bacterium cultures decompose paraffin hydrocarbons in the presence of mineral salts to produce proteins.

2.0 LITERATURE SURVEY - ADSORPTION ON MOLECULAR SIEVES

2.1. Adsorption by Zeolites

The study of adsorption of gases and vapours on solids dates from early times. In 1840 Damour observed that crystals of zeolites could be reversibly dehydrated without any apparent change in their transparency or morphology. The concept that the structures of dehydrated zeolites consist of open-spongy-frameworks is due to Friedel, who observed that various liquids such as alcohols, benzene, chloroform, carbon disulfide and mercury were occluded by zeolites (1).

Barrer and Ibbitson (2) described an investigation of the adsorption of hydrocarbons on chabazite. They found that hydrocarbons such as n-propane, n-butane, n-pentane and n-heptane were adsorbed quite rapidly at temperatures above 373 K. However, branched chain hydrocarbons, such as isobutane and iso-octane, were totally excluded. The adsorption equilibria were reversible. Isotherms and isosteres were determined for some normal hydrocarbons on chabazite and analcite, where it was shown that the affinity of solutes for the lattice increased in the order

$$He < H_2 < O_2 \text{ and } CH_4 < C_2H_6 < C_3H_8 < n\text{-}C_4H_{10}$$
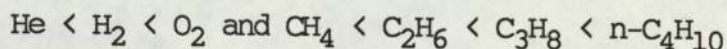
Thermodynamic properties of the zeolitic solid solutions were obtained as functions of charge of gas in the crystal, chain length, or temperature. Where possible the thermodynamic data were interpreted physically.

Adsorption by molecular sieves has become the standard method of treatment for propane and butane containing H_2S and mercaptans. They perform well in sweetening light hydrocarbon liquids. Clark (3) used exactly the same principles for butane or natural gasoline sweetening. In a typical process propane passes down through the packed bed of molecular sieve to provide an outlet product free of water, H_2S and mercaptans. Typically, a pressure swing arrangement is incorporated where a bed will stay on stream for 8 hours, whilst, a second bed, which performed 8 hours service previously, is being desorbed.

Molecular sieves are required to selectively remove the polar compounds from the relatively non-polar paraffinic hydrocarbon. Molecular sieves do have the selectivity required to make this separation. However, there are other compounds such as carbon disulfide, carbon sulfide and elemental sulfur that may, or may not, be removable by molecular sieves.

No data has been found on the ability of molecular sieves to adsorb, or desorb, elemental sulfur from a hydrocarbon stream, but carbon disulfide would be expected to be removed from a propane or butane stream if the CO_2 content was not excessive. In a typical natural-gasoline plant it is unlikely that mercaptans, below ethyl mercaptans, will have to be removed from gasoline. Generally, the narrower the cut processed, the higher will be the molecular sieve-design capacity for sulfur compounds.

Mair et al. (4) separated paraffins from cycloparaffins and alkylbenzenes from cyclobenzenes by selective adsorption on Sephadex LH-20 which was previously pre-wetted with acetone. The samples were added in an acetone solution to a chromatographic column and the compounds were eluted with acetone. The separations of dinuclear aromatic petroleum fractions near C_{19} and C_{21} with Sephadex were superior to those obtained with thermal diffusion. Separation of fractions up to C_{30} were obtained using a 75:25 vol% acetone-tetrahydrofuran mixture.

In 1958, Mair and Shamaiengar (5) developed a method for separating certain aromatic hydrocarbons according to the shape and size of the molecules by introducing a mixture of aromatic hydrocarbons into a column containing the molecular sieve adsorbent. The method was tested with mixtures of pure aromatic hydrocarbons and with petroleum fractions comprising, respectively, mononuclear, dinuclear and trinuclear aromatics in the C_{18} to C_{25} range. Results showed that fractionation with molecular sieve adsorbents is a useful tool for investigating the composition of the higher boiling fractions of petroleum, besides providing information concerning the structure of hydrocarbon molecules, since separation occurs according to the shape and size of the molecules.

In this investigation, iso-octane was used as an eluant since it can enter the pores of both the 10X and 13X adsorbent. Its use is possible with aromatic hydrocarbons because the latter are very strongly adsorbed and can enter the pores even in the presence of iso-octane as demonstrated in Table 2.1.

TABLE 2.1

PERCENTAGE OF HYDROCARBON ADSORBED ON MOLECULAR SIEVE
ADSORBENTS TYPE CaX (10X) and NaX (13X)

Name	Formula	Approximate % adsorbed on	
		CaX (10X)	NaX (13X)
n-Decylbenzene	$C_{16}H_{26}$	100	100
1,3,5-Triethylbenzene	$C_{12}H_{18}$	6	100
6-Decyl-(1,2,3,4-tetrahydro-naphthalene)	$C_{20}H_{32}$	50	100
2-Butyl-1-hexylindan	$C_{19}H_{30}$	-	100
2-Butyl-5-hexylindan	$C_{19}H_{30}$	60	100
1,2,3,4,5,6,7,8,13,14,15,16-Dodecahydrochrysene	$C_{18}H_{24}$	5	100

Satterfield and Cheng (6) studied factors influencing selective
adsorption from a binary liquid system on molecular sieve zeolites. They
reported that selective adsorption is caused by the relative affinity, or
interaction energy, of the molecules for the zeolite structure. On NaY
adsorbent, aromatic compounds were selectively adsorbed in preference to
paraffins and naphthenes. Within a group of aromatic compounds those hav-
ing the smallest and most compact structure, for example benzene and
cumene, were selectively adsorbed in preference to larger aromatics, e.g.
1,3,5 tri-isopropylbenzene, because the isopropyl group causes shielding
of the ring from the pore so that the bond interaction becomes less impor-
tant and alkyl group interaction more significant. Thus steric considera-
tions appear to be particularly important in adsorption selectivity.

Benzene > Cumene > mesitylene > 1, 3, 5 tri-ethylbenzene >
isopropylbenzene

They concluded that for a fixed temperature, the most important factor
affecting the rate of intracrystalline diffusion in type Y zeolites is the
critical molecular diameter of the diffusing molecules. The diffusion
rate decreases with increasing critical diameter.

Gupta et al. (7) studied liquid phase adsorption of binary and ternary systems of n-paraffins on LMS-5A at 279, 291, 303 and 315 K and found that equilibrium adsorption was independent of temperature for loadings of hexane-heptane and heptane-octane systems. However, for pentane-hexane, pentane-heptane and pentane-octane systems the amount of pentane adsorbed at 303 K decreased compared with the lower temperatures.

α and β parameters, where $\tan \alpha = \frac{1}{A_m}$ and β is the mutual displacement as defined in the Nomenclature, can be calculated from the slope of the adsorption isotherm at very low concentrations. The nature of the experimental isotherms did not permit direct measurement of the slope because of experimental limitations in the determination of equilibrium loadings at very low concentrations.

The heats of adsorption were calculated from the slopes of the plots. They were approximately equal to latent heats of vaporization; e.g. for n-octane, the heat of adsorption was found to be 38.1 kJ/mol, whereas, the latent heat of vaporization is 34.8 kJ/mol.

Adsorption of benzene from artificial mixtures of benzene and n-heptane was carried out by Fominykh et al. (8). Experiments were conducted both in the liquid and the vapour phase using synthetic zeolites of type NaX or CaX as adsorbents. They verified that synthetic zeolites of the NaX or CaX type possessed high dynamic activity and selectivity with respect to benzene in adsorption either from the liquid or the vapour phase, but the dynamic activity of zeolites decreased with the increase in the feed rate of crude. NaX zeolites had a greater dynamic activity than CaX zeolites.

Both physico-chemical adsorption and steric effects play an important role in selectivity for adsorbance of one component from a binary mixture. For example, Satterfield and Smeets (9) studied the steric effect for binary liquid phase mixtures of n-octane with either n-decane, n-dodecane or n-tetradecane to obtain a better understanding of systems where steric effects would be expected to be dominant. They concluded that, for all three binary systems studied, the lower molecular weight paraffin was preferentially adsorbed on molecular sieve 5A, relative to the higher molecular weight paraffin. They also studied briefly the adsorbance of cyclooctane on molecular sieve type NaX from a binary mixture containing n-paraffin of the same carbon number. They concluded that a cycloparaffin

in general was preferentially adsorbed from a binary mixture of
n-paraffin. Steric effects cannot explain this and the cyclic structure
must cause some physico-chemical effect more strongly than that existing
with the n-paraffins.

Aromatic hydrocarbons are the most undesirable impurity in liquid
paraffins, and there is insufficient information on their composition.
Various methods have been used for investigation of the composition of
those aromatics such as gas liquid chromatography, UV spectroscopy and
mass spectrometry.

Siryuk and Barabadze (10) established the limit of applicability of a
procedure known as Method I through which the composition of aromatic
hydrocarbons containing various polycyclic systems could be analyzed on
the basis of UV spectra. They were able to determine the absolute con-
tents of benzenes, naphthalenes, phenanthrenes, and anthracenes with a
relative accuracy of 10% and a sensitivity from 0.01% to 0.1%. The advan-
tages of the method are its high sensitivity and its complete independence
of the quality, or type, of paraffins or alkylnaphthenes present in the
product. Thus this method can be used to analyze various petroleum cuts
without first removing the saturated hydrocarbons and it is applicable not
only for a cut with a 673 K end point, but also for those with a higher
boiling point. A disadvantage of the method is that the accuracy of anal-
ysis is affected by the presence of hydrocarbons with four or five con-
densed aromatic rings.

Cherednichenko et al., (11) studied the composition of aromatic
hydrocarbons present as impurities in liquid paraffins by means of a set
of methods consisting of adsorption, gas liquid chromatography, UV and IR
spectroscopy. They used three types of sample

o   Sample 1: Obtained from a diesel fuel cut produced from Arlan crude.
o   Sample 2: Obtained from a diesel fuel cut produced from Sunzha crude.
o   Sample 3: Obtained from a kerosene gas oil cut produced from Stavro-
    pol crude.

The qualitative composition of the aromatic hydrocarbon was investigated
by means of thin layer chromatography and UV spectroscopy. The use of
thin layer chromatography could provide separation of the aromatic hydro-
carbons into monocyclic, bicyclic aromatics and phenanthrene hydrocarbons.
UV spectroscopic data could support certain tentative conclusions on the

structure of the aromatic hydrocarbons and micropreparative gas chromatography could determine the individual composition of the fractions of aromatic hydrocarbons.

Epperly and Pramuk (12) patented a process related to the separation of aromatics and/or non-hydrocarbons from saturated hydrocarbons and/or olefins. More particularly, their invention related to an improved process for the separation of aromatics from gasolines, kerosenes, lube oils and, most important of all, the preparation of thermally-stable hydrocarbons for use as jet fuels for supersonic aircraft. The separation of the aromatic hydrocarbons from the oil was accomplished by treating it with molecular sieve type X so that a maximum of about 3 wt. percent of aromatics was allowed to remain in the product. If any greater amount of aromatics was present the thermal stability would not be satisfactory.

Separation of unsaturated compounds from paraffin-rich hydrocarbon mixtures has for a long time been carried out by treating the crude hydrocarbon mixture with a liquid such as concentrated sulphuric acid or a selective solvent, such as liquid sulfur dioxide or furfural. For economic reasons these processes are usually used for the primary purification. However, for further economical purification, e.g. down to 0.01 wt% of aromatics, solid adsorption agents such as aluminium oxide and zeolite molecular sieves are used.

Epperly and Pramuk's process was carried out in either the liquid or the vapour phase. When the liquid phase was utilized the preferred temperature was 294-421 K. The preferred pressure was $1 \times 10^5 - 6.8 \times 10^5$ N/m^2 and the preferred feed rate, in order to limit the aromatics in the product to a maximum of about 3 wt percent, would be 0.4-3 w./w./hr.

Vapour phase operation is preferred. The temperature in the molecular sieve zone should be maintained at about 588-685 K. Pressure may vary between 1.0×10^5 to 3.4×10^5 N/m^2. The feed rate should be 0.5-3 w./w./hr. The amount of feed per cycle to maintain a critical level of no more than about 3 wt percent aromatic in the product would vary between 0.02 and 5 weight per weight of an adsorbent.

Usually aromatics are present in a typical feed to the extent of at least 10% by weight. The aromatics and the undesired hydrocarbon and non-hydrocarbon materials would remain on the molecular sieve. The molecular sieve was treated with various desorbing agents e.g., steam, CO_2, SO_2,

C_1-C_5 alcohols (such as, methyl, ethyl, glycols) or halogenated compounds (such as, methyl and ethyl chloride). Preferably, the desorption temperature should not exceed the adsorption temperature used for vapour phase adsorption, to avoid decomposition of the adsorbed material, and the pressure might vary between 1.0×10^5 to 3.4×10^5 N/m^2.

Dielacher and Hansen (13) described and claimed a process for the separation of aromatic compounds from liquid hydrocarbon mixtures where only traces of the aromatic occurs in the mixture. The process comprises adsorbing the aromatic compound onto a macro-porous, dehydrated cation exchange resin having a specific surface area of at least one m^2/g and pore diameter greater than 10 A°. They also described another process for the purification of crude oil paraffin (slack wax) in which the liquified starting material is treated with a dehydrated macroporous ion exchange resin which is charged almost completely with metal ions, in particular silver or copper ions. This process supplies a product which fulfils the purity requirements for the pharmaceutical industry, and is suitable for biogenic protein synthesis, for cosmetic purposes as well as for use in the food industry.

Aveisi, F. et al., (14) studied dearomatization of n-paraffin based on equilibrium and kinetic processes by using zeolite type NaX without binder. The work was conducted at 293 and 343 K, with a mesh size of 1-2 mm for zeolite. Model compounds such as tetralin, naphthalene, phenanthrene, fluorene, thiophene, etc. were used. Iso-octane was used as a solvent for the aromatic hydrocarbons in liquid-phase adsorption. They concluded that the energy of interaction depends on the temperature and on the chemical structure of the molecules.

When a molecule is attached to a long alkyl chain it weakens the net specificity of adsorption. The presence of a thiophene ring conjugated with an aromatic ring increases the net specific adsorption to a greater degree than does the presence of a saturated ring. Thus the adsorptivity from iso-octane solutions at 343 K increases in the following order: alkyl benzene < α-decylthiophene < tetrelin < benzothiophene < acenaphthene < 1, 3-di-p-xylyl-2 pentyl propane. At 293 K, the greatest adsorptivity is shown by naphthalene.

The common way to evaluate adsorbents for a specific application is to make isotherm tests, i.e. a series of experiments in which the value of

adsorption is determined as a function of adsorbate concentration at constant temperature followed by pilot column tests. The isotherm is used to determine the feasibility of using an adsorbent for a particular application.

Sundstrom and Krautz (15) studied the adsorption of n-paraffins from the liquid phase on type 5A molecular sieve. They studied the effect of molecular size, concentration and temperature on equilibrium loadings. Experiments were performed in a 200 cm^3 glass vessel. Dry molecular sieves from a regeneration column were charged to the vessel immersed in a constant temperature water bath. Samples of liquids were withdrawn periodically with a microliter syringe and analyzed with an Abbe refractometer. Equilibrium loadings on the sieves were calculated from the change in concentration of a known amount of binary mixture.

The normal paraffins studied were heptane, decane, dodecane and tetradecane. Measurements were made at 303, 333, and 363 K. Pressure was held constant at 98.06 kN/m^2 for all experimental runs. Results showed that for binary adsorption the normal paraffin with the lower molecular weight was preferentially adsorbed. The selectivity for the lower molecular weight paraffin was determined mainly by steric factors. The shorter the chains the easier the paraffin could enter the cavities. The equilibrium adsorptive capacity of the molecular sieves decreased slightly with increasing temperature. Over the temperature range studied, however, temperature had a negligible effect on the equilibrium when expressed on a volume basis, whilst on a weight basis the equilibrium loading capacity decreased with increasing temperature.

Dorogchinskii et al., (16) studied dearomatization of a kerosene cut by using commercial sorbent, synthetic zeolite of the fujasite type. The content of aromatic hydrocarbons in the feed stock was 8.3 wt.%. The experiments were conducted in continuously repeating cycles in a laboratory apparatus of 0.03 m diameter and 0.37 m height, charged with 200 cm^3 of binder-free NaX zeolite in the form of 0.4-1.5 mm granules. The run was conducted at 438 K with a linear feed velocity of 1 cm/min. The amount of feedstock in each cycle was 290% of the adsorbent (by volume). Desorption was performed at 573 K with benzene as displacing agent, using 0.5 volume of benzene per volume of zeolite per cycle. The content of aromatic hydrocarbons in the treated product was determined by a photoelectric-

colorimetric method and was found to be less than 0.2% by wt. The dynamic activity of the zeolite was 3.4% by weight.

Neuzil (17) claimed, in his invention, the separation of C_8 aromatic hydrocarbons from a feed using a solid crystalline, aluminosilicate adsorbent. The selectively adsorbed component was then recovered from the adsorbent through a desorption step employing a desorbent containing para diethylbenzene. The C_8 aromatic hydrocarbons which had been used in the feed streams of the adsorptive separation process include ortho xylene, meta-xylene, para-xylene and ethylbenzene. Other materials that may be included in the feed stream, but which are not necessarily determined in this adsorptive separation process, include relatively small amounts of paraffins, olefins, naphthenes and other types of hydrocarbon that are necessarily found in a C_8 aromatic stream. Crystalline alumino-silicate adsorbent Type X and Type Y zeolites were used.

Adsorption conditions included temperatures within the range from 303 K to about 623 K, and preferably within the range of about 313 K to about 522 K, and pressures within the range of atmospheric to about 40×10^5 N/m^2, and preferably within the range from about atmospheric to about 27×10^5 N/m^2. Both liquid phase and vapour phase operations can be used in the adsorption step but it is preferable to employ liquid phase operations because of the reduced temperature requirements and the decreasing opportunities for any type of side reactions to occur in the separation process.

The adsorption by CaA zeolite of normal alkanes from dilute iso-octane solutions at 293, 373, and 423 K is satisfactorily described by Fal'kovich et al., (18). The adsorption was calculated from Gibbs equation. They verified that the maximum adsorption is approximately equal to the limiting adsorption value. They also found that the values of maximum adsorption, A_m, and adsorption or separation coefficient f, characterizing collective interactions occurring in the zeolite solution system, decreased with an increase in temperature. This appears to be explained by an increase in the molecular mobility in the cavities, a weakening in their bonds with the cavity surfaces, and an increase in the effect of the force field due to the solution.

The molar volume of a normal alkane increases with an increase in temperature but the product of the maximum adsorption value and the molar

volume, termed the "limiting adsorption volume" decreased with increasing temperature. This decrease was quite sharp in some cases. The extent to which the large cavities were filled did not exceed 66% and usually decreased with increase in temperature and number of carbon atoms.

Heats of adsorption of ethane, ethylene and water on LiX, NaX, KX, RbX and CsX zeolites, as well as heats of adsorption of the homologous series of n-alcohols C_1-C_4 on NaX zeolite, were investigated by Avgul et al., (19). The contribution of specific interactions to the total energy of adsorption of ethylene on zeolites was found to decrease from LiX to CsX. The heats of adsorption of ethylene exceed those of ethane because of specific interactions due to the π bond present. The curves of the heat of adsorption of water have a wave-like form, especially for KX. The dependence of the differential heats of adsorption of n-alcohols by zeolite NaX on adsorption level were very large (83.6-108.6 kJ/mole) for initial values. Therefore, at room temperature it was difficult to determine the heat of adsorption of alcohols at small coverages. The heat of adsorption of methanol decreased with increasing adsorbate loading (a) in the low-coverage region. The heat of adsorption of 1-butanol did not depend to any large extent on a. Evaluation of the heat of adsorption of complicated molecules with branched chains, π bonds and conjugated bonds on zeolites is still needed.

In the process of propylene polymerization, at the stage of washing the polymer from the catalyst complex, the unreacted propylene becomes contaminated with isopropyl alcohol and water. The spent propylene makes up a significant part of the total volume of the raw material which undergoes polymerization. Therefore, its recovery and recycle is a very important problem. In order to regenerate the propylene, Gel'ms et al., (20) used NaX zeolites. Experiments were carried out in the liquid phase in a laboratory apparatus designed for pressures up to 1569 kN/m^2. They concluded that NaX - type zeolite is an effective adsorbent for purification of liquified propylene from isopropyl alcohol and water. NaX zeolite was also stable in multi-cyclic operations, e.g. after 13 cycles had been carried out, the adsorption capacity of the zeolite and the degree of purification of the propylene remained constant. The true dynamic activity of the adsorbent sample that was used with respect to water vapour was 146 kg/m^3. The static capacity of the zeolite with respect to the isopropyl

alcohol was determined and was equal to 0.014-0.017 kg per 0.1 kg of the adsorbent. Based upon the results obtained for the purification of propylene from alcohol and water, by the zeolite layer, a process was developed for the industrial production of polypropylene.

Hansjoerg et al., (21) studied the adsorption of mixtures of alkanes of medium chain length on X and Y zeolites. The heats of immersion, the isotherms, and the separation factors were determined. The adsorption and separation depended on the nature and sites of the zeolite cations. The alkenes have higher heats of immersion than the alkanes due to interactions with adsorption centres.

Epperly et al., (22) published an invention relating to a process for purifying saturated hydrocarbons and/or olefins of aromatic contents utilizing zeolite adsorbent type X, having pore sizes of 6.5 to 13A with monovalent or divalent cations. Adsorption was carried out at 588.5 K and 103.4 kN/m^2. The aromatic contents in the product were less than 0.1%.

Rosback et al., (23) claimed an improved process for the separation of olefins from a hydrocarbon feed mixture using zeolite adsorbent type X. The conditions used included temperatures within the approximate range of 298 to 423 K and pressures within the approximate range of atmospheric to 3450 kN/m^2. They claimed an improved prepared zeolite by contacting an X structure zeolite and an amorphous binder selected from the group (consisting of silica, alumina and silica-alumina) and having a Na_2O/Al_2O_3 ratio of less than about 0.7, with an aqueous sodium hydroxide solution at ion exchange conditions, for 0.5 to 5 hours to increase the sodium cation content to a Na_2O/Al_2O_3 ratio of greater than about 0.7 and to remove from 1 to about 15 wt% of SiO_2 and Al_2O_3 from the NaX zeolite.

The competitive adsorption of fuel-type compounds on zeolite 13X was studied by Jean et al. (24). They reported that in the removal of nitrogen compounds, oxygen compounds, and olefins from synthetic petroleum fractions such as naphtha on zeolite 13X, both nitrogen and oxygen compounds were strongly adsorbed, but the low basicity compounds such as 2,4,6 collidine were poorly adsorbed. Olefins competed for adsorption with nitrogen compounds only at very high concentrations.

Selectivity of adsorption of dimethylnaphthalenes on zeolites was reported by Casellato (25). He studied the adsorption of naphthalene, of the monomethylnaphthalenes and of 8 dimethylnaphthalenes from n-hexane

solution on LZY zeolite in the Na, K and Ca forms and on 13X zeolite in the Na form. The adsorption capacity of these zeolites towards the methylnaphthalene was relatively high, particularly of the Na-LZY form. 1,4- and 1,8-dimethylnaphthalene behaved differently, the former being completely excluded from the 3 LZY zeolites and the latter being excluded also from the K-LZY zeolite. This behaviour of the methylnaphthalenes was apparently attributable mainly to steric factors.

It is clear that there are only limited data in the literature on the adsorption of high molecular weight aromatic compounds (such as aromatics present in wax with a boiling range of 620 K to 720 K). The adsorption of such compounds would be expected to involve more complex phenomena, e.g. due to blockage of pores. However, if their removal proved technically feasible and economic it would greatly assist wax processing.

3.0 A STUDY OF EQUILIBRIUM ISOTHERM ADSORPTION OF INDIVIDUAL AROMATIC COMPOUNDS FROM BINARY SOLUTIONS WITH ISO-OCTANE

The adsorptive separation of petroleum products and petroleum hydro-carbons can be predicted by using physico-chemical properties of the sorbent-sorbate system; especially the adsorption isotherm which is the most significant property of the system. Practically, for a wide range of applications, static methods are used for determination of the adsorption isotherms.

The latest scientific studies show that dynamic methods can be used for the determination of the adsorption isotherms, using liquid chromatography columns packed with non-porous and highly porous adsorbents. However, detailed research work is required on the factors which affect the breakthrough curves of each specific system, i.e. the plot of effluent concentration/feed concentration versus time or volume of effluent after passing through a specific fixed bed.

This investigation deals with the study of physico-chemical characteristics of the adsorbent-sorbate system, using the static method.

3.1 Selection of the Materials

3.1.1 Molecular Sieves Type X

Molecular adsorbents which exhibit ultraporosity and which are generally used for the separation of gas, vapour and liquid hydrocarbon mixtures include: activated carbon, activated clays, inorganic gels (such as silica gel), activated alumina and crystalline alumino-silicate zeolites (molecular sieves).

Breck (1) found that the activated carbons, activated alumina and silica gel do not possess an ordered crystal structure and consequently the pores are non-uniform. The distribution of the pore diameters within the adsorbent particles may be narrow (20-50A°) or wide (20-1000A°) as in carbons. Hence, all molecular species, with the exception of high molecular weight polymeric materials, may enter the pores.

Zeolite molecular sieves have pores of uniform size (3-10A°). These pores will completely exclude molecules which are larger than their diameter. In contrast with other types of adsorbent the molecular sieves have a high internal surface area available for adsorption due to the channels or pores which uniformly penetrate the entire volume of the solid. The

external surface of the molecular sieve particles contributes only a small amount of the total available surface area, see Figure 3.1.

Barrer (26) studied the saturation capacities of water for different types of adsorbent. He estimated that the saturation for molecular sieves type X, silica gel and molecular sieves type A are 445, 0, 357 cm^3 at Standard Temperature and Pressure STP/kg of adsorbent respectively.

Owaysi (27) studied the dynamic capacity of different types of adsorbent such as silica gel, alumina and molecular sieve type X, by using a mixture of alkylbenzene in tridecane. He concluded that the dynamic capacity for adsorption of aromatic hydrocarbons was much higher when using molecular sieve type X, i.e. it was 12.0, 6.0, and 4.6 g/100 g of adsorbent for molecular sieve, silica gel and alumina, respectively.

The adsorbent used in the present work was Linde Molecular Sieve type 13 X which has the properties summarized in Table 3.1.A according to Breck (1), and in Table 3.1.B according to characterization performed at KISR's laboratories.
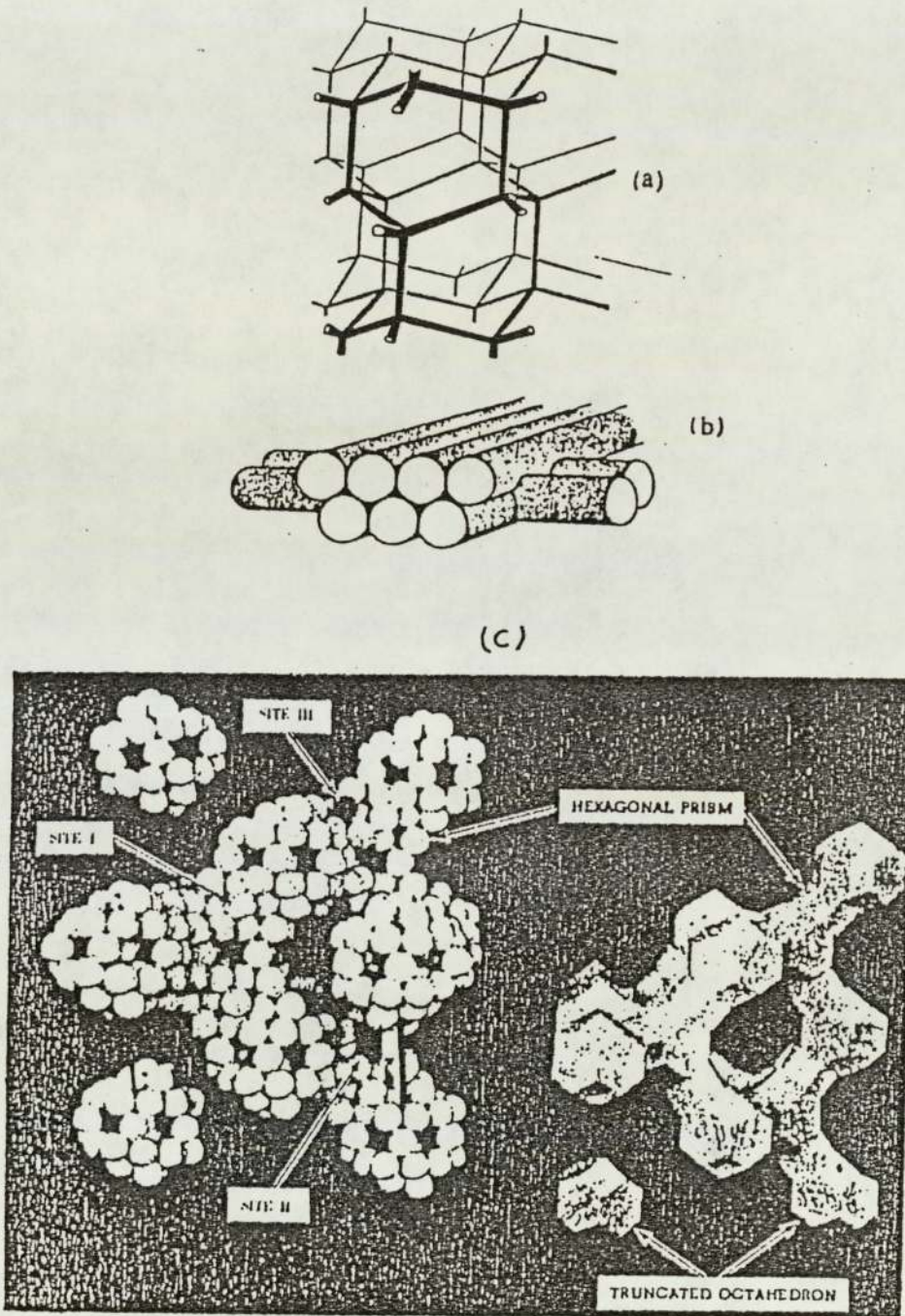
Figure 3.1   Illustration of the Channel System
in the Zeolite   (a) The 4-Connected
Net Work,   (b) The Channels as an
Array of Overlapping Tubes and   (c)
The Structure of Zeolite by a Model.

TABLE 3.1.A

PHYSICO-CHEMICAL AND THERMODYNAMIC PROPERTIES OF
MOLECULAR SIEVES TYPE NaX (13X)

Physical Properties	Typical Unit Cell Contents
Nominal Pore Size ...10 Angstroms	Na_{86}
Type of Crystal .....Body Centre Cubic (Diamond Structure)	$[(AlO_2)_{86}(SiO_2)_{106}]$ 264 H_2O
Bulk Density	
Powder .... 770 kg/m^3	
Beads .... 688.8 kg/m^3	
Crushing Strength * - Beads	
(4-8 Mesh) .... 7.25 kg	
(8-12 Mesh) .... 3.1 kg	
Pore volume 0.352 cm^3/g	

TABLE 3.1.B

CHARACTERIZATION OF MOLECULAR SIEVES TYPE NaX

1. Mechanical Properties
   a. Average length (mm)   6.448
   b. Average diameter (mm)   3.302
   c. Bulk density (kg/m^3)   620.2

2. Physical Properties
   a. Surface area (m^2/g)   539.05
   b. Pore volume (cm^3/g)   0.296
   c. Pore radius (°A)   9.8

3. Chemical Structure in Oxide Forms
   Al_2O_3 (wt %)   32.8
   SiO_2 (wt %)   33.1
   Na_2O (wt %)   15.1
   Water capacity (wt %)   19.5

-40-

3.1.2 Solvents and Adsorbate Hydrocarbons

The main objective of this investigation was to study the effect of adsorption of low concentrations of aromatic hydrocarbons from a binary mixture with paraffin waxes and iso-octane using selective molecular sieves type X. The hydrocarbons selected as models of impurities in waxes are listed in Table 3.2.

The selection of such aromatic components was based upon Cherednichenko's (11) identification of some hydrocarbons in an oil cut with boiling ranges 520-630 K, such as naphthalene, 2, methylnaphthalene, fluorene and phenanthrene. Aveisi (14) also identified some aromatics in a high boiling point paraffin fraction such as naphthalene, phenanthrene, fluorene and alkyl-benzene. Newman (28) also identified different types of aromatics, i.e. mono, di, tri and polynuclear, such as dibenzofuran, phenanthrene, etc. in high boiling-point range petroleum fractions.

Siryuk and Barabadze (10) also identified some aromatic compounds in high boiling petroleum cuts such as naphthalene, phenanthrene and anthracene etc. by using a modified UV spectroscopy method.

3.2 Methodology

3.2.1 Molecular Sieve Preparation

The molecular sieve pellets were crushed by grinding and were then screened using a shaker to obtain particle sizes between 1 to 2 mm in diameter. The molecular sieve was then kept in a covered container ready for use.

3.2.2 Molecular Sieve Activation

All zeolites have a high affinity for polar molecules particularly water, and can, in general, be used for removing water from gases and liquids and for general drying.

Activation of molecular sieves type 13 X was carried out by drying a weighed amount in a weighing bottle in an oven to remove the water present in the pores at 673-720 K for 4 hours. Then the weighing bottle was covered firmly and taken out of the oven and cooled down in a desiccator. The bottle was then weighed at room temperature (~298 K).

The loss in weight was related to the water present in the molecular sieves pores. Percentage loss was 19% ± 0.5% for each run.

3.2.3 Solution Preparation

Several weights of each aromatic compound were weighed into a volumetric flask of 50 cm^3 volume; the range of weights are illustrated in Table 3.3.

Iso-octane was used, as solvent and each flask was well-shaken until all the component dissolved and a homogeneous solution was obtained.

Cumene, dodecylbenzene, naphthalene, 1-methylnaphthalene, dimethylnaphthalene and fluorene were easy to prepare because of their complete miscibility with isooctane. However, dibenzothiophene, dibenzofuran and phenanthrene were difficult to dissolve and needed some heating.

TABLE 3.2
THE PHYSICAL PROPERTIES OF THE INDIVIDUAL AROMATIC COMPOUNDS

Name	General Formula	Structural Formula	Mol. Wt. g/mole	Density g/cm^3	
				303 K	343 K
Cumene	C_9H_{12}		120.2	0.8551	0.8277
Dodecyl-benzene	$C_{18}H_{30}$		246	0.8495	0.8215
Naphthalene	$C_{10}H_8$		128.18	0.9979	0.9928
1, methyl-naphthalene	$C_{11}H_{10}$		142.2	1.012	0.9923
1,3,Dimethyl-naphthalene	$C_{12}H_{12}$		156.26	1.0119	0.9913
Phenanthrene	$C_{14}H_{10}$		178.24	0.9664	0.9455
Fluorene	$C_{13}H_{10}$		166.21	1.1864	1.1642
Dibenzo-thiophene	$C_{12}H_8S$		184.26	1.0835	1.0629
Dibenzofuran	$C_{12}H_8O$		168.2	1.0778	1.0572
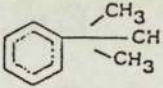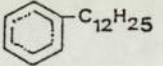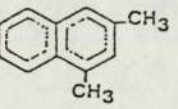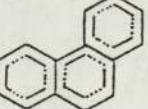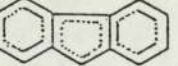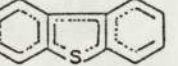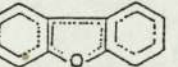
TABLE 3.3
CONCENTRATION RANGE OF ORIGINAL SOLUTIONS AND THEIR
EQUILIBRIUM TIME

Constituents Name	Range Conc. of original solution $g/10^3 cm^3$	Range Conc. of original solution $mole/10^6 cm^3$	Mol. wt.	Equilib. Time at 303 K	Equilib. Time at 323 K	Equilib. Time at 343 K
Cumene	7-35	58-291	120	4 days	2 days	24 hrs
Dodecylbenzene	5-46	20-191	246	4 days	-	24 hrs
Naphthalene	5-35	39-273	128	4 days	-	16 hrs
1, Methylnaph-thalene	8-56	56-394	142	4 days	-	16 hrs
1,3 Dimethyl-naphthalene	8-58	51-371	156.26	4 days	2 days	20 hrs
Dibenzothiophene	3-26	16-141	184.26	10 days	2 days	24 hrs
Fluorene	4-34	24-204	166.21	10 days	-	24 hrs
Phenanthrene	6-30	33-168	178.24	10 days	-	24 hrs
Dibenzofuran	4-34	17-202	168.2	10 days	-	24 hrs

The change in concentration of a known amount of binary mixture was measured by UV Vis NIR spectrometer (Perkin Elmer Model 330) and the adsorption value G was calculated from the formula:

$$G = \frac{(X_o - X_1)}{m} \sum n_1 n_2 \tag{3.1}$$

where X can be calculated according to the following equation:

$$X_o = \frac{(0.001) C_o}{(0.001) C_o + \left(1000 - \frac{Mol. \ wt}{\rho \times 1000} \cdot C_o\right) \frac{\rho \ solv.}{Mol. \ wt \ solv.}} \tag{3.2}$$

The equilibrium adsorption of aromatic compounds from iso-octane solutions on zeolite was investigated in the region of initial concentrations up to approximately 5-35 kg/m^3, equal to 1-5% wt.

3.2.4 Experimental Procedure

Equilibrium measurements were made in a 100 cm^3 capacity, stainless steel, autoclave of 0.14 m length and 0.03 m in diameter (Figure 3.2).

A constant temperature of 273 K was maintained during each experiment by means of a water bath.

(10 cm^3) of a certain concentration of an aromatic compound was introduced into a numbered autoclave by injection from a disposable syringe. A known quantity, about 1 g, of freshly-prepared, dry activated molecular sieve of size 1-2 mm was poured quickly into the autoclave which was then closed firmly.

The autoclave was immersed in the water bath at the required temperature of 303, 323 or 343 K, for a specific time (Table 3.3) to attain equilibrium. Equilibrium was established experimentally for each compound and temperature, by plotting the adsorption value vs. time. When no more adsorption occurred, i.e., the value of adsorption remained constant with time, this indicated that the maximum equilibrium was attained. Table 3.3 contains the values established for each compound and temperature.

3.3 Results and Discussion

The development and extensive commercial use of liquid phase processes for the recovery of pure n-paraffins and waxes by means of synthetic zeolites is closely related to the problem of improving the feedstock quality, mainly its hydrocarbon composition.

Little is known about diffusivity in the large-pore zeolites such as type X and type Y that are of interest in catalysis and as noted in Chapter 2, very little has been published relating to hydrocarbon molecules of high molecular weight which are of interest in chemical processing.

The study of zeolite dearomatization of n-paraffin or waxes must be based on adsorption equilibrium and kinetic characteristics of the process of aromatic compound adsorption by the zeolite.
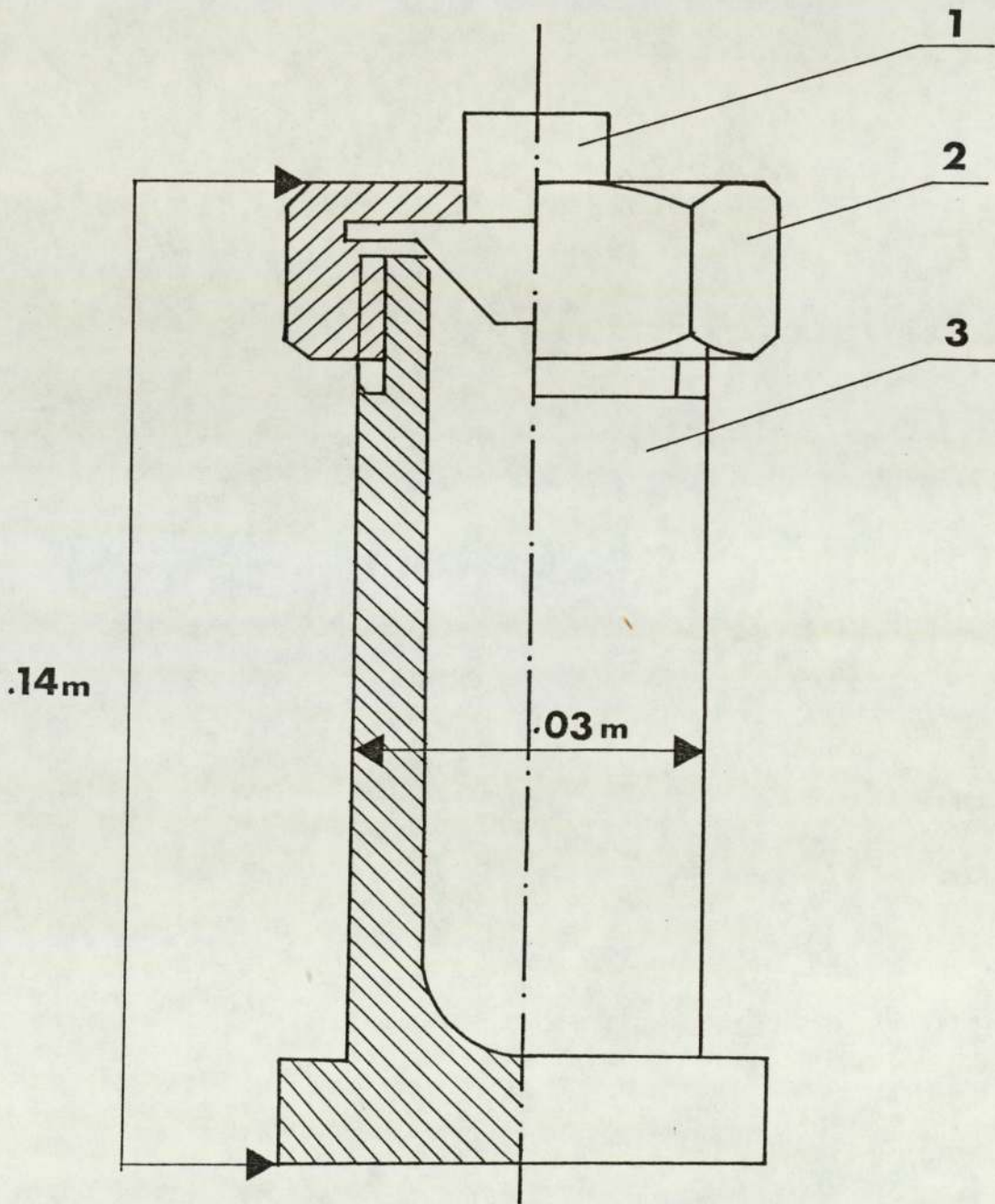
Figure 3.2   Autoclave: 1 Cone,
2 Nut, 3 Body.

3.3.1 Equilibrium Isotherm Adsorption of Aromatic Hydrocarbons from Binary Solution With Iso-octane.

The plot of the quantity of the hydrocarbon adsorbed as a function of equilibrium concentration gives the experimental adsorption "isotherm".

The adsorption isotherm is generally determined by two methods. The first method, is the volumetric method: which determines the quantity of hydrocarbon present in the system by measurement of the solution concentration volume, and temperature. After exposing the activated molecular sieves to a quantity of hydrocarbons (in the present case aromatic organic compounds in iso-octane) in a closed system, the quantity adsorbed is determined from the concentration, temperature and volume of contacted solution with adsorbents when equilibrium is attained.

The second method is the gravimetric method, which measures the amount of gas, vapour or liquid adsorbed by weighing the sample in a closed system on a balance, generally of the quartz-spring type. This balance was first used by McBain and is commonly referred to as a MacBain adsorption balance (1).

When the solution of aromatic component is contacted with the adsorbents, the molecules of the aromatic component will be distributed among the zeolites cavities along with the molecules of the solvent. Due to some interaction between the molecules of the component (adsorbates) and the cations in cavities of zeolite crystals, adsorption occurs. These interactions can be divided into specific and non-specific interactions. The specific interactions can be characterized by the energy which arises from the constant dipole or quadrupole moments of the adsorbate molecules.

Non-specific interactions are related to dispersion, repulsion and polarization (the energy which is related to electrostatic charges of molecular sieves van der Waals energy).

The initial sections of adsorption isotherms for the aromatic hydrocarbons and heterogeneous compounds are shown in Figures 3.3 through 3.8. The points represent the experimental data determined by the Gibbs equation, and the curves were calculated from a suggested equation by Eltekov and Kiselev (29) for pore filling in the form of multilayers referred to as Brunauer-Emmett-Teller (BET) and expressed as:

$$G = A_m \, \beta(f-1) \, \frac{X_1 \, (1-X_1)}{1 + (\beta f - 1) \, X_1} \tag{3.3}$$

The limiting value of maximum adsorption capacity A_m and separation coefficient f can be calculated from a graphical solution of the (BET) equation in the form

$$\frac{X_1(1 - X_1)}{G} = \frac{1}{\beta A_m \, (f-1)} + \frac{X_1}{A_m} \tag{3.4}$$

This was done by plotting $X_1(1-X_1)/G$ versus X_1 to give a straight line, from which the slope was determined according to the following equations:
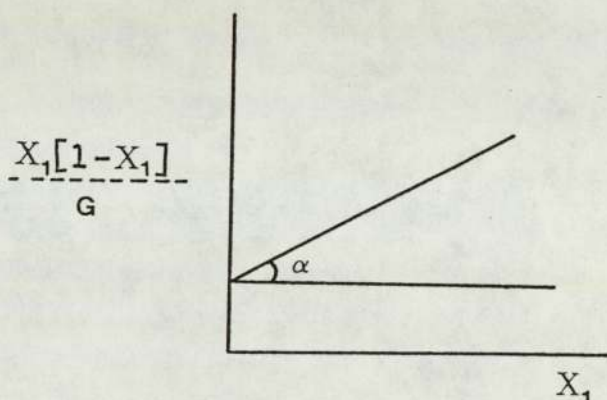
The slope equals $\tan \alpha = \dfrac{1}{A_m}$ $\qquad\qquad$ (3.5)

The intercept $= \dfrac{1}{\beta A_m \, (f-1)} = b$ $\qquad\qquad$ (3.6)

$$\beta = \left[\frac{Mol. \ wt.}{\rho} \ compound \right] \left[\frac{\rho}{Mol. \ wt.} \ solvent \right] \tag{3.7}$$

then $f = (\tan \alpha/\beta b) + 1$ $\qquad\qquad$ (3.8)

As demonstrated by Figures 3.3-3.8, adsorption of the aromatic hydro-carbons under study was reasonably well described by equation 3.3 and the limiting amounts of adsorption as determined experimentally (i.e., points on the isotherm curves) were in a good agreement with the values calculated from equation 3.3.

Adsorption of aromatic hydrocarbons has been classified for three groups: mono aromatics, di aromatics and triaromatic rings.

Adsorption Isotherms for Mononuclear Aromatics.

The sorption isotherms for the two aromatic hydrocarbons cumene and dodecylbenzene on sodium-molecular sieves 13 X at 303, and 343 K are shown in Figures 3.3 and 3.4. Adsorption of such aromatic hydrocarbons, occurs as a result of interaction of the Π-electron system of the benzene ring with the cations in the cavities of zeolite crystals. The benzene ring is attached to the surface or within the zeolite cavities. The interaction between Π-electrons and the hydroxyl groups has also been observed on amorphous silica, although the interaction on amorphous silica was weaker compared to that on molecular sieves (1). However, such interaction resulting in the strong adsorption of aromatics onto zeolite crystals, is affected by many parameters. The zeolite is characterized by its uniform pore structure with the size typical of aromatic hydrocarbons. Such a pore structure may be a cause of strong "physical" interaction with aromatic hydrocarbons.

The adsorption isotherms of aromatic hydrocarbons on molecular sieves have a typical form characterized by the slightly tailed-out maximum of Gibb's adsorption. They rise steeply and reach maximum values at equilibrium concentrations of the hydrocarbons in iso-octane. These equalled 8×10^{-3} mole fraction for cumene and dodecylbenzene at 303 K, and $18 \times 10^{-3} - 5.10^{-3}$ mole fraction for cumene and dodecylbenzene respectively at 343 K.

An increase in temperature also affects the orientation of the dodecylbenzene molecules. Hence diffusivity increases according to an Arrhenius type equation; thus the equilibrium decreases (the maximum adsorption value for dodecylbenzene at 303 and 343 K were 0.53 and 0.38 mole/kg respectively).
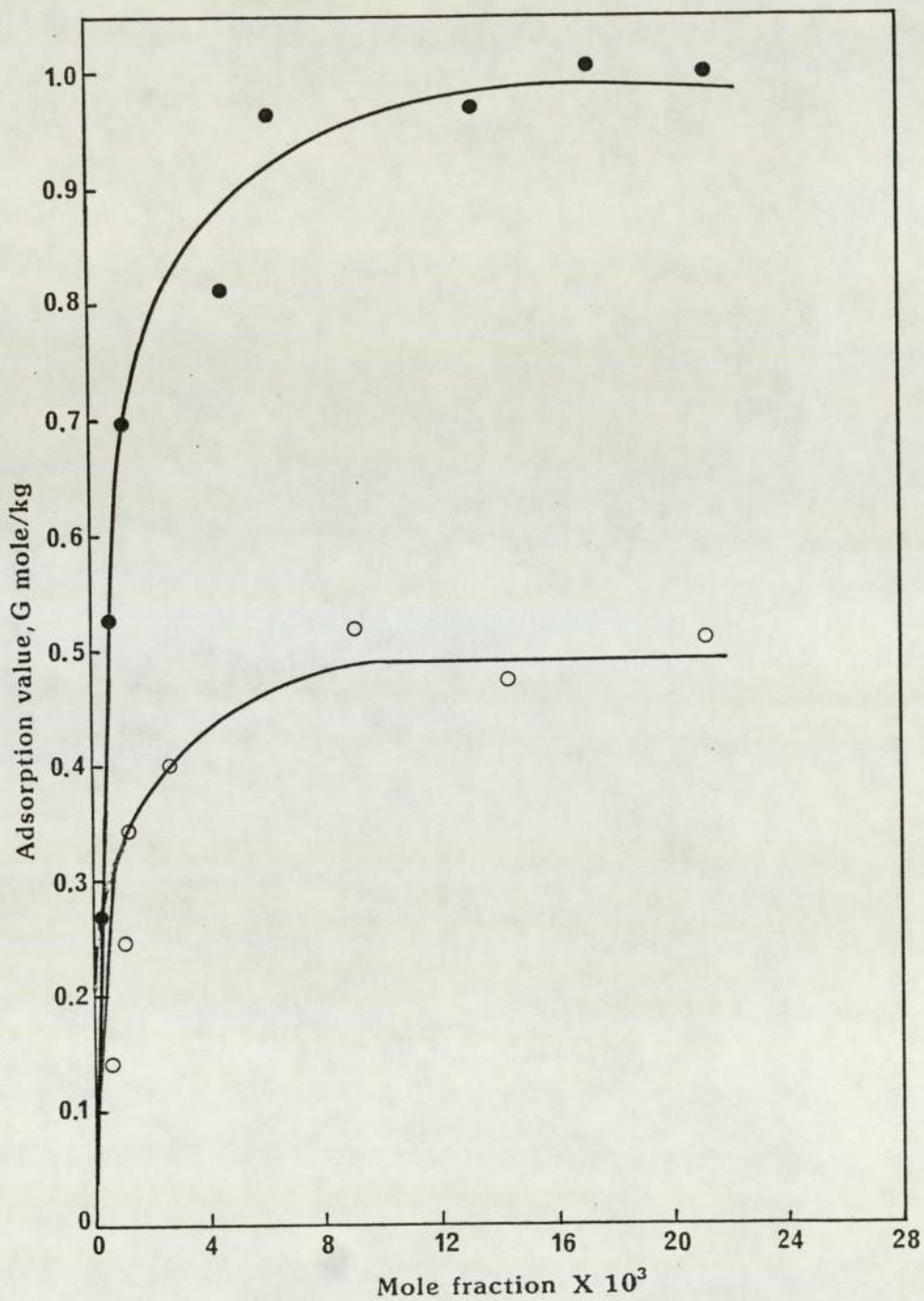
Figure 3.3   Adsorption Isotherms of ● Cumene
and ○ Dodecylbenzene on Pellets
of Zeolite NaX (13X) at 303 K.
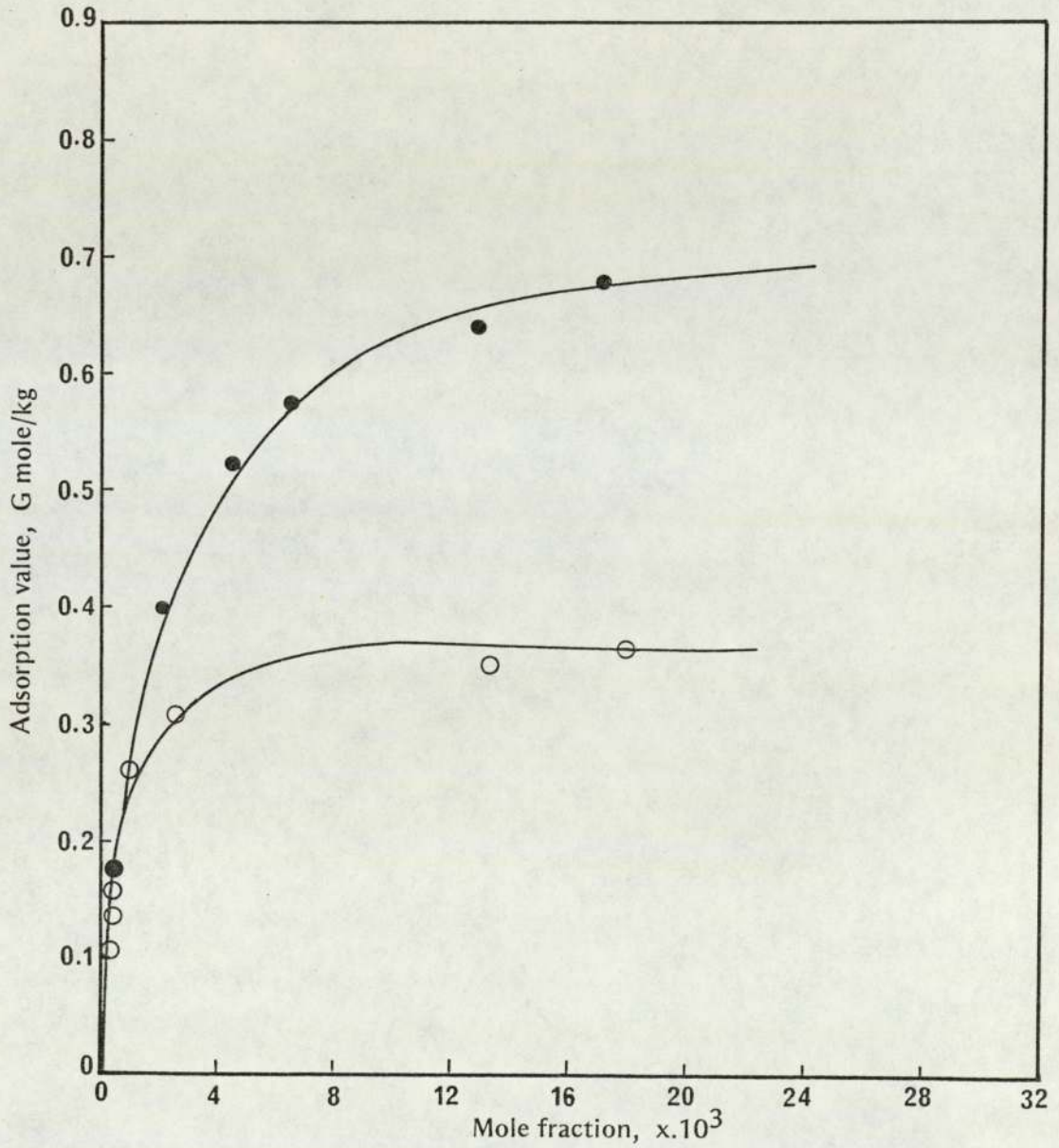
Figure 3.4   Adsorption Isotherms of ● Cumene
and ○ Dodecylbenzene on Pellets
of Zeolite NaX (13X) at 343 K.

Separation Coefficients of Mononuclear Aromatics.

Values of the separation coefficients (log f) determined for cumene and dodecylbenzene using equation (3.3) are illustrated in Table 3.4. These show that the logarithm of the separation coefficient log f > 2, indicative of a high selectivity of adsorption of these aromatic hydrocarbons from iso-octane solution by molecular sieves 13 X.

The free energy of adsorption depends on the temperature and on the chemical structure of the molecules. The influence of temperature on the adsorption of aromatic hydrocarbons shows up particularly for those molecules in which the aromatic ring is shielded by a small alkyl chain (as in cumene) and a long alkyl chain (as in dodecylbenzene).

In general increasing the adsorption temperature from 303 K to 343 K resulted in a decrease in the separation coefficient for cumene, from 3.3 to 2.5, and for dodecylbenzene, from 3.1 to 3.0. This indicates that an increase in the adsorption temperature results in weakening of the interaction of the π-bonds of the molecules of aromatic compounds with the electrostatic charges of the cations in the cavities of zeolite crystals. The increase in temperature also results in more rapid diffusion of the molecules in the zeolite cavities with a consequent reduction in time for the physical interaction to occur. The long alkyl chain connected with the benzene ring, such as in dodecylbenzene, at a low temperature will weaken the nonspecific interaction compared with that for cumene. Hence the separation coefficient of cumene at 303 K (log f = 3.3) is higher than that for the dodecylbenzene (log f = 3.1). An increase in the adsorption temperature up to 343 K would be expected to result in an increase in the free energy of adsorption for dodecylbenzene molecules due to the increase in the nonspecific interactions (total repulsion, dispersion and polarization energy) between the molecules of dodecylbenzene and cations in the cavities of zeolite crystals. These are higher than the interactions between the cumene molecules and the cations in cavities of zeolite crystals, e.g. at 343 K the values of log f for dodecylbenzene and cumene were 3 and 2.5 respectively. Non-specific interaction is in fact characteristic of the alkyl chain rather than the aromatic ring.

-52-

TABLE 3.4. THE CALCULATED THEORETICAL EQUILIBRIUM LIMITING VALUES OF AROMATIC COMPOUNDS FROM BINARY SOLUTION WITH ISO-OCTANE USING MOL SIEVES TYPE NaX AT DIFFERENT TEMPERATURE

TYPE OF HC	303 K						343 K					
	TAN α	A_m THEORETICAL MOLE/KG	b	B	f	LOG f	TAN α	A_m MOLE/KG	b	B	f	LOG f
CUMENE	0.9	1.00	0.5×10^{-3}	1.06	1817.0	3.3	1.2	0.83	4×10^{-3}	0.82	366.8	2.5
DODECYL-BENZENE	2.0	0.50	1.0×10^{-3}	1.7	1177.4	3.1	2.6	0.38	1.4×10^{-3}	1.65	1131.0	3.0
NAPHTHA-LENE	1.1	0.92	0.2×10^{-3}	0.76	7106.2	3.8	1.15	0.86	1×10^{-3}	0.73	1576.3	3.2
METHYL-NAPHTHALENE	1.2	0.83	1×10^{-3}	0.84	1429.5	3.1	1.6	0.62	3×10^{-3}	0.81	667.0	2.8
DIMETHYL-NAPHTHALENE	1.3	0.77	0.5×10^{-3}	0.92	2811.8	3.4	1.8	0.54	1×10^{-3}	0.89	2079.0	3.3
DIBENZO-THIOPHENE	1.2	0.82	0.1×10^{-3}	1.01	12129.0	4.1	1.27	0.78	0.1×100^{-3}	0.98	12960.0	4.1
FLUORENE	1.3	0.73	1.75×10^{-3}	0.83	6555.0	3.8	1.43	0.69	0.5×10^{-3}	0.8	35947.0	3.5
PHENAN-THRENE	1.9	0.52	0.25×10^{-3}	1.1	6910.0	3.8	2.3	0.43	0.5×10^{-3}	1.07	4303.0	3.6
DIBENZO-FURAN	1.5	0.66	2.5×10^{-3}	0.88	679.7	2.8	1.8	0.55	2.5×10^{-3}	0.9	801.0	2.9

Number of Molecules Occupied by Unit Cell of Zeolite Crystals of Mononuclear Aromatics.

At both adsorption temperatures, 303 K and 343 K, the number of molecules occupying a unit cell of zeolite crystals 13X for cumene is higher than that for dodcylbenzene (13.3, 7.1 at 303 K and 9.1, 5.1 at 343 K for cumene and dodecylbenzene, respectively). This occurs due to the molar volume of the dodecylbenzene which is twice that of cumene. Also from Table 3.5, the coverage of cumene molecules adsorbed by the cavities of the molecular sieves crystals appears to be lower than that of dodceylbenzene; i.e. the values (at 303 K and 343 K), are 47.4 and 33.3 for cumene and 51.7 and 37.5 for dodecylbenzene respectively. This occurred due to the steric effect in adsorption and close packing of aromatic molecules with aliphatic chain, the coverage ratio usually decreases at higher temperature.

Adsorption Isotherms of Binuclear Aromatics.

Figures 3.5 and 3.6 illustrate the adsorption equilibrium isotherms for binuclear aromatic hydrocarbons: naphthalene, 1 methylnaphthalene and 1, 3 dimethylnaphthalene over a wide range of equilibrium concentrations up to 32×10^{-3} mole fraction at temperatures of 303 K and 343 K. These suggest that the isotherms are characterized by achievement of the maximum of Gibbs adsorption. The isotherms rise steeply and reach maximum values of equilibrium concentration of the aromatics in iso-octane equal to 8×10^{-3} mole fraction at 303 K and 12×10^{-3} mole fraction at 343 K.

As mentioned above, with increasing temperature, the diffusivity increased according to the Arrhenius type equation but the equilibrium amount adsorbed decreased and this was confirmed for the adsorption of naphthalene group which, at 343 K, had lower values of adsorption than at 303 K. This means that the temperature maximum occurs at a low amount adsorbed, and the increased rate, owing to increased diffusivities, is nearly compensated for by the decreased equilibrium adsorption at the observed temperature.

Usually the aromatic with the lower molecular weight was preferentially adsorbed. This is demonstrated by the naphthalene group adsorption. According to the data of Figures 3.5 and 3.6, the adsorptivity of naphthalenes from iso-octane solutions by zeolite 13 X at 303 K and 343 K increased in the following order:

TABLE 3.5. LIMITING VALUES OF ADSORPTION OF AROMATIC COMPOUNDS FROM BINARY SOLUTION WITH ISO-OCTANE AT DIFFERENT TEMPERATURES

TYPE OF HC	MAX. ADSORPTION EXP. G MOLE/KG	303 K				343 K				
		VOL. OCCUPIED BY MOLECULES $G\mu$ cm³/g	COVERAGE $\dfrac{G\mu\%}{V_p}$	NO. OF MOLECULES ADSORBED BY 1 g GN	NO. OF MOLECULES ADSORBED BY 1 UNIT CELL $\dfrac{GN}{n}$	G	$G\mu$	$\dfrac{G\mu\%}{V_p}$	GN	$\dfrac{GN}{n}$
CUMENE	1.00	0.14	47.4	6×10^{20}	13.3	0.68	0.09	33.3	4.09×10^{20}	9.1
DODECYL-BENZENE	0.53	0.15	51.7	3.2×10^{20}	7.1	0.38	0.11	37.5	2.3×10^{20}	5.1
NAPHTHALENE	0.92	0.12	40.0	5.5×10^{20}	12.3	0.85	0.11	37.5	5×10^{20}	11.4
1, METHYL-NAPHTHALENE	0.83	0.12	39.3	4.9×10^{20}	11.1	0.65	0.09	20.5	3.9×10^{20}	8.7
1, 3 DIMETHYL-NAPHTHALENE	0.78	0.14	40.6	4.7×10^{20}	10.4	0.54	0.08	15.5	3.3×10^{20}	7.2
DIBENZO-THIOPHENE	0.84	0.14	48.2	5.0×10^{20}	11.2	0.78	0.13	45.3	7×10^{20}	10.5
FLUORENE	0.72	0.10	34.3	4.4×10^{20}	9.7	0.69	0.09	33.2	4.2×10^{20}	9.2
PHENANTHRENE	0.51	0.09	31.7	3×10^{20}	6.8	0.42	0.07	26.7	2.5×10^{20}	5.6
DIBENZOFURAN	0.60	0.09	31.6	3.6×10^{20}	8.0	0.54	0.09	29.1	3.2×10^{20}	7.2

V_p = LARGE PORE SIZE FOR ZEOLITE X

= 0.296 cm^3/g

n = 0.45 x 10^{20} unit cell/g

1,3 dimethylnaphthalene < methylnaphthalene < naphthalene

Separation Coefficients of Binuclear Aromatics.

The limiting values of adsorption and the separation coefficient for binuclear aromatic hydrocarbons are listed in Table 3.4.

From Table 3.4 it was shown that the separation coefficients, log f > 3, for the naphthalene group. This indicates strong interactions between the molecules of naphthalene and the local electrostatic field in the cavities of the molecular sieve crystals. Increase in adsorption temperature will lead to a decrease in the separation coefficients log f of the naphthalene adsorbate molecules.

Number of Molecules Occupied by Unit Cell of Zeolite Crystals of Binuclear Aromatics.

The number of adsorbate molecules captured by unit cell of the zeolite crystals decreased as the molecular weight of the adsorbate molecules increased. For example at 303 K for naphthalene only 12.3 molecules were located in one cavity of molecular sieve crystal, whereas for 1-methyl naphthalene and 1, 3 dimethylnaphthalene the numbers were 11.1 and 10.4 molecules respectively. The value of adsorption will affect the total number of adsorbate molecules and, as already mentioned, an increase in adsorption temperature will result in a decrease in the value of adsorption. Hence, the number of adsorbed molecules of naphthalene group will decrease as the temperature increases (see Table 3.5).

In similar work, Hedge (30) studied the use of molecular sieve type X for the separation of 2, 7 Dimethylnaphthalene from 2, 6 Dimethylnaphthalene. He concluded that the dimensions of the molecule are a major factor affecting the separation process.
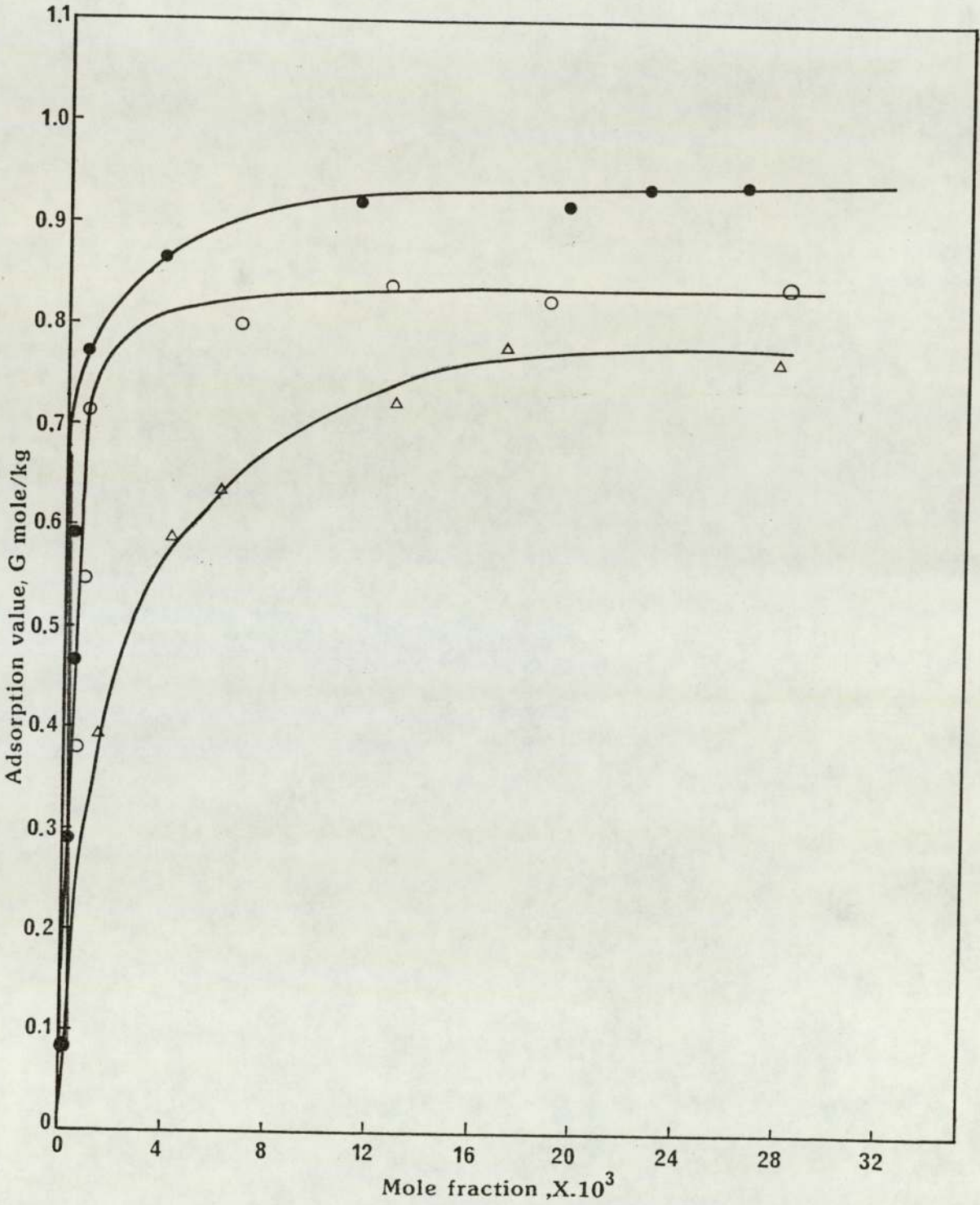
Figure 3.5 Adsorption Isotherms of ● Naphthalene,
○ 1-Methylnaphthalene and △ 1-3-Di-
methylnaphthalene on Pellets of
Zeolite NaX at 303 K
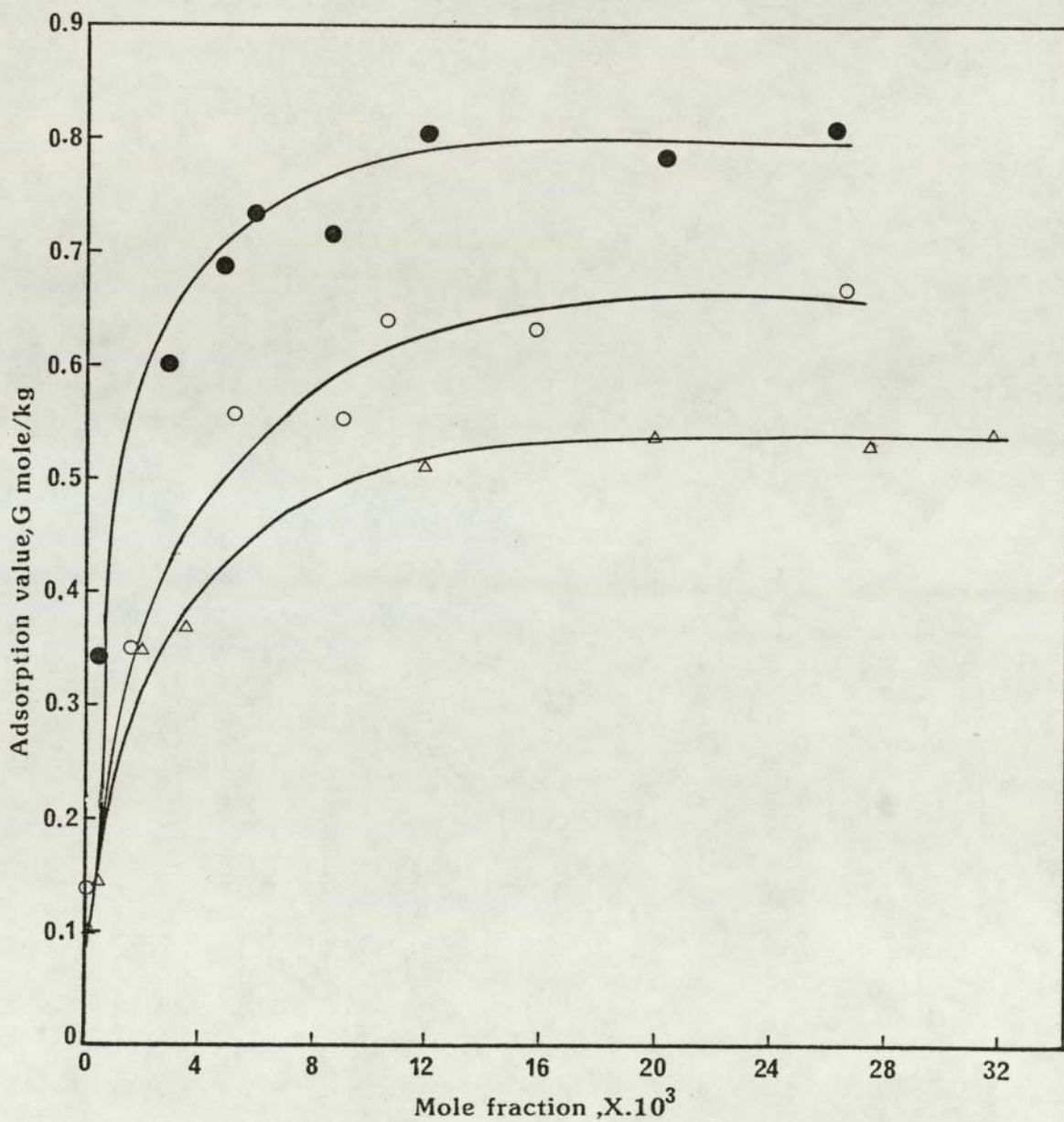
Figure 3.6   Adsorption Isotherms of ● Naphthalene,
            ○   1-Methylnaphthalene and △ 1-3-Di-
            methylnaphthalene on Pellets of
            Zeolite NaX at 343 K.

Adsorption Isotherms of Trinuclear Aromatics.

The adsorption isotherms of trinuclear aromatics from a binary solution with iso-octane, over a range of equilibrium concentration (up to 24 x 10^{-3} mole fraction) and at temperatures of 303 and 343 K are illustrated in Figures 3.7 and 3.8. The solid curves represent calculated adsorption isotherms and the points denote the experimental data.

From the adsorption isotherms, it is clear that equation (3.3) provides a good fit of the experimental data of the equilibria measured for dibenzothiophene, dibenzofuran, fluorene and phenanthrene.

The adsorption isotherms are characterized by the slightly tailed-out maximum of Gibbs adsorption. They rise steeply and reach a maximum value at equilibrium concentrations of approximately 4-6 x 10^{-3} mole fraction for dibenzothiophene, fluorene and phenanthrene and 14 x 10^{-3} mole fraction for dibenzofuran. The adsorptivity of trinuclear aromatics from isooctane solution at 303 K and 343 K increased in the following order:

Phenanthrene < Dibenzofuran < Flourene < Dibenzothiophene

Separation Coefficients of Trinuclear Aromatics.

The separation coefficients, log f, of the trinuclear aromatic compounds dibenzothiophene, dibenzofuran, fluorene and phenanthrene is greater than 3 (see Table 3.4), which indicates that the interactions of adsorbate molecules with the cations of cavities of zeolite crystals are very strong. In particular, the organic sulfur compounds which possess two pairs of free electrons which have a high value of dipole moment (specific energy). For heterogeneous hydrocarbons, such as dibenzofuran, the adsorption bond between the oxygen atom in the ring of the aromatic compound and cations of the cavities of the porous crystals is weak with comparison with the one for the dibenzothiophene. This means that the interactions

between the heterogeneous compounds and zeolite crystals have a specific character. Actually the specific interaction energy arises from the interactions between the adsorbate molecules, which have dipole or quadrupole moments, and the electrostatic charges of the cations in the cavities of zeolite 13 X. Breck (1) attributed the adsorption interaction energies
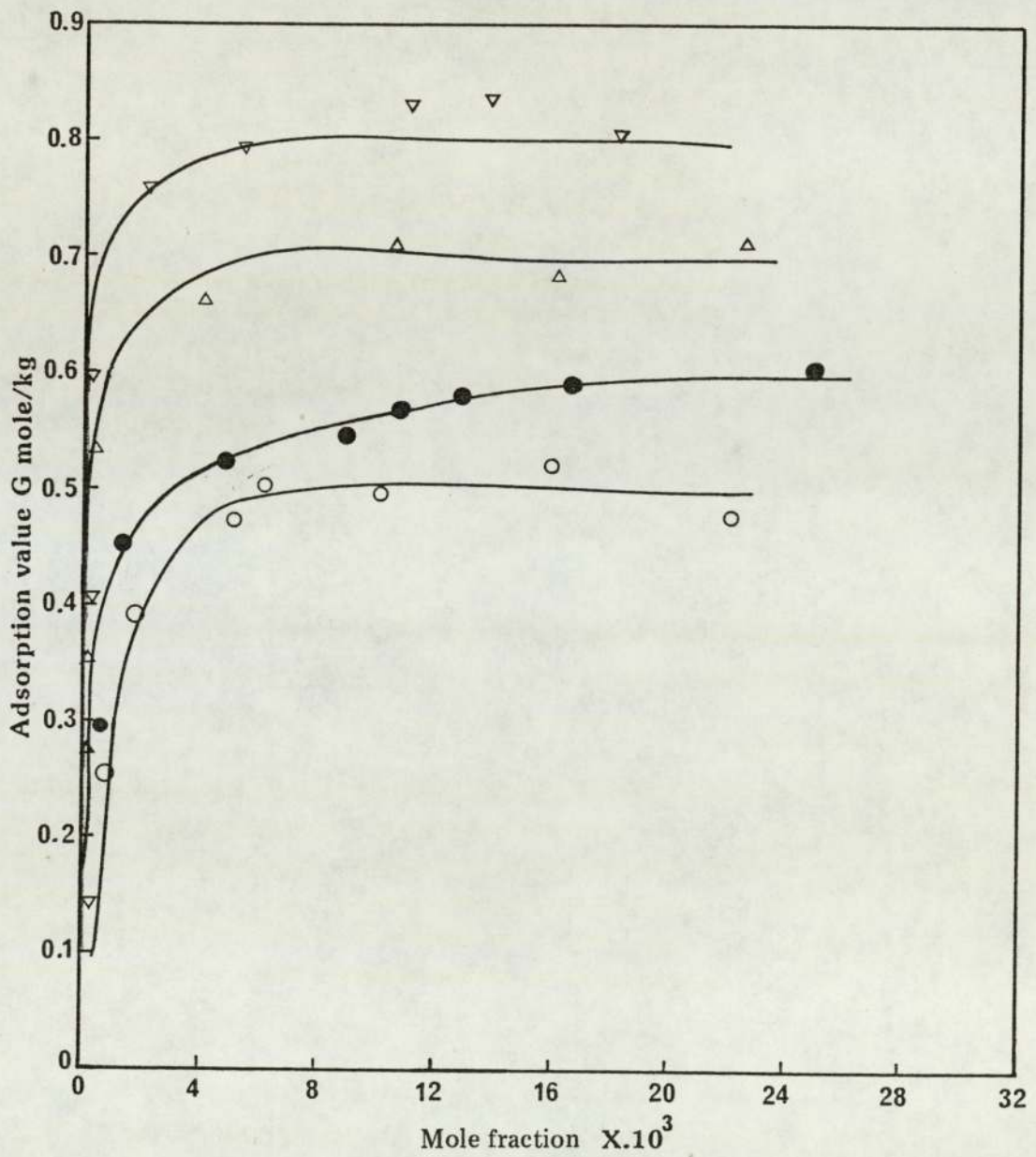
Figure 3.7 Adsorption Isotherms of
▽ Dibenzothiophene, △ Fluorene,
● Dibenzofuran and O Phenanthrene
on Pellets of Zeolite NaX (13X)
at 303 K.
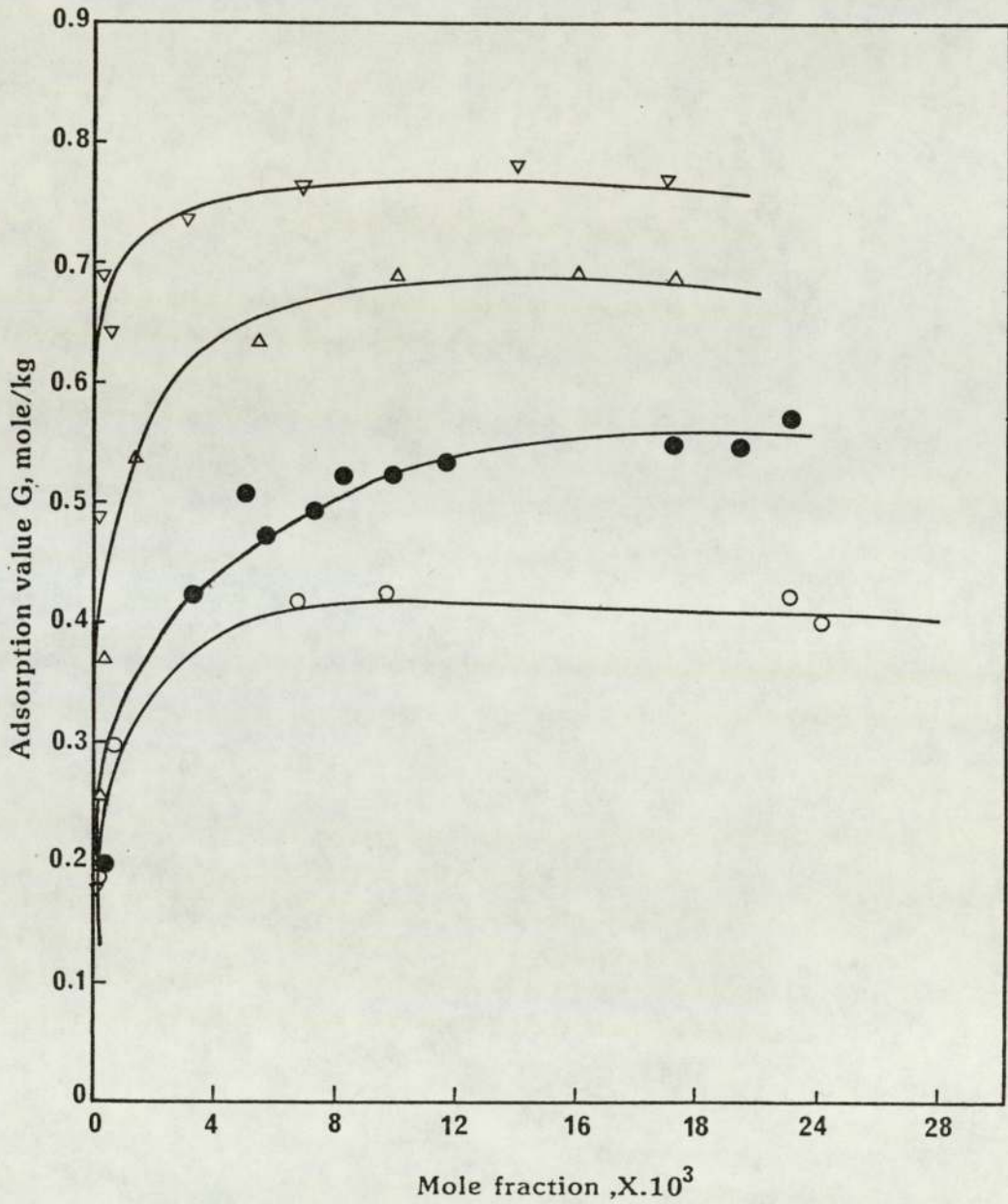
Figure 3.8   Adsorption Isotherms of
           ∇ Dibenzothiophene, △ Fluorene,
           ● Dibenzofuran and o Phenanthrene
           on Pellets of Zeolite NaX (13X)
                   at 343 K.

of oxygen and nitrogen organic compounds with the zeolites to cation qua-
drupole interactions. The presence of heterogeneous atoms in the organic
compounds (dibenzothiophene and dibenzofuran) causes a small difference in
the degree of separation coefficients at temperatures of 303 and 343 K.
This is demonstrated by the separation coefficients, log f, for dibenzo-
thiophene and dibenzofuran. The increase of the adsorption temperature
from 303 to 343 K does not significantly alter their separation coeffi-
cients.

The adsorption value of phenanthrene from the binary solution with
iso-octane was very low in contrast with other types of heterogenous
hydrocarbons and fluorene compounds. This is due to the steric effect
restricting migration of phenanthrene into the pores of the molecular
sieves. Adsorption of phenanthrene in the molecular sieves occurs mainly
as a result of the interaction of Π-electron density of the aromatic rings
with the cations, or the hydroxyl groups, at the cavities of the zeolite
crystals so that phenanthrene molecules are attached to the surface, or
within, the zeolite cavities. The separation coefficients, log f, for
phenanathrene and fluorene at 303 and 343 K are close.

Numbers of Molecules Occupied by Unit Cell of Zeolite Crystals of
Trinuclear Aromatics.

The numbers of adsorbate molecules occupied by unit cell of zeolite
crystals were,

	At 303 K	At 343 K
Dibenzothiophene	11.2	10.5
Flourene	9.7	9.2
Phenanthrene	6.8	5.6
Dibenzofuran	8.0	7.2

These data indicate that molar volume, forms and orientations are impor-
tant parameters which characterize the adsorption process. Adsorbed mol-
ecules of dibenzothiophene were distributed in the cavities of the zeolite
crystals more densely. The orientation factor for other compounds, such
as flourene, dibenzofuran, and phenanthrene has a sealing effect on the

distribution of the adsorbate molecules in the cavities of the molecular sieves. An increase in the molecular volume of the adsorbed molecule will result in a reduction in their packing density within the cavities of the molecular sieves. But the orientation effect and flexibility of the long alkyl chain can change these assumptions. The adsorption of high molecular weight aromatic hydrocarbons and heterogeneous compounds can be clarified as follows:-

The molecular sieve's specificity regarding the adsorbate molecules can be determined by the value of the different types of interactions: namely repulsion-interaction at small distances between the adsorbate molecules and the cations in the cavities of the zeolite crystals, dispersed attraction, and polarization of the local electrostatic fields of the cations of the molecular sieves crystals. The adsorbate molecules which exhibit a constant dipole moment, such as dibenzothiophene, can interact strongly with the electrostatic charge of the cations of the molecular sieves crystals. If the dipole moment does not exist in the adsorbate molecules, as in fluorene and phenanthrene, then the determining factor in the specificity of adsorption is the dispersed attraction energy. This energy is increased by increasing the number of zeolite cations which interact with the adsorbate molecules.

As shown in Table 3.4 the separation coefficients (log f) of aromatic hydrocarbons and heterogeneous compounds from solution with iso-octane at 303 K were in the order: dibenzofuran < dodecylbenzene < methylnaphthalene < cumene < dimethylnaphthalene < fluorene < phenanthrene < naphthalene < dibenzothiophene. At 343 K the maximum separation coefficient was also obtained with dibenzothiophene; the minimum separation coefficients were observed for cumene and methylnaphthalene.

An increase in temperature leads to an increase in the molar volume of adsorbate molecules μ given by,

$$\mu = \frac{Mol\ wt.}{\rho} \tag{3.9}$$

The product of μ (molar volume) and G (value of adsorption, mole/kg) gives the limiting adsorption volume, cm^3/g. The total volume of the large pore size for zeolite type NaX has been reported to be 0.296 cm^3/g (1).

The coverage or pore filling of the adsorbate molecules can be defined as the ratio between the limiting adsorbate volume and the total volume of the large pores of the molecular sieves. The number of molecules adsorbed by one gram of molecular sieves can be determined by multiplying the value of adsorption by the Avogadro's number.

The number of adsorbed molecules, N_A, per unit cell of molecular sieves can be calculated by

$$N_A = \frac{GN}{n} \tag{3.10}$$

The value of the limiting adsorption, and number of adsorbed molecules per unit cell are demonstrated in Table 3.5. At a temperature of 343 K, the number of adsorbed molecules of hydrocarbons, such as dodecylbenzene, cumene, naphthalene, 1-methylnaphthalene, 1,3-dimethylnaphthalene, dibenzothiophene and phenanthrene, decreased as a result of an increase in temperature. The lowest numbers of adsorbed molecules were for phenanthrene and dodecylbenzene. This indicated that molecules which have enough active energy can migrate through the cavities of zeolite crystals; conversely molecules, such as dodecylbenzene and phenanthrene at 343 K, diffused through the pores of the molecular sieves at low velocity because these hydrocarbons have insufficient activated energy to equal the diffusivity of the other hydrocarbons. Barrer and Ibbitson (2) and Breck (1) found that the apparent activation energy for diffusion in chabazite increased with chain length of the hydrocarbons. Hence, as would be expected, with an increase in temperature to 343 K, the number of adsorbed molecules per unit cell for the dodecylbenzene (5.1 molecules) was lower than for cumene (9.1 molecules/unit cell).

3.4 Conclusions

1. Type 13X molecular sieves exhibited a high affinity towards aromatic compounds. Those compounds having the smallest and most compact structure or lower molecular weight, and more polar compounds, were selectively adsorbed in preference to the compounds, of large critical molecular diameters, or with higher molecular weights, or molecules with long side chains.

2.   The equilibrium adsorptive capacity of the molecular sieves decreased with increasing temperature, over the temperature range studied.

3.   The maximum experimental values of adsorption, G, were approximately equal to the theoretical limiting adsorption values, A_m for each compound. The values of separation coefficient, f indicate that the individual aromatic molecules were strongly adsorbed by NaX zeolite.

4.0 A STUDY OF HEAT OF ADSORPTION OF INDIVIDUAL AROMATIC COMPOUNDS USING MOLECULAR SIEVES TYPE 13 X

The magnitude of the adsorption heat is a useful criterion for differentiation of the structure of the adsorbing molecules. The greatest values of adsorption heat observed in physical adsorption are for molecular sieves (zeolites) which arise from the interactions of active cations in zeolite crystals with adsorbate hydrocarbon molecules.

When molecules with π-bonds, as in aromatic hydrocarbons, or polar functional groups, or in heterogeneous compounds, are adsorbed by porous crystals of zeolite sieves, they interact very strongly with the exchange cations of zeolite cavities (31) and (32). The magnitude of this additional contribution to the total interaction energy depends on the type, charge, radius, position and concentration of the exchange cations, degree of decationization, type of zeolite, and chemical structure of adsorbed molecules. The particular features of the structure of importance are the nature of the π-bonds, the value and localization of dipole and quadrupole moments, and the presence of a free electron pair in the adsorbed molecule. In the present study changes of the heat of adsorption were investigated for different types of aromatic and heterogeneous compounds on X-type molecular sieves.

Usually all processes of physical adsorption are exothermic. For adsorption to take place the free energy change, ΔG must be negative from the thermodynamic relation.

$$\Delta G = \Delta H - T \Delta S \qquad (4.1)$$

The change in enthalpy, ΔH, is negative since the change in entropy, ΔS, is negative because the adsorbate molecules are in an ordered configuration. Three heats of adsorption are of relevance,

1. The isothermal integral heat of adsorption. This is the total heat involved in the adsorption process from zero adsorbate loading to some final adsorbate loading (filling rate) at a constant temperature.

2. The differential heat of adsorption. This is the change in integral heat of adsorption with a change in adsorbate loading. It is dependent upon pressure (or concentration), temperature, and adsorbate coverage or loading (1).

3.   The isosteric heat of adsorption is derived from adsorption isost-
     eres. It is obtained from a plot of the log of the concentration in
     mole fraction versus the reciprocal of the absolute temperature,
     $1/T$, at a constant adsorbate loading, a m^3/kg, by means of the
     Clausius-Clapeyron equation.

From pairs of isotherms at different temperatures (303 K and 343 K)
q^a_{iso} may be calculated by:

$$-\frac{\partial (\ln x)}{\partial \left(\frac{1}{T} \right)} = \frac{q^a_{iso}}{R} \tag{4.2}$$

Equation (4.2) can be written as,

$$q^a_{iso} = 18.8 \; \frac{T_1 - T_2}{T_2 \quad T_1} \; \log \; \frac{X_2}{X_1} \tag{4.3}$$

where T_1, T_2 are the adsorption temperatures, equal in this work to 303 K
and 343 K respectively, and X_1, X_2 are the equilibrium concentrations at
different temperatures and at constant adsorbate loading (a) for each
adsorbate hydrocarbon. The isothermal integral heat of adsorption can
also be obtained from isosteric heats. As shown in Figures 4.1 to 4.9, a
plot of logarithim of concentration log X versus $1/T$ gives a straight line
with a slope equal to q^a_{iso}/R at different fractional coverage from which
the limiting isosteric heat of adsorption can be calculated. Alterna-
tively, the isosteric heat of adsorption can be calculated from isotherms
using the Clausius-Clapeyron equation as shown in equation (4.2).

Figures 4.5 and 4.6 present isosters for 1, 3 dimethylnaphthalene and
for dibenzothiophene at three different temperatures 303, 323, 343 K, at
different fractional coverages.

The superscript a in equation 4.2 is an indication that the isosteric
heat of adsorption must be calculated at a fixed coverage of adsorption.
Thus, if q^a_{iso} is assumed to be independent of temperature, equation 4.2
suggests that a plot of lnX versus $1/T$ will give a straight line of slope
q^a_{iso}/R.
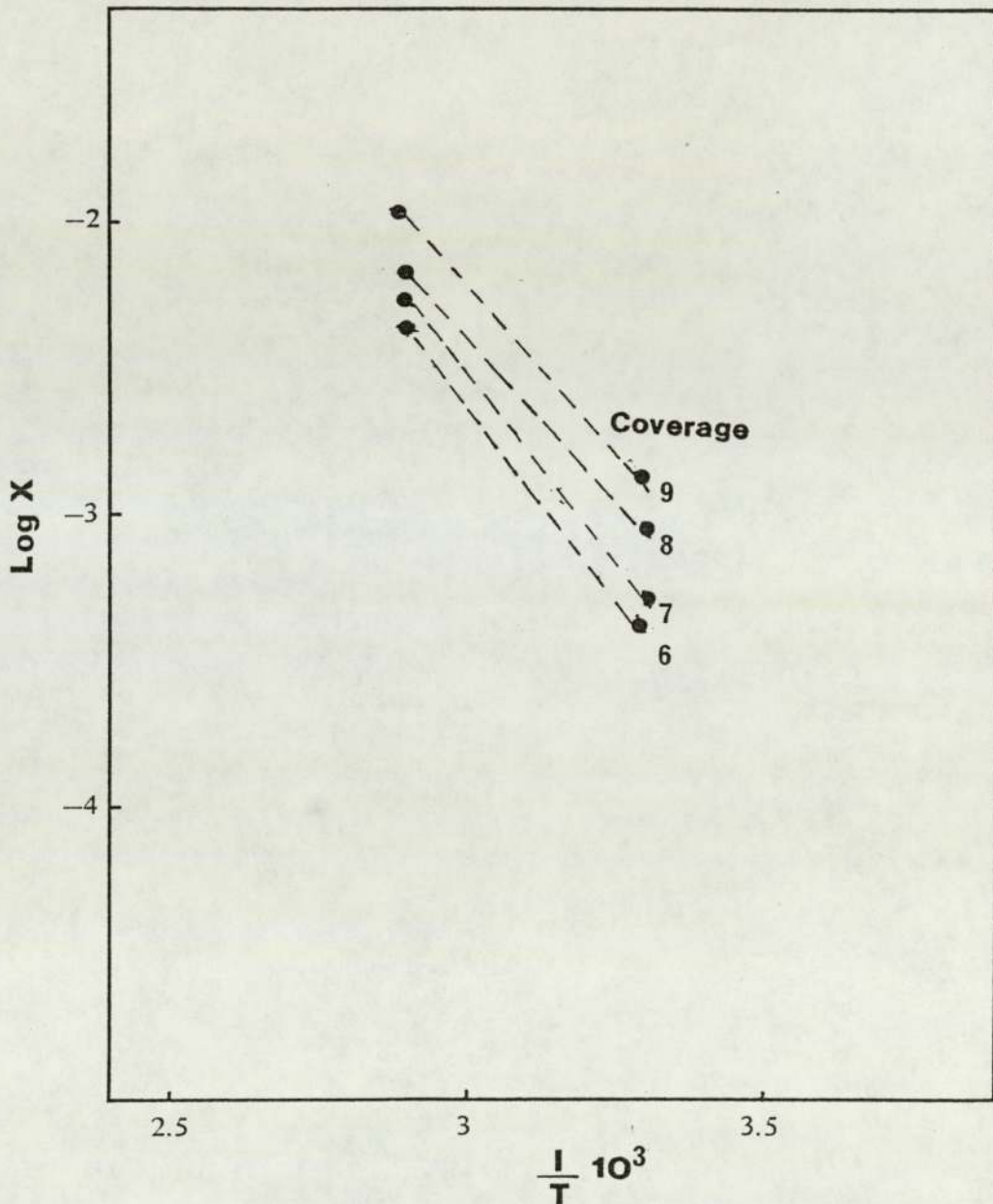
Figure 4.1   The Isosters for Cumene on
Molecular Sieves Type 13X
at Different Coverages
a x 10^{-5} m^3/kg.
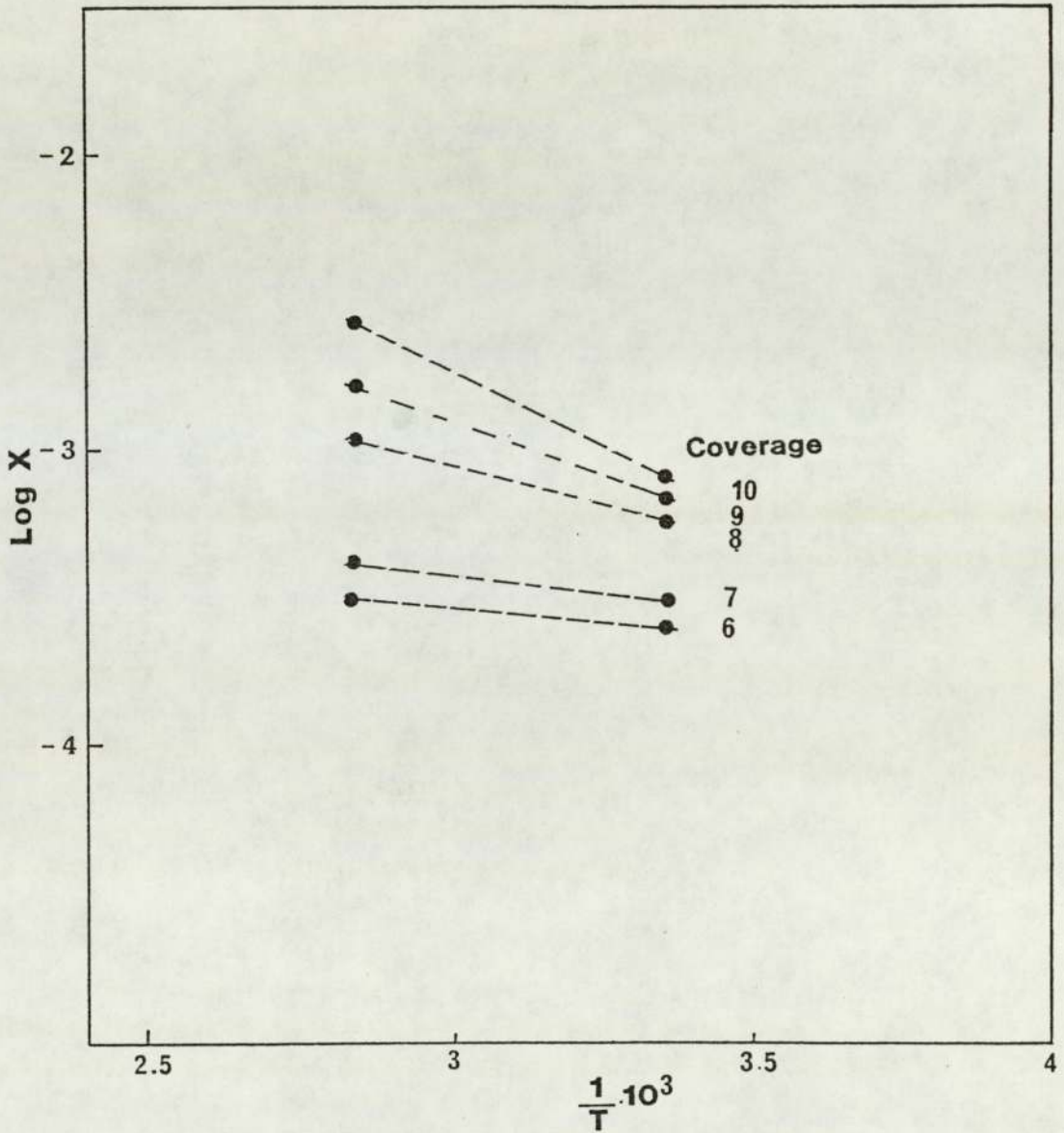
Figure 4.2   The Isosters for Dodecylbenene
on Molecular Sieves Type 13X
at Different Coverages
a x 10^5 m^3/kg.
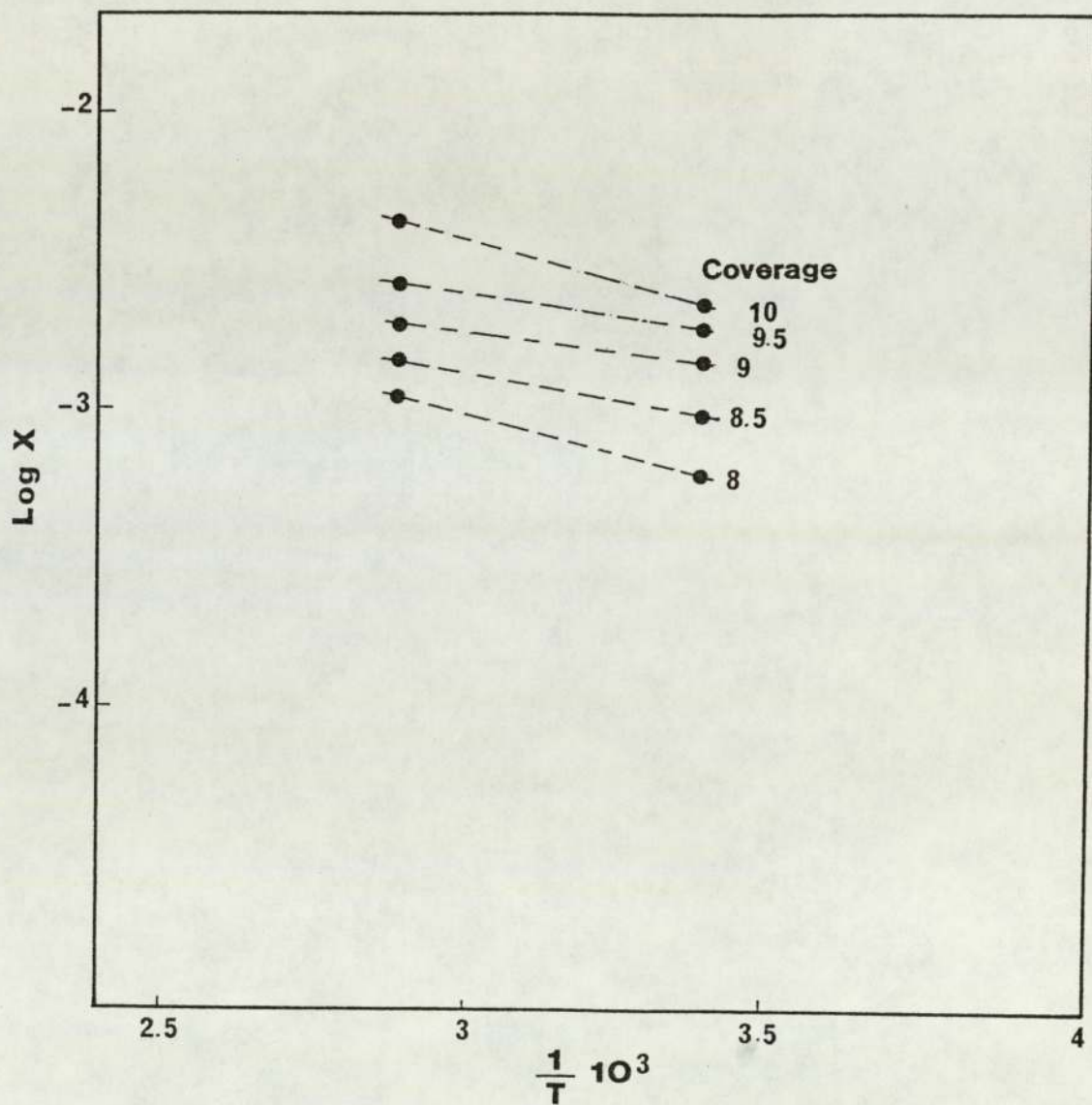
Figure 4.3   The Isosters for Naphthalene
             on Molecular Sieves Type 13X
             at Different Coverages
                a x 10^5 m^3/kg.
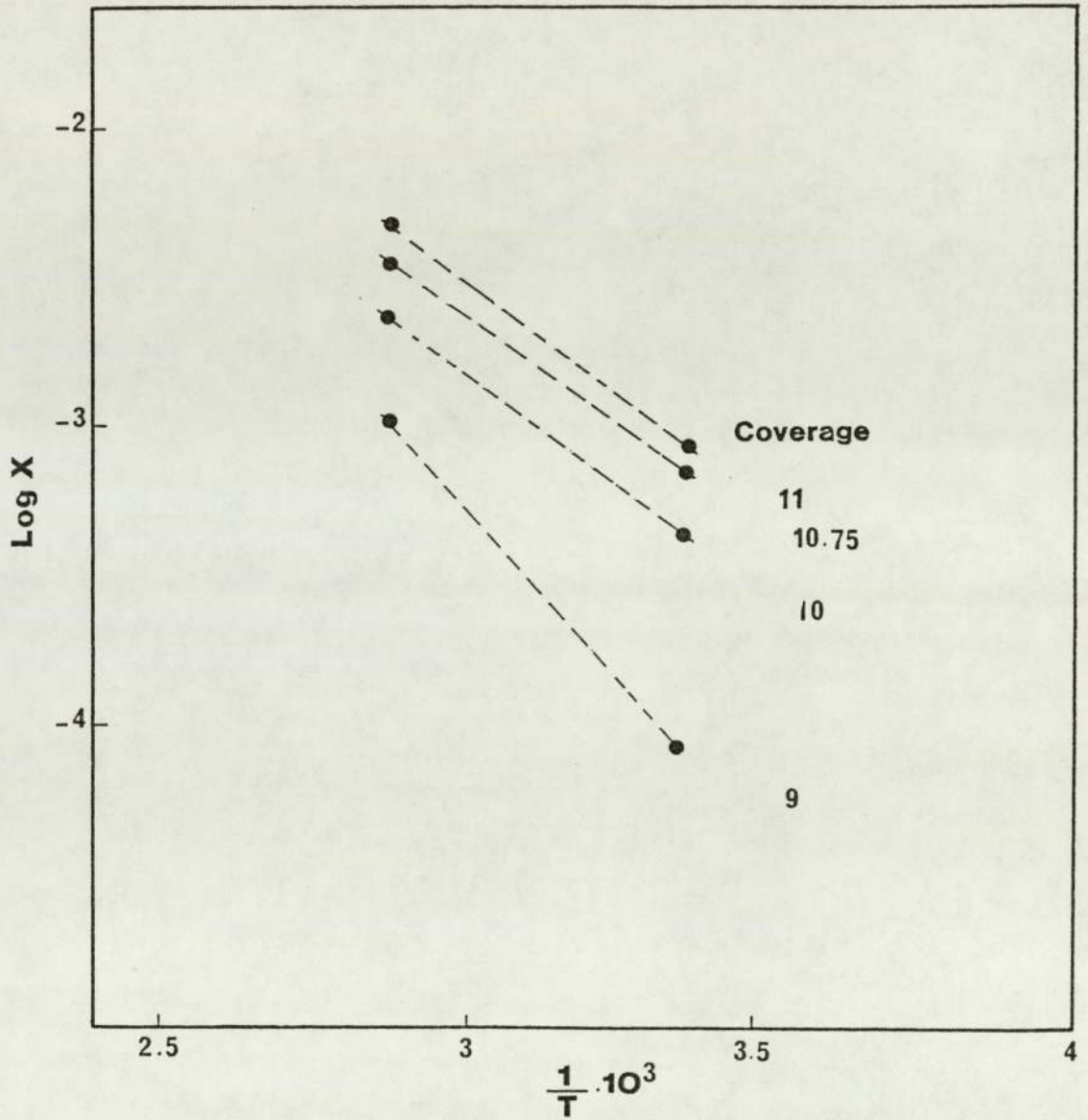
Figure 4.4   The Isosters for 1-Methylnaphalene on
              Molecular Sieves Type 13X at Different
              Coverages a x 10^5 m^3/kg.
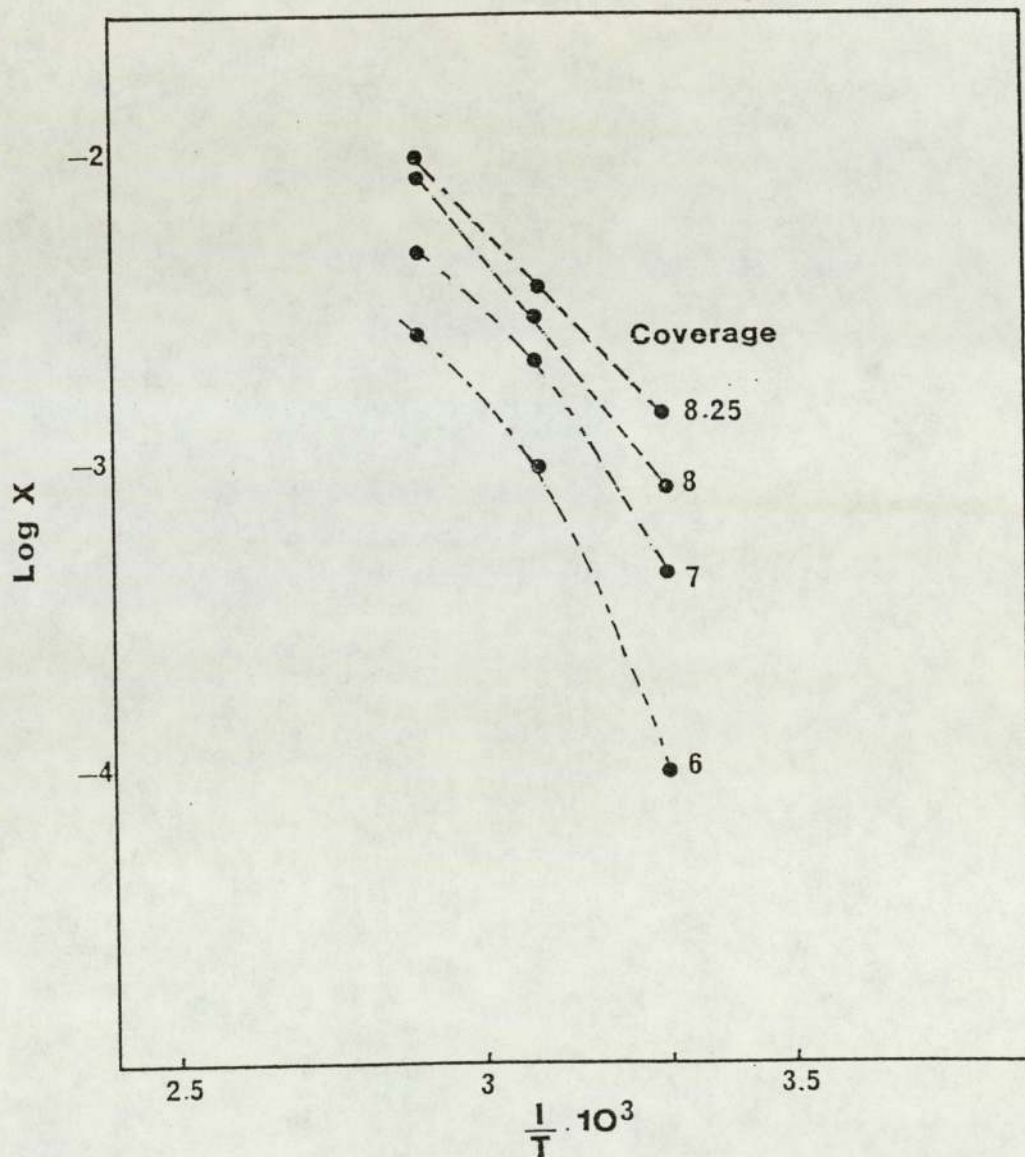
Figure 4.5   The Isosters for 1, 3-Dimethyl-
naphthalene on Molecular Sieves
Type 13X at Different Coverages
a x 10^5 cm^3/kg.
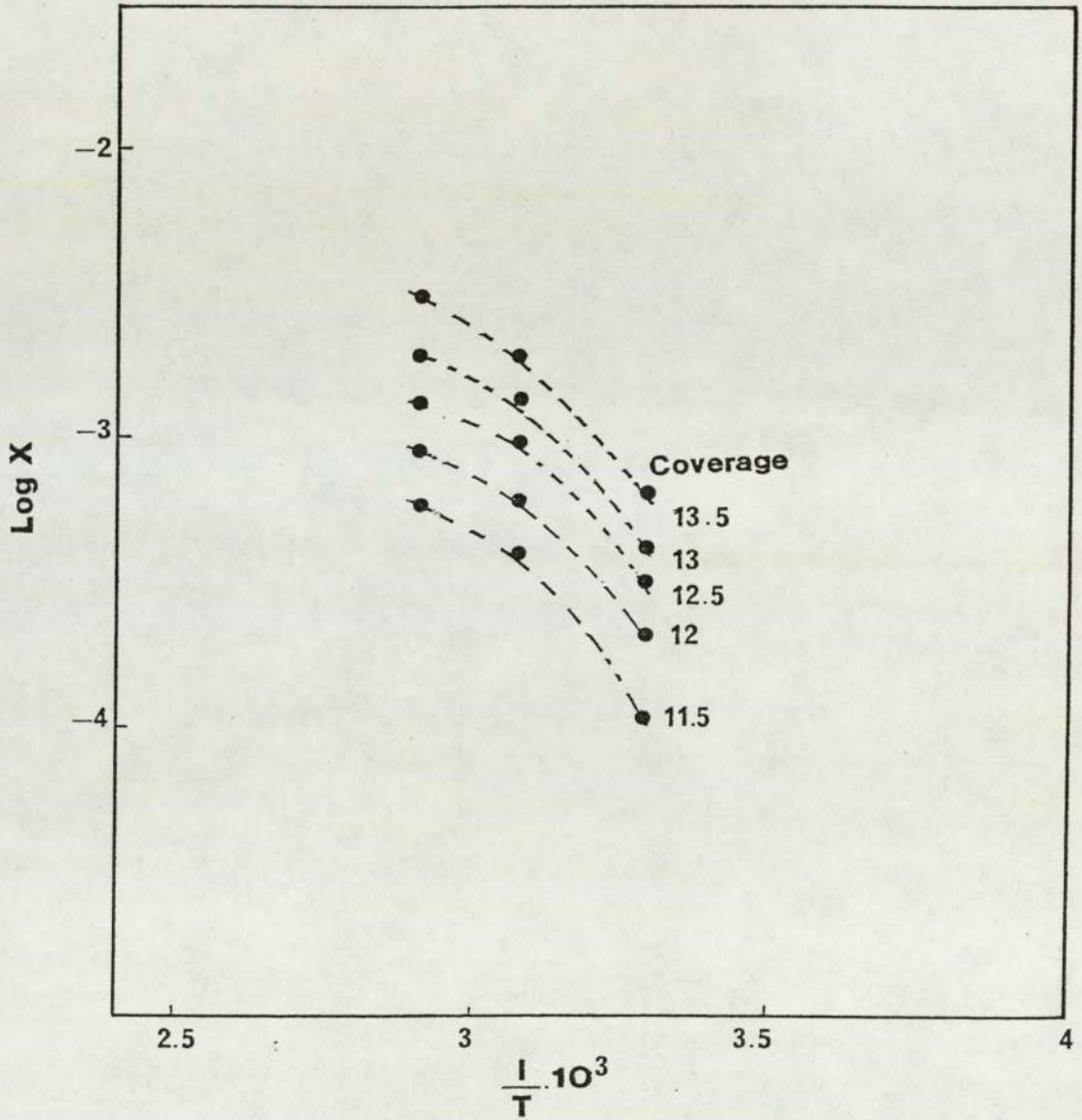
Figure 4.6   The Isosters for Dibenzothiophene
on Molecular Sieves Type 13X at
Different Coverages
a x 10^5 m^3/kg.
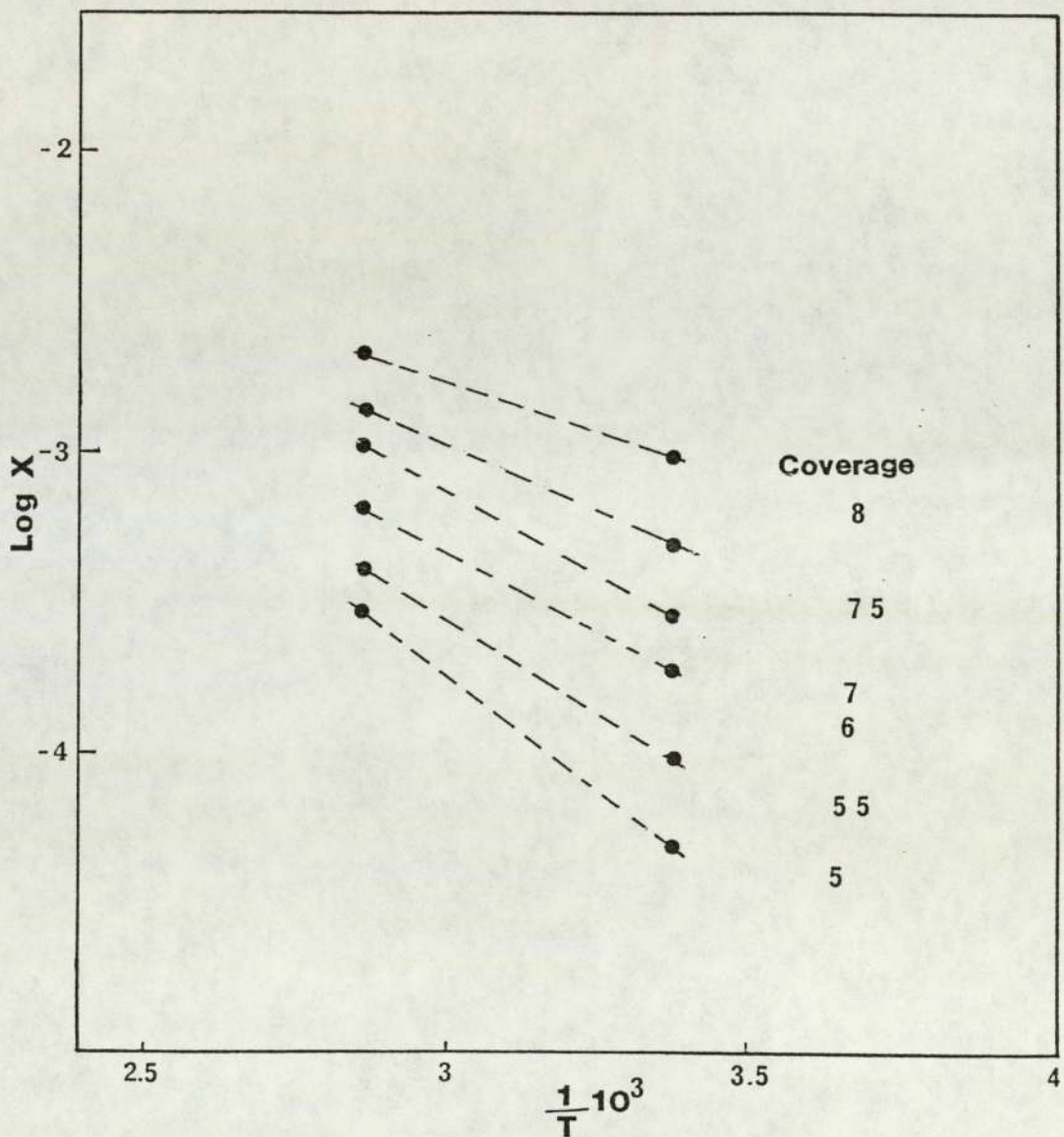
Figure 4.7   The Isosters for Flourene on Molecular
Sieves Type 13X at Different Coverages
a x 10^5 m^3/kg.
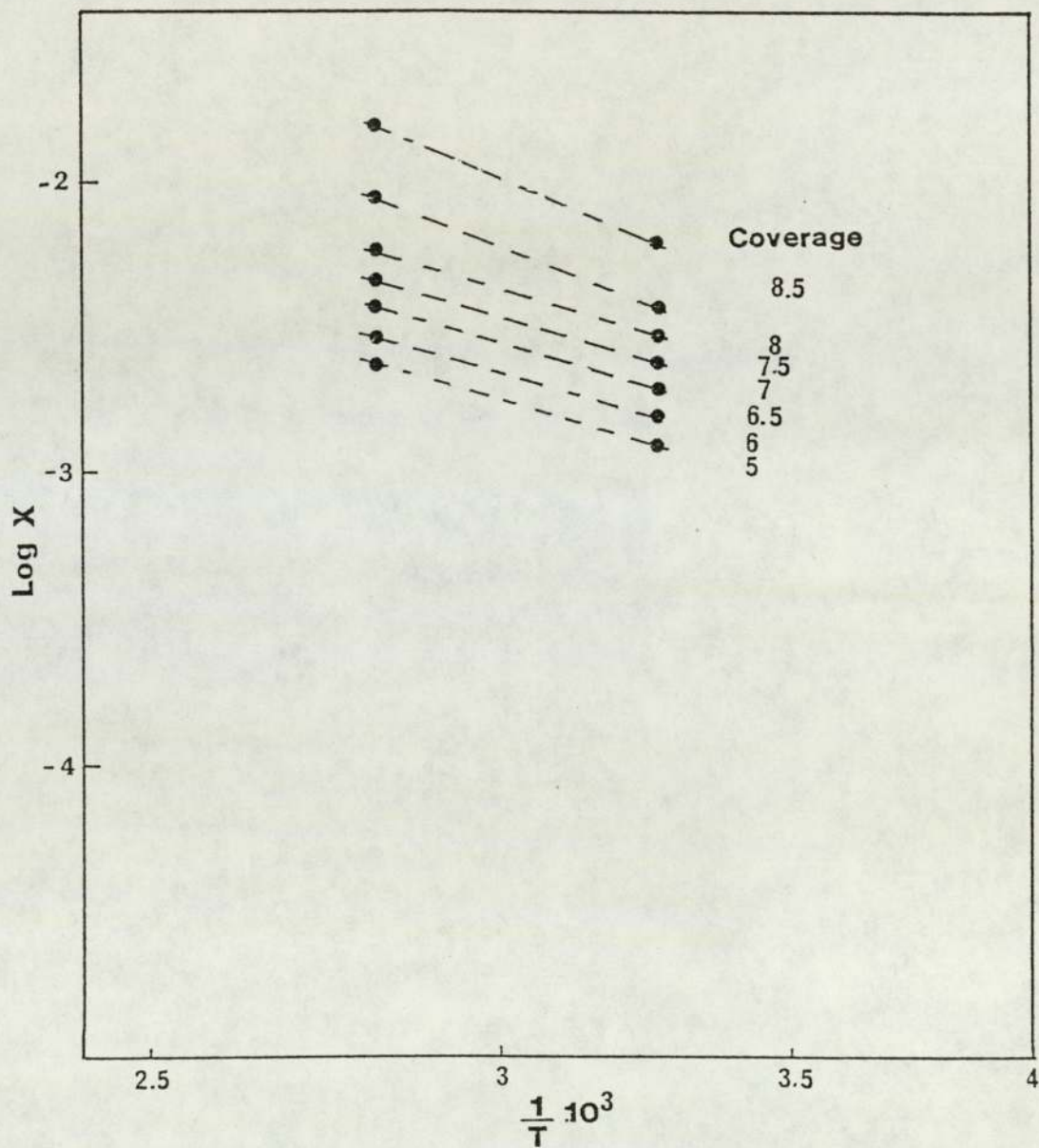
Figure 4.8   The Isosters for Dibenzofuran
on Molecular Sieves Type 13X
at Different Coverages
a x 10^5 m^3/kg.
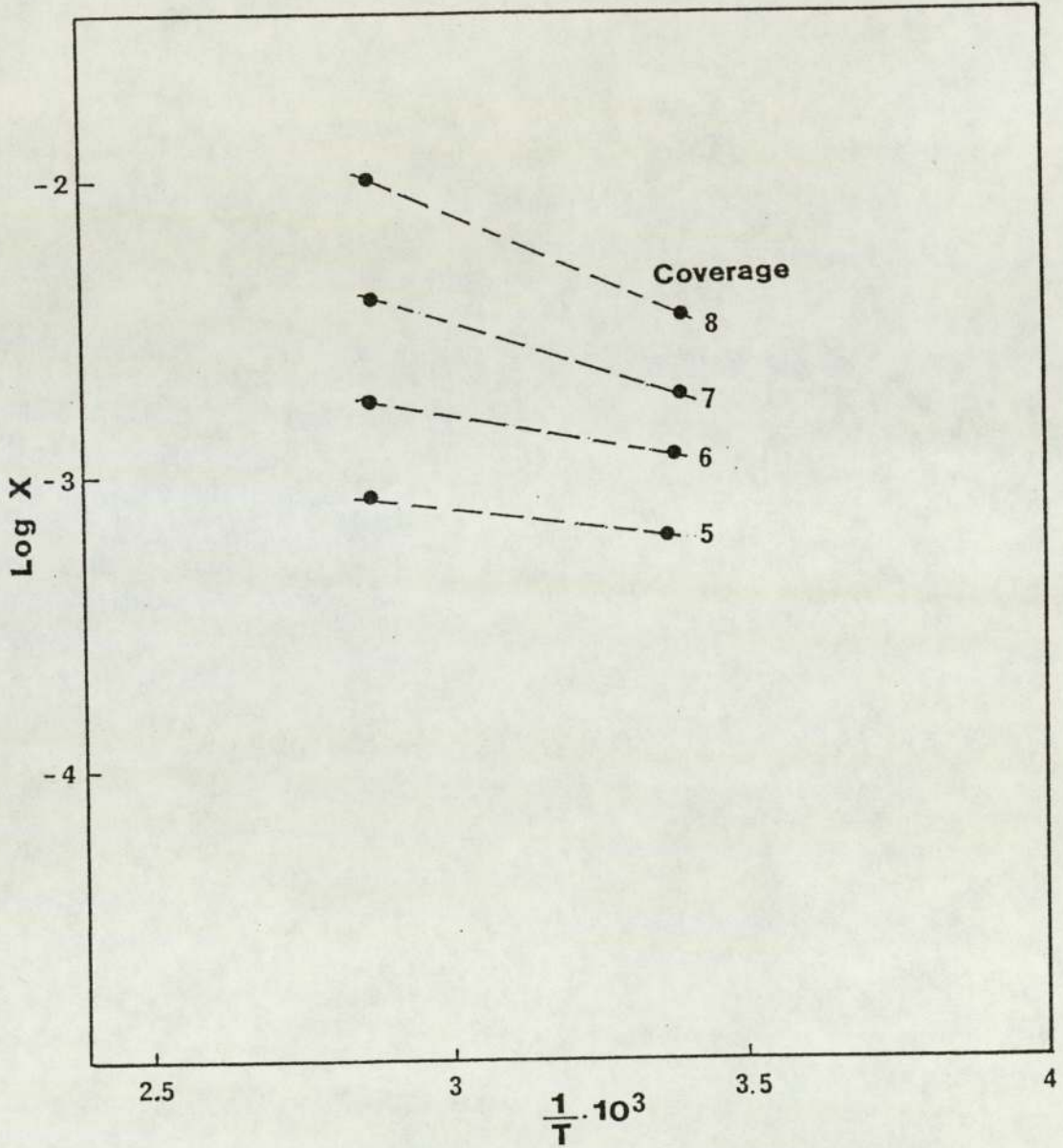
Figure 4.9   The Isosters for Phenanthrene
on Molecular Sieves Type 13X
at Different Coverages
a x 10^5 m^3/kg.

Figure 4.10 is a plot of the calculated isosteric differential heats of adsorption as a function of the coverage. This shows that isosteric heat curves for cumene and dodecylbenzene increase monotonically up to coverage 11×10^{-5} m^3/kg.

The corresponding values of isosteric heat obtained using equation 4.3 and Figure 4.10 show that the interaction energies between the adsorbate molecules of cumene and dodecylbenzene with cations of zeolite crystals were greater than those between the iso-octane molecules and the cations of zeolite crystals. The energy required to leach-out the iso-octane molecules from sites within molecular sieves using the adsorbate molecules of cumene and dodecylbenzene in the range of low concentrations was 26.25 kJ/mole and 4.2 kJ/mole respectively. Hence the adsorbate molecules of cumene interacted with cations of zeolite crystals more strongly than dodecylbenzene molecules. The increase in isosteric heat of adsroption for cumene is due to the strong interactions between the π-bond of the cumene and electrostatic charges of the molecular sieves. Increase in the length of the alkylchain attached to the benzene ring will weaken the π-bond of the benzene ring, and result in weakening of the interactions between the adsorbate molecules and eletrostatic charges of the molecular sieves.

In addition to the interaction energies between the π-bonds of adsorbate molecules and the molecular sieves, there are other types of the interaction at maximum coverage rate of the cumene and dodecylbenzene e.g. dispersion energies of interaction and repulsion interaction over a small distance between the adsorbate molecules. The increase in the isosteric heat of adsorption with coverage has been attributed not only to adsorbate-adsorbent interactions but also to mutual interactions between the adsorbate molecules (33), (1). Dubinin (34) also found that after filling the adsorbent centres by adsorbate molecules such as cyclohexane, benzene, and n-pentane, a free space may remain in the zeolite cavities for adsorption as a result of the manifestation of both dispersion forces, (adsorbent-adsorbate-interaction) and the forces of interaction between the adsorbate molecules themselves which are influenced by the force adsorbent field.

Figure 4.11 shows the dependence of isosteric heat of adsorption on the coverage for different types of hydrocarbons, viz, naphthalene,
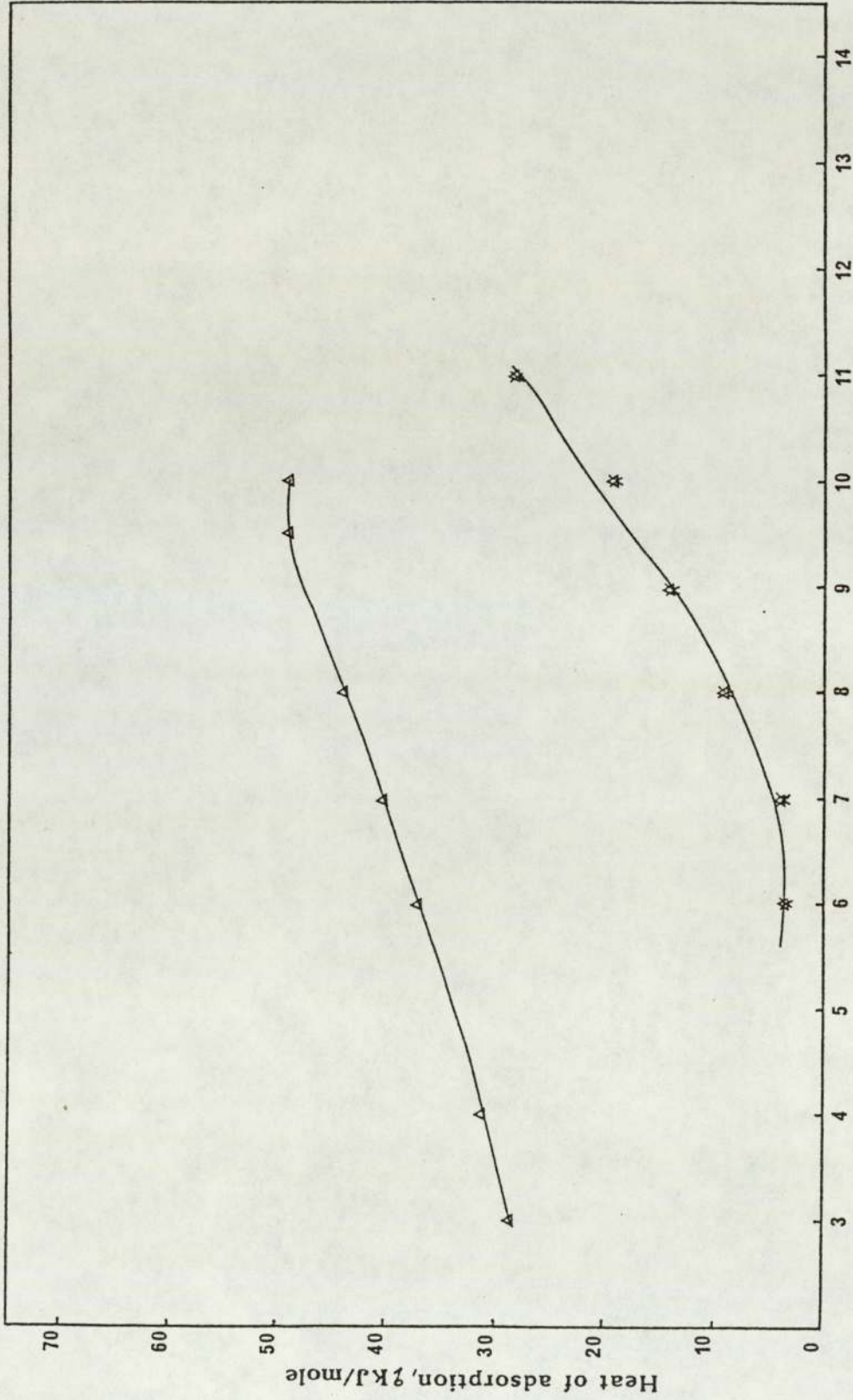
Figure 4.10 The Relationship Between the Isosteric
Heat of Adsorption and Coverage
on Molecular Sieves for
△ Cumene and ✳ Dodecylbenzene.

1-methylnaphthalene and dimethylnaphthalene. The maximum heat of adsorption was for 1-methylnaphthalene, and the lowest for naphthalene; dimethylnaphthalene had an intermediate value of heat adsorption. The isosteric heat of the naphthalene group decreased with increase in the coverage of adsorption, because the most active sites of the molecular sieves had been filled and addition of further molecules resulted in weakening adsorbent-adsorbate interaction. The behaviour of the dimethylnaphthalene was different since continued increase in the pore filling resulted in a further increase in the isosteric heat. This second stage increase in the isosteric heat is explainable in terms of adsorbate-dispersion interaction, i.e., adsorbate-adsorbate interactions influenced by the electrostatic charge field of the molecular sieves. Orientation of the dimethylnaphthalene molecules also has an effect on the increase in the isosteric heat with increase in the loading (filling). In this case orientation assists adsorbate-adsorbate interactions.

The observed behaviour of the isosteric heat with the level of adsorbate loading, or coverage, of different aromatic hydrocarbons corresponds in general with that reported by previous investigators. Khudieve (35), reported differential heats of adsorption for benzene and toluene at coverages of 50×10^{-5} and 40×10^{-5} m^3 STP/kg respectively on molecular sieves 13X; the calculated values of the isosteric heats were 73 and 77.28 kJ/mole respectively. This demonstrates that addition of the alkyl group to the benzene ring leads to an increase in the heat of adsorption. Furthermore it confirms that the results of previous workers are similar to those obtained in this study for adsorption of naphthalene group compounds on molecular sieves type NaX.

Figure 4.12 illustrates the relationship between the isosteric heat of adsorption and the coverage for the trinuclear aromatic hydrocarbons fluorene and phenanthrene, and the heterogeneous compounds dibenzothiophene and dibenzofuran. The fluorene molecules exhibit a maximum heat of adsorption at the lowest coverage rate. An increase in the filling results in a decrease in the heat evolved because the most active sites of the zeolite have been filled and the addition of further molecules appears to result in weaker adsorbate-adsorbent interaction energies.

The differential heat of the phenanthrene as a function of adsorption loading behaves in a similar manner initially to fluorene, i.e., the ini-
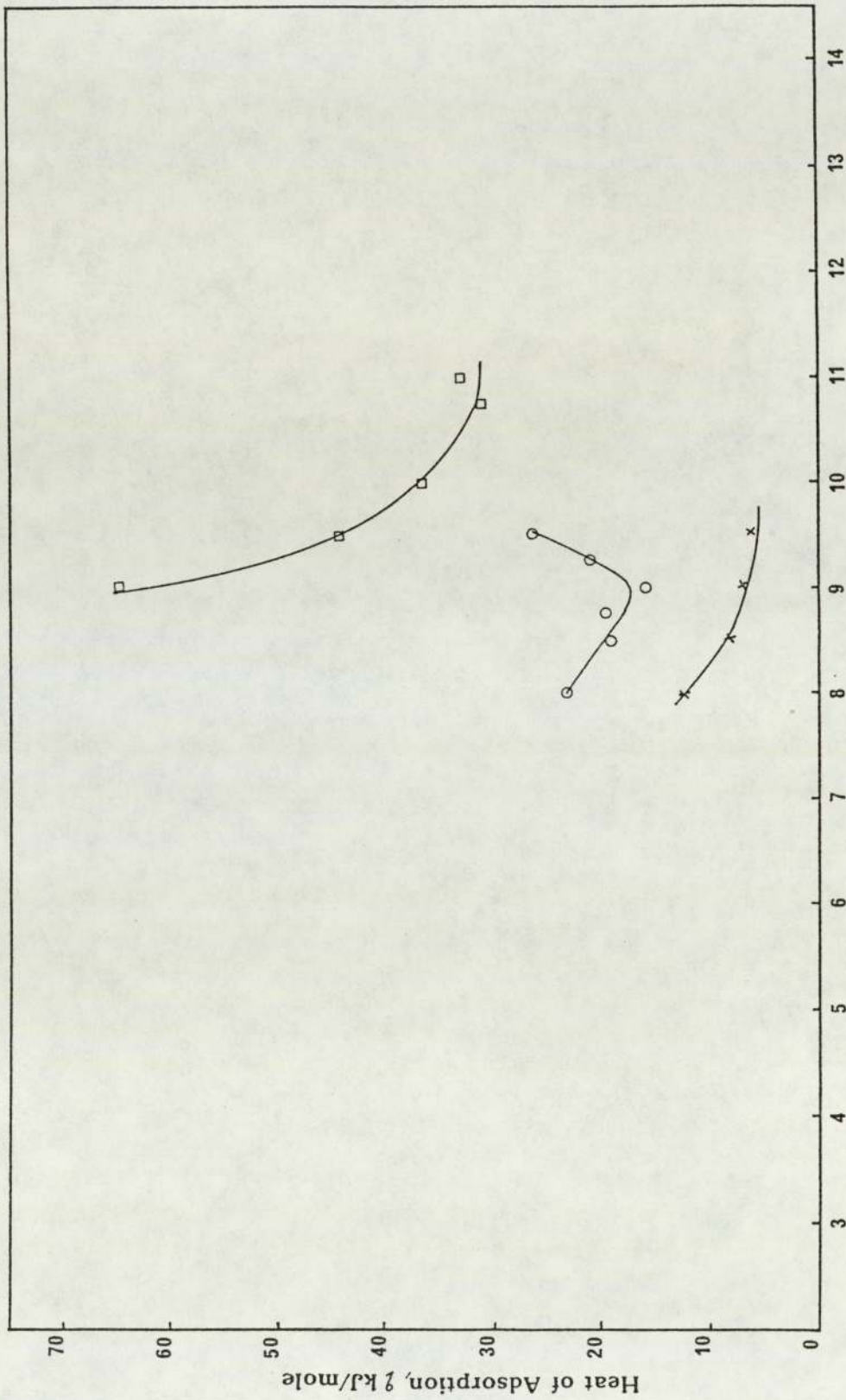
Figure 4.11 The Relationship Between the Isosteric Heat of Adsorption and Coverage on Molecular Sieves for x Naphthalene, □ 1-Methylnaphthalene and o 1-3-Dimethylnaphthalene.

Coverage, $a.10^5$ m^3/kg

Heat of Adsorption q kJ/mole

tial heat is high but drops off to a minimum. Further increase in the loading results in the isosteric heat increasing to a maximum as the pore volume of the molecular sieves becomes filled. In this instance, the maximum is the result of mutual interaction between the phenanthrene molecules. Since fluorene has a more symmetrical configruation than phenanthrene, orientation of the fluorene molecules is more easily accomplished and the interactions between the adsorbate molecules of fluorene with electrostatic charges of molecular sieves will consequently be higher. The magnitude of the isosteric heats of adsorption and their variation with the level of adsorbate loading or coverage have been studied by previous workers. Barrer (36) found that the differential heats of adsorption at coverage rate of 50% were 73.5 and 77.7 kJ/mole for benzene and cyclopentane on NaX respectively. This demonstrates that the geometrical structure and symmetricity had an effect on the heat of adsorption, similar to that noted in the present work with phenanthrene and flourene adsorbed molecules.

The variation in isosteric heat of adsorption with loading for the heterogeneous aromatic compounds dibenzothiophene and dibenzofuran is exemplified in Figure 4.12. Two effects are shown for dibenzofuran,

i.   a high initial heat of adsorption, characteristic of the cation quadrupole interactions plus interactions of the π-bond of aromatic nuclei with electrostatic charges of the cation cavities of zeolite crystals and

ii.   a minimum followed by a maximum heat of adsorption with increase in loading.

The following increase of the isosteric heat is due to interaction between the adsorbate molecules. The magnitude of the decrease in the isosteric heat of adsorption accompanying an increase in loading arises because the most active centres of the molecular sieves have been filled. The addition of more molecules leads to an increase in the isosteric heat due to interaction between the adsorbate molecules. The magnitude of the increase in isosteric heat for dibenzofuran is attributable to a strongly directional interaction between the eight dibenzofuran molecules within each unit cell. The increase in the heat of the adsorption for dibenzofuran is related to the strong specific interactions which can be formed from an additional hydrogen bond with negatively-charged oxygen atoms of
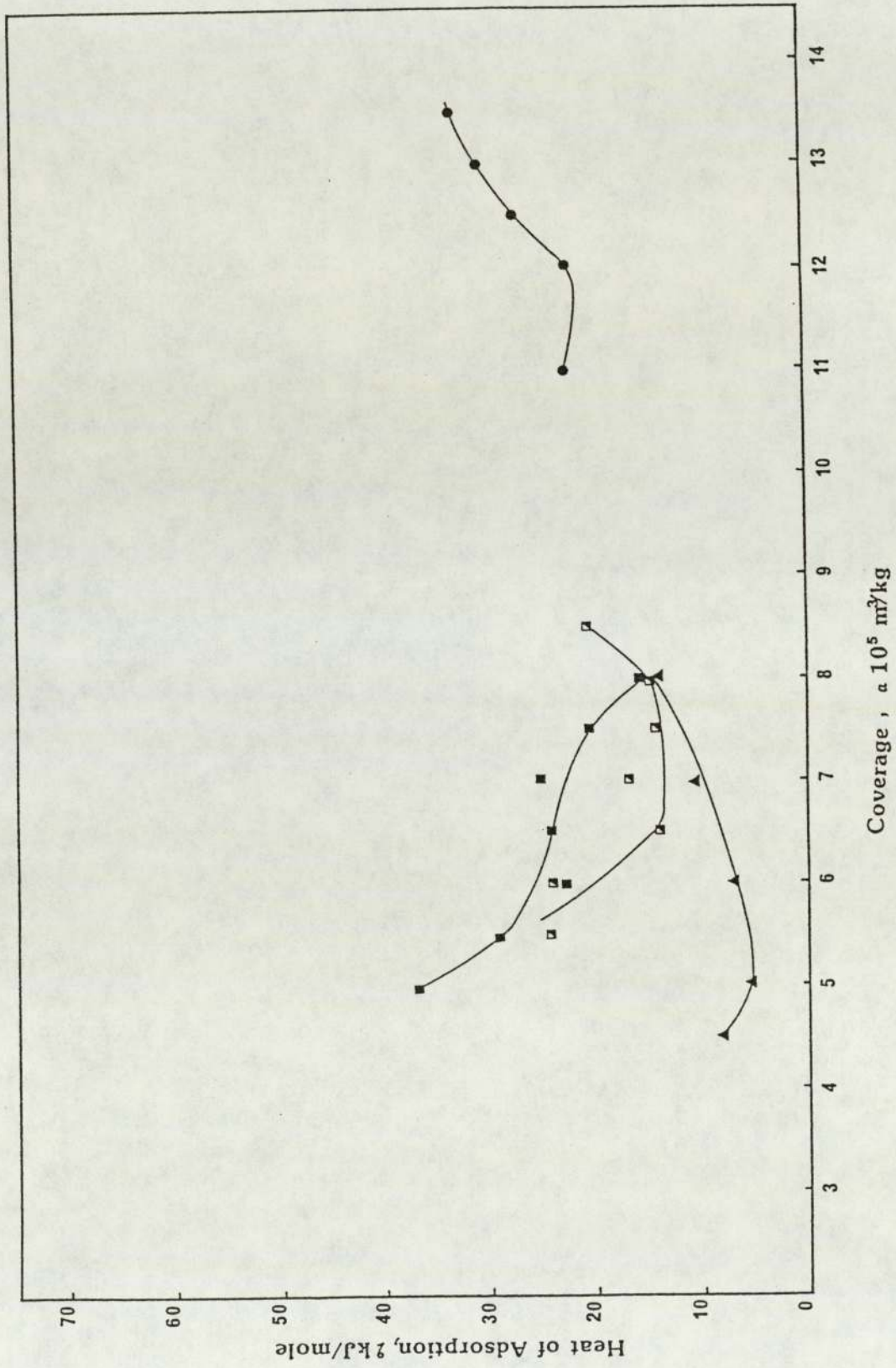
Figure 4.12 The Relationship Between the Isosteric
Heat of Adsorption and Coverage
on Molecular Sieves for
▲ Phenanthrene,   ● Dibenzothiophene,
■ Fluorene and   ◨ Dibenzofuran.

the zeolite structure. The conjugation of the electrons of the oxygen atom with π-bond in dibenzofuran molecule causes a more uniform distribution of the electron density in this molecule. Heats of adsorption for dibenzothiophene are larger than for dibenzofuran and the molecular sieves show a greater affinity for the dibenzothiophene molecules. The isosteric heat of adsorption for dibenzothiophene was calculated at a high loading rate. At low coverage the adsorbate molecules of the dibenzothiophene are localized in the cavities of the molecular sieves. As the cavities of the zeolite crystals are filled with dibenzothiophene molecules, the filled surface will acquire more energy due to the quadrupole interactions and the interactions between the π-electron system of aromatic rings with the cation or the hydroxyl groups of zeolite crystals. The increase in the coverage will also result in a mutual interaction between the adsorbate molecules of dibenzothiophene.

A particular example is the adsorption of different type of components such as carbon dioxide provided by Kiselev (33). The effect of isosteric heat of adsorption for carbon dioxide was studied as a function of adsorption loading. It was observed that the isosteric heat of adsorption behaved in a similar manner in the present work, i.e., the initial heat was high, decreased to a minimum, then rose to a maximum as the pore volume became filled. The last maximum was the result of mutual interaction between four carbon dioxide molecules within one cavity of the structure of the molecular sieves.

Figure 4.13 shows the relationship between the isosteric heat of adsorption versus coverage for all the aromatic components studied. The lowest heat of adsorption at 3-5 x 10^5 m^3/kg i.e. at low coverage was for dodecylbenzene and phenanthrene, whilst at high coverage 14 x $10^5 m^3$/kg the highest heat of adsorption was for dibenzothiophene.

4.1 Conclusions

Heats of adsorption of pure aromatic compounds on NaX zeolites were calculated. The data show that the most important criteria affecting the interaction between the adsorbate molecules and the cations in the zeolite crystals are the nature of the π bonds, the value and localization of dipole or quadrupole moments, and the presence of a free electron pair in the adsorbed molecule.
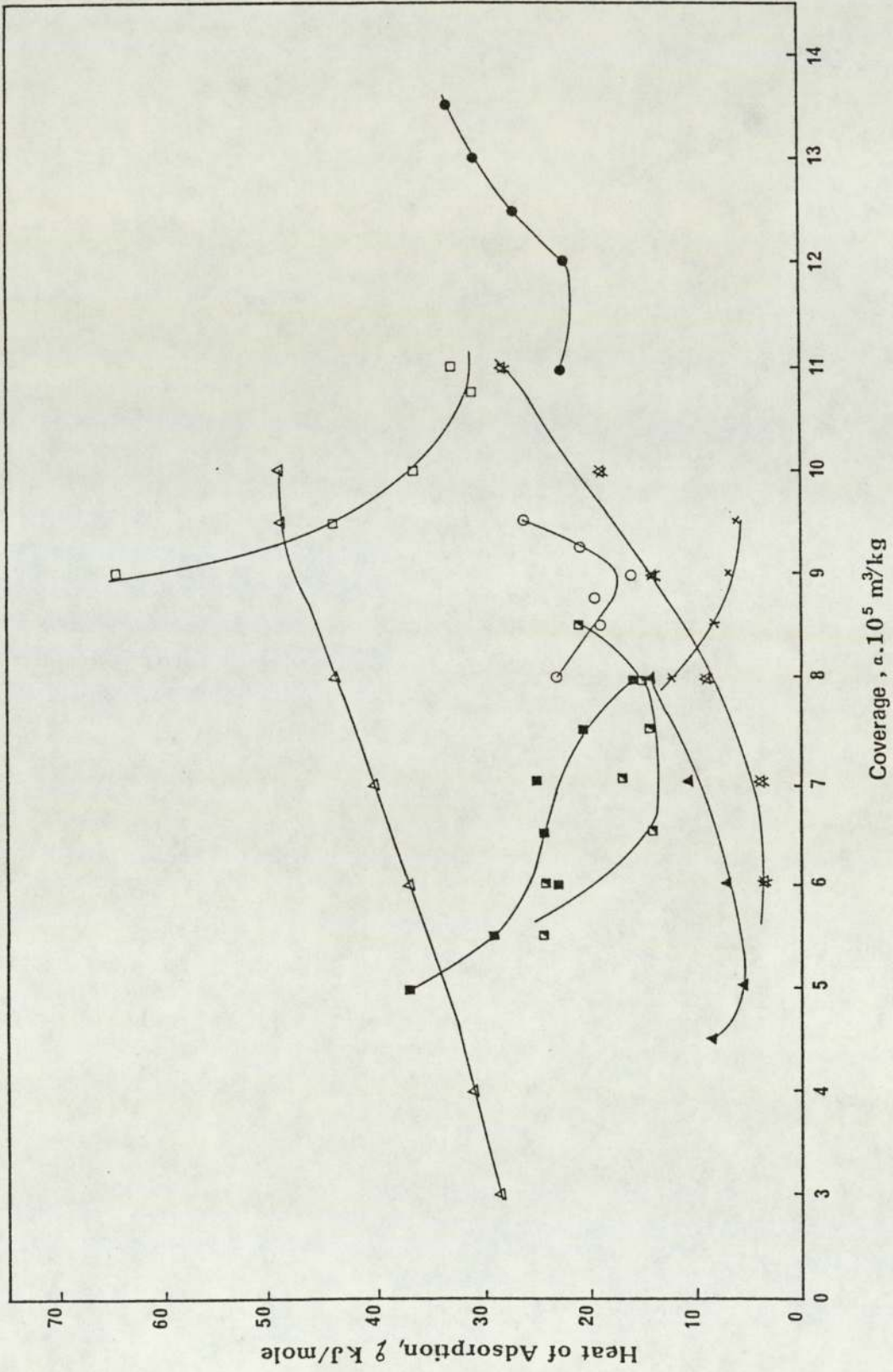
Figure 4.13 The Relationship Between the Isosteric Heat of Adsorption and Coverage of Molecular Sieves for ✹ Dodecylbenzene, △ Cumene, ✕ Naphthalene, ☐ 1-Methyl-naphthalene, ○ 1-3-Dimethylnaphthalene, ⬭ Dibenzofuran, ▲ Phenanthrene, ● Dibenzothiophe and ■ Fluorene.

5.0 A STUDY OF EQUILIBRIUM ISOTHERM ADSORPTION OF AROMATIC MIXTURES (EXTRACT FRACTIONS) FROM BINARY SOLUTIONS WITH ISOOCTANE

5.1 Introduction

The adsorption properties of porous crystals of molecular sieves, and in particular their faculty for adsorption from liquid solutions, depends upon the concentration and nature of the components, upon the composition and structure of the molecular sieves, and upon temperature.

Adsorption of individual aromatic and heterogeneous compounds from iso-octane results in selective adsorption from solutions of those molecules whose sizes are smaller than the windows of the zeolite channels. This ability to adsorb molecules according to their geometry leads to high selectivity of separation of many liquid mixtures. If, however, molecules can freely penetrate into zeolite cavities adsorption will be determined by interaction of these molecules with zeolite.

Zeolite type 13X (NaX) is a specific adsorbent capable of strong selective adsorption of heterogeneous and aromatic compounds of high molecular weight. This property was utilized to study the relationships between Gibbs adsorption of extract fractions and their initial mole fractions. Equilibrium isotherms were determined for 3 extract fractions at two different temperatures 303 and 343 K.

The heats of adsorption of extract fractions using the same type of molecular sieves were determined by the isosteric method.

5.2 Experimental Procedure

The literature contains a considerable amount of multicomponent adsorption data for inorganic gases. The bulk of the published data deal with mixtures of organic vapours or inorganic adsorbates at liquid nitrogen temperatures (90 K).

Joubert and Zwiebel (37). studied the adsorption isotherms of oxygen, nitrogen, carbon dioxide, and sulfur dioxide as a mixture on hydrogen-mordenite at several temperatures in the range of 273-373 K. SO_2 and CO_2 were found to exhibit considerably greater affinity for the adsorbent than O_2 and N_2.

As already discussed molecular sieves have a high affinity to adsorb standard, individual aromatic compounds. Their advantage in industrial applications is in removing impurities, e.g. aromatic compounds, from waxes resulting from dewaxing of the slack wax after extraction of heavy distillates to produce different types of lubricating oils.

To study the effect of adsorption of aromatic mixtures from binary solution with waxes, aromatic mixtures (extracts) were prepared by extraction of petroleum heavy distillate (623-753K) with phenol. 5% of water in phenol (12.5g H_2O in 237.5g phenol) was added to 125 g of a heavy distillate cut and mixed by stirring at 328K (above the aniline point of the cut). The mixture was left to settle for 3.6 ks. Two layers separated: a top layer (raffinate) and a bottom layer (extract). The raffinate layer was washed several times with 10% NaOH solution and finally dried overnight using calcium chloride granules. The extract layer was washed with 300 cm^3 of dichloromethane CH_2Cl_2 and 800 cm^3 of 10% NaOH and left to settle for 1.8 ks. The bottom layer was then recovered and washed several times with 250 cm^3 of NaOH, then with water. Finally CH_2Cl_2 was removed by evaporation in a rotary vacuum evaporator to obtain the free extract which was then dried over-night using calcium chloride. The extract was vacuum distilled to yield three fractions,

Extract Fraction 1, boiling point range 633 - 653 K

Extract Fraction 2, boiling point range 673 - 693 K

Extract Fraction 3, boiling point range 713 - 747 K

Standard methods were used for the determination of the physico-chemical properties of the aromatic extraction fractions given in Table 5.1. Using Van Ness and Van Westen's method (38) the structural groups of the aromatics extract fractions were determined and are illustrated in Table 5.2.

TABLE 5.1
PHYSICO-CHEMICAL PROPERTIES OF DIFFERENT TYPES OF AROMATIC
EXTRACT FRACTIONS

Test Required	Reference No.	Units	Extract Fraction 1	Extract Fraction 2	Extract Fraction 3
Boiling point range			633-653 K	673-693 K	713-747 K
Density at					
303 K	IP160 or 190	kg/L	0.9977	1.0154	1.0493
343 K			0.9707	0.9884	1.0223
Refractive index at 293K	D 1747	-	1.5682	1.5808	1.6002
Kinematic vis. at 373 K	IP 71	cst	3.490	4.640	20.26
Saturates	BAM 74	% wt	9.5	5.2	2.1
Aromatics			88.4	91.7	90.4
Resins			2.1	3.1	7.5
Sulfur	Coulomax	% wt	3.83	4.14	5.19

TABLE 5.2
STRUCTURAL GROUP ANALYSIS OF DIFFERENT FRACTIONS OF EXTRACTS
(ASTM D3238-74) VAN NEES AND VAN WISTON METHODS

Extract No.	Density at 293K $kg/m^3 10^{-3}$	Ref. Ind. at 293K	Mol. wt.	%S	Carbon Content, Wt%				No. of Rings		
					$\%C_A$	$\%C_R$	$\%C_N$	$\%C_P$	R_A	R_T	R_N
1	1.0042	1.5682	293	3.8	47.1	63.4	16.2	36.5	1.7	2.6	0.9
2	1.0219	1.5808	320	4.1	52.1	62.7	10.5	37.3	2.1	2.8	0.7
3	1.0558	1.6002	366	5.1	57.0	65.7	8.7	34.2	2.6	3.4	0.8

The adsorption isotherms of the aromatics extract fractions were determined using Analar iso-octane as inert solvent. The static method was used for the determination of the adsorption isotherms of these extract fractions from binary solutions at temperatures of 303 and 343 K using the method discussed in Chapter 3.

The time needed to reach the adsorption equilibrium was: 864 ks for extract fraction 1, 902 ks for extraction fraction 2 and 1296 ks for extract fraction 3 at 303 K. At 343 K it was 86.4 ks for extract fraction 1, 90 ks for extract fraction 2 and 130 ks for extract fraction 3. The concentrations of aromatic extract fractions before, and after, adsorption were determined using ultraviolet spectrometry.

5.3 Results and Discussion

Adosrption Isotherms of Extract Fractions.

The adsorption isotherms of aromatics extract fractions from iso-octane solutions on type 13 X molecular sieves was investigated over a range of initial concentrations from 5 to 35 kg/m^3, equivalent to 1-3% aromatics by weight. The adsorption values of the extract fractions were determined using Gibbs free energy method as in Chapter 3. The initial sections of the adsorption isotherms for the three extract fractions are shown in Figures 5.1 and 5.2.

The points represent the experimental data which were determined by Gibb's equation and the curves were calculated using the BET equation (Brunauer-Emmett-Teller) for multilayer adsorption system. The value of maximum adsorption capacity A_m and separation coefficient f were determined from the graphical solution of the (B.E.T.) equation and are presented in Table 5.3.

As illustrated in Figures 5.1 and 5.2, for equilibrium isotherm adsorption of the extract fractions there was good agreement between adsorption values derived theoretically using B.E.T. equation (i.e., the solid curves) and the adsorption value determined experimentally using Gibbs method of calculation (i.e. points on the isotherm curves). This means that the mechanism of adsorption of extracts using molecular sieves is in agreement with the theory for a binary system shown for individual aromatic compounds in Chapter 3.

Table 5.2 shows that the extract fractions generally consisted of naphtheno-aromatic compounds. An increase in the boiling point of the
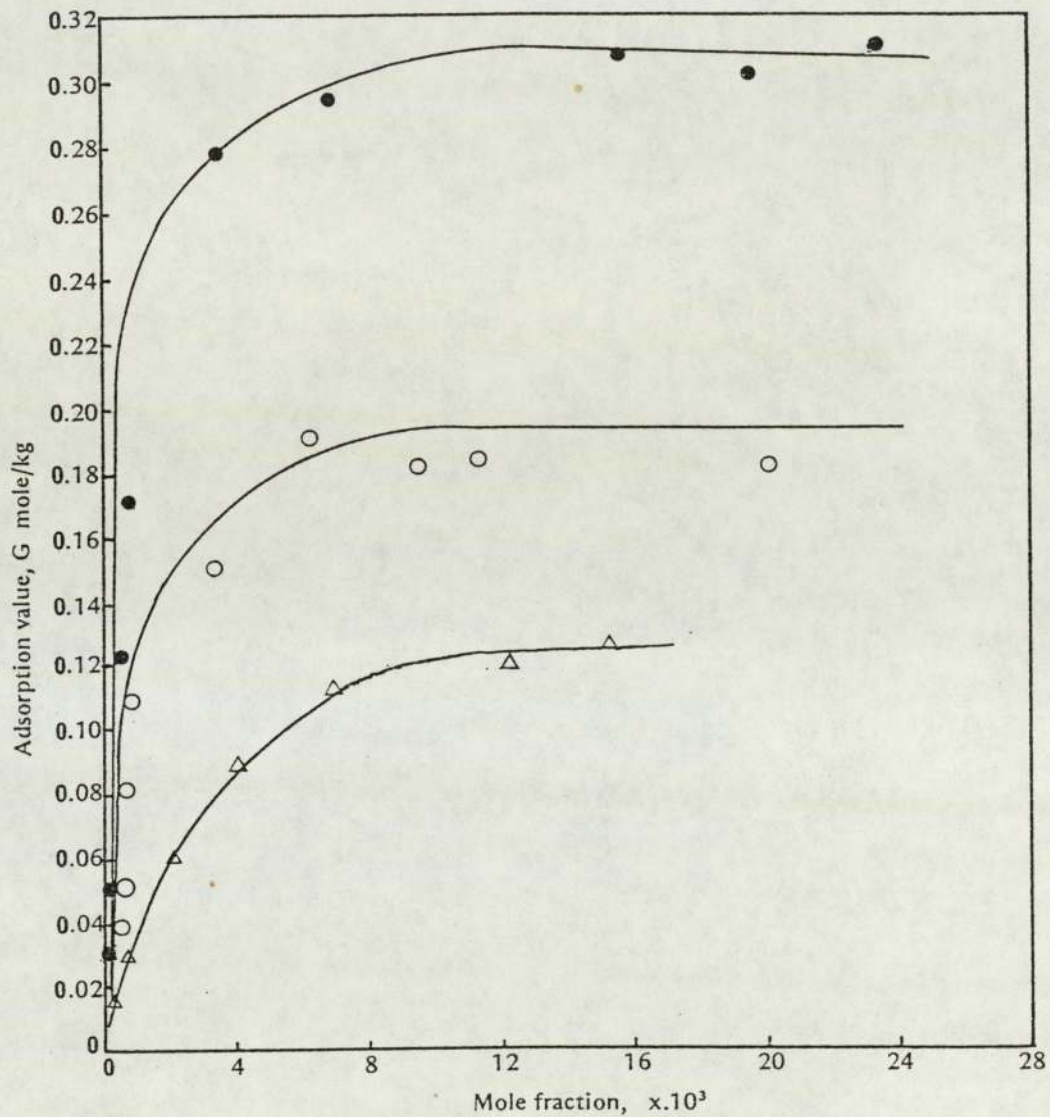
Figure 5.1   Adsorption Isotherms of Extract
Fractions   • 1, o 2, and △ 3 on
Pellets of Zeolite NaX at 303 K.

Figure 5.2   Adsorption Isotherms of Extract
             Fractions ● 1, ○ 2, and △ 3 on
             Pellets of Zeolite NaX at 343 K.

TABLE 5.3. THE CALCULATED THEORETICAL EQUILIBRIUM LIMITING VALUES OF ADSORPTION OF AROMATIC EXTRACTS FROM BINARY SOLUTION WITH ISO-OCTANE USING MOL. SIEVES TYPE 13X AT DIFFERENT TEMPERATURES

Extract No.	303 K						343 K					
	$\tan a$	Am theoretical mole/kg	b	B	f	Log f	$\tan a$	Am theoretical mole/kg	b	B	f	Log f
1	3.1	0.32	1×10^{-3}	1.75	1772	3.2	3.2	0.30	1×10^{-3}	1.71	1901	3.2
2	5.0	0.2	2×10^{-3}	1.88	1330	3.1	5.3	0.18	2.5×10^{-3}	1.84	1172	3.1
3	5.5	0.18	20×10^{-3}	2.08	133	2.1	8.5	0.11	24×10^{-3}	2.00	178	2.2

fractions resulted in an increase in the aromaticity and in sulfur content. The three extract fractions exhibited an affinity for adsorption on molecular sieves as illustrated in the equilibrium isotherms. Hence, there is an interaction between the active sites of the molecular sieves and π-bond of the aromatic compounds of the extract fractions. There are also specific interactions, since the polar compounds, i.e. the sulfur compounds, have strong interactions with the electrostatic field of the molecular sieves crystal. Figures 5.1 and 5.2 show that the adsorption isotherms of extract fractions have a form typical of the adsorption isotherm of an individual aromatic compound. They rise steeply and reach maximum values at equilibrium concentration of the extract fractions equal to 6×10^{-3} to 10×10^{-3} mole fraction at 303 K and 4×10^{-3} to 8×10^{-3} mole fraction at 343 K.

The maximum value of adsorption for the extract fractions is very low compared with the isotherms of the individual aromatic compounds due to the complexity of the molecules. Increase in the molecular weight of the extract fraction affects the diffusion rate of the adsorption and results in a decrease in the adsorption value as shown in Table 5.4. Increase in molecular weight from 293 to 366 led to a decrease in the adsorption value from 0.31 to 0.11 for the first to third extract fractions respectively at 303 K and from 0.3 to 0.09 at 343 K.

Separation Coefficients of Extract Fractions.

The separation coefficients, f, was determined for each of the 3 extract fractions and are illustrated in Table 5.3. The separation coefficient log f > 2 indicate a high selectivity of adsorption of these aromatic compounds from the extract fractions. The increase of the molecular weight of the aromatic compounds in the extract fractions from 293 to 366 resulted in a decrease in separation coefficients. The separation coefficients (log f) for the three extract fractions changed by increase of the temperature from 303 to 343 K. At lower temperatures the high molecular weight extract fractions must be activated to permit the adsorbate molecules to penetrate through the crystal of the molecular sieves. The increase in the energy level of the adsorbate molecules results in increased diffusivity of the compounds; hence they are able to penetrate rapidly through the cavities of the molecular sieves. The steric effect also affects the diffusivity of the adsorbate molecules through the cavi-

ties, i.e. the critical diameter of the aromatic compounds present in the extract fraction. Depending upon the aperture diameter of the molecular sieves, there is a hind rance effect on adsorption. High molecular weight aromatic compounds tend to block the surface of the crystal of the molecular sieves thus preventing the diffusion of other molecules. This is demonstrated for the third extract fraction see Table 5.3. Table 5.4 illustrates the limiting values of adsorption, and number of adsorbate molecules occupied per unit cell of the molecular sieves.

Number of Molecules Occupied by Unit Cell of Zeolite Crystals Of Extract Fractions

Table 5.4 shows that the numbers of adsorbate molecules captured per one unit cell of molecular sieves decreased as the molecular weight of the extract fractions increased. For example, at 303 K for the first extract fraction only 4.2 molecules were located in one unit cell of molecular sieves, whereas for the second and third extract fractions, 2.5, 1.5 molecules respectively were located in one unit cell.

Increase in temperature resulted in an increase in the mobility of molecules adsorbed in cavities of zeolite crystals. Hence the number of adsorbate molecules in the cavities will decrease as the temperature of the adsorption increases. This can be seen from Table 5.4. Increase in the temperature from 303 to 343 K led to a decrease in the number of adsorbate molecules captured by one unit cell of the molecular sieves to: 4, 2.3 and 1.2 for the extract fractions 1, 2 and 3 respectively.

It was shown in Chapter 3 that the maximum adsorption values for individual aromatic compounds by zeolite 13X were for the more compact molecules such as cumene and for molecules with the more delocalized electron density such as naphthalene and for the more polar compounds such as dibenzothiophene. It can be assumed that first stage of the adsorption of the aromatic compounds of the extract fractions would therefore comprise adsorption of lower molecular weight aromatics and the second stage adsorption of polar molecules that possess a high dipole moment. As the sulfur content increased in the extract fractions, the adsorption value decreased (see Table 5.4). The adsorption of sulfur compounds results in a reduction in the packing density of adsorbed molecules into cavities of the zeolite crystals. Adsorption of high molecular weight aromatic hydrocarbons and heterogeneous compounds such as sulfur compounds using zeolite

TABLE 5.4. LIMITING VALUES OF ADSORPTION OF EXTRACTS FROM BINARY SOLUTION WITH
ISO-OCTANE AT DIFFERENT TEMPERATURES USING MOL. SIEVES TYPE 13X.

Extract No.	303 K					343 K				
	G Exp. mole /kg	$G\mu$	$\dfrac{G\mu}{V_p}$ %	GN	$\dfrac{GN}{n}$	G Exp. mole /kg	$G\mu$	$\dfrac{G\mu}{V_p}$ %	GN	$\dfrac{GN}{n}$
1	0.31	0.088	29.7	1.87×10^{20}	4.2	0.30	0.09	30.0	1.80×10^{20}	4.0
2	0.19	0.059	20.2	1.14×10^{20}	2.5	0.17	0.05	19.0	1.05×10^{20}	2.3
3	0.11	0.040	13.6	0.66×10^{20}	1.5	0.09	0.03	10.6	0.54×10^{20}	1.2

13X can be caused by specific and nonspecific interactions between the adsorbing molecules and cations of the cavities of zeolite crystals. The adsorbate molecules which possess constant dipole moment, such as sulfur aromatic compounds, can interact very strongly with the electrostatic charges of the cavities of the molecular sieve. This results in blockage of the pores of the molecular sieves and hence decreases the adsorption value.

As shown in Table 5.4 the adsorption efficiency of the extract fractions from solution in iso-octane at 303 and 343 K were in the order: third fraction < 2nd fraction < 1st fraction.

5.4 Conclusions

Unlike solvent extraction, adsorption by silica gel or alumina, or azeotropic distillation, which are used principally to separate hydrocarbons according to type of molecule, this investigation shows that molecular sieves type 13X can be used successfully for separation of multicomponent aromatic compounds from petroleum fractions, according to the shape, and size of the molecules. This is practicable despite the low adsorption values compared with adsorption values for the pure aromatic compounds. However, a reliable method is required for the prediction of equilibrium adsorption data for mixtures from the isotherms of pure components.

6.0 A STUDY OF HEAT OF ADSORPTION FOR EXTRACT FRACTIONS ON MOLECULAR SIEVES TYPE 13X

6.1 Determination of Heats of Adsorption for Extract Fractions on Molecular Sieves Type 13X

The adsorption properties of zeolites are determined by the geometry of the opening of the channels in porous crystals and by the chemical composition of their skeleton. Zeolites are specific adsorbents because their surface carries positive charges concentrated in exchange cations, while the negative charges are distributed over the internal bonds of complex $(AlO_4)^-$. This determines the adsorption properties of zeolites. With respect to polar molecules of the extract fractions which are capable of specific interaction with the surface of the molecular sieves type X, the attachment of these molecules will be at specific sites of cation cavities. The heat of adsorption associated with electrostatic interactions can be calculated from the Clasius Clapeyron equation mentioned in Chapter 4. As discussed earlier, heats of adsorption may comprise two contributions, specific and non-specific heats of adsorption. The heat of adsorption of aromatic compounds is solely due to non-specific interactions whereas the hetero-aromatic compounds also have a specific contribution. The evaluation of the heats of adsorption by molecular sieve at small and high pore filling have been calculated from adsorption isosters for the extract fractions in the range of temperatures 303 - 343 K.

Different types of components are present in extract fractions such as polar compounds, aromatic hydrocarbons in which the rings are shielded with alkyl chains, naphthalenes, etc. Therefore the heat of adsorption of these hydrocarbons consists of specific and non-specific interactions. If the adsorbed molecules are aromatic rings with π bonds or with polar functional groups as in the sulfur compounds, then these molecules interact strongly with the exchange cations of the molecular sieves. The most important features of the component's structure are the nature of the π bonds, the value of localization of the dipole and quadropole moments, due to the presence of a free electron pair in the adsorbed molecule. The heats of adsorption were calculated from pairs of isotherms at temperatures of 303 to 343 K. Figures 6.1, 6.2 and 6.3 illustrate the isosters of adsorption of the extract fractions at different coverages.

Figure 6.4 is a plot of the calculated isosteric heat of adsorption as a function of the coverage of each extract fraction on molecular sieves 13X. It demonstrates that the interaction energies between the adsorbate molecules of the extracts with molecular sieve crystals are greater than those between the iso-octane molecules and the crystals. The heat required for removing iso-octane molecules from cavities of the zeolite crystals by molecules of extract fractions at low concentrations were 14, 20 and 19 kJ/mole for the 1st, 2nd and 3rd extract fractions respectively. With extract fraction 1 and 2, by increasing the pore filling, the heat of adsorption decreased. This indicates that at higher temperatures (343 K), the concentration of the molecules of aromatic extract fractions 1 or 2 in the zeolite cavities decreased and interaction between them became weaker. As a result, the isosteric heat of adsorption for these extract fractions depends on coverage. During the adsorption of the aromatic components on zeolite, the electro-negative nature of the sulfur atoms led to an additional specific interaction with zeolite cations.

During the earlier stage, the heat of adsorption of the 2nd extract fraction was higher than that of the first fraction. This can be attributed to the increase in the specific strong interactions between the polar compounds of the 2nd fraction and electrostatic charge of the cations of molecular sieves. The concentration of polar compounds in the 2nd fraction was higher than in the 1st fraction. The aromatic content was also higher. So that the total π bond, dipole and quadrupole moments of the 2nd fraction would be higher.

	Sulfur Content	Aromatic Content
Extract Fraction 1	3.8	88.4
Extract Fraction 2	4.1	91.7

During the early stage of coverage, the heat of adsorption of the 3rd fraction was high, indicative a strong interaction between the total π-bonds and free pairs of electrons of sulfur compounds with the electrostatic field of the molecular sieves. An increase in the packing of the adsorbate molecules of the 3rd fraction resulted in a slight decrease in the heat of adsorption. Further increase in the coverages led to a slight increase in the heat of adsorption which can be explained as follows: Mol-
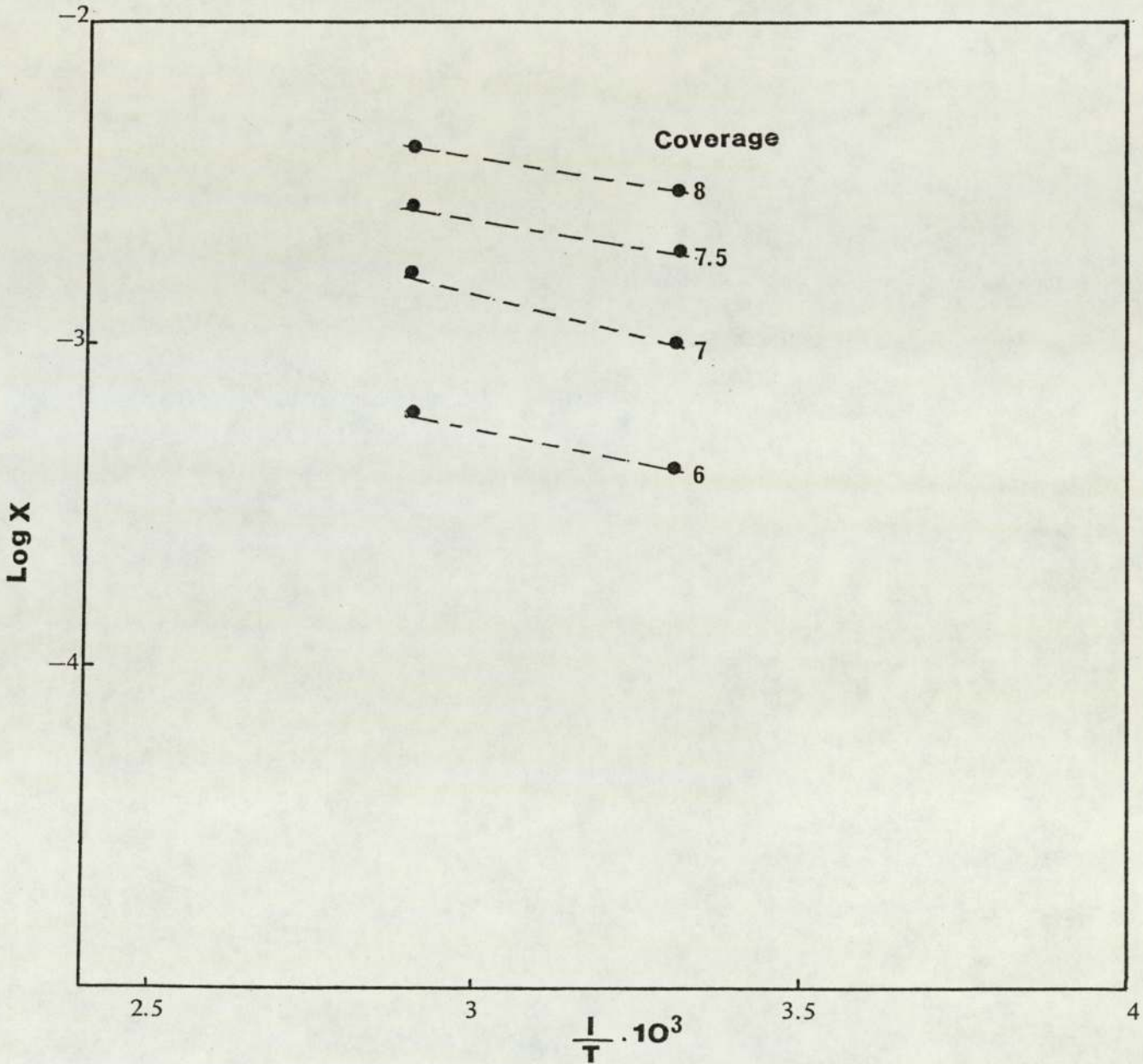
Figure 6.1   The isosters for Extract Fraction l
on Molecular Sieves Type 13X at
Different Coverages
a x 10^5 m^3/kg.
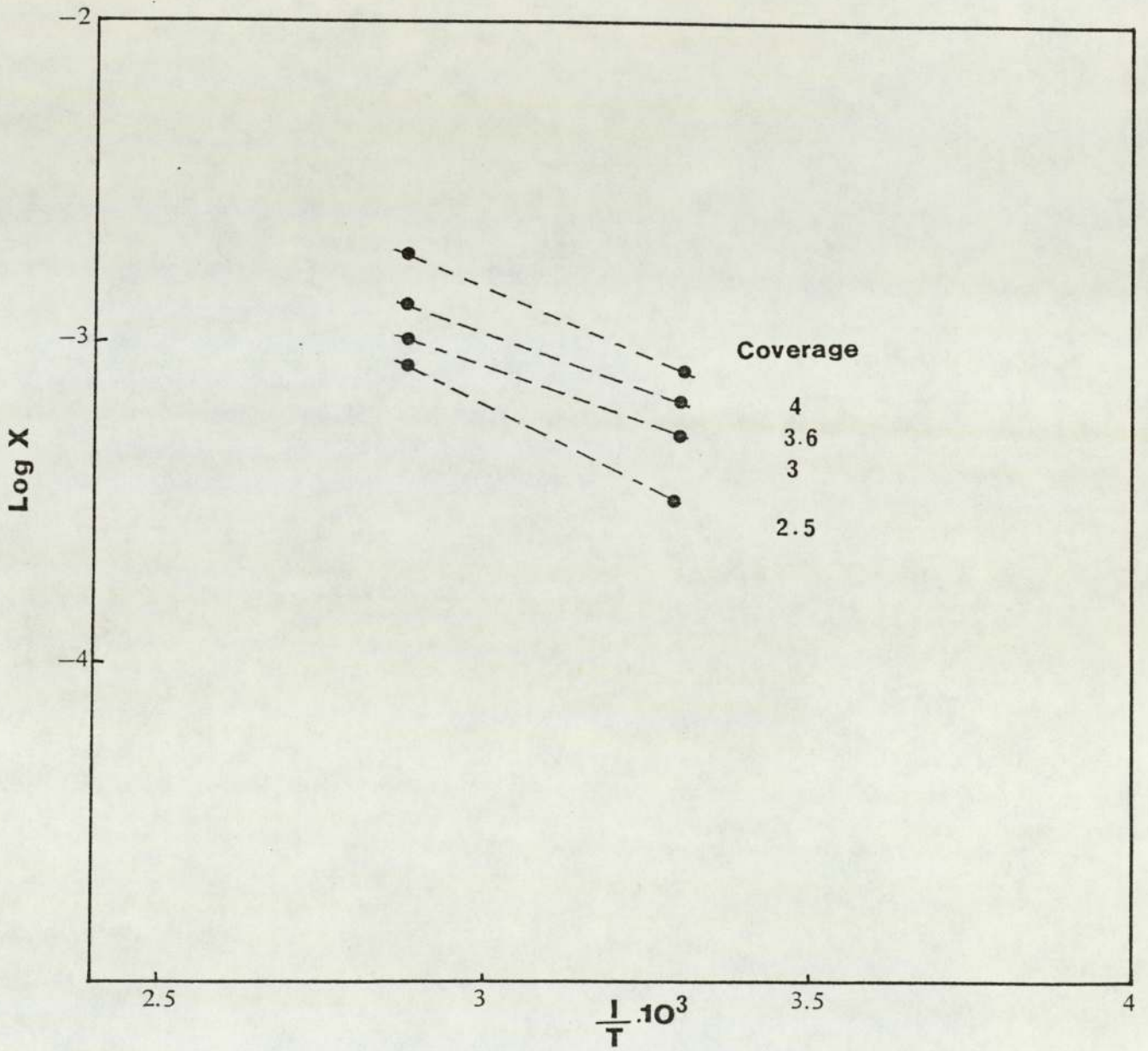
Figure 6.2   The Isosters for Extract Fraction 2
on Molecular Sieves Type 13X at
Different Coverages
a x 10^5 m^3/kg.
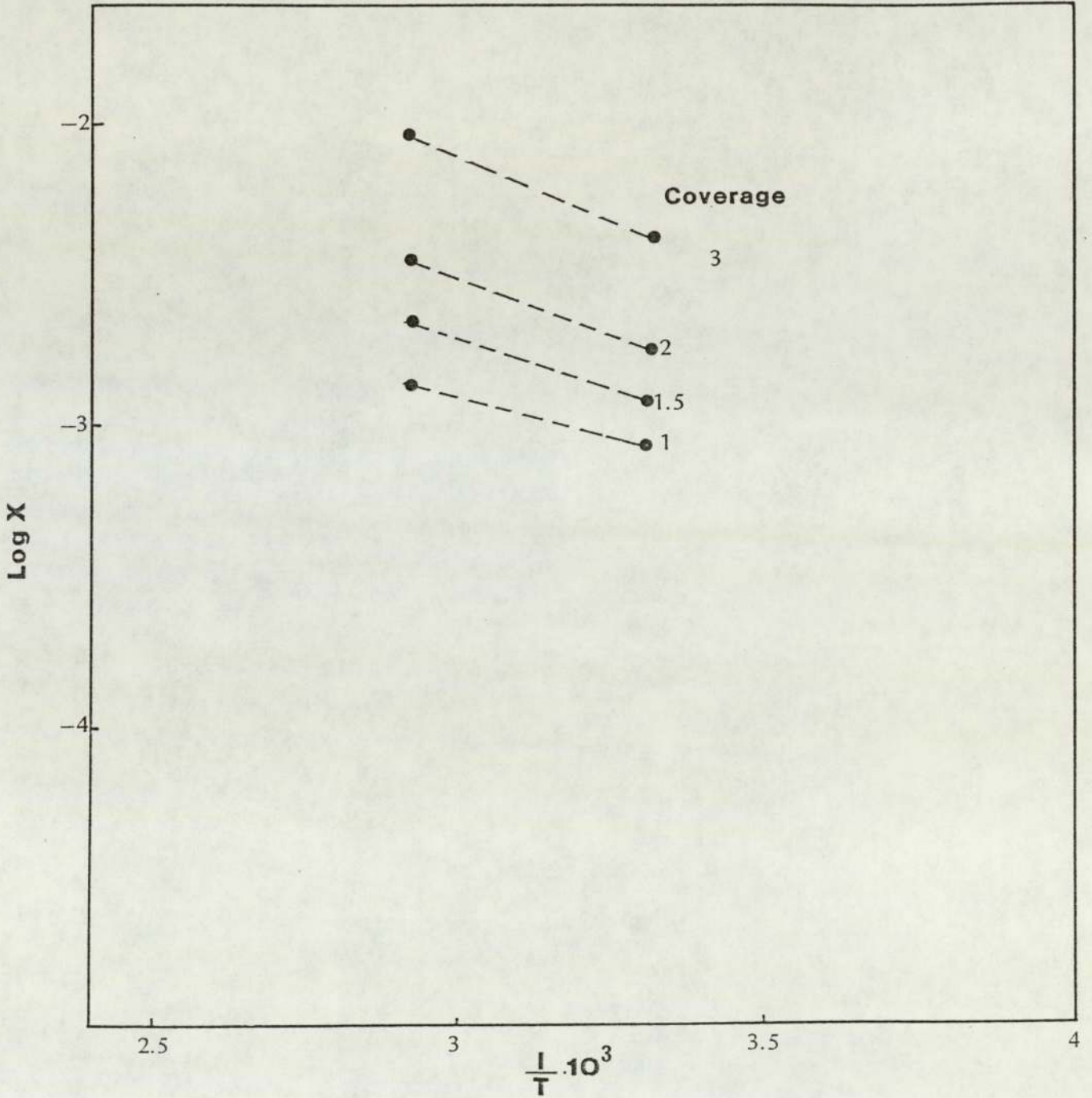
Figure 6.3   The Isosters for Extract Fraction 3
on Molecular Sieves Type 13X at
Different Coverages
a x 10^5 m^3/kg.
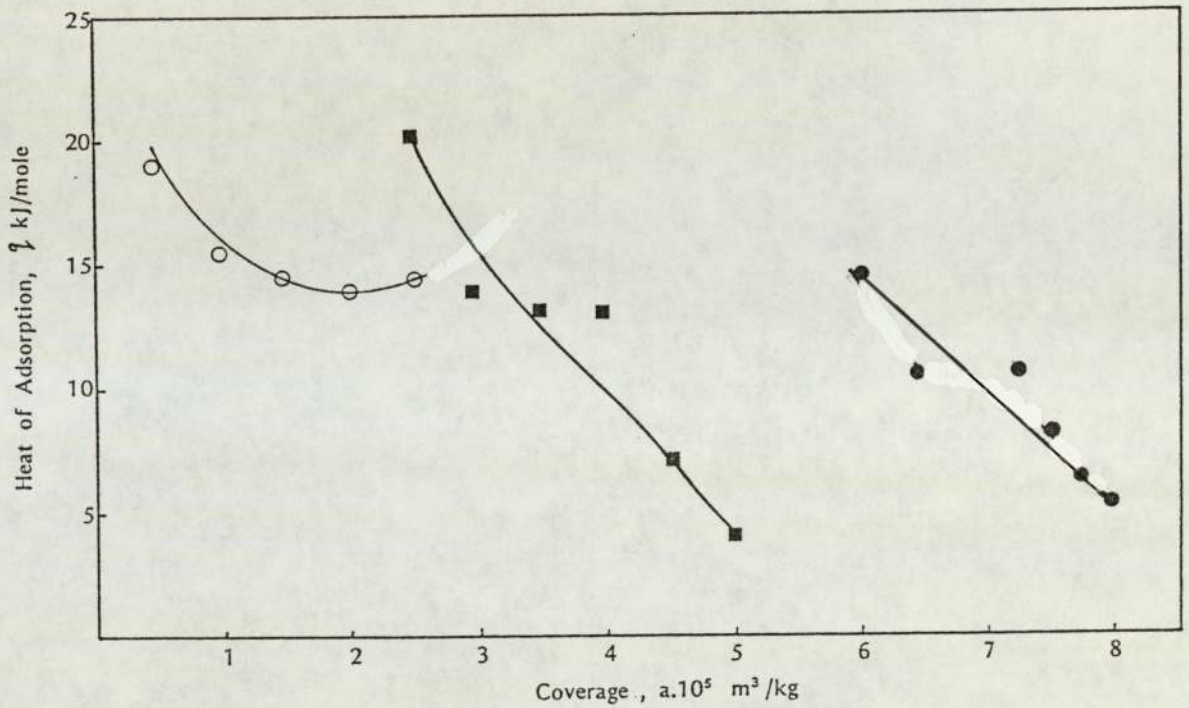
Figure 6.4   The Relationship Between the Isosteric
              Heat of Adsorption and Coverage
              on Molecular Sieve Type 13X for:
                   ● Extract fraction 1
                   ■ Extract fraction 2
                   ○ Extract fraction 3

ecules of the third fraction have a high content of sulfur (5.2 wt%) and heterogeneous compounds in the form of resins (resin content 7.5 wt%). This percent is high in comparison with the first and second fractions (resin contents of 2.1 wt% and 3.1 wt% respectively). The heterogeneous molecules of the third fraction can interact specifically not only with the electrostatic field of zeolite but also with themselves forming mutual bonds creating longer side chains, or bigger molecules of larger critical diameter. Therefore, the adsorption value will be lowered and the number of molecules adsorbed by one unit cell of molecular sieves will be less than expected (see Table 5.4). This can be attributed particularly to the steric effect, i.e., the geometry of the adsorbed molecules. This also results in a decreased heat of adsorption because the polar compounds and the polycycloaromatic compounds present in the resin or the extract itself possess a large molecular diameter, i.e., larger than the critical diameter of the zeolite cavity. During adsorption these molecules block the window of the pore site thus hindering penetration by molecules of smaller diameter, such as naphthenes and mono or diaromatics. Since molecules having dipole, quadropole moments and free electron pairs, can diffuse very quickly and be directly adsorbed ahead of the mono and di-aromatic molecules forming a multilayer resistance.

This summarizes factors in the reduction of the interaction between the extract molecules and the electron density of the zeolite sites. Thus the total value of isosteric heat of adsorption will be lower than the heat of adsorption of individual aromatic compounds discussed in Chapter 4.

6.2 Conclusions

Heats of adsorption of extract fractions were considerably less than those of the individual aromatic compounds described in Chapter 4. An increase in complexity of the extract fraction resulted in a reduction in the heat of adsorption.

7.0 KINETICS OF ADSORPTION OF INDIVIDUAL AROMATIC COMPOUNDS FROM BINARY SOLUTIONS WITH ISO-OCTANE USING MOLECULAR SIEVES

7.1 Introduction

The kinetics of adsorption depend upon mass transfer of the adsorbate molecules through a pellet or through a layer of the molecular sieves at a certain rate. The rate of adsorption is always controlled by the mass transfer resistance and the temperature rather than by the intrinsic sorption kinetics. Therefore factors affecting the rates of diffusion of hydrocarbons in molecular sieves are of significant importance in the use of zeolitic catalysts in reactors and of zeolitic sorbents in separation processes under dynamic conditions.

The transient flow of hydrocarbons within the adsorbent consists of three stages:

1. Transfer of the adsorbate material from the solution to the external surface of the adsorbent.

2. Diffusion of the adsorbate molecules through the pore window to the surface of the adsorbent crystal, and

3. Migration of the adsorbate molecules inside the cavities of the adsorbent.

The kinetics of sorption are governed by two distinct diffusional resistances; the macropore resistance of the pellet and the micropore resistance of the zeolite crystals. To interpret kinetic data for such systems, it is therefore necessary to take account of both diffusional processes although, under certain conditions, either of the resistances may be rate-controlling.

Under equilibrium conditions, the quantity of sorbate molecules occluded by the zeolite crystals is generally very much greater than the quantity remaining within the macropores of the pellet. Adsorption within the micropores may be neglected and the adsorbate molecules occluded within the zeolite crystals may be treated as a single adsorbed phase.

The adsorption velocity is limited by the slowest stage of adsorption. Hence the sorption kinetics in the small pores of zeolites such as type A, erionite, and chabazite can be controlled. There are difficulties in controlling the sorption kinetics in zeolites types X and Y because the diffusion in the open framework of these types of molecular sieves is rapid and is not easily measured by conventional methods, particularly for

adsorption of molecules of very small kinetic diameter such as low molecular weight gases.

The migration of molecules is generally described as an activated diffusion process with activation energies ranging from 0.5 to 19 k cal/g mole. The migration of adsorbate molecules depends on two factors:

i.   energy considerations which determine the direction of the process, i.e., to result in a decrease in the free energy of the system,

and

ii.   the steric factor which determines the ability of the adsorbate molecules to migrate through the cavity window of the pores.

Hence the adsorption isotherm is influenced by both these effects.

The rate of diffusion of adsorbate molecules within the pores of molecular sieves is related to the probability of the transition of the molecules through the windows between adjacent cavities. This probability is proportional to:

$$\exp\left(-\frac{E_1 - E_2}{KT}\right) \qquad (7.1)$$

An increase in the interactions between the adsorbate molecules and the molecular sieves leads to a decrease in the E_2 and the mean lifetime of the adsorbate molecules inside the pores of the crystal will increase. The migration of the adsorbate molecules in the pores will be retarded.

The energy of adsorbate molecules in the pores is equal to the difference between their energy in the gas phase and the heat of adsorption.

$$E = H - q \qquad (7.2)$$

Equation 7.2, implies that an increase in the heat of adsorption will lead to a decrease in the energy of adsorbate molecules in the pores. This also results in an increase in the lifetime of the adsorbate molecules in the pores, thus decreasing the rate of adsorption.

A decrease in adsorption rate is also attributable to the increase in the energy of adsorbate molecules at the boundary of two pores. This energy comprises energy of interactions of adsorbate molecules with cations distributed in the channels of the sites of the molecular sieves plus the energy of dispersion interactions with oxygen ions.

The potential of these interactions decreases sharply with increase in the distance between the nearest neighbours of the active sites of the molecular sieves. Hence an increase in the critical diameter of the adsorbate molecules results in a sharp increase in this energy level.

If the critical diameter of adsorbate molecules is approximately equal to the effective diameter of the aperture of the macropore, physical adsorption will occur. The effect of the low affinity of macropores to adsorb hydrocarbon molecules is observed only over a specific temperature range. An increase in the temperature up to a specific limit results in an increase in the adsorption value. This occurs due to the input of excess activation energy to the process so that the adsorbate molecules can penetrate into the pores of the molecular sieves crystal.

In kinetic studies, it is important to clarify how diffusion coefficients within zeolites are related to:

1.   Intracrystalline channel geometry and dimensions.
2.   Shape, size and polarity of penetrant molecules.
3.   Presence of molecules of impurity in channel.
4.   Structural changes brought about by penetrants.
5.   Structural damage associated with physical and chemical treatment.
6.   Concentration of penetrant within the crystal (1).

However, information on these topics relating to high molecular weight aromatics as penetrants is still limited.

7.2 Literature Survey

Barrer and Ibbitson (39) found that the pressure of the gas (concentration of the adsorbate molecules) and the temperature significantly affected the rate of occlusion of adsorbate molecules inside the pores of molecular sieves. They considered that from the kinetic point of view, adsorbate molecules could be divided into three categories:

R = molecules occluded extremely rapidly

L = molecules occluded slowly at room temperature

C = molecules excluded from the zeolite lattice

Most of these groups were defined but little is known about the kinetics of the adsorption of high molecular weight compounds in the large-pore zeolites, such as type X and type Y, of interest in catalysis. Little has

been published regarding the kinetics of adsorption of such types of compound. Diffusion constants and activation energies have been determined for the adsorption of gases, medium chain-length hydrocarbon molecules and some light and medium aromatic hydrocarbons on mineral zeolites, synthetic zeolite and modifications of both. The modifications include the effect of cation replacement, decationization, and the effect of a pre-adsorbed polar compound such as ammonia, CO_2, or CO. The results support the model of diffusing molecules encountering a periodic potential field within the zeolite. Various calculations were made of these potential fields.

In early work on the rate of adsorption by zeolite, Barrer and Ibbitson studied the kinetics of occlusion of different hydrocarbons such as n-hydrocarbons and different polar compounds, e.g. NH_3 and H_2O, using different types of zeolitic solids such as chabazite and active and inactive analcite. A relationship was found between the kinetics of occlusion of hydrocarbons in the molecular sieves,

$$\frac{Q_t - Q_o}{Q_\infty - Q_o} = K' \sqrt{t} \tag{7.3}$$

K' depends on particle size and the diffusion constant D. The latter depends on the temperature and the concentration of the adsorbate molecules in the zeolite. Plotting $(Q_t - Q_o)/(Q_\infty - Q_o)$ versus $\sqrt{t}$ illustrates the kinetic behaviour of the adsorption.

Barrer and Ibbitson also stated that as the molecular weight increases the diffusion coefficient decreases and consequently the rate of adsorption in zeolites decreases. The rate of adsorption depends upon the cross-section of the solute molecule; for example ethane (C_2H_6) propane (C_3H_8) and isobutane (Iso C_4H_{10}) have cross-sectional diameters of the order of 4.0, 4.89 and 5.50 A° respectively. Molecules with a cross-sectional diameter $\leq$ 4.0 A° are taken-up by minute channels. Molecules with a cross-sectional diameter equal to 4.89A° (n-paraffins) are occluded by a slow process of diffusion, in which an energy of activation is needed to move the molecule along the interstitial channel from one position of maximum sorption potential to another. Molecules with cross-sectional diameter $\geq$ 5.58A° (isoparaffin and aromatic hydrocarbons) are totally excluded.

Based on these results Barrer and Ibbitson suggested a method of measuring cross-sectional diameters of molecules. They also concluded that:

i.   The rate of sorption is decreased as the chain length increases;

ii.   The rate of occlusion decreases as the concentration of the solute
      within the zeolite increases;

      and

iii. The sorption rate is increased exponentially by rise in temperature.

Barrer and Brook (40) studied the kinetics of sorption for various gases in zeolites by a volumetric method under both constant pressure and constant volume conditions. They studied the kinetics of occlusion of methylchloride and methylamine in chabazite degassed at 673-693 K but found them too rapid to be followed quantitatively. The occlusion rates of the larger molecules $CHFCl_2$, CH_2Cl_2, CHF_3, $(CH_3)_2NH$, C_3H_8 and C_4H_{10} could however, be measured conveniently. They found that whilst diffusivity decreases activation energy E_A increases considerably as the chain length, or the cross-section of the diffusing molecules, increases. Comparing three molecules of comparable size and shape in which polarity increases - C_3H_8, CH_2Cl_2, $(CH_3)_2NH$, E_A undergoes a large increase in the same order. This arises because a polar molecule is attracted more strongly to each cationic equilibrium position than a non-polar molecule. The molecule with a dipole is likely to require a higher energy to breakaway and jump to the next equilibrium position.

Eberly (41) reviewed the study by Ruthven et al. of the relationship between critical diameter of different types of hydrocarbon and their adsorption rate upon different types of molecular sieve. He stated that as the critical diameter of the hydrocabons increases the rate of adsorption decreases. He also studied the activation energy for gases on natural chabazite and found that they increased with increase in the length of hydrocarbon chain. The heavier hydrocarbons $n-C_5H_{12}$ and $n-C_7H_{16}$ were appreciably sorbed only at elevated temperatures. The diffusivity was found to decrease as the amount of material initially sorbed increased. Activation energy was determined for C_3H_8 on 5A molecular sieve and a value of 14.63 kJ/mole was reported. The long chain, $n-C_{14}H_{30}$ had a high activation energy of 67.29 kJ/mole. Activation energies were reported for various sorbates on zeolites 3A and 4A.

A study of the rates of adsorption of highly purified liquid hydrocarbons in NaY and HY was made by Satterfield and Cheng (42). The critical molecular diameters were evaluated from bond lengths, angles and van

der Waals radii. The results with NaY clearly showed that the diffusivities increase quite markedly with decreasing molecular size, e.g. hexadecane diffused at a rate > 20,000 times faster than 1,3,5 triisopropylbenzene. Also 2,4,6 trimethyl-aniline, containing a permanent dipole, diffused at a much slower rate than the 1,3,5 trimethylbenzene even though the molecular diameters are identical. This is attributed to the higher energy of interaction between the polar molecule and the surface cations. Similarly, 1,3,5 triisopropylcyclohexane diffused at a faster rate in NaY than 1,3,5 triisopropylbenzene even though the former molecule has a larger diameter. This is again due to the higher energy of interaction between the aromatic π electrons and the zeolite surface.

Loughlin et al. (43) studied sorption of n-butane from two different samples of Linde 5A zeolite crystals at 323 K and under comparable butane pressures (2000-4770 N/m^2). There were significant differences between the sorption curves and diffusivity due to the difference in pore diameter and size distribution. Diffusion was shown to depend strongly on the concentration of the adsorbate and not on the zeolite type.

As mentioned in Section 2.1, Satterfield and Cheng (6) focussed their study on elucidating two aspects,

i.   the relationship between the size and physicochemical properties of the diffusing molecule and its rate of diffusion in type Y zeolite in either the Na or H form,

      and

ii.   the relationship between unidirectional, that is single component, diffusion and counter diffusion in binary systems.

They studied diffusion of cumene in cyclohexane and mesitylene in cyclohexane on NaY zeolite at 303 K. Mesitylene, which has the largest critical molecular diameter 8.4 A° diffuses much slower than cumene which is of smaller critical diameter (6.8 A°). They also studied the adsorptivity of 2,4,6 trimethylaniline (mesidine), which has a similar molecular shape and size to mesitylene but is an aromatic amine. The diffusion rate of mesidine is much slower than that of mesitylene, indicating that steric considerations were by no means the only factor determining diffusivities in zeolites. Other factors affect the mobility of diffusate, resulting from strong interactions between molecules and zeolite. The diffusion coefficient for mesitylene at 303 K in NaX was about 10 times that of mesidine.

In the unidirectional studies, the activation energy was 37 kJ/mole for mesitylene and 71 kJ/mole for mesidine. It can be postulated that, due to the presence of the amine group, mesidine interacts more strongly with the zeolite than does mesitylene.

The effect of the zeolitic cation was also studied and the diffusivity was found to increase with an increasing degree of ion exchange converting NaY to HY. The cation effect can also be explained from the viewpoint of molecule-zeolite interactions, but this was not demonstrated in the diffusion rate for mesidine (amine group) which was similar in the two forms of Y zeolite.

Ruthven et al., (44) presented diffusivity data for ethane, ethylene, propane, propylene, cyclopropane, n-butane, 1-butene, cis-2-butene, and trans-2-butene in Linde 5A zeolite. The diffusivity was found to increase with increase in sorbate concentration. As would be expected, for diffusion of small molecules in larger pore zeolites a concentration-dependent mobility was observed.

Activation energies for different hydrocarbons were determined and it was found that as the molecular diameter of the sorbate molecules increases the activation energy increases. Propylene, 1-butene and trans-2 butene all have the same critical diameter 2.65 A°, and the diffusivities and activation energies for these species were found to be similar. Cis-2-butene has a considerably larger critical diameter, and its activation energy was found to be greater. This provides strong evidence that activation energy for zeolite diffusion is determined by the critical diameter of the molecule and that other factors such as molecular weight, chain length or type of bond are only of minor significance.

Ruthven et al., also studied the kinetics and equilibria of sorption of light hydrocarbons and some other simple non-polar molecules, in 5A zeolite. They showed that many features of the sorption kinetics and equilibria may be explained by simple theoretical considerations.

Fal'kovich et al. (18) studied kinetics of adsorption of n-decane, n-tetradecane, n-hexadecane, and n-heptadecane from isooctane solutions by granules of Ca A-zeolite at 293, 373 and 423 K. They found that the diffusion coefficient for n-heptadecane was increased, then remained constant for a definite period as the zeolite cavities were filled, and finally decreased rapidly near the equilibrium point. It was concluded that the

diffusivities of all the n-alkanes studied had similar values and did not depend on the length of the hydrocarbon chain, but there was a general rise in diffusion coefficient values with increasing temperature. Activation energies appeared to depend only slightly on chain length of the alkane. It was shown that at 373 and 423 K activation energies were 41.8-62.7 kJ/mole while at lower temperature range 293 and 373 K they were 12.5-16.7 kJ/mole, indicative of a change in the nature of the diffusion.

Doetsch et al., (45) studied the kinetics and the equilibrium of the sorption of n-heptane in 5A zeolite. A satisfactory interpretation of the equilibrium data was obtained on the basis of a simple theoretical model in which it was assumed that there were both active and inactive sites within each crystal of the zeolite lattice. Other workers have attributed the difference between active and inactive sites to the presence of the cation, which generates the electrostatic energy necessary for activation. These sites might correspond to the region close to the cavity wall in which adsorption was energetically favourable giving rise to localized adsorption, and the central region of the cavity in which the sorbate was less strongly bound with greater rotational and translational freedom. The difference in mass transfer increased strongly with sorbate concentation. The limiting diffusional activation energy for n-heptane was 31.3 kJ and this value was somewhat higher than the activation energy for the lighter paraffins in the range C_2-C_4.

Caro et al. (46) studied sorption of n-decane from a nonadsorbing liquid solvent. The nature of the solvent and traces of impurities were found to significantly affect the rate of sorption. They also studied sorption of n-decane in cyclohexane, ethyl- and butylbenzene and found that blocking effects caused by the solvent molecules strongly interacted with the outer crystal surface. Hence they concluded that sorption rate depends strongly on the nature of solvent. It was demonstrated that when using cyclohexane as a solvent the probability of n-decane entry into the zeolite micropores through the crystal surface is at least three orders of magnitude higher than when using ethylbenzene. This is attributed to weak interaction of the cyclohexane molecules with the outer crystal surface due to the difference in the molecular structure between cyclohexane and ethylbenzene.

Ruthven and Doetsch (47) studied equilibrium isotherms for four hydrocarbons $n-C_6H_{14}$, C_6H_{12}, C_6H_6 and $C_6H_5CH_3$ in specially-prepared, samples of 13X zeolite with crystal size 16.5 μm at 409 to 513 K and pressures of 13.3 to 13300 N/m^2. Extensive diffusivity data were presented showing the dependence on sorbate concentration and temperature. Over the range of the experimental measurements, the diffusivities for the C_6 and C_7 species in 13X sieve were 10^{-12} to 10^{-13} m^2/s. Diffusional activation energies for the C_6 and C_7 hydrocarbons in 13X sieve ranged from 21 to 26 kJ/mole.

Ruthven and Derrah (48) developed a simple transition state theory of zeolitic diffusion of methane CH_4 and tetrafluoromethane CF_4 in 5A zeolite. Theoretical diffusivities were calculated for CH_4 and CF_4 in 5A zeolite and found to agree well with experimental data. Experiments were carried out over a range of pressures from 400 to 40000 N/m^2. The isotherms for tetrafluoromethane were essentially linear (Henry's law region) and the diffusivities were found to be independent of concentration.

Vavlitis, et al. (49) reported sorption and diffusion data for n-pentane, n-octane, and n-decane in Linde 5A zeolite crystals. The diffusivities of these hydrocarbons all increased strongly with concentration, and the activation energy increased monotonically with carbon number. The experiments were conducted at 520-620 K. Diffusion of pentane was found to be relatively rapid and heat effects were found to be significant, whilst octane and decane diffused more slowly.

Fal'kovich et al. (50) studied the kinetics of adsorption of aromatic hydrocarbons and organic sulfur compounds from binary solutions in isooctane at a concentration of 0.01 mole fraction at 293 K using crystals of binder-free NaX zeolite. Benzene and naphthalene exhibited very similar adsorption rates. Replacement of four hydrogen atoms on the benzene ring by symmetrically-located methyl groups (durene) led to a slight decrease in the adsorption rate. The adsorption process was much slower when the benzene ring in the molecule was conjugated with a thiophene ring (benzothiophene) or was shielded by a long alkyl chain (alkylbenzene). The rate of adsorption was found to be similar for phenanthrene and fluorene.

The adsorption rate was shown to depend on the size of the molecules and upon the temperature of the process; the lower the temperature and the greater the sizes of the molecules, the flatter was the curve for this relationship.

The values of effective diffusion coefficient and the apparent activation energy of some of the aromatic hydrocarbons and organic sulfur compounds were reported. The greatest diffusion was shown by molecules with two condensed rings. If the benzene was conjugated with a thiophene ring (thionaphthene), or shielded by a long alkylchain (alkylbenzene), the diffusion coefficients for such molecules were smaller. An increase in temperature to 343 K increased the rate of diffusion of the organic sulfur compound molecules to a greater degree than in the case of the alkybenzene molecules.

A study of kinetics of high-temperature sorption of C_{10}-C_{19} n-alkanes on 5A zeolites was reported by Amerik and Novikov (51). They studied the sorption and desorption kinetics of C_{10}-C_{19} n-alkanes on CaA zeolite with or without CaO binder and on MgA zeolite with or without MgO + CaO binder. They found that sorption was a rapid process, 90% of the alkanes were adsorbed in $\leq$240 s. Desorption was much slower, it took 18-108 ks, depending on zeolite type, molecular weight of the alkane, temperature and pressure. Thus the proper choice of desorption conditions can be used to separate C_{10}-C_{19} alkanes in the dewaxing of lubricating oils.

Most of the literature indicates that in a porous adsorbent, the diffusional mechanism is generally controlling. Therefore, adsorption processes are frequently treated as diffusional problems. Diffusion coefficients for liquids adsorbed in zeolite crystals have often been calculated from experimental transient uptake curves on the assumption that the system may be regarded as isothermal. Because of the heat of adsorption, this approximation is only valid if the adsorption rate is slow compared with the rate of heat transfer. The significance of thermal effects in zeolite of molecular sieves type X was demonstrated in the experimentation described in Chapters 4 and 6. During adsorption measurements, the temperature rose from 303 - 343 K i.e. 40° and the form of uptake curves deviated significantly from the curve for an isothermal system, at 303K; they were faster in the initial region and slower in the final approach to equilibrium. There are two distinct effects. The increase in the initial uptake rate is due to the temperature dependence of the diffusivity while in the later stages, the sorption rate is related to the equilibrium position.

In accordance with most previous investigations, the zeolite crystals were treated as homogeneous media in which the rate of transport of molecules was characterized by an effective diffusion coefficient, and the flux was assumed to follow Fick's law,

$$J = -D \frac{\partial c}{\partial x} \tag{7.4}$$

At least two pore structures generally exist inside a zeolite pellet. Since zeolite can rarely be synthesized or found as large particles, reasonably-sized pellets are formed by compaction of micron or submicron particle size crystallites. The macropore structure is defined as that existing in the pellet between the individual zeolite crystals. If the dimensions of this structure are such that the mean free path of the diffusing molecule is greater than the pore diameter, Knudson type diffusion occurs in which the diffusivity is given by,

$$D_k = \frac{2d}{3} \sqrt{\frac{2RT}{\pi M}} \tag{7.5}$$

For a material having a distribution of irregularly-shaped pores, the average pore radius can be defined as 2v/A, where v and A are the pore volume and surface area of the macropore structure, respectively. This diffusivity, D_k does not depend on pressure or concentration and is independent of the presence of other gases. It depends only upon the temperature $(T^{1/2})$.

It is difficult to devise a generalized equation relating the zeolitic diffusion constant to the properties of the adsorbed molecules, size and shape of the intracrystalline pore, concentration and temperature. The diffusing molecules are always in intimate contact with the pore walls, so the flow depends strongly upon these variables and upon the chemical nature of the pore walls themselves. These factors contribute to the general non-ideality of zeolitic diffusion. Hence, the diffusivity is generally a function of pressure or more explicitly, a function of the concentration of sorbed molecules. The dependence is frequently expressed as

$$D = D_o \quad \frac{\partial \ln P}{\partial \ln C} \tag{7.6}$$

As stated earlier, the relationship between pressure (P) and concentration of sorbed molecules (C) can often be expressed by the Langmuir isotherm in which case

$$\partial \ln P / \partial \ln C = 1/(1-\theta)$$

Consequently,

$$D = \frac{D_o}{1-\theta} \tag{7.7}$$

The limiting diffusivity at zero sorbate concentation is considered to be a more fundamental constant. It is equal to D only in the case of a linear adsorption isotherm in which case $\partial \ln P / \partial \ln C = 1$.

Timofeev (52), Ruthven (53), Novoselova (54) and others all reported that surface diffusion coefficients vary with the amount adsorbed. The general form of these dependencies is typified as described below.

Surface diffusion has generally been analysed in terms of energy considerations. Since a molecule gives up heat during adsorption, the process is exothermic; this energy barrier must be overcome before desorption occurs. However, before a molecule gains sufficient energy to desorb, it may acquire enough energy to move along the surface. This requirement would be expected to be less than for desorption since there is no change in state. The surface diffusion coefficient can then be expressed in terms of the distance between sites and the average time a molecule resides at a site.

$$D_S = \delta^2/4\tau \tag{7.8}$$

τ has been related to the period of vibration of the molecule by,

$$\tau = \tau_o \quad \exp \left(-\frac{E_A}{RT} \right) \tag{7.9}$$

The period of vibration is approximated to the time required to cover the jump distance at the molecular velocity.

$$\tau_o \approx \frac{\delta}{V} \tag{7.10}$$

where V - mean molecular velocity

Substitution of equations 7.9 and 7.10 for D_S yields,

$$D_S \approx 1/4 \ V \ \delta \ \exp(-E_A/RT) \tag{7.11}$$

This equation yields surface diffusion coefficients in the range of 10^{-9} or 10^{-10} m^2/s. The value is highly sensitive to the activation energy and, to a lesser degree, to the jump distance which is very difficult to evaluate.

Equation 7.11 is frequently written with the constants combined as,

$$D_S = D_o \ \exp(-E_A/RT) \tag{7.12}$$

where D_o is constant and $-E_A$ is the activation energy for the diffusion process. Equation (7.12) shows that diffusion in zeolite is strongly dependent on temperature. It generally increases exponentially with this variable as expressed by the Arrhenius type of relationship (Barrer, 1949).

Equation (7.12) has been used to evaluate activation energies by plotting D_S against $1/T$,

$$E_A = R \left(\frac{\partial \ln D}{\partial \frac{1}{T}} \right) \tag{7.13}$$

Barrer reported activation energies in the range of 8.3 to 83.6 kJ/mole for different types of hydrocarbon gases (26). Barrer and Brook (40) had studied the kinetics of sorption of various gases in zeolite and obtained values for mean diffusion coefficients of C_3H_8, n - C_4H_{10}, CH_2Cl_2 and $(CH_3)_2$-NH at several temperatures in chabazite type molecular sieves. They developed a method for determining true diffusion coefficients and their dependence on the concentration of the diffusing species in the region where the kinetics follow a $t^{1/2}$ diffusion law. The diffusion equation was solved for diffusion in cubes, parallelopipeds, spheres and cylinders. They proved that edges, corners and curvature had no effect on the slope of the $t^{1/2}$ diffusion law for small times. It takes the form,

$$\frac{d}{dt^{1/2}} \left(\frac{Q_t - Q_o}{Q_\infty - Q_o} \right) = \frac{2A}{v} \left(\frac{D}{\pi} \right)^{1/2} \tag{7.14}$$

As an approximation, 2A/v may be replaced by an average 2A/v, which cannot however be specified exactly. The kinetics equation 7.14 may be written,

$$\frac{Q_t - Q_o}{Q_\infty - Q_o} = \frac{2A}{v} \left(\frac{Dt}{\pi} \right)^{1/2} \tag{7.15}$$

If the $Q_o = 0$ at $t = 0$, then,

$$\frac{Q_t}{Q_\infty} = \frac{2A}{v} \left(\frac{Dt}{\pi} \right)^{1/2} \tag{7.16}$$

There are numerous publications concerned with diffusion and adsorption kinetics in the various ion forms of zeolite A involving adsorbates such as the permanent gases and hydrocarbon molecules (44), (1). In these studies the rates of adsorption of both argon and nitrogen were found to decrease rapidly with decreasing temperature. For an assembly of spherical or cubic particles of zeolites, the equation at constant pressure (or concentration) is:

$$\frac{Q_t - Q_o}{Q_\infty - Q_o} = \frac{2A}{v} \left(\frac{Dt}{\pi} \right)^{1/2} = \frac{6}{r_o} \left(\frac{Dt}{\pi} \right)^{1/2} \tag{7.17}$$

This applies for small amounts of adsorption.

Henry's law confirms such relationships for the adsorption isotherms. Over large ranges of adsorbate concentration, D depends on the concentration and the $t^{1/2}$ law is not applicable. The diffusion coefficient calculated by any of the preceeding methods is an effective coefficient. If $Q_o = 0$ at time $t = 0$, then

$$D = \frac{\pi}{4t} \left(\frac{Q_t}{Q_\infty} \right)^2 \left(\frac{v}{A} \right)^2 \tag{7.18}$$

From equations 7.17 and 7.18 the value $1/r_o$, where r_o is the radius of the spherical particles, can be replaced by A/3v.

In the present work measurements were made for determination of kinetics adsoprtion value, rate of adsorption, diffusion coefficient and activation energies of pure aromatic hydrocarbons and aromatic compounds containing heteroatoms from binary solution with iso-octane over molecular sieves type 13X.

7.3 Methodology

Materials: Kinetic adsorption was studied using different types of aromatic compounds, viz, mononuclear, di and trinuclear compounds as listed in Table 3.2. The quantities used depended upon the chemical structure of the compound and upon the field of interest, namely the removal of traces (1-3%) of aromatic compounds from waxes.

Hence the maximum concentration used for cumene, dodecylbenzene i.e., mononuclear compounds; and for naphthalene, 1, methylnaphthalene and 1, 3-dimethylnaphthalene, i.e., dinuclear components was 30 kg/m^3. For dibenzothiophene, fluorene, dibenzofuran and phenanthrene i.e., trinuclear compounds it was only 20 kg/m^3 due to difficulty in dissolving them in isooctane. The molecular sieve type was 13X (NaX) with the properties listed in Table 3.1. The method of activation is summarised in 3.2.2.

7.3.1 Experimental Procedure

Fifteen clean, dry, numbered autoclaves were prepared. 10 cm^3 of a solution, e.g. cumene in isooctane, of known concentration was withdrawn by disposable syringe and poured into each autoclave.

1.0 gram of freshly-dry, activated molecular sieve was poured quickly into each autoclave. The cover was closed firmly and the autoclave immersed into a waterbath at the desired temperature of 303 K ±1. The time was calculated from the moment of contacting the molecular sieves with the solution. After specific time intervals of 15 s, 30 s, 60 s, 120 s, 300 s, 900 s, 1800 s, 2700 s, 3.6 ks., 7.2 ks., 14.4 ks., 22.7 ks., 32.4 ks., 45 ks., and 90 ks. each autoclave was taken out of the bath quickly, opened and the solution decanted into a numbered test tube. Its concentration was then determined by UV spectroscopy. If maximum equilibrium adsorption was reached, then there was no need for testing for a longer time. Alternatively, a longer time was allowed until maximum equilibrium adsorption was achieved.

The same procedure was repeated for all aromatic compounds at temperatures of 303 K and 343 K.

7.4 Results and Discussion

Many investigations have been reported on the sorption of gases and liquids, both in the pure state and as mixtures on zeolitic materials. Much of this work has been concerned with equilibrium studies, and less extensive studies have been made of rates and kinetics of sorption.

Rate of adsorption clearly depends on temperature; it generally increases exponentially with increasing temperature.

This investigation was concerned with,

1. The relationship between the size and physicochemical properties of the diffusant molecule and its rate of diffusion in type X zeolite (NaX).

2. Effect of temperature on the rate of diffusion.

Kinetics of adsorption in terms of G_t as a function of $\sqrt{t}$, where G_t is the amount of adsorption at time t, was studied in detail for mononuclear aromatic compounds (cumene, dodecylbenzene), dinuclear compounds (naphthalene, 1 methylnaphthalene, 1-3 dimethylnaphthalene) and trinuclear compounds (dibenzothiophene, phenanthrene, fluorene and dibenzofuran). NaX zeolite crystals were used at two temperatures, 303 and 343 K, and at initial concentrations of ~ 30 g/L for the mono and the dinuclear hydrocarbons and ~ 20 g/L for the trinuclear species.

The rate of adsorption at 343 K was rapid and equilibrium was reached within several hours. With cumene the equilibrium was reached within 5.4 ks whilst with dodecylbenzene equilibrium was reached after just 3.6 ks. With naphthalene, 1-methylnaphthalene and 1-3-dimethylnaphthalene, it took 5.4, 14.4, 3.6 ks respectively to approach equilibrium. In the case of trinuclear compounds all of them took 23.4 ks to reach equilibrium except phenanthrene which took 176.4 ks.

The rate of adsorption at 303 K was slower and therefore more time was required to reach equilibrium. For cumene it took 14.4 ks and remained steady up to the measurement at 86.4 ks. With dodecylbenzene equilibrium was reached after 48.6 ks and a slight decrease was shown after 86.4 ks. Naphthalene, 1-methylnaphthalene and 1-3 dimethylnaphthal-

ene had reached equilibrium after 86.4, 86.4 and 50 ks respectively the rate of adsorption decreased with further times. In the case of dibenzothiophene and phenanthrene it required 54 ks and with fluorene and dibenzofuran 90 ks to reach equilibrium.

Figures 7.1 and 7.2 show typical kinetic curves for adsorption, G_t mole/kg and g/g, versus $\sqrt{t}$ for cumene and dodecylbenzene in isooctane on NaX zeolite at 303 K. Since dodecylbenzene has a larger critical molecular diameter it diffuses much more slowly than cumene; thus the maximum equilibrium adsorbance was 1.15 mole/kg for cumene whilst for dodecylbenzene it was only 0.52 mole/kg. In the case of dodecylbenzene this could be due to steric hindrance restricting its passage into the pores. The effect of increasing the temperature from 303 to 343 K, is shown in Figures 7.3 and 7.4, for the kinetic adsorption G_t mole/kg and g/g for cumene and dodecylbenzene from isooctane at 343 K on NaX zeolite pellets. Figure 7.3 shows that the maximum adsorption value for cumene was 1.15 mole/kg; for dodecylbenzene it was 0.52, i.e. slightly higher than at 303 K.

Temperature does not appear to have a great influence on adsorption value in the case of monoaromatics, but as mentioned earlier, affects the time to reach equilibrium. Maximum equilibrium was reached within 5.4 ks at 343 K for cumene; at 303 K it was reached after 14.4 ks for the same inlet concentration.

For dodecylbenzene, maximum equilibrium was approached within 3.6 ks at 343 K and within 48.6 ks at 303 K. This could be due to the temperature-dependence of the energy of interactions. Increasing the temperature from 303 to 343 K enhanced the mobility of the molecules towards the molecular sieves pores. This accelerated the interactions between the bonds of the adsorbate molecules and the electrostatic charge of the zeolite crystals resulting in a more rapid approach to equilibrium. Of greatest interest is the time dependence of the relative adsorption G_t/G_∞ (where G_t is the adsorption at the moment of time t; G_∞ is the equilibrium adsorption). This relationship expresses the degree of the saturation of the sorption capacity at any given time. For the adsorption of aromatic hydrocarbons from binary solutions with isooctane, the relationship between the G_t/G_∞ and $\sqrt{t}$, at temperatures of 303 and 343 K are illustrated in Figures 7.5 and 7.6. These show that the adsorption kinetics at intermediate degrees of coverage of the zeolite void spaces follow a lin-
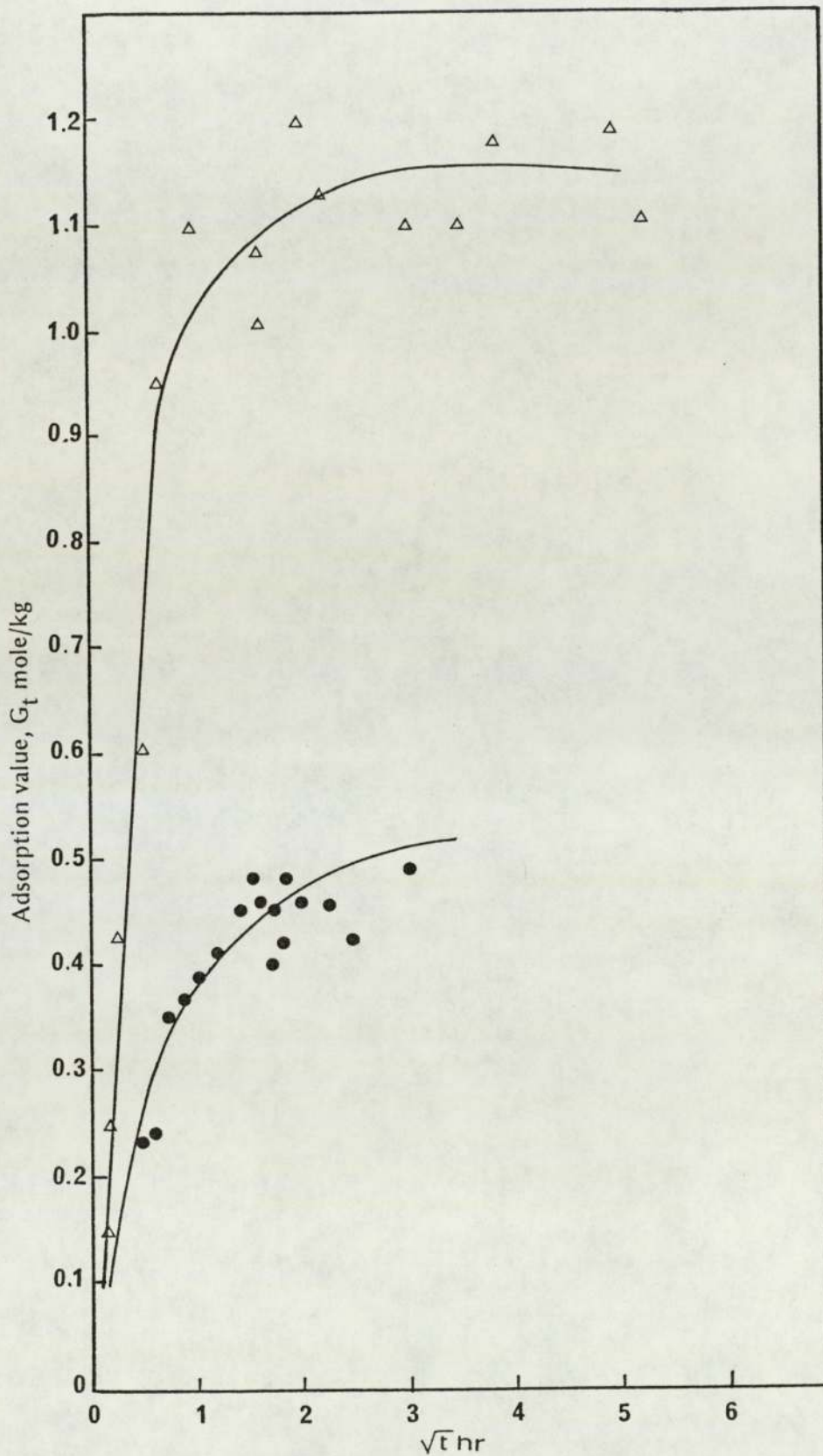
Figure 7.1   Kinetic Curve for Adsorption
G_t mole/kg for △ Cumene and
● Dodecylbenzene from
Isooctane at 303 K on
NaX Zeolite Pellets.
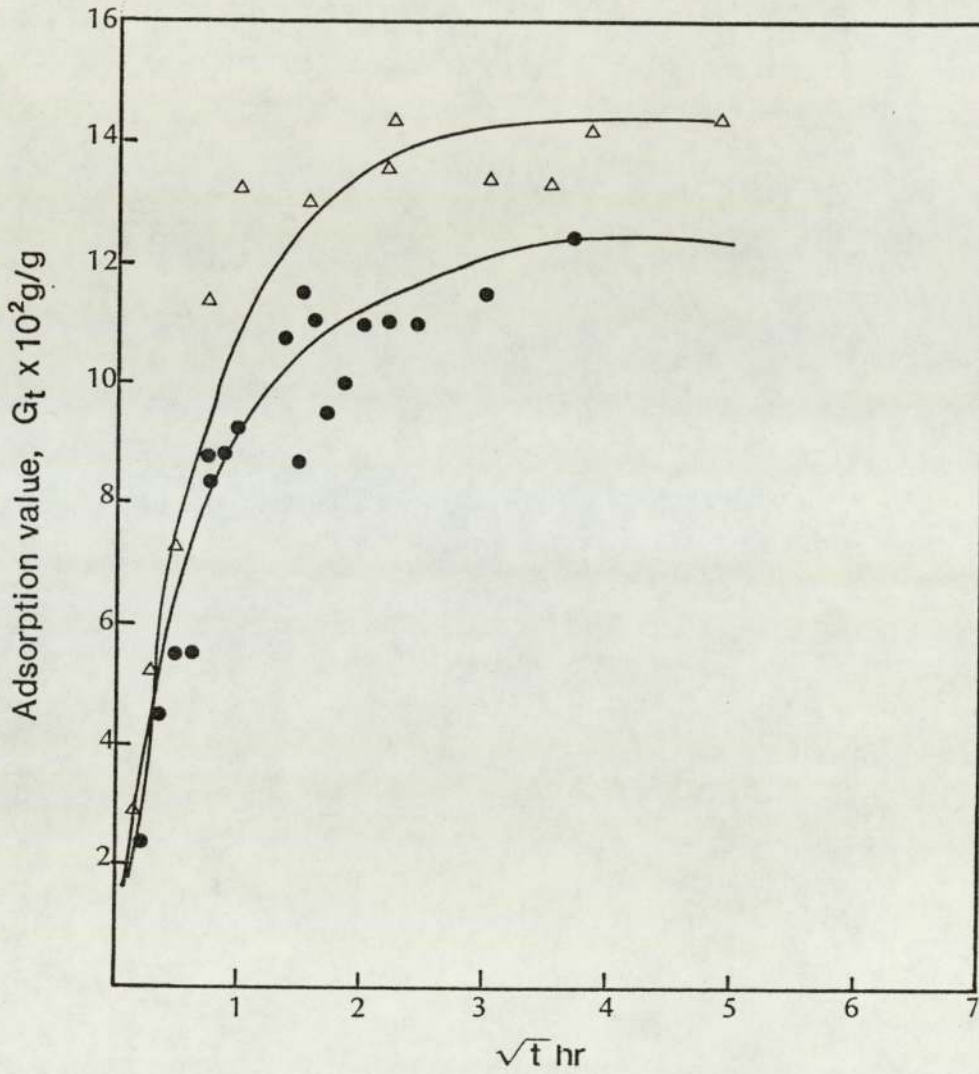
Figure 7.2   Kinetic Curve for Adsorption
             G_t g/g for △ Cumene and
             ● Dodecylbenzene from
             Isooctane at 303 K on
             NaX Zeolite Pellets.
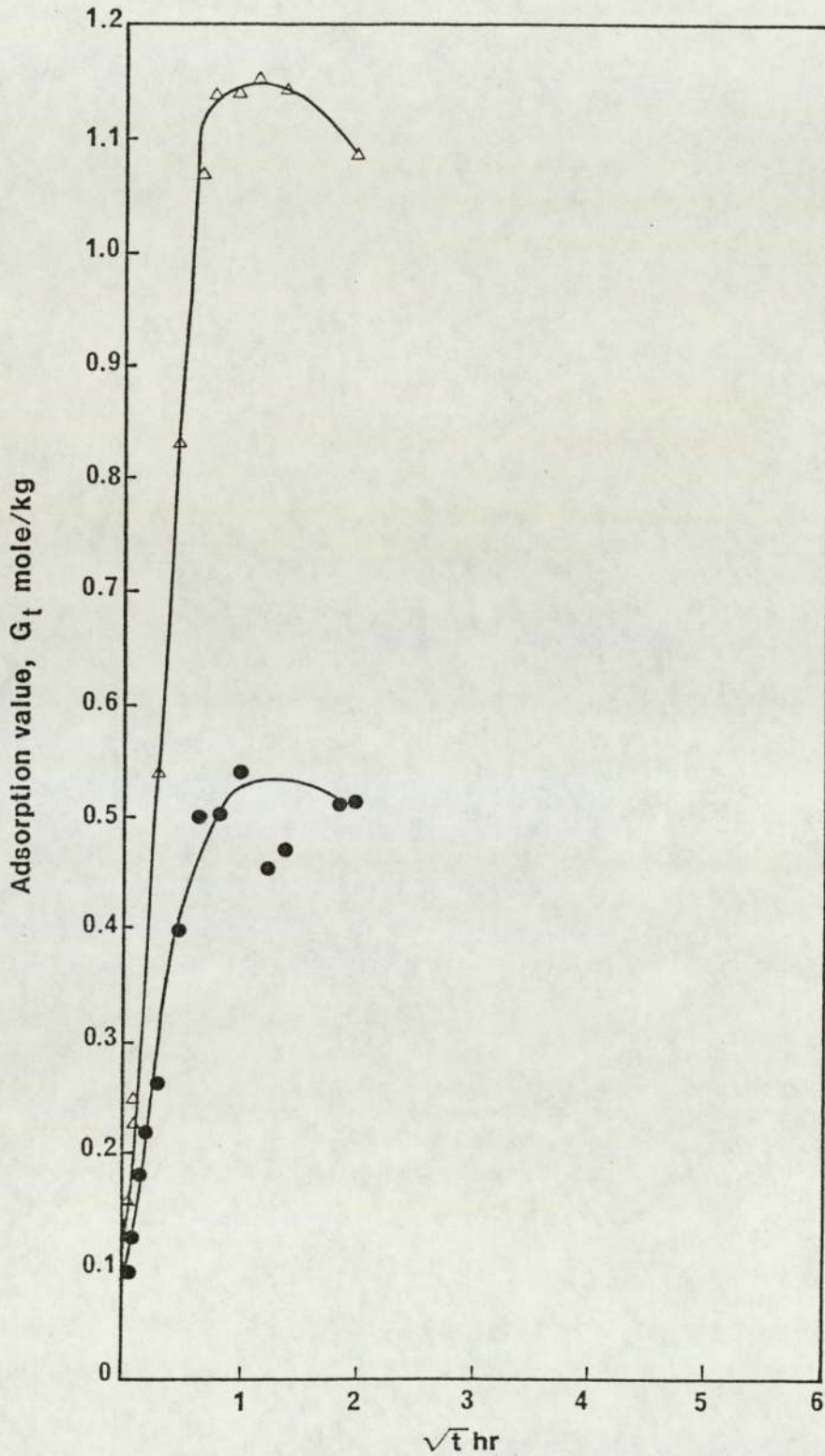
Figure 7.3   Kinetic Curve for
              Adsorption G_t mole/
              kg for △ Cumene and
              ● Dodecylbenzene
              from Isooctane at
              343 K on NaX
              Zeolite Pellets.
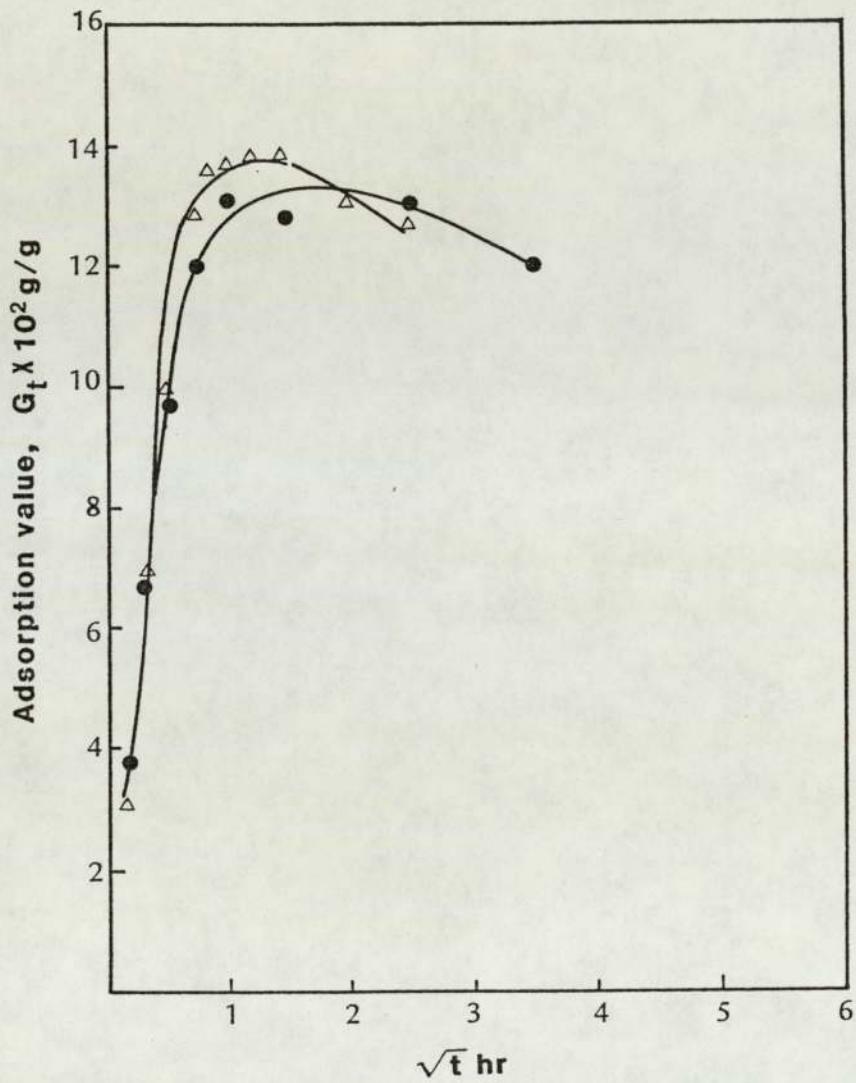
Figure 7.4   Kinetic Curve for
Adsorption G_t g/g
for △ Cumene and
● Dodecylbenzene
from Isooctane at
343 K on NaX
Zeolite Pellets.

ear relationship, i.e., the kinetics are determined by the rate of internal diffusion. Figures 7.5 and 7.6 show that equilibrium points for cumene and dodecylebenzene can be achieved at temperature 343 K faster than at 303 K, i.e., the rate of adsorption increases with increase in the temperature.

The rate of adsorption depends on the rate of diffusion of the sorbate component to the activated molecular sieve crystals, the relative size of the molecule and pores, the strength of the adsorptive forces, and the temperature. The sorption rate decreases with increasing molecular weight of adsorbate molecules as shown in Figure 7.7. The rate of adsorption for cumene is higher than that for dodecylbenzene, and this affects the loading capacity of the adsorbate molecules. At higher temperatures, the rate of sorption is higher, but the capacity of the molecular sieves is reduced. At 303 K, as shown in Figure 7.7 the rates of adsorption for cumene and dodecylbenzene were lower than that for the same components at 343 K (Figure 7.8).

Because of their industrial importance diffusion in zeolites has been extensively studied. For diffusion of hydrocarbons in open structures of the X and Y zeolites only very limited data are available, although such information is of considerable practical importance in view of the widespread use of zeolites as cracking catalysts.

Figures 7.9 and 7.10 show effective diffusivities plotted against coverage rate for cumene and dodecylbenzene at 303 and 343 K. At 303 K the diffusivity initially increased gradually with coverage rate both for cumene and dodecylbenzene; it reached a maximum at coverage rate of 0.6, then decreased to equilibrium to a minimum with De 3.4 x 10^{-12} m^2/s for cumene and 1.1 x 10^{-12} m^2/s for dodecylbenzene at 303 K. The maximum De values were 18.5 x 10^{-12} and 10.5 x 10^{-12} m^2/s respectively.

Figure 7.10 shows that at 343 K the diffusivity reached a maximum at a coverage rate 0.47 then decreased to reach equilibrium for cumene at 9-13 x 10^{-12}, and for dodecylbenzene at 13.6 x 10^{-12} m^2/s. The diffusivity for cumene molecules was higher than for dodecylbenzene at 343 K. This can be attributed to the smaller critical diameter of cumene compared with the dodecylbenzene molecule, in which the benzene ring is shielded with a long alkylchain which prevents it penetrating easily through the molecular sieves pores. With temperature increase from 303 K to 343 K the
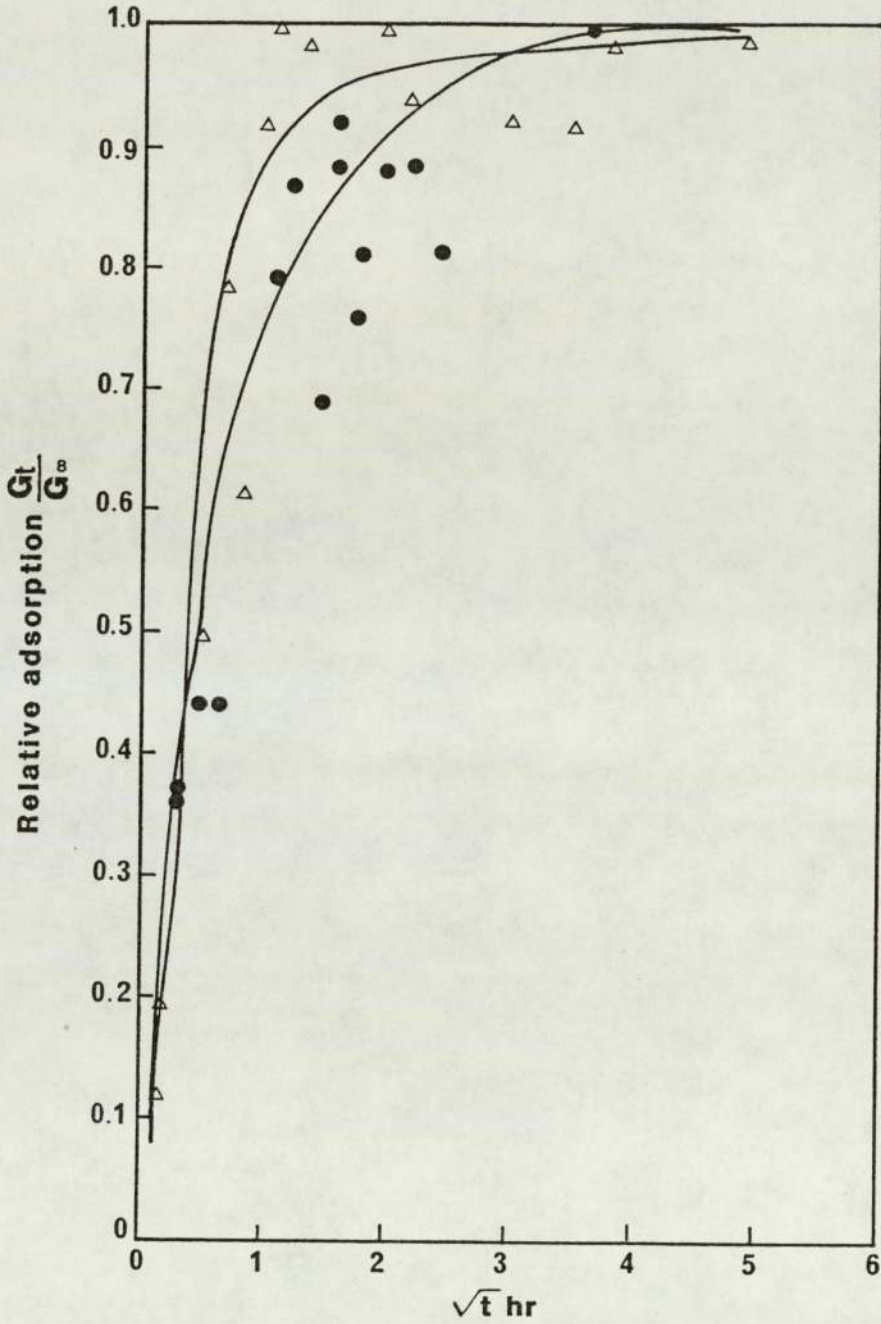
Figure 7.5   Kinetics of Relative
            Adsorption $\frac{G_t}{G_\infty}$ of
            △ Cumene and
            ● Dodecylbenzene
            from Isooctane at
            303 K on NaX Zeolite
                Pellets.
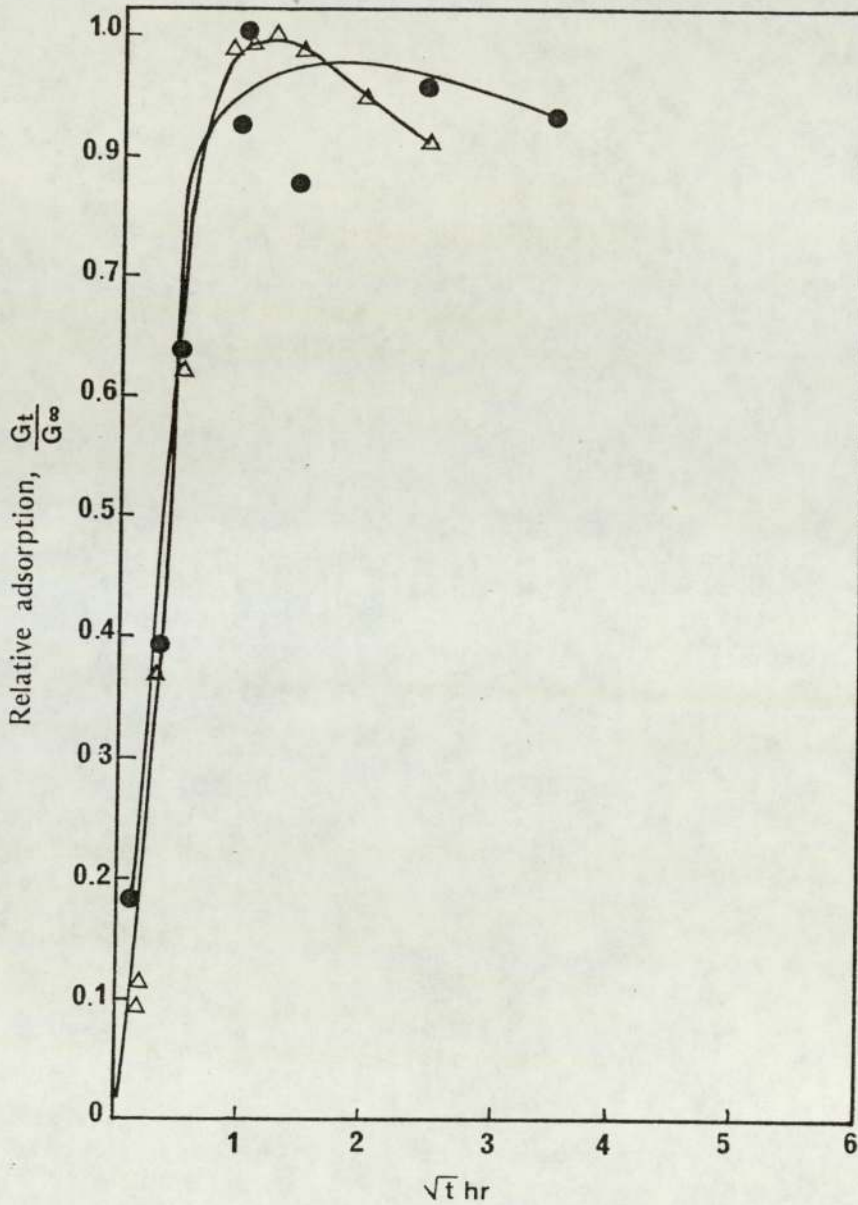
Figure 7.6 Kinetics of Relative
Adsorption $\frac{G_t}{G_\infty}$ of
△ Cumene and
● Dodecylbenzene
from Isooctane at
343 K on Nax Zeolite
Pellets.
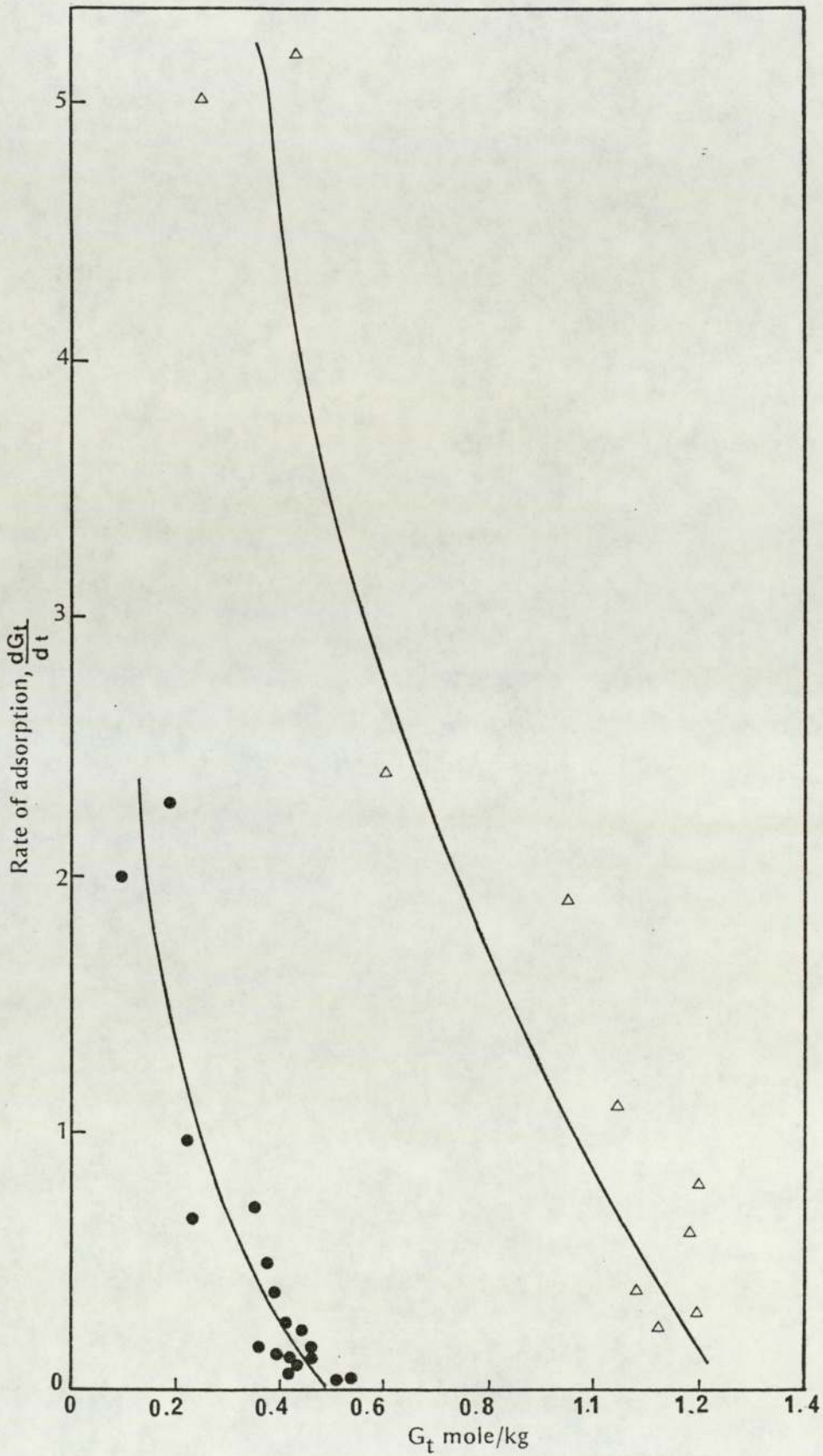
Figure 7.7   Rate of Adsorption $\dfrac{dG_t}{dt}$ of
△ Cumene and   ● Dodecyl-
benzene at 303 K NaX
Zeolite Pellets.
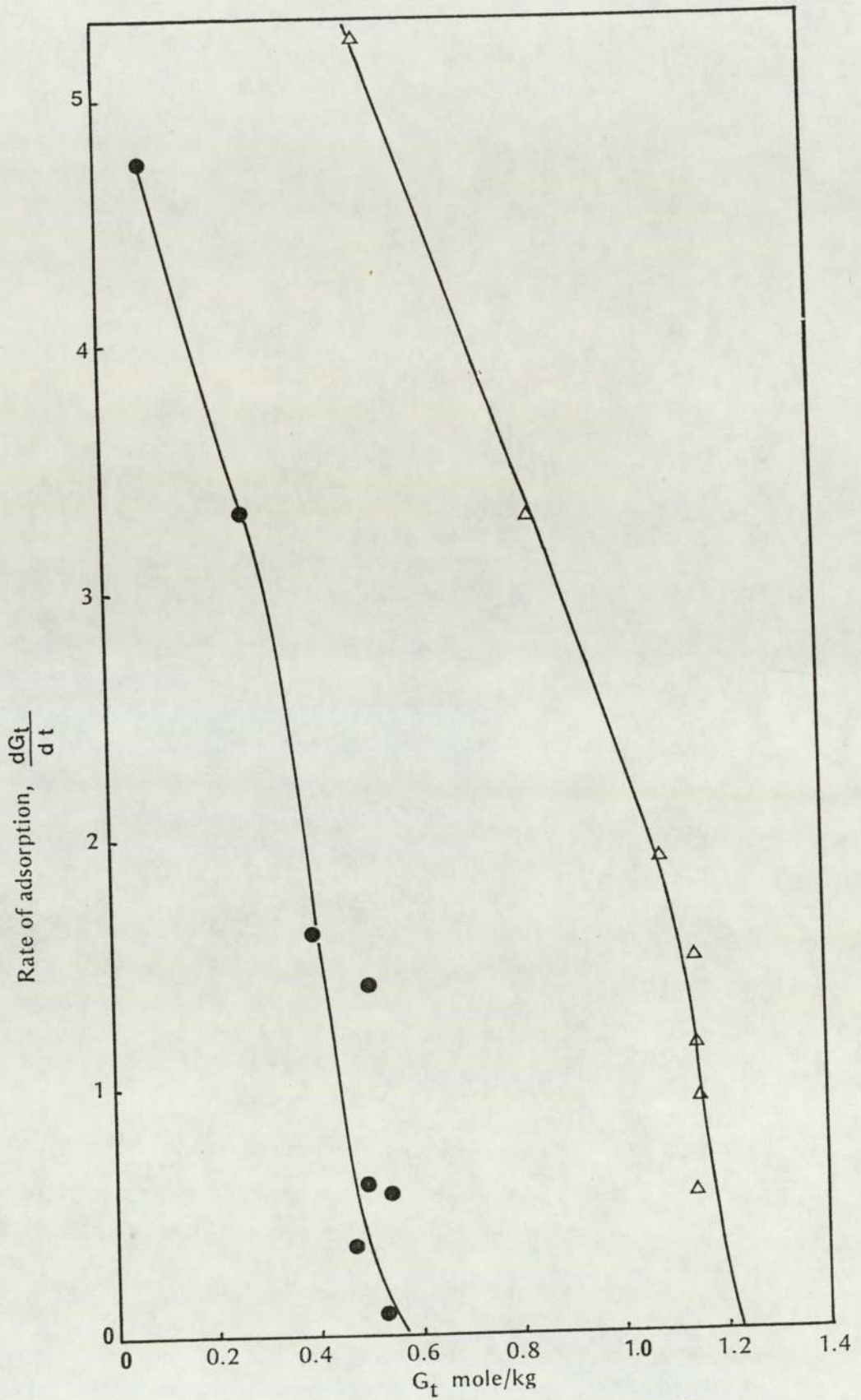
Figure 7.8   Rate of Adsorption $\frac{dG_t}{dt}$ of
$\triangle$ Cumene and $\bullet$ Dodecyl-
benzene at 343 K on NaX
Zeolite Pellets.
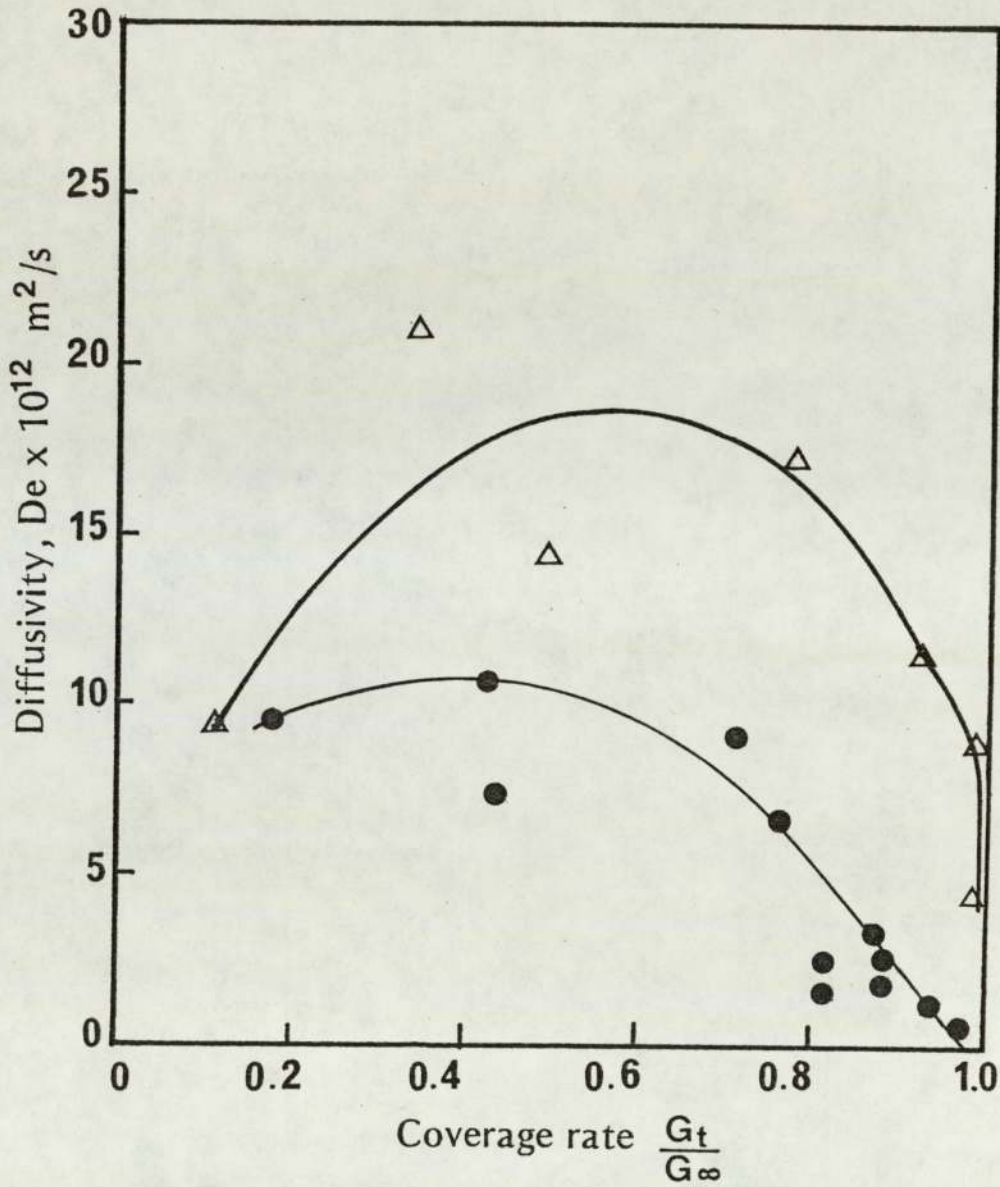
Figure 7.9   Effective Diffusion
Coefficient De of
△ Cumene and ● Do-
decylbenzene as a
Function of Degree
of Coverage Rate $\frac{G_t}{G_\infty}$
at 303 K on NaX
Zeolite Pellets.
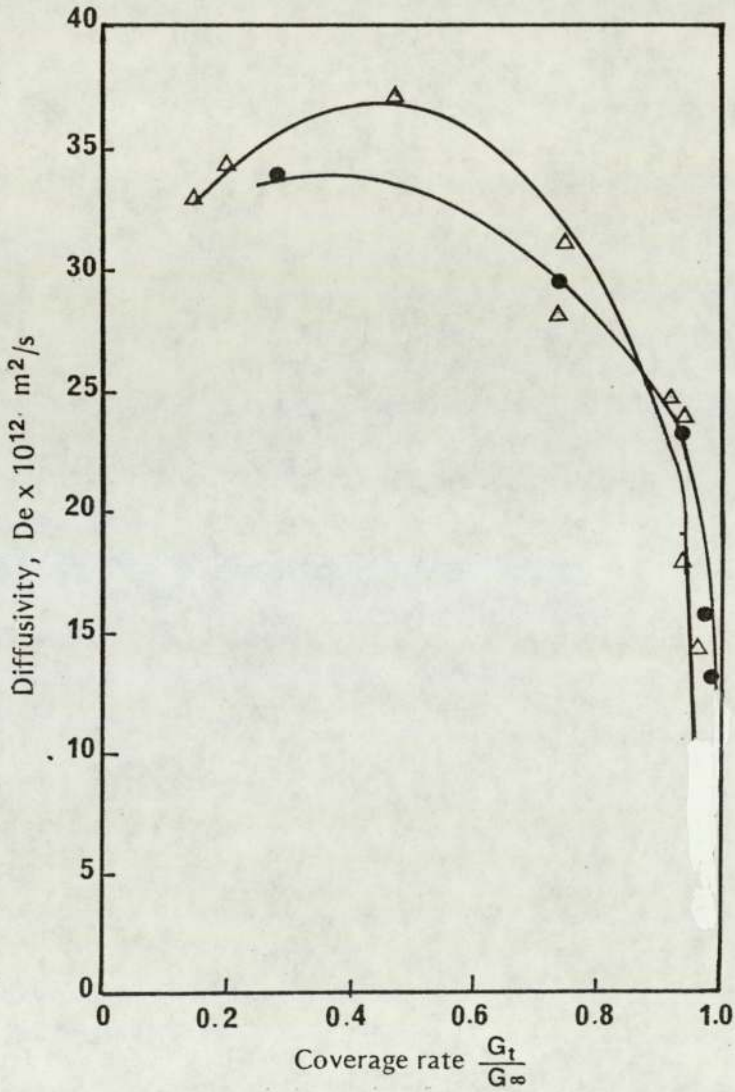
Figure 7.10   Effective Diffusion
                Coefficient De of
                $\triangle$ Cumene and $\bullet$ Do-
                dectlbenzene as a
                Function of Degree
                of Coverage Rate
                $\frac{G_t}{G_\infty}$ at 343 K on NaX
                Zeolite Pellets.

orientation factor apparently played a major role in the case of dodecylbenzene where the diffusivity increased to 13.6×10^{-12} at equilibrium. At lower coverage rates the diffusivity reached a maximum of 37×10^{-12} m^2/s for cumene, and slightly lower, 34×10^{-12} m^2/s for dodecylbenzene.

It has been suggested that when the diffusing molecule is large relative to the sieve aperture, the dominant diffusion mechanism involves single activated jumps between cages. When the molecule is relatively small, a multiple jump mechanism becomes dominant (53), (45).

Breck (1) studied the diffusion coefficient for different types of hydrocarbons such as CH_4 and $n-C_4H_{10}$ on synthetic sodium zeolite at temperature 25 K. The diffusion coefficients were found to decrease with increasing molecular size: hence the diffusion coefficient for cumene with a short alkyl chain would be expected to be more than for dodecylbenzene which is shielded with a long alkyl chain ($C_{12}H_{25}$). Adsorption kinetics and diffusion of cumene at 303 K over molecular sieves type NaY were studied by Satterfield and Cheng (42). They found that the diffusion coefficient at coverage rate $G_t/G_\infty = 0.3$ was equal to $>700 \times 10^{-17}$ m^2/s. By comparison the diffusion coefficient for cumene at 303 K at $G_t/G_\infty = 0.3$ in the present study using molecular sieves type NaX was equal to 15.5×10^{-12} m^2/s, (see Table 7.1). Therefore, the ratio of Si/Al in the molecular sieves has a major effect on the kinetics of adsorption; the increase in the ratio of Si/Al leads to a decrease in the diffusion coefficient: for NaY and NaX the ratios of Si/Al are 1.5-3 and 1-1.5 respectively. Hence the filler in the molecular sieves significantly affects the kinetics of adsorption.

In the case of the naphthalene group, Figures 7.11 and 7.12 illustrate kinetic curves for adsorption G_t mole/kg and g/g vs $\sqrt{t}$ for naphthalene 1, methylnaphthalene and 1-3 dimethylnaphthalene at 303 K. It appears that the maximum equilibrium adsorbance were 1.0, 0.6, and 0.47 mole/kg respectively. The higher rate of adsorption for naphthalene in comparison with 1, methyl and 1,3 dimethylnaphthalene can be attributed to the strong interaction between the bond of the two adjacent rings of naphthalene and the cationic charge of the zeolite.

The presence of one methyl group decreases the negativity of the electron charge of the π bond of the two adjacent rings thus weakening the interaction between the 1, methylnaphthalene molecules and the cation of the zeolite lattice.
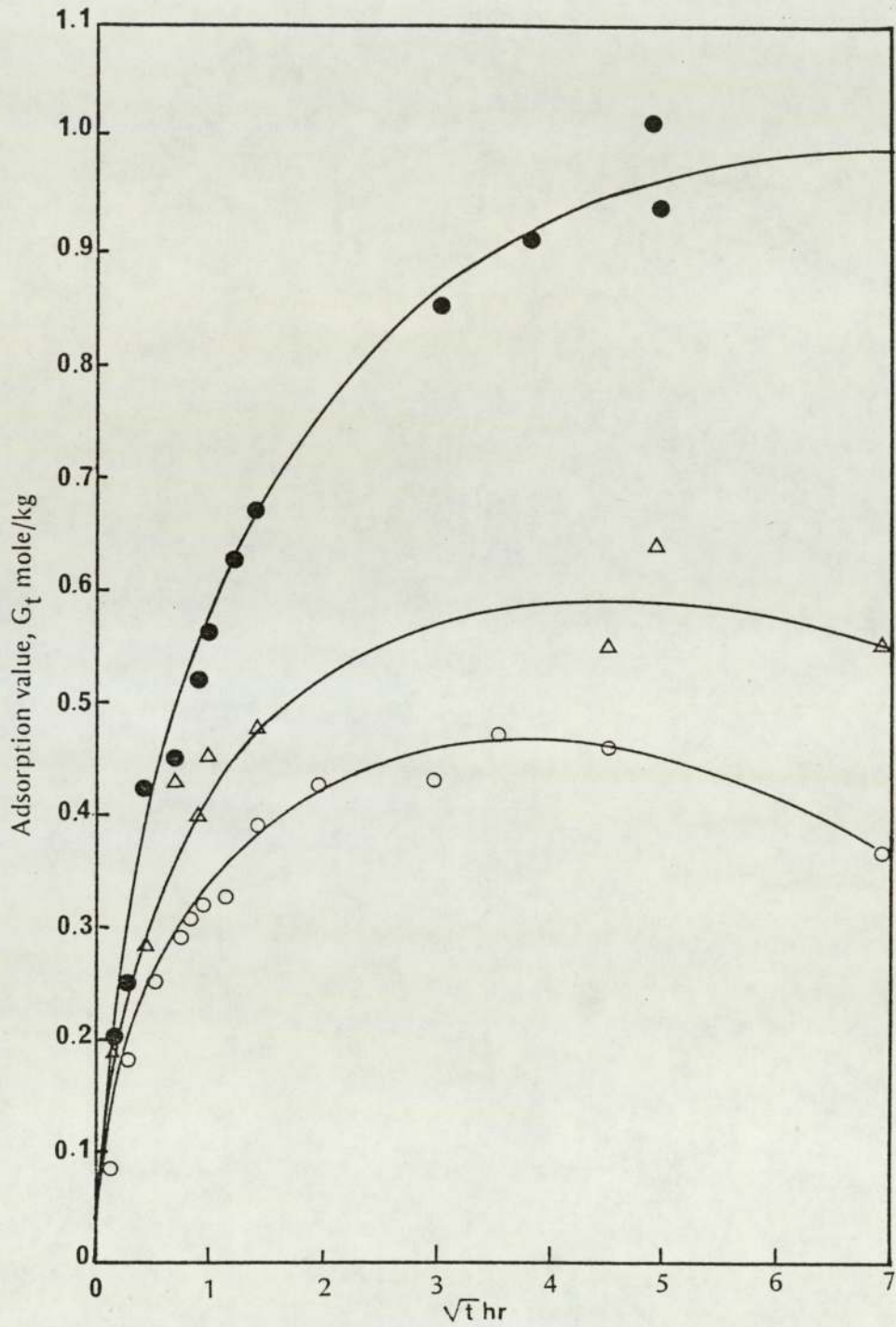
Figure 7.11   Kinetic Curve for Adsorption
G_t mole/kg for ● Naphthalene,
△ 1-Methylnaphthalne,
○ 1-3 Dimethylnaphthalene
from Isooctane at 303 K on
Nax Zeolite Pellets.
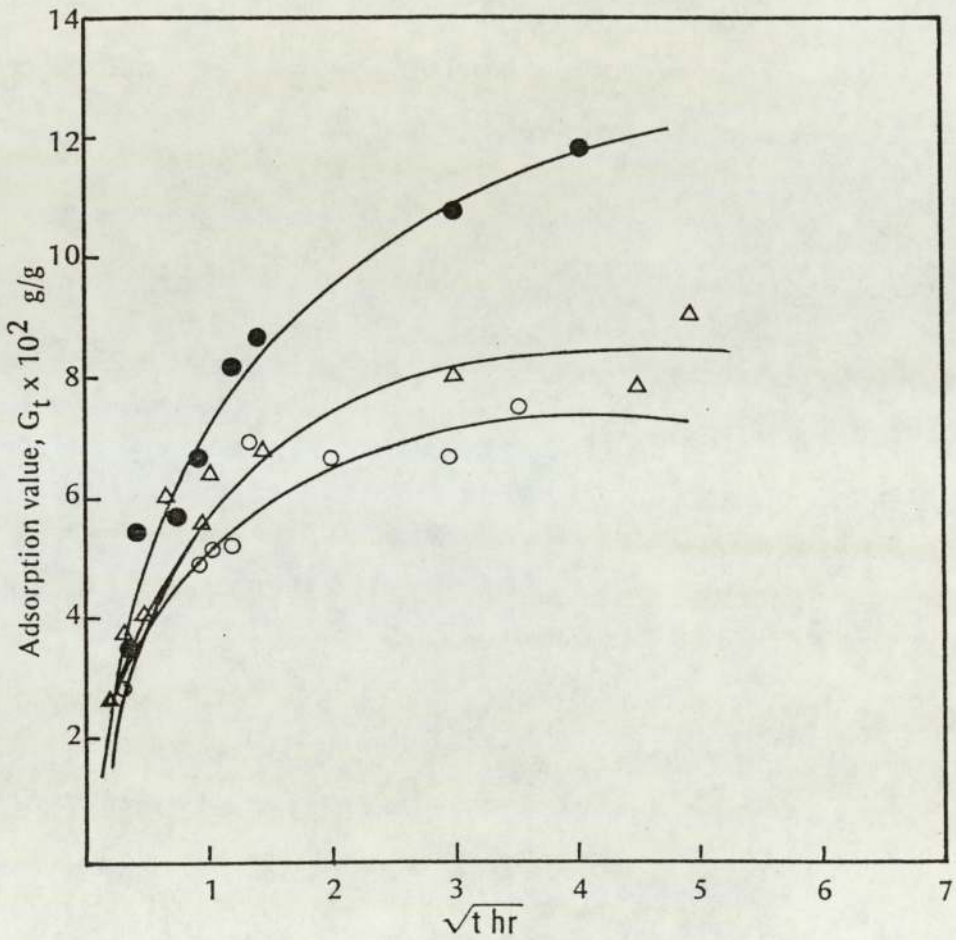
Figure 7.12 Kinetic Curve for Adsorption
G_t g/g for ● Naphthalene,
△ l-Methylnaphthalene, and
○ l-3 Dimethylnapthalene
from Isooctane at 303 K on
Nax Zeolite Pellets.

The presence of two methyl groups in 1, 3 dimethylnaphthalene results in a reduction in the adsorption value to a greater extent (0.47 mole/kg) due to more delocalization of the negative charge in the naphthalene ring.

Figures 7.13 and 7.14 show kinetic adsorption G_t mole/kg and g/g for naphthalene, 1, methylnaphthalene and 1, 3 dimethylnaphthalene at 343 K on NaX zeolite pellets. It is clear that the maximum adsorption values for the three components were much higher at 343 K, than at 303 K. They were attained more rapidly, and the equilibrium declined rapidly with time after reaching maximum equilibrium.

For naphthalene the maximum adsorption value was 1.3 mole/kg; this was reached within 5.4 ks whereas at 303 K it was reached after 86.4 ks. In the case of 1, methylnaphthalene the maximum equilibrium value of 0.91 mole/kg was approached after 14.4 ks, whilst at 303 K it was approached after 86.4 ks. For 1,3 dimethylnaphthalene equilibrium was approached after 3.6 ks but took 50 ks at 303 K; the maximum adsorption value was 0.7 mole/kg at 343 K whilst it was 0.47 mole/kg at 303 K.

Decrease in time to reach equilibrium and the increase in the maximum adsorption value with temperature increase can be explained in terms of increasing mobility of the molecules in the solution, thus increasing the diffusivity of such molecules to pass into the molecular sieve pores. The interactions created between the bonds of the adsorbate molecules and the high energy electrostatic charges of the zeolite crystals allow more molecules to migrate from the isooctane solutions through the windows of the molecular sieves pores. Hence an increase in the adsorption value and a decrease in the time to reach equilibrium can be achieved by increasing the temperature to a certain limit.

Figures 7.15 and 7.16 illustrate kinetic data for the adsorption of naphthalene, 1, methylnaphtalene and 1, 3 di-methylnaphthalene at 303 and 343 K in terms of G_t/G_∞ as a function of $\sqrt{t}$. These show that the rate of adsorption of the naphthalene group at 303 K was not a linear function and was slower than at 343 K.

The filling rate of the naphthalene group at 343 K was very rapid and reached a maximum more rapidly than at 303 K. This can be attributed to the increase in the temperature activating the hydrocarbons, thus facilitating penetration of the adsorbate molecules into the cavities of the molecular sieve crystals, because the intracrystalline diffusion rates increase with increasing temperature.
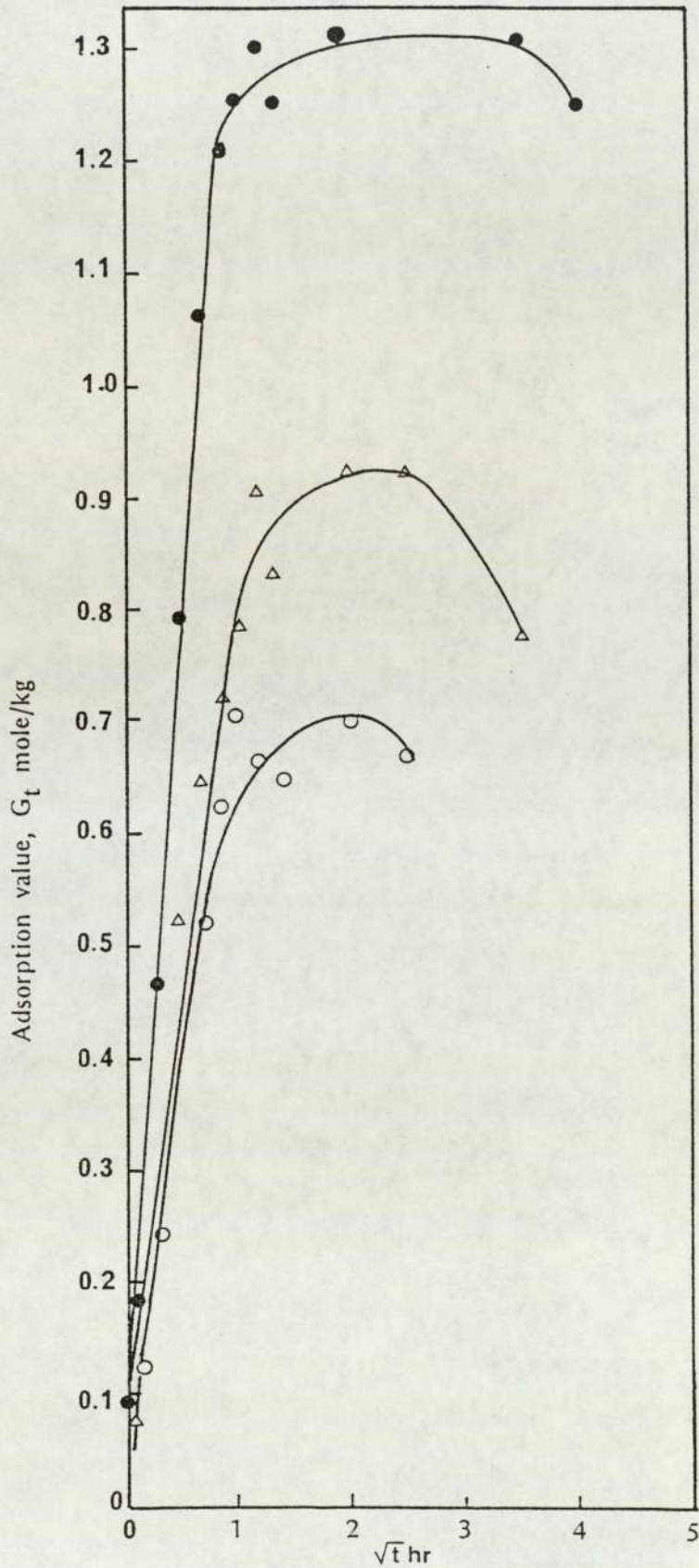
Figure 7.13 Kinetic Curve for
Adsorption G_t mole/
kg for • Naphthalene,
△ l-Methylnaphthalene
and o 1-3 Dimethyl-
naphthalene from Iso-
octane at 343 K on NaX
Zeolite Pellets.
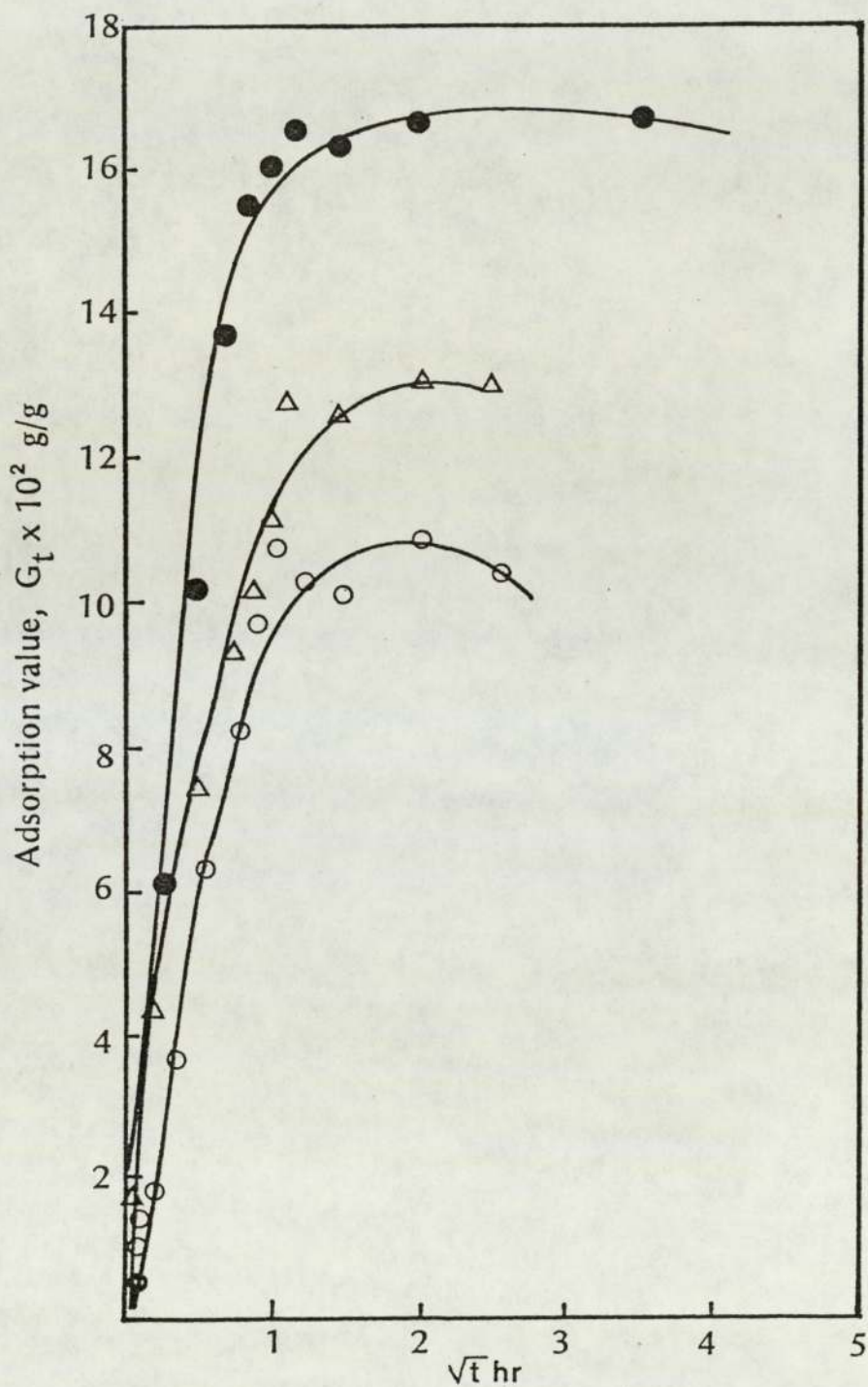
Figure 7.14   Kinetic Curve for
Adsorption G_t g/g
for ● Naphthalene,
△ 1-Methylnaphthalene,
and ○ 1-3 Dimethyl-
naphthalene from Iso-
octane at 343 K on NaX
Zeolite Pellets.
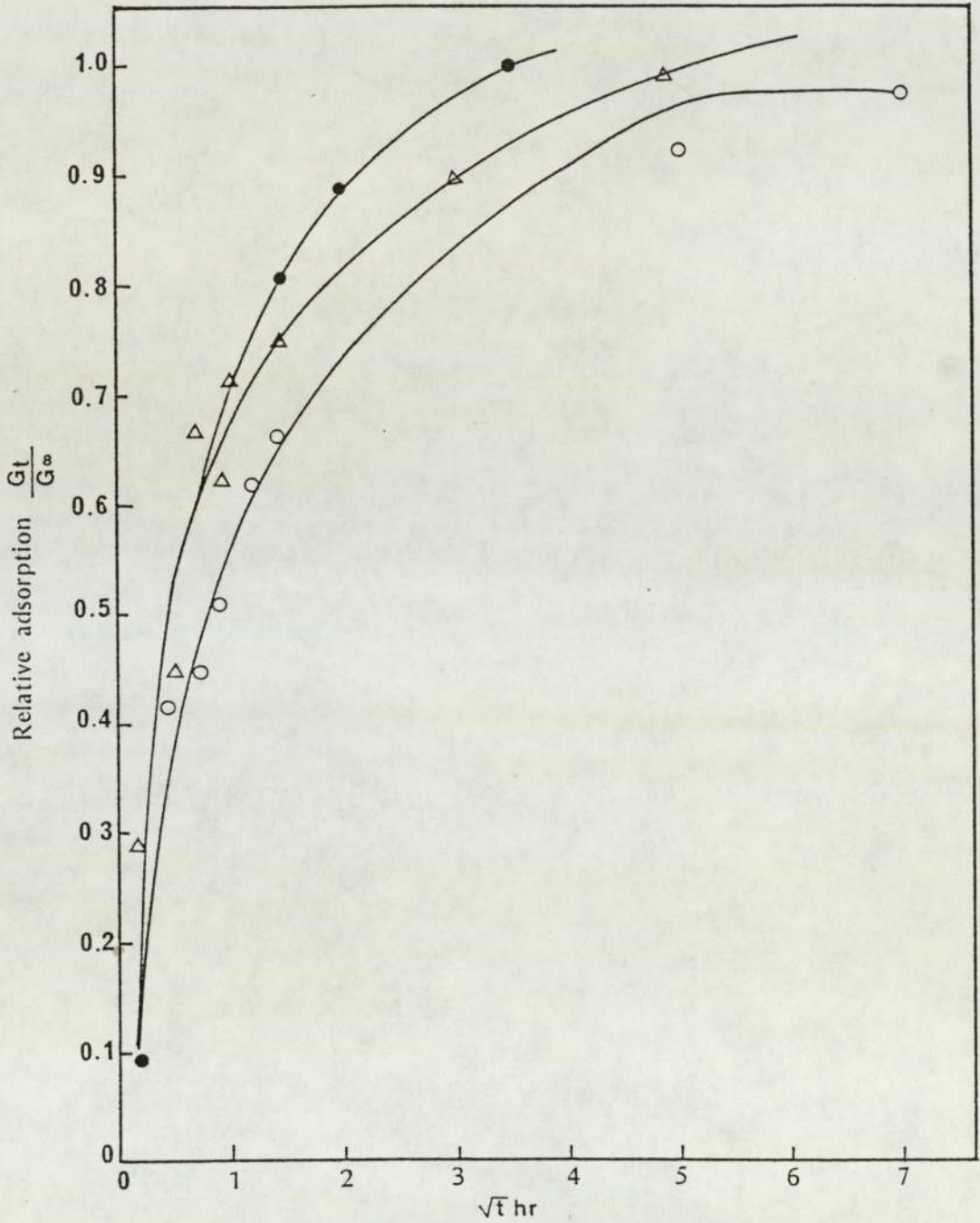
Figure 7.15   Kinetics of Relative Adsorption
$\frac{G_t}{G_\infty}$ of ● Naphthalene, △ 1-Methyl-
naphthalene and ○ 1-3 Dimethyl-
naphthalene from Isooctane at
303 K on NaX Zeolite Pellets.
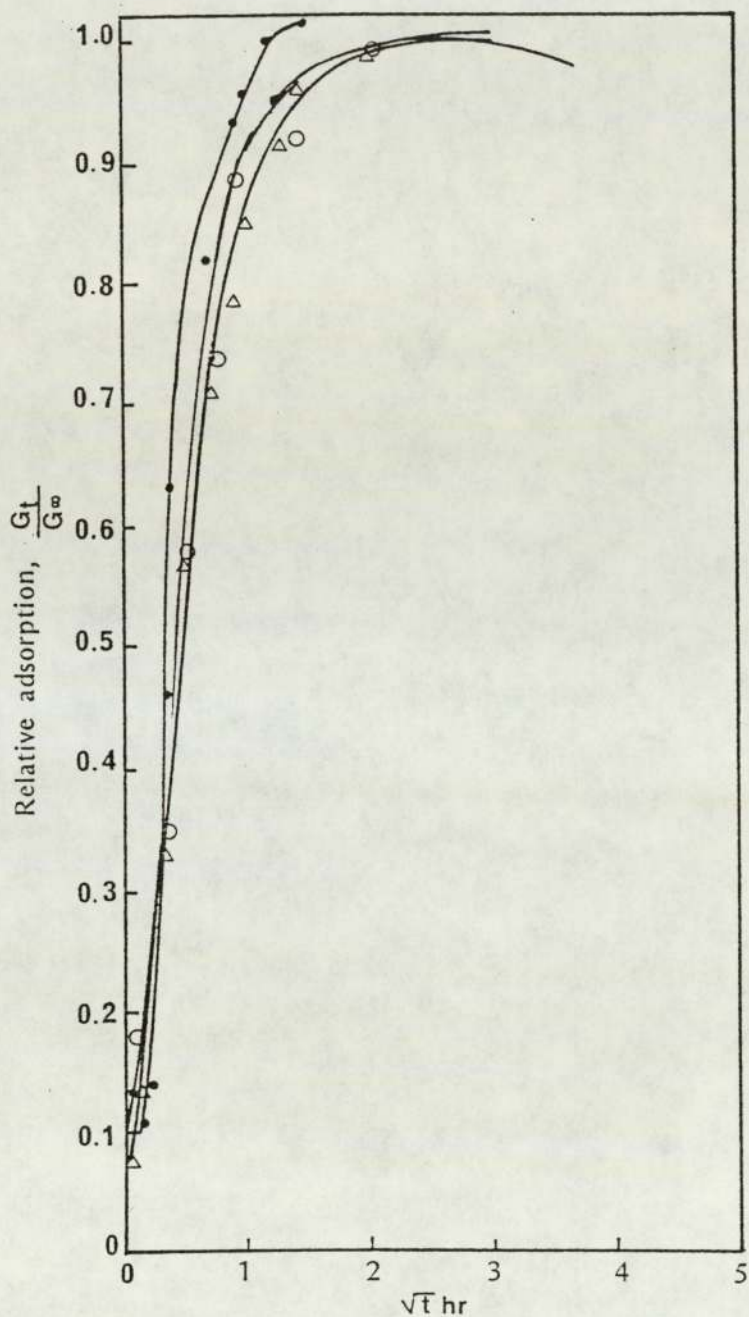
Figure 7.16   Kinetics of Relative

Adsorption $\frac{G_t}{G_\infty}$ of

•Naphthalene, △
1-Methylnaphthalene
and o 1-3 Dimethyl-
naphthalene from
Isooctane at 343 K on
NaX Zeolite Pellets.

Whilst there are numerous publications concerned with adsorption kinetics and diffusion in the various ion forms of zeolite A and Y, little is known about kinetic adsorption of aromatic compounds in zeolite type X (NaX). Illustrative data for determination of the rate of adsorption of different types of naphthalene groups using molecular sieves type NaX at different temperatures 303 and 343 K are shown in Figures 7.17 and 7.18. The rate of the adsorption dG_t/dt of naphthalene, 1-methylnaphthalene, and 1,3 dimethylnaphthalene increased rapidly with increasing temperature during initial packing of the molecular sieves. As shown in Figures 7.17 and 7.18 the rate of adsorption of the naphthalene group decreased with increasing adsorption value. This indicates that the packing of the voids of the cavities of the molecular sieves crystal significantly affects the rate of adsorption. The first packing stage will be in the form of a monolayer which is followed by multilayers of packing. The thick package of adsorbate molecules will eventually close the aperture cavities, thus hindering penetration of sorbate molecules through the cavities of the molecular sieves. This will lead to a decrease in the rate of adsorption.

Increase in temperature will result in more rapid packing of the adsorbate molecules in the molecular sieve crystals. Figures 7.17 and 7.18 show that the best packing in the cavities is for naphthalene, then 1-methylnaphthalene followed by 1,3-dimethylnaphthalene. This action can be attributed to the interactions between the π-bond of naphthalene with the electrostatic charge on a site within a molecular sieve. When the naphthalene ring is shielded by one or two methyl groups the interactions will be weakened. The kinetics of sorption have been studied for mononuclear aromatic hydrocarbons such as cumene and dodecylbenzene, and values have been obtained for diffusion coefficients of these hydrocarbons. It is of interest in this work to study the diffusion resistance of some aromatic hydrocarbons which have large molecular diameter such as naphthalene, 1-methylnaphthalene, and 1,3-dimethylnaphthalene. Figures 7.19 and 7.20 illustrate the dependence of diffusion coefficient on the rate of adsorption for naphthalene, 1-methylnaphthalene, and 1,3-dimethylnaphthalene at temperatures of 303 and 343 K. The diffusion coefficients have been determined using the formula of Barrer and Brook, equation 7.18, taking into account the granule shape and the particle size of the adsorbent. At the lower values of coverage rate the diffusion coefficient was lower
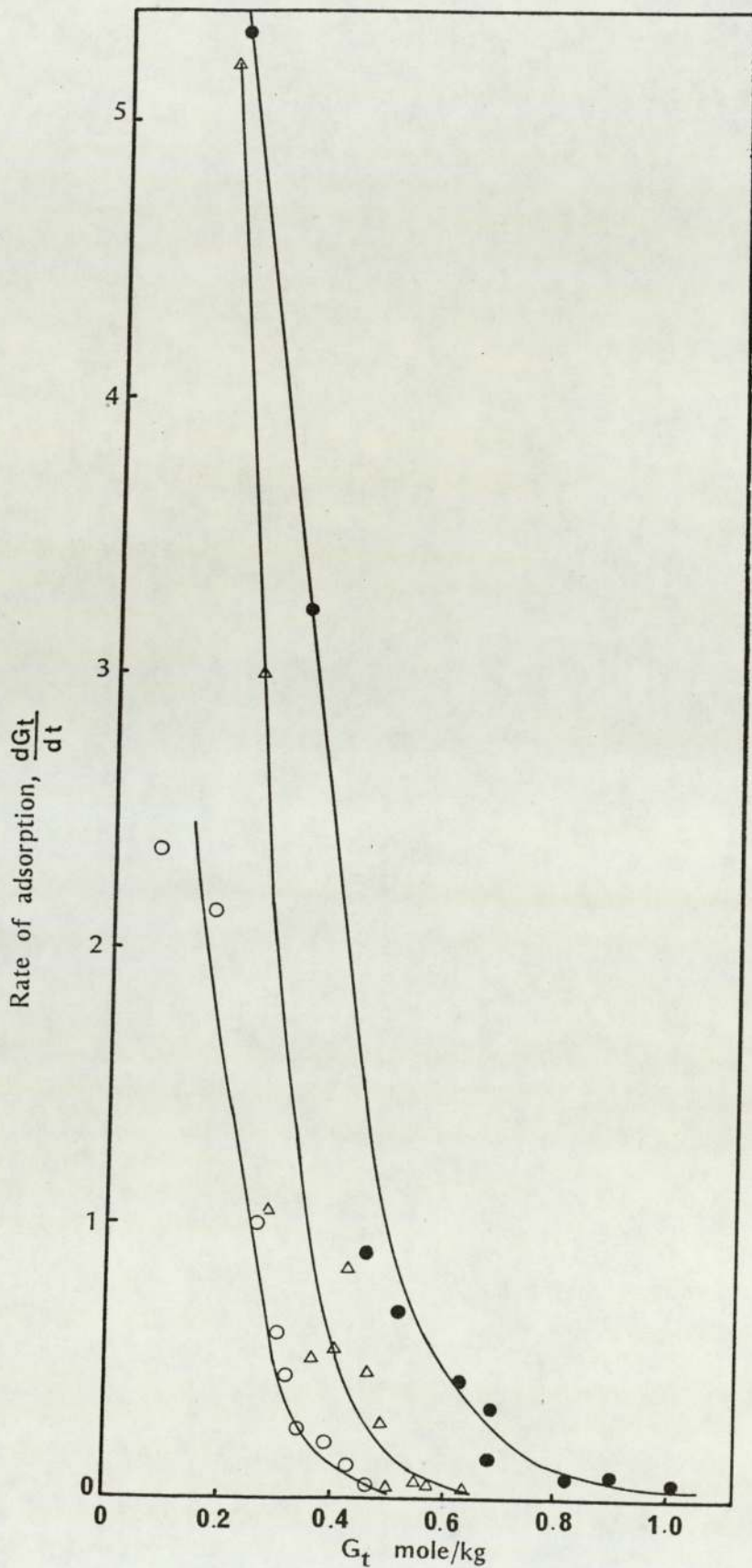
Figure 7.17   Rate of Adsorption $\dfrac{dG_t}{dt}$
of ● Naphthalene,
△ 1-Methylnaphthalene
and o 1-3 Dimethyl-
naphthalene at 303 K on
NaX Zeolite Pellets.
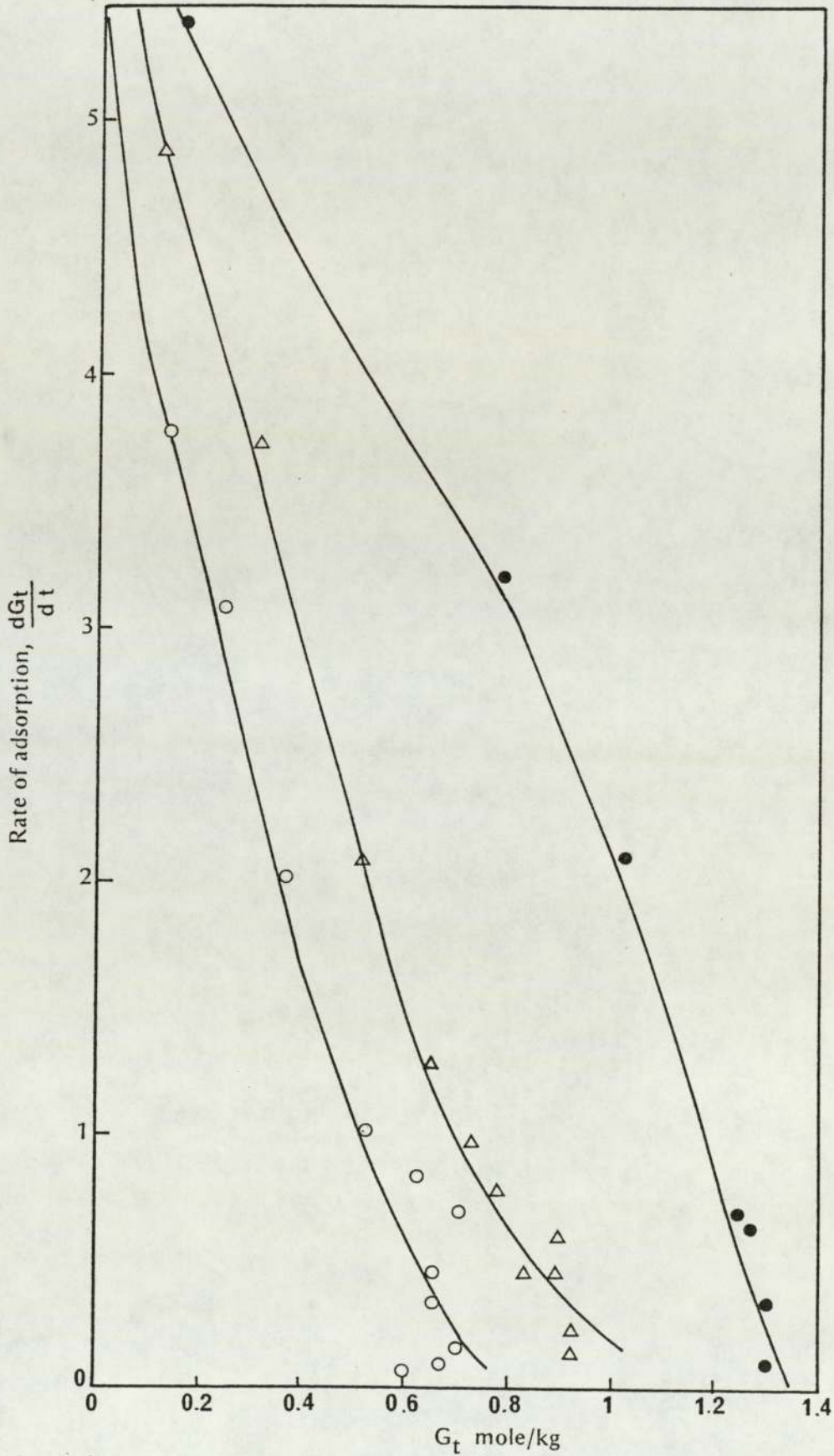
Figure 7.18 Rate of Adsorption $\frac{dG_t}{dt}$ of
● Naphthalene, △ 1-Methyl-
naphthalene and O 1-3 Dimethyl-
naphthalene at 343 K on NaX
Zeolite Pellets.

at the higher temperature. Increasing the coverage rate of adsorption resulted in an increase in the diffusion coefficient upto a limit, where the voids of the molecular sieve crystals would be filled < 0.6. The penetration of the adsorbate molecules through the voids of adsorbent crystals would be decreased and this results in a decrease in the diffusion coefficient.

Figure 7.19 illustrates the change of diffusivity versus coverage rate for naphthalene, 1, methylnaphthalene and 1, 3 dimethylnaphthalene at 303 K. With naphthalene there was a regular decrease in the diffusivity as the coverage rate was increased to reach a minimum at equilibrium. Its diffusion rate corresponded to 0.56×10^{-12} m^2/s and maximum diffusivity was observed at 0.19 coverage rate where De corresponds to 14×10^{-12} m^2/s. 1, methylnaphthalene exhibited a rapid decrease in the diffusivity with increasing coverage rate from 33×10^{-12} m^2/s at 0.29 coverage rate passing through a minimum of 0.57×10^{-12} m^2/s as saturation was approached. With 1, 3 dimethylnaphthalene diffusivity increased gradually from 12×10^{-12} m^2/s at 0.18 to reach a maximum intermediate value at 0.375 coverage rate where De corresponds to 23×10^{-12} m^2/s; it then decreased gradually to reach equilibrium where the rate of diffusion was 1.1×10^{-12} m^2/s.

Figure 7.20 demonstrates the change of diffusivity vs coverage rate for naphthalene, 1, methylnaphthalene and 1, 3 dimethylnaphthalene at 343 K. Clearly the three components behaved in a similar manner. Their diffusivities increased gradually to approach an intermediate maximum then fell off gradually to a minimum at equilibrium. The maximum diffusivities for naphthalene, 1, methylnaphthalene and 1, 3 dimethylnaphthalene were 20×10^{-12}, 18.5×10^{-12}; and 31×10^{-12} m^2/s respectively associated with coverage rates of 0.5, 0.33 and 0.57 in each case. The diffusivities at saturation were 3.4×10^{-12}, 3.3×10^{-12} and 3.6×10^{-12} respectively in the same order.

Fal'kovich et al. (18) studied the adsorption kinetics of naphthalene from binary solution with isooctane at 293 K over crystals of binder-free NaX zeolite. The diffusion coefficient of naphthalene at coverage rate $G_t/G_\infty = 0.5$ was reported as 17.0×10^{-11} m^2/s, whereas in the present investigation the diffusion coefficient at 303 K and $G_t/G_\infty = 0.5$ was 6×10^{-12} m^2/s, using molecular sieves type NaX with 20 wt.% of inert filler.
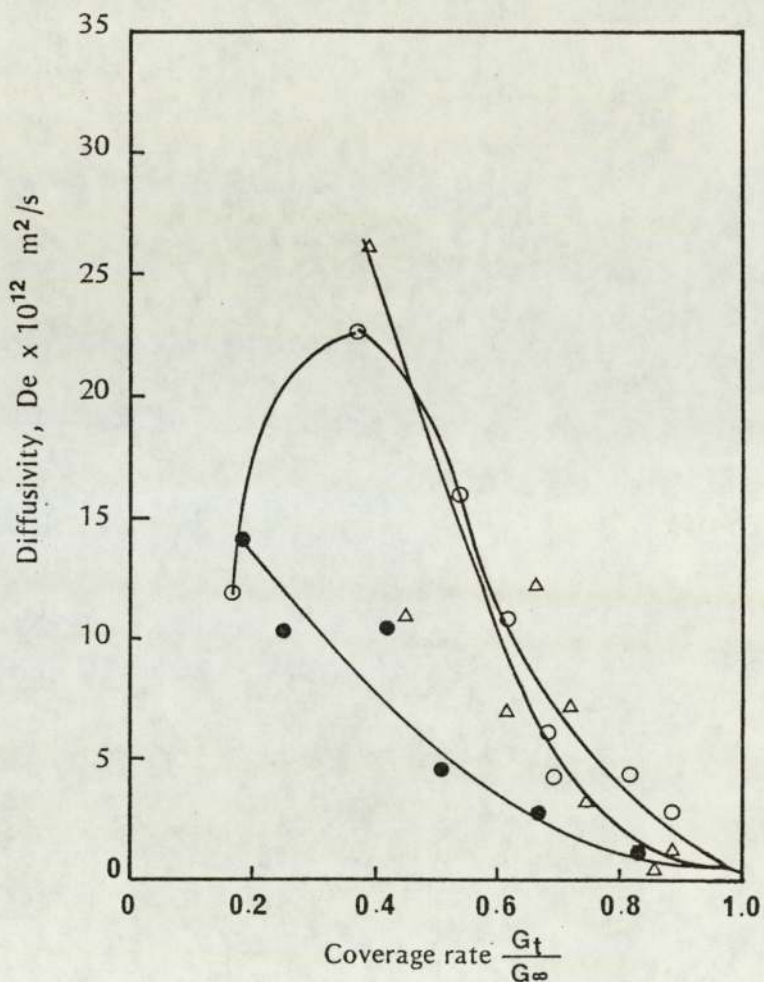
Figure 7.19   Effective Diffusion
Coefficient De of
● Naphthalene, △
1-Methylnaphthalene,
O 1-3 Dimethyl-
naphthalene as a
Function of Degree of
Coverage $\frac{G_t}{G_\infty}$ at 303 K
on Nax Zeolite Pellets.
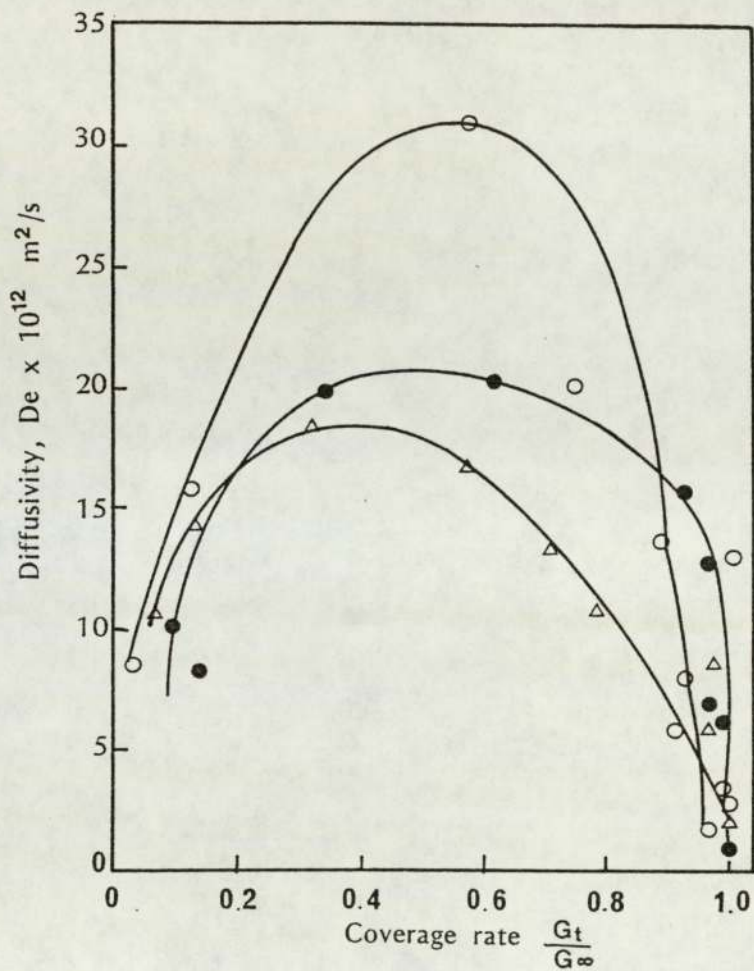
Figure 7.20 Effective Diffusion
Coefficient De of
● Naphghalene, △
1-Methylnaphthalene
and o 1-3 Dimethyl-
naphthalene as a
Function of Degree of
Coverage $\frac{G_t}{G_\infty}$ at 343 K
on NaX Zeolite Pellets.

Clearly, then the 'inert' filler or binder has an effect on the kinetics of adsorption and the filler by itself hinders the penetration diffusivity of the molecules; because the number of the micropores in the filler are more than in the binder free zeolite. Transition of adsorbate molecules occurs from one pore to another in the molecular sieve crystals (i.e., in macropores) and any decrease in the macropores would therefore be expected to result in a decrease in the diffusion coefficient.

Figures 7.21 and 7.22 demonstrate kinetic curves for adsorption G_t mole/kg and g/g vs $\sqrt{t}$ for dibenzothiophene, fluorene, phenanthrene and dibenzofuran at 303 K on NaX zeolite. The maximum equilibrium adsorbance for dibenzothiophene was clearly much higher than for the others 0.49 mole/kg. The maxima for fluorene and phenanthrene were close to each other 0.44, 0.41 mole/kg respectively but for dibenzofuran it was very low, 0.25 mole/kg. This can be explained since the presence of the sulfur atom with two pairs of lone electrons increases the activity of the dibenzo-thiophene. Thus the molecules penetrate through the pores of the zeolite crystals more easily, and interact with the cations present on the surface of molecular sieve pores more strongly, and so increase the value of the equilibrium adsorbance. But comparing the critical diameter of cumene with dibenzothiophene molecules, obviously cumene has a smaller critical diameter and a more compact molecule, resulting in a higher adsorbance value and faster approach to equilibrium.

In the case of fluorene the presence of just one pair of electrons will affect the activity of the molecule to a lesser extent than with dibenzothiophene. Dibenzofuran molecules would have less negativity than the two others; thus a lower value of equilibrium adsorbance. Dibenzofu-ran appeared to have the lowest value of equilibrium adsorbance and the longer time needed to reach equilibrium. This can be related to the ster-ic hindrance effect.

Figures 7.23 and 7.24 indicate kinetic curves for adsorption G_t mole/kg and g/g vs $\sqrt{t}$ hr for dibenzothiophene, fluorene, phenanthrene and dibenzofuran at 343 K on NaX zeolite pellets. Figure 7.23 shows that the maximum adsorption value for the whole group (trinuclear aromatic com-pounds) were higher at 343 K than at 303 K, namely 0.85, 0.766, 0.63, and 0.48 mole/kg respectively. The time to reach equilibrium at 343 K was within 23.4 ks for all of them.
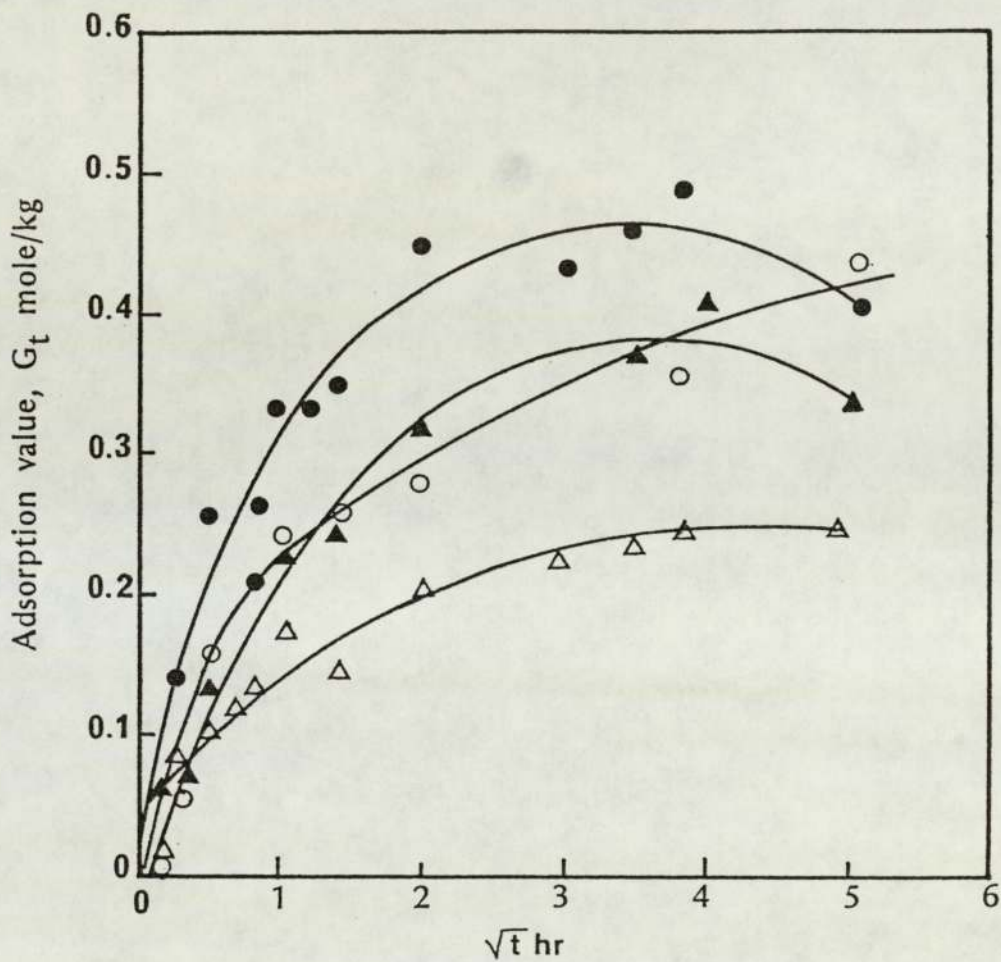
Figure 7.21 Kinetic Curve for
Adsorption G_t mole/
kg for ● Dibenzo-
thiophene, o Fluorene,
△ Dibenzofuran and
▲ Phenanthrene from
Isooctane at 303 K on
NaX Zeolite Pellets.
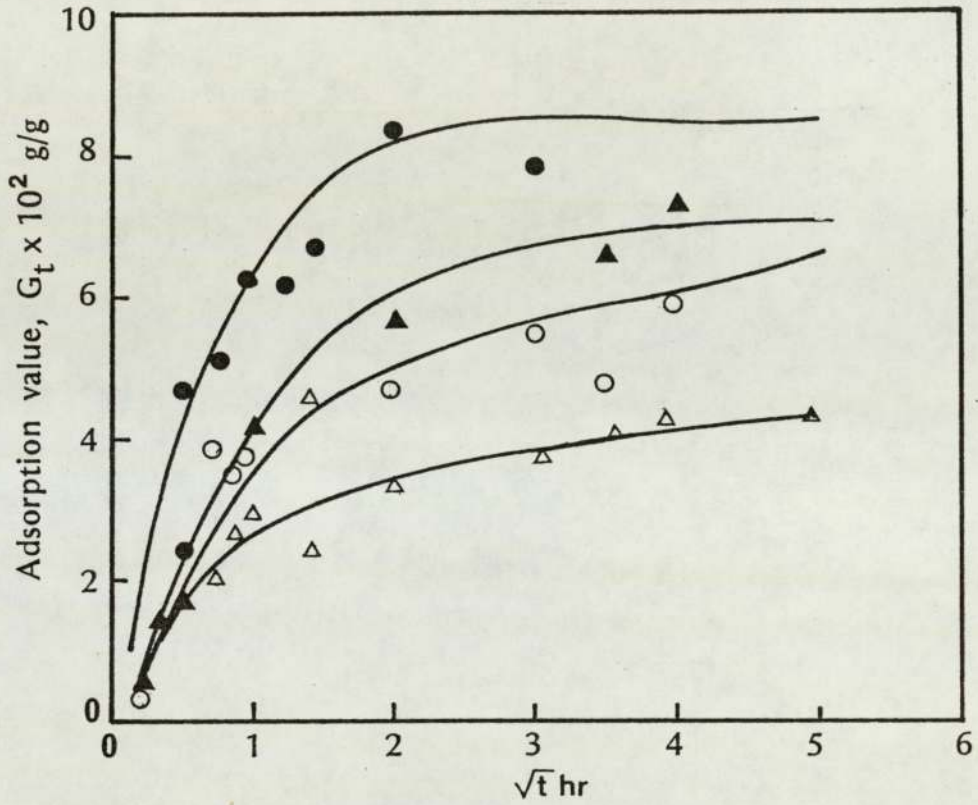
Figure 7.22   Kinetic Curve for Adsorption
G_t g/g for ● Dibenzothiophene,
○ Fluorene, △ Dibenzofuran
and ▲ Phenanthrene from
Isooctane at 303 K on NaX
Zeolite Pellets.

An increase in adsorption value with temperature can be attributed to a gain in high energy from the surrounding medium. Mobility of the molecules facilitates orientation of molecules of critical diameter so that they penetrate more easily and rapidly through the pores of the molecular sieves, and interact more strongly with the electrostatic charges of the cations of the zeolite crystals.

The value of adsorption of dibenzothiophene, fluorene, phenanthrene, and dibenzofuran decreased rapidly with decreasing temperature from 343 to 303 K. At the higher temperature linear portions of the kinetic curves correlate with the √t for the first hour of adsorption. Dibenzothiophene exhibited the greatest value of adsorption at both temperatures, indicating that the total interactions between the dibenzothiophene molecules and electrostatic charges of molecular sieves are very high. This is attributable to the π-bond of aromatic hydrocarbons of the aromatic ring in the dibenzothiophene, and also to the free pair electrons of the sulfur which has a dipole moment which interacts strongly with the electrostatic ions of the molecular sieve crystals.

For the polar compounds the free pair of electrons of sulfur are stronger than the pair electrons of the oxygen; hence the interactions between the dibenzothiophene and molecular sieves are higher than those between the dinenzofuran and crystals of the molecular sieves. From the kinetic curves in Figures 7.21, 7.22, 7.23 and 7.24, the lowest adsorption value is for dibenzofuran, suggesting that the oxygen atom in the dibenzofuran weakened the total interactions between the dibenzofuran molecules and cation of molecular sieve crystals.

The dependence of the coverage rate of adsorption on $t^{1/2}$ has been studied for the above mentioned hydrocarbons. Results of this study have been illustrated in Figures 7.25 and 7.26 at temperatures of 303 and 343 K. The fractional amount sorbed was linear with the square root of time within certain limits. Therefore Fick's law of diffusion, as expressed by equation (7.4), could be utilized. As shown in Figure 7.26 the saturation point was reached faster at 343 K but phenanthrene was slower than the others. This means that during the initial stages the adsorption was very fast according to Henry's law. However, after a short period the rate of adsorption slowed down, due to the decrease in the effective diameter of the pore of the molecular sieve crystals. The diffusion rate of the phe-
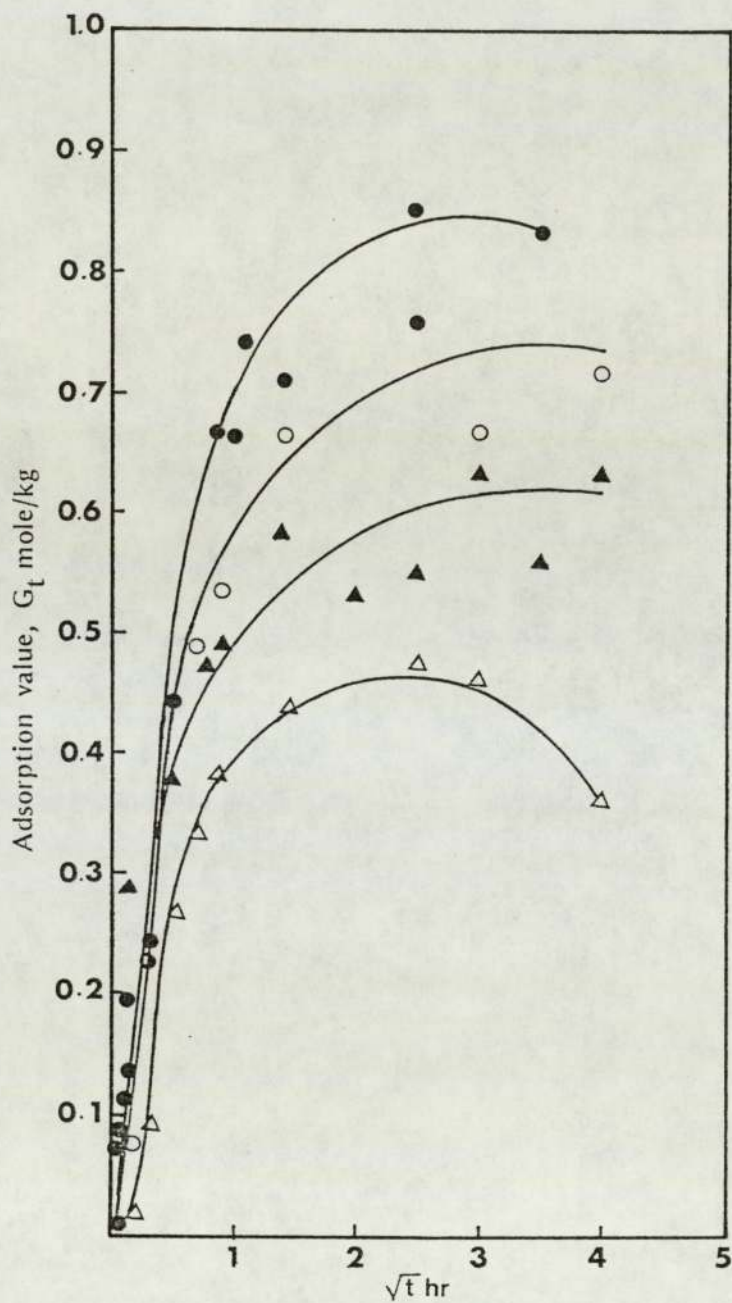
Figure 7.23   Kinetic Curve for
               Adsorption G_t mole/
               kg for ● Dibenzo-
               thiophene, ○ Fluorene,
               △ Dibenzofuran and
               ▲ Phenanthrene from
               Isooctane at 343 K on
               NaX Zeolite Pellets.
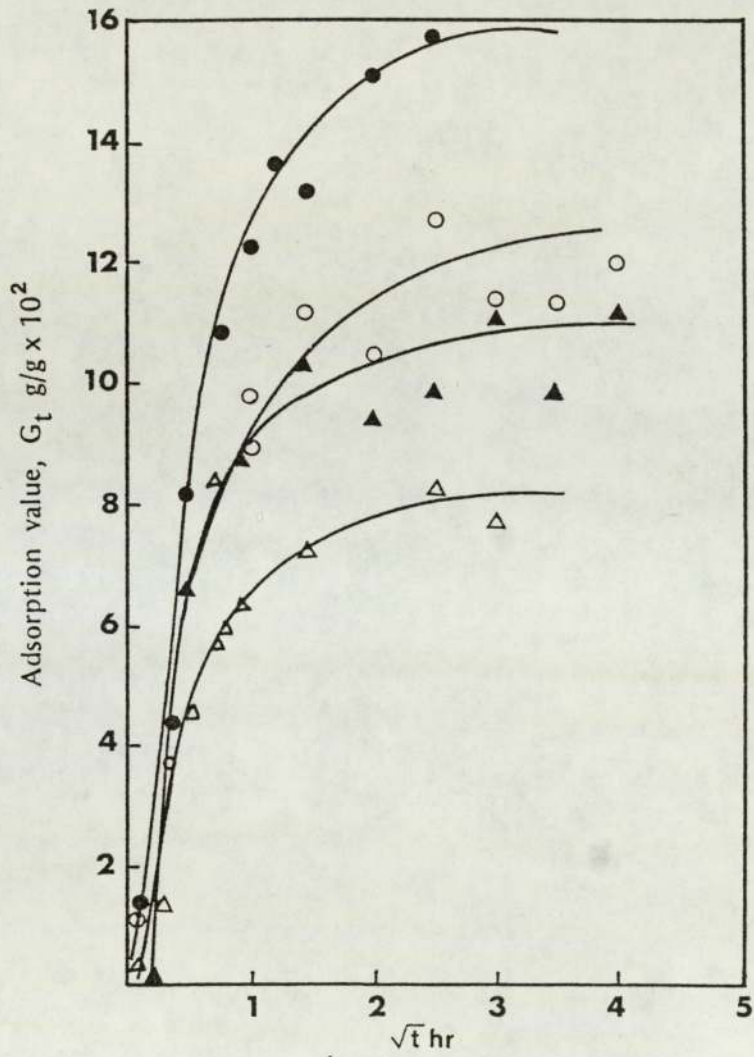
Figure 7.24   Kinetic Curve for
Adsorption G_t (g/g)
for ● Dibenzo-
thiophene, ○ Fluorene,
△ Dibenzofuran and
▲ Phenanthrene from
Isooctane at 343 K on
NaX Zeolite Pellets.

nanthrene molecules was hence very slow and a longer time was required to achieve the saturation point. The adsorption rate of phenanthrene was lower at 303 K than at 343 K.

An increase in the temperature of adsorption will tend to increase the instability and the activation of adsorbate molecules. This will increase the diffusivity but reduce the adsorption on the packing, because any increase in temperature will weaken the interactions between the π-bond of the molecules and active site of the pores in the molecular sieve crystals. More time was needed to achieve the saturation point for adsorbate molecules at the lower temperature than for adsorption at high temperature. Figures 7.25 and 7.26 suggest that the dipole moment of the sulfur atom in dibenzothiophene is stronger than that of the oxygen atom in dibenzofuran. It appears therefore that at both temperatures the interactions between the dibenzothiophene and active sites of the molecular sieves are higher than with dibenzofuran. The rate of adsorption of trinuclear aromatic hydrocarbons and polar compounds are of special interest. Figures 7.27 and 7.28 illustrate the dependence of rate of adsorption on the value of adsorption for these compounds.

The rate of adsorption dG_t/dt of dibenzothiophene, dibenzofuran, flourene and phenanthrene were measured at temperatures of 303 and 343 K and the results are illustrated in Figures 7.27 and 7.28. These show that the increase in the value of adsorption leads to a decrease in the rate of adsorption. This was consistent for all hydrocarbons at the two temperatures. It also appears from Figures 7.27 and 7.28 that during the initial stage of adsorption the rate of adsorption is very high and diffusion of hydrocarbon molecules is very rapid. However, the rate decreases rapidly due to blockage of the pores. For dibenzofuran blockage of adsorbate-molecules was complete at 0.3 mole/kg at 303 K and 0.5 at 343 K, hence the rate of adsorption reduced to zero. This means that when diffusion of these molecules in a zeolite channel is subjected to attachment on the active sites they cluster around the channel of located cations thus hindering penetration of more adsorbate molecules into the pores of the molecular sieve crystals. Adhesion is due to the cation-dipole interactions. This adherance of adsorbate molecules on the active sites of the molecular sieve crystals has a different efficiency for each aromatic compound in the order: dibenzofuran < fluorene < phenanthrene < dibenzothiophene at

-151-
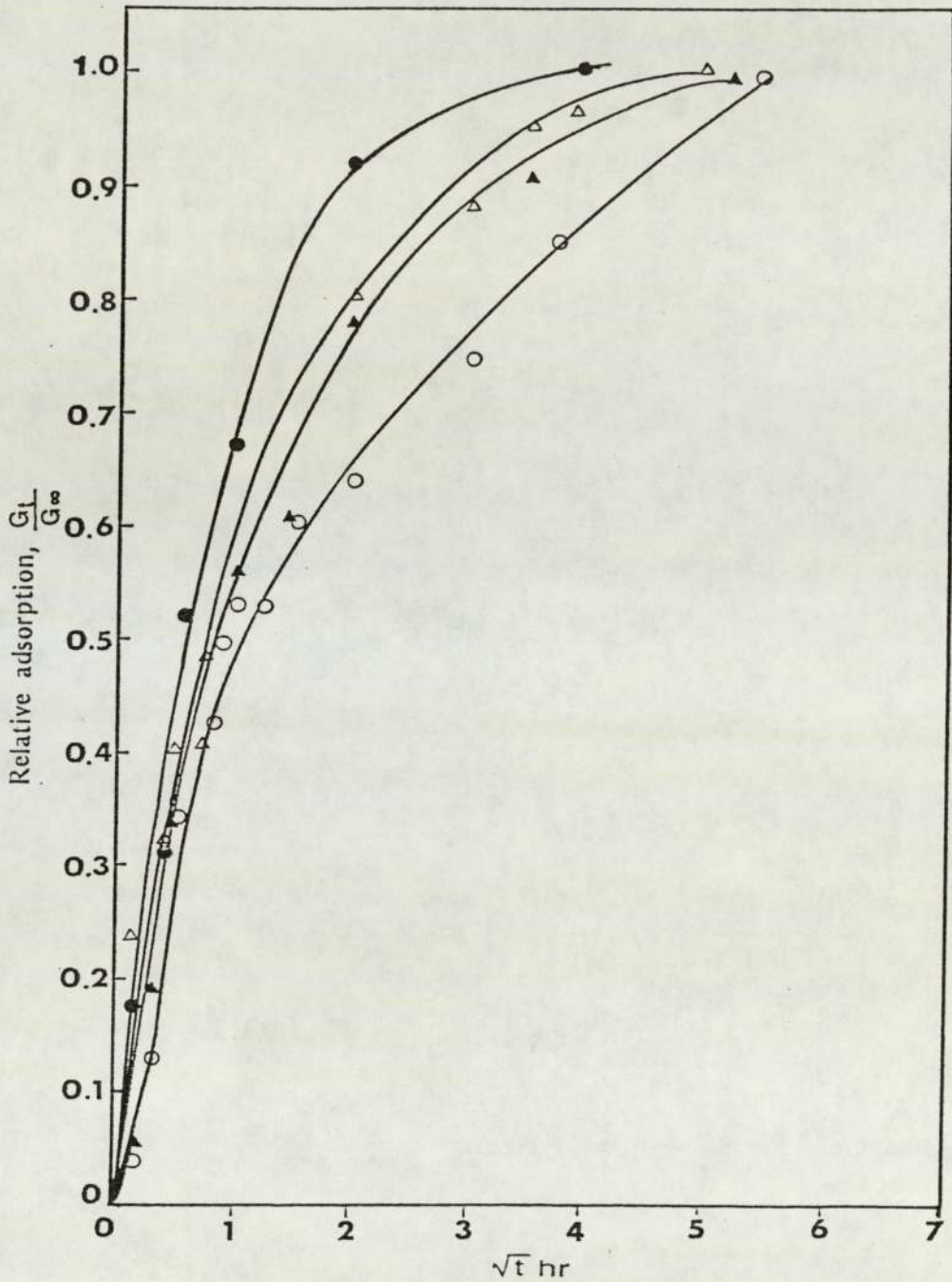
Figure 7.25 Kinetics of Relative Adsorption
$\frac{G_t}{G_\infty}$ of ● Dibenzothiophene, ▲
Phenanthrene, ○ Fluorene and
△ Dibenzofuran from Isooctane
at 303 K on NaX Zeolite Pellets.
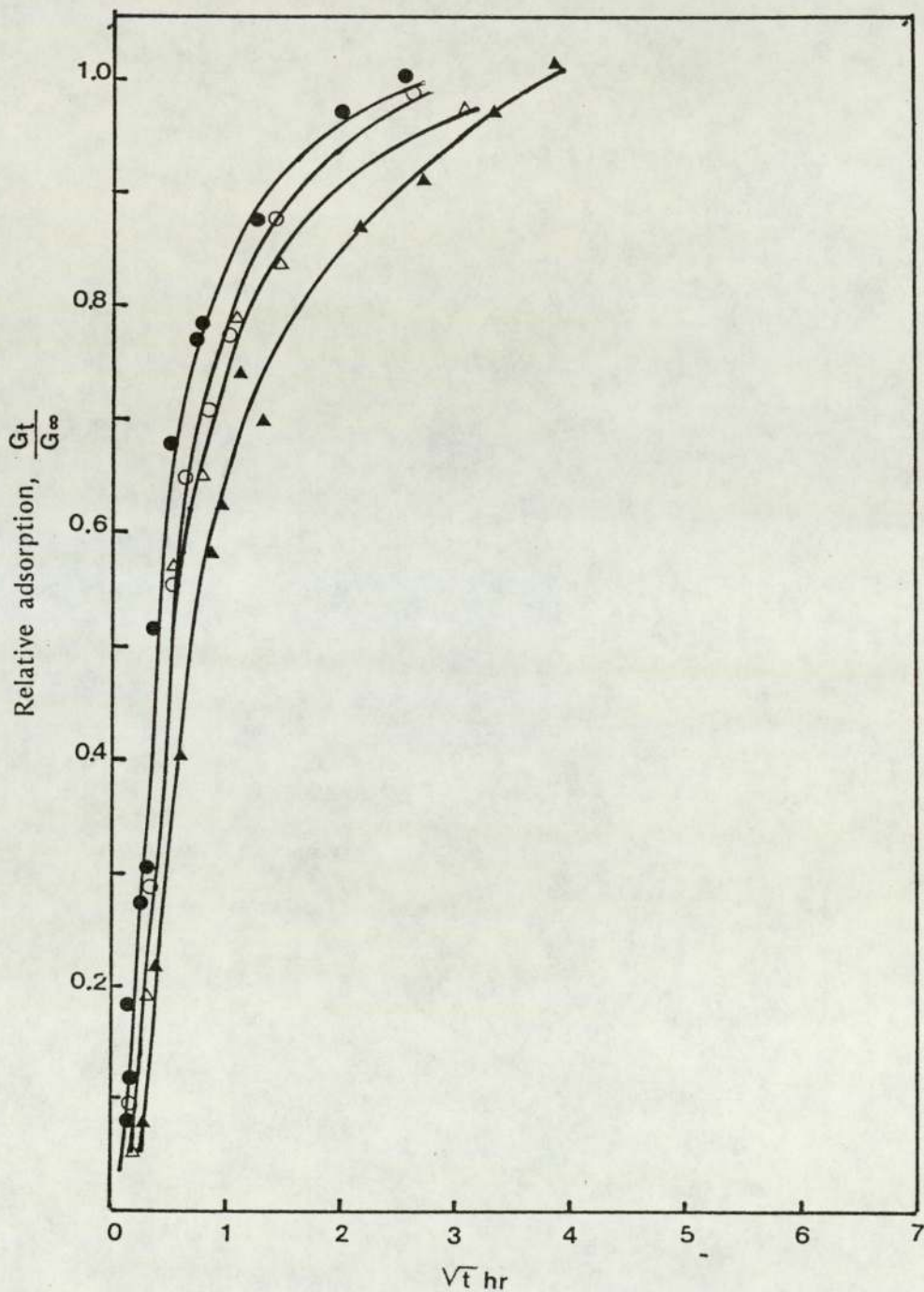
Figure 7.26 Kinetics of Relative Adsorption
$\dfrac{G_t}{G_\infty}$ of ● Dibenzothiophene, ▲
Phenanthrene, o Fluorene and
△ Dibenzofuran from Isooctane
at 343 K on NaX Zeolite Pellets.

303 K. At 343 K the efficiency has the order: dibenzofuran < phenanthrene < fluorene < dibenzothiophene. Increase in temperature will activate the adsorbate molecules of phenanthrene to adhere more strongly to the active sites of the molecular sieves, which (i.e. after G = 0.7 mole/kg) will subsequently prevent further molecules penetrating through the channels of the molecular sieves. This will result in a decrease in the rate of adsorption at the higher temperature, as shown for 343 K in Figure 7.28.

Experimental data regarding the relationship between the effective diffusion coefficient De and the coverage rate for adsorbate molecules of trinuclear aromatic and polar compounds are presented in Figures 7.29 and 7.30. The data were obtained using molecular sieves type 13X at two temperatures, 303 and 343 K. The diffusivities of relatively large organic molecules, e.g. trinuclear aromatic compounds, from the liquid phase in NaX are related to the molecular diameter and to the interactions of the adsorbate molecules with the cations in zeolite crystals. For all hydrocarbons the diffusion coefficient had an optimum value, i.e. at the initial stage of coverage rate the diffusion coefficient increased; subsequently it decreased, and reached the minimum at a coverage rate G_t/G_∞ = 0.8 - 1.0. At 303 K the diffusion coefficients for phenanthrene and fluorene were lower than for the polar compounds. This indicates that the interaction of these aromatic compounds with active sites of the molecular sieve is higher than for polar compounds.

Dibenzothiophene molecules were an exception. Increase in the temperature from 303 to 343 K will lead to an increase in the interactions of phenanthrene molecules with active sites of the molecular sieves and so result in an increase in the diffusivity of phenanthrene at the higher temperature. At a higher coverage rate ($G_t/G_\infty \sim 0.5$) the diffusion coefficient of dibenzofuran is higher than that of dibenzothiophene. The critical diameter of both molecules seems to be similar but the interactions of dibenzothiophene with molecular sieves were higher than for dibenzofuran, because the dipole moment of the sulfur atom in dibenzothiophene is stronger than the dipole moment of the oxygen atom in dibenzofuran and this action will result in a decrease in the diffusivity of the dibenzothiophene, at both temperatures.
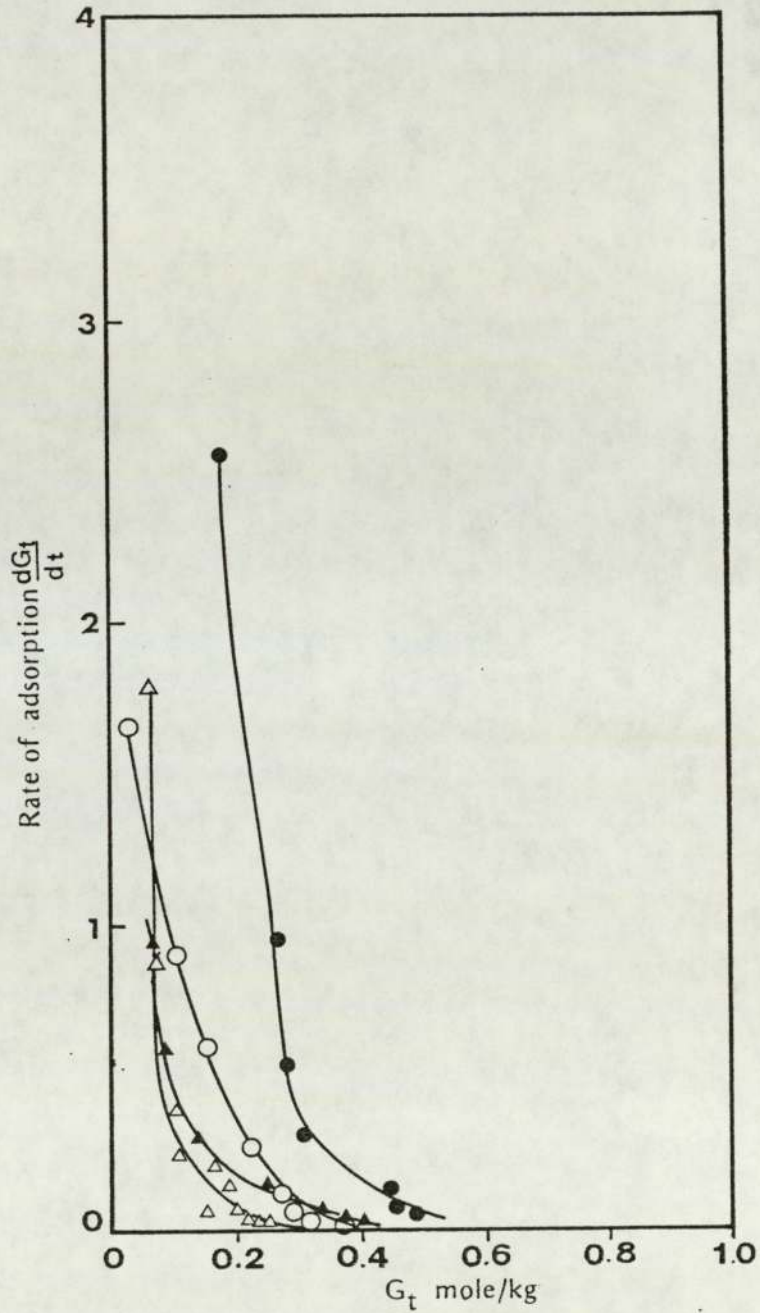
Figure 7.27   Rate of Adsorption $\frac{dG_t}{dt}$
of ● Dibenzothiophene,
○ Fluorene, △ Dibenzo-
furan and ▲ Phenanthrene
at 303 K on NaX Zeolite
Pellets.
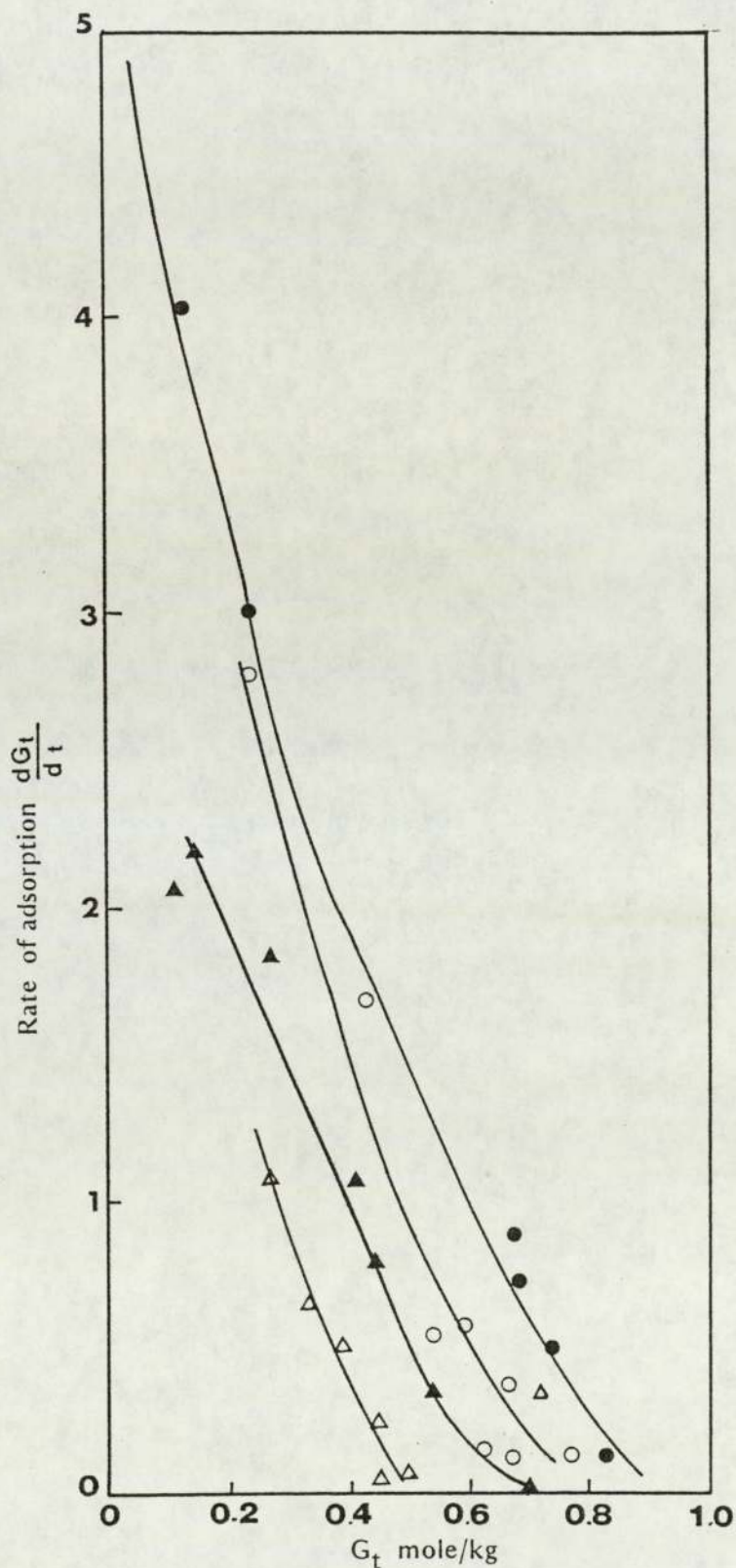
Figure 7.28 Rate of Adsorption $\dfrac{dG_t}{dt}$
of ● Dibenzothiophene,
o Fluorene, △ Dibenzo-
furan and ▲ Phenanthrene
at 343 K on Nax Zeolite
Pellets.
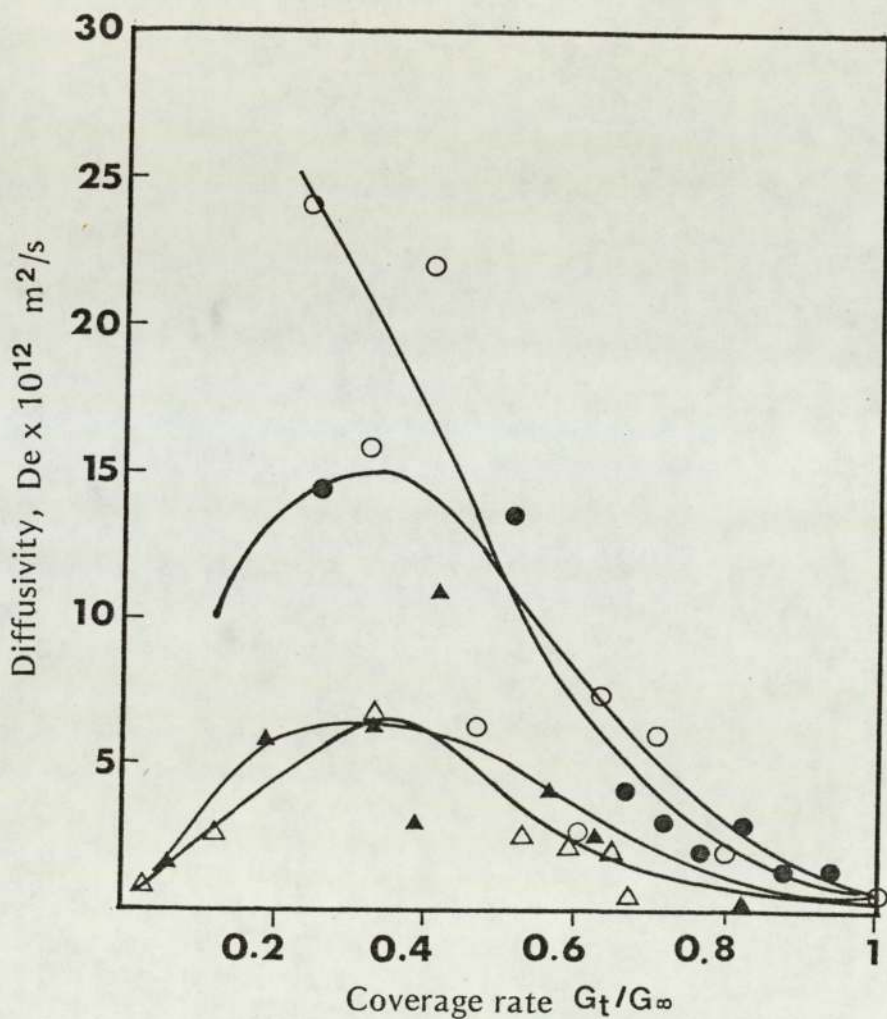
Figure 7.29 Effective Diffusion
Coefficient De of
● Dibenzothiophene,
△ Fluorene, ○ Di-
benzofuran and ▲
Phenanthrene as a
Fuction of Degree
of Coverage Rate $\frac{G_t}{G_\infty}$
at 303 K on NaX
Zeolite Pellets.
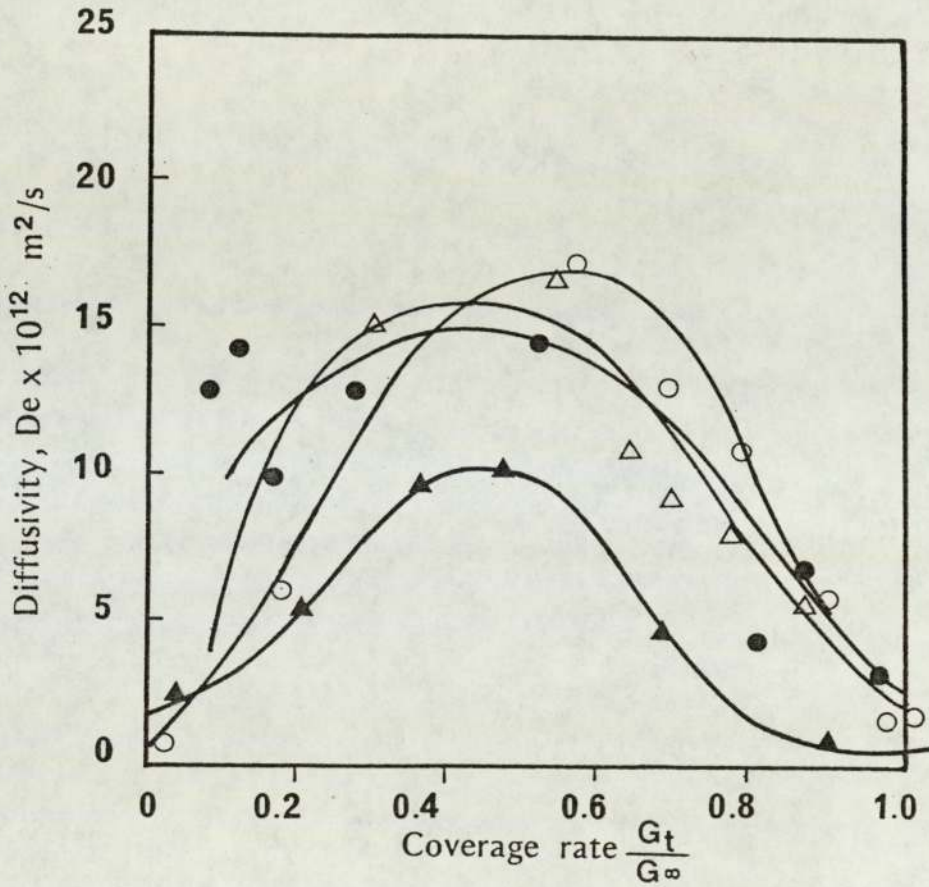
Figure 7.30 Effective Diffusion
Coefficient De of
● Dibenzothiophene,
△ Fluorene, O Di-
benzofuran and ▲
Phenanthrene as a
Function of Degree
of Coverage Rate
$\frac{G_t}{G_\infty}$ at 343 K on NaX
Zeolite Pellets.

158-

TABLE 7.1
AVERAGE DIFFUSION COEFFICIENTS IN MOLECULAR SIEVES
TYPE 13X (NaX)

| Sorbate | Temperature K | | $\dfrac{G_t}{G_\infty}$ |
| | 303 | 343 | |
	De x 10^{12}	m^2/s	
Cumene	15.5	36.3	0.3
	18.5	37.0	0.5
	18.0	33.8	0.7
Dodecylbenzene	10.8	33.8	0.3
	10.5	33.5	0.5
	8.0	31.0	0.7
Naphthalene	10.0	19.0	0.3
	6.0	20.0	0.5
	2.0	19.5	0.7
1, methylnaphthalene	14.0	18.5	0.5
	8.0	17.0	0.6
	5.0	15.0	0.7
1, 3 dimethylnaph-thalene	21.5	25.5	0.3
	20.5	31.0	0.5
	7.0	28.0	0.7
Dibenzothiophene	15.0	15.5	0.3
	12.8	14.5	0.5
	4.8	10.5	0.7
Fluorene	6.0	15.3	0.3
	4.3	16.0	0.5
	1.3	10.3	0.7
Phenanthrene	5.8	9.5	0.3
	5.3	9.5	0.5
	2.5	4.0	0.7
Dibenzofuran	14.0	15.0	0.4
	9.0	17.0	0.6
	4.5	14.6	0.7

Figure 7.29 shows a plot of diffusivity versus coverage rate for the trinuclear compounds: dibenzothiophene, fluorene, phenanthrene and dibenzofuran at 303 K. Dibenzothiophene, fluorene and phenanthrene exhibited similar behaviour to the naphthalene group at 343 K. Diffusivities started at a low value, increased slowly to reach a maximum, then decreased sharply to a minimum. The maximum diffusivities were 15×10^{-12}, 6.3×10^{-12} and 6.3×10^{-12} m^2/s respectively at a coverage rate 0.34. In the case of dibenzofuran the diffusivity decreased gradually to reach a minimum at a coverage rate of 1, i.e. at equilibrium, and the maximum diffusion rate was 24×10^{-12} m^2/s at 0.24 coverage range. Figure 7.30 illustrates diffusivity versus coverage rate for trinuclear aromatic compounds at 343 K.

The diffusional behaviour of the four components is seen to be qualitatively similar. Their diffusivities increased slowly to approach an intermediate maximum then declined to reach a minimum value at saturation.

Maximum diffusivity, m^2/s at 0.5 coverage

14.5×10^{-12}	dibenzothiophene
16.0×10^{-12}	fluorene
9.5×10^{-12}	Phenanthrene
17.0×10^{-12}	dibenzofuran

The minimum diffusivities corresponded to $1-3 \times 10^{-12}$ m^2/s for the four species.

No significant influence of temperature was found for the diffusivity of dibenzothiophene molecules particularly in the initial coverage rate region (0.2 - 0.5), see Table 7.1. This was contrary to the behaviour of other species in this group for which diffusivities increased very markedly when the temperature was raised from 303 to 343 K due to their increased mobility.

7.5 Activation Energy

The activation energies for the adsorption of aromatic compounds by zeolite type 13X from isooctane solutions at concentrations of 0.015 mole fraction are listed in Table 7.2.

These were calculated from the differences in the logarithm of effective diffusion coefficients, De, with the reciprocal of the difference of

absolute temperatures at a coverage rate $\frac{Gt}{G_\infty} = 0.5$, by applying Eyring's equation

$$E_A = R \left(\frac{\partial \ln De}{\partial \frac{1}{T}} \right) \qquad (7.19)$$

A plot of De versus (1/T) is not linear, indicating that the nature of the diffusion is different at different temperatures.

TABLE 7.2
APPARENT ENERGIES OF ACTIVATION FOR DIFFUSION IN MOLE-
CULAR SIEVES TYPE 13X (NaX) AT A COVERAGE RATE $\frac{Gt}{G_\infty} = 0.5$.

Sorbate	Temp. Range K	E_A K cal/mole	E_A kJ/mole
Cumene	303 – 343	3.4	14.2
Dodecylbenzene	" "	5.7	24.0
Naphthalene	" "	6.8	28.0
1, methylnapthalene	" "	3.7	15.6
1, 3 dimethylnaph-thalene	" "	2.0	8.6
Dibenzothiophene	" "	0.7	2.7
Fluorene	" "	6.2	26.0
Phenanthrene	" "	2.9	12.5
Dibenzofuran	" "	2.7	11.0

The energy needed for activation of dodecylbenzene molecules to penetrate through the pores of the molecular sieves is approximately 24.0 kJ/mole compared with 14 kJ/mole for cumene. Although cumene molecules exhibit a higher adsorption value, due to their stronger interactions with the electrostatic charges of the molecular sieve sites, the activation energy required to break-away from the attracted sites and jump from one equilibrium position to another is less. This can be attributed to its compact structure, since its critical diameter is much less than that of dodecylbenzene which has a long alkyl chain attached to the ring. Hence cumene molecules can penetrate through the molecular sieve pores more easily, with less energy consumption.

In the case of naphthalene groups, the naphthalene molecules required a higher activation energy, 28.0 kJ/mole, than 1,methylnaphthalene, and 1,3 dimethylnaphthalene which required just 15.6 and 8.6 kJ/mole respectively to attain the equilibrium point. This can be attributed to the fact that the polarity of naphthalene is higher than that of 1,methylnaphthalene, in which the methyl group is present, and of the 1,3 dimethylnaphthalene, in which two methyl groups are present since the adsorption value increases as the polarity increases. Thus the interaction of naphthalene molecules with molecular sieve sites is much stronger than that of 1,methylnaphthalene and 1,3 dimethylnaphthalene molecules. Hence the naphthalene molecules require more energy to break away and jump from one equilibrium position to another than 1,methylnaphthalene and 1,3 dimethylnaphthalene. Polarity in the sorbate molecules contributes substantial energy barriers to diffusion along the channels of molecular sieves and to overcome these energy barriers, to permit the sorbate molecules transition from one pore to another, the sorbate molecules have to be activated by gaining a certain amount of energy. The more polar the molecules the more activation energy is required. This is clear in the case of the naphthalene group where naphthalene required 28 kJ/mole to overcome the energy barriers to diffuse through the pores of the molecular sieves, whereas 1,methylnaphthalene required 15.6 kJ/mole and 1,3 dimethylnaphthalene 8.6 kJ/mole.

The activation energy for the third group, the trinuclear aromatic compounds (dibenzothiophene, fluorene, phenanthrene and dibenzofuran), were determined and their values are also illustrated in Table 7.2. The lowest activation energy value was for dibenzothiophene, although it exhibited a higher adsorption value at both temperatures, because it possesses a strong polarity due to the sulphur atom in which two free electron pairs are available.

The activation energy for dibenzothiophene molecules was lower than for the other aromatic compounds in this group. This is attributable to the energy barriers of the pores for transition of a dibenzothiophene molecule from one equilibrium position to another being much less than for the other trinuclear compounds, i.e. it consumed just 2.7 kJ/mole. For fluorene molecules 26 kJ/mole were required to transmit a molecule from one equilibrium position to another, because fluorene molecules are

strongly attracted to the molecular sieve sites. By comparison phenan-
threne and dibenzofuran required 12.5 and 11 kJ/mole respectively. Since
the adsorption value for phenanthrene is higher than that for dibenzofu-
ran, phenanthrene molecules required a higher activation energy to break
away and jump from one equilibrium position to another. However, dibenzo-
furan molecules are less attracted to the sites of molecular sieves
because the interaction between the electrostatic charges of the molecular
sieves and dibenzofuran molecules are very weak, thus needing a lower
activation energy.

7.6 Conclusions

Solutes of aromatic components are adsorbed in the lattices of active
zeolites, at rates which are a function of their cross-sectional diameter.
Molecules with small cross-sectional diameter (e.g. cumene   6.8 A$^\circ$) are
taken-up very rapidly by a process resembling free diffusion. The rela-
tively larger cross-sectional diameter molecules are taken-up by a slower
diffusion process because their mobility in the zeolitic channels is
greatly reduced due to geometrical obstructions.

The rate of sorption tends to decrease considerably when a long
alkylchain is attached to a benzene ring (e.g. dodecylbenzene), because of
steric hindrance and intermolecular interactions; therefore the diffusion
coefficient would be expected to be significantly reduced. The sorption
rate is increased exponentially by a rise in temperature.

Apparent energies of activation were determined for all individual
aromatic components and found to increase as the polarity increased, (the
exception was dibenzothiophene) and with increase in the side chain
attached to the aromatic ring (e.g. dodecylbenzene). This is explained by
the stronger interaction of the polar compounds with the cations of the
zeolite crystals than the non-polar compounds, so that such molecules then
require a higher energy to break-away and jump to the next equilibrium
position.

Thus these results have shown that for thorough treatment of a paraf-
finic feedstock to remove traces of aromatic hydrocarbons and organic
sulphur compounds, there may be kinetic hindrance due to the low diffusion
coefficients of the molecules of these compounds at low degrees of cover-
age rate of the zeolite void spaces.

8.0 KINETICS OF ADSORPTION OF EXTRACT FRACTIONS FROM BINARY SOLUTIONS WITH ISOOCTANE USING MOLECULAR SIEVES TYPE 13X

8.1 Results and Discussion

As shown in Chapter 7, the diffusivities of aromatic and polar compounds, as single components in the liquid phase into zeolite type NaX (13 X) at specified temperatures are predominantly affected by the critical molecular diameter of the diffusant and the specific and nonspecific interactions between adsorbate molecules and active sites of the molecular sieve crystals. To extend this study to the dearomatization of waxes it was necessary to investigate the kinetics of adsorption of the multi-component aromatic compounds referred to as the extract in previous Chapters. Three fractions from the extract were selected for this study. The physico-chemical characteristics and structures of these fractions are listed in Tables 5.1 and 5.2.

The experimental data obtained relating to the kinetics of adsorption of the three fractions at temperatures of 303 and 343 K are shown in Figures 8.1 to 8.4. These demonstrate that an increase in temperature from 303 to 343 K resulted in an increase in the adsorption value for each of the three fractions. The rate of adsorption at 343 K was more rapid, and the saturation point was reached within a shorter time, than at 303 K. The adsorption value vs. time for the fractions was in the order:

extract 1 > extract 2 > extract 3

The heavier molecular weight extract had a lower adsorption value, which can be attributed to the critical diameter of the adsorbate molecules. The complexity of the components present in the extract fractions increased with their boiling point. Thus extract fraction 3 was more complex and more polar with long side chain components, i.e. the critical diameter of the components were much bigger than the aperture of the molecular sieve pores. Hence, due to the steric effect, penetration through the pores was more difficult resulting in a lower adsorption value. From Table 5.1, the resins content in the first extract fraction was

lower than in the other two fractions. The resin materials have a differ-
ent structure from the poly-aromatics and polar compounds. They have a
low adsorption efficiency on the molecular sieves and can be easily
occluded on their surface; this can result in blockage of the pore aper-
tures and hindrance of any further diffusion through the channels.

Of greatest interest is the time dependence of the relative adsorp-
tion $\frac{G_t}{G_\infty}$, where G_t is the adsorption at the moment of time t; and G_∞
is the maximum adsorption. Figures 8.5 and 8.6 illustrate the relation-
ship of $\frac{G_t}{G_\infty}$ with $\sqrt{t}$ for three extract fractions. The degree of satu-
ration of the sorption capacity at a given moment can be judged from Fig-
ures 8.5 and 8.6. The kinetics of adsorption at initial and intermediate
degrees of coverage of the zeolite void spaces follow a linear relation-
ship. Hence the kinetics are determined by the rate of internal diffu-
sion, usually described by Fick's equation taking into consideration the
shape and size of the adsorbent grains. In this case the particle size of
the molecular sieves was 1-2 mm. At 303 K the degree of coverage of the
void spaces of the molecular sieves for the second extract fraction was
higher than the other two fractions. This indicates that the structure of
the extract fraction had a strong effect on the coverage rate, since the
naphthene rings are smaller than the other two fractions and these
naphthenes weakened the interactions between the aromatic compounds and
the active sites of the molecular sieves.

Increase in temperature from 303 to 343 K facilitated interactions
between the π-bond of the aromatic compounds present in the extract frac-
tions and the active sites of the molecular sieve crystals. Activation of
the molecules enabled them to penetrate faster through the pores of the
molecular sieves.

The rate of adsorption of the three extract fractions from solution
with isooctane were measured on zeolite type NaX (13X) at 303 and 343 K.
The results are shown in Figures 8.7 and 8.8.

At 303 K the rate of adsorption for highly polar compounds present in
extract fraction 3 was slow, due to the high percent of resins present and
its high molecular weight. The rate of adsorption was much higher for the
first extract fraction due to the low percent of resins and lower molecu-
lar weight. An increase in temperature would be expected to increase the
rate of adsorption since at a higher temperature the molecules will be
occluded more.
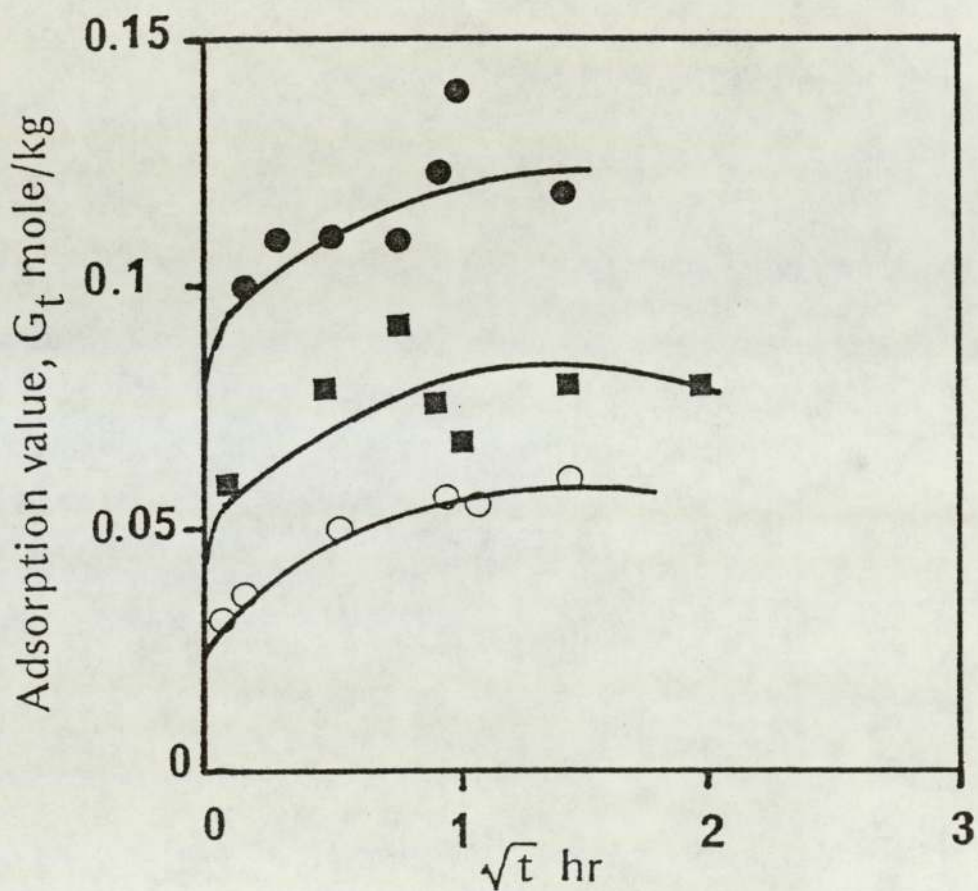
Figure 8.1 Kinetic Curve for
Adsorption G_t mole/
kg for ● Extract
fraction 1, ■ Extract
fraction 2, and O
Extract fraction 3
from Isooctane at
303 K on NaX Zeolite
Pellets.
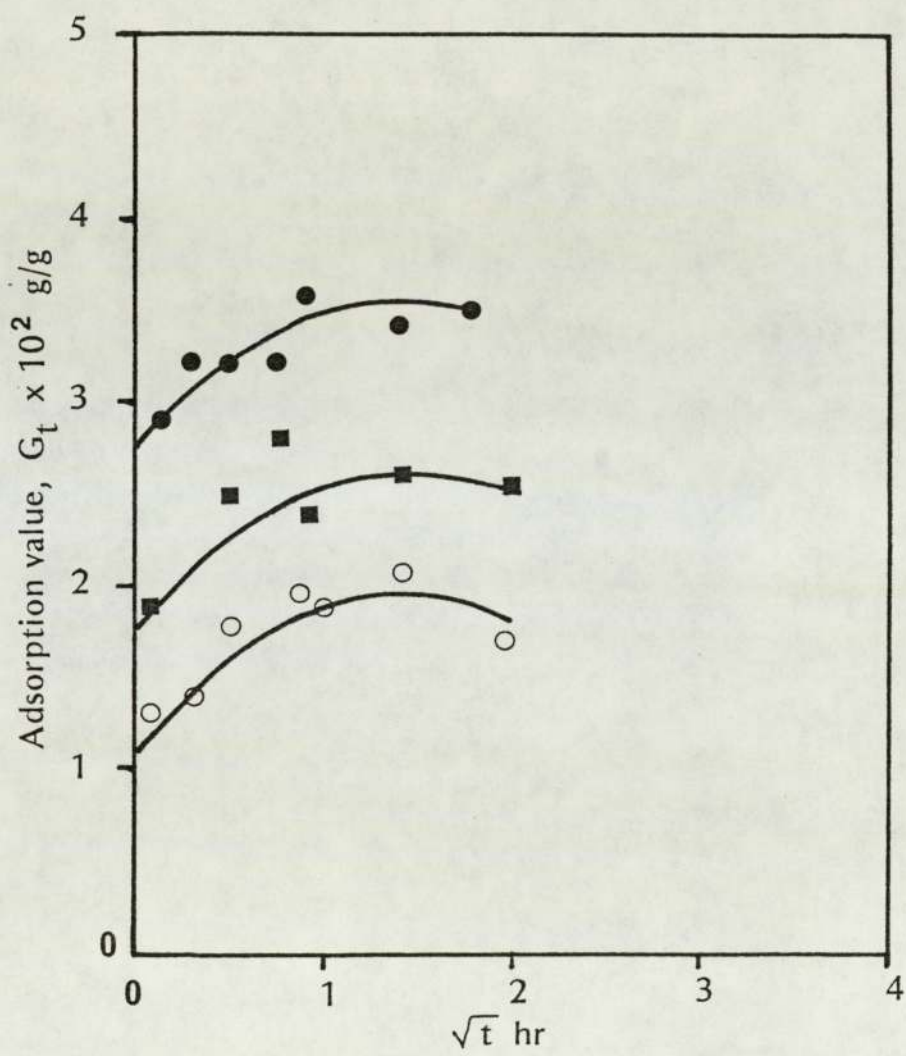
Figure 8.2   Kinetic Curve for
             Adsorption G_t g/g
             for ● Extract
             fraction 1, ■
             Extract fraction 2,
             and O Extract
             fraction 3 from
             Isooctane at 303 K
             on NaX Zeolite
                 Pellets.
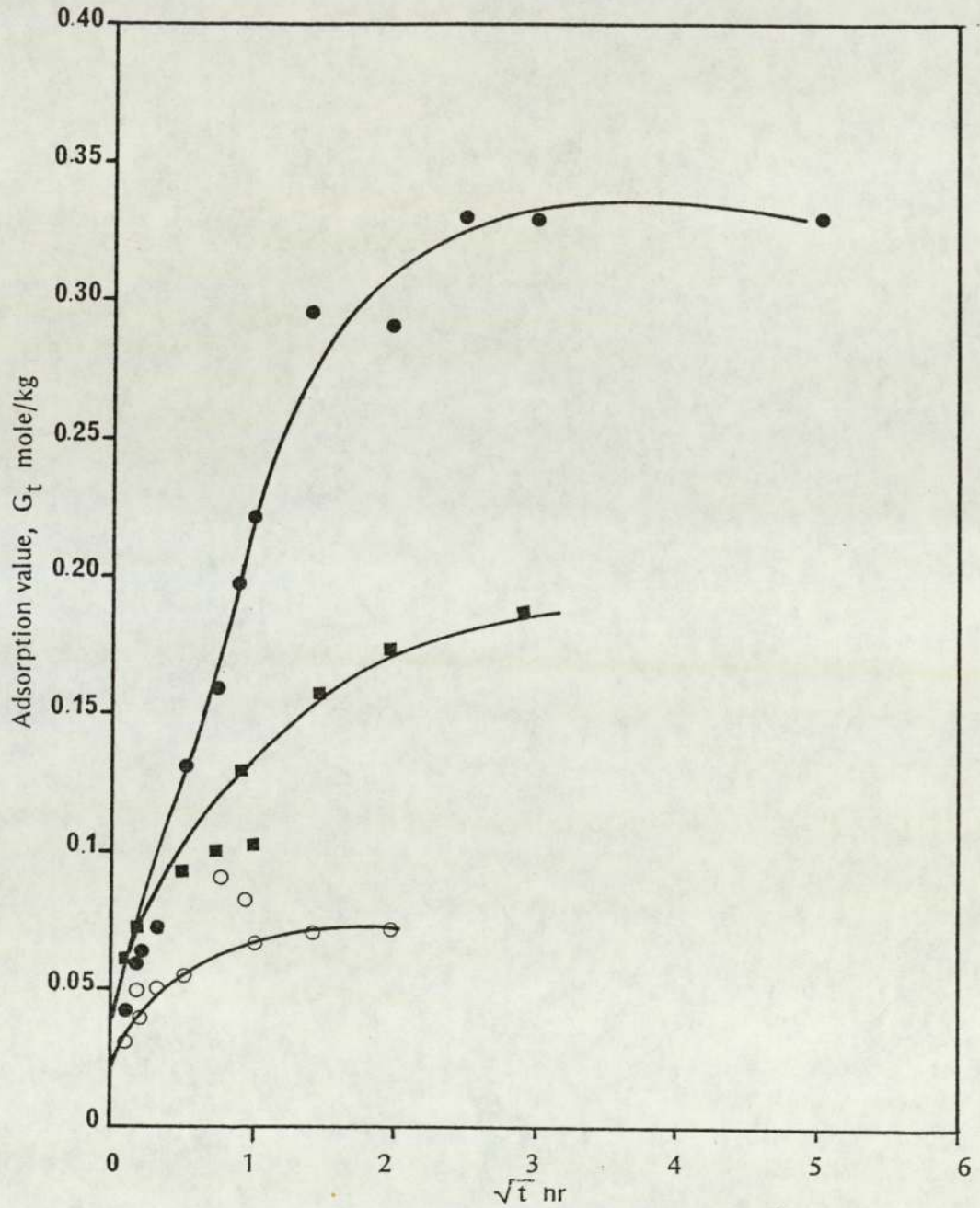
Figure 8.3 Kinetic Curve for Adsorption
G_t mol/kg for ● Extract
fraction 1, ■ Extract
fraction 2, and O Extract
fraction 3 from Isooctane at
343 K on NaX Zeolite Pellets.
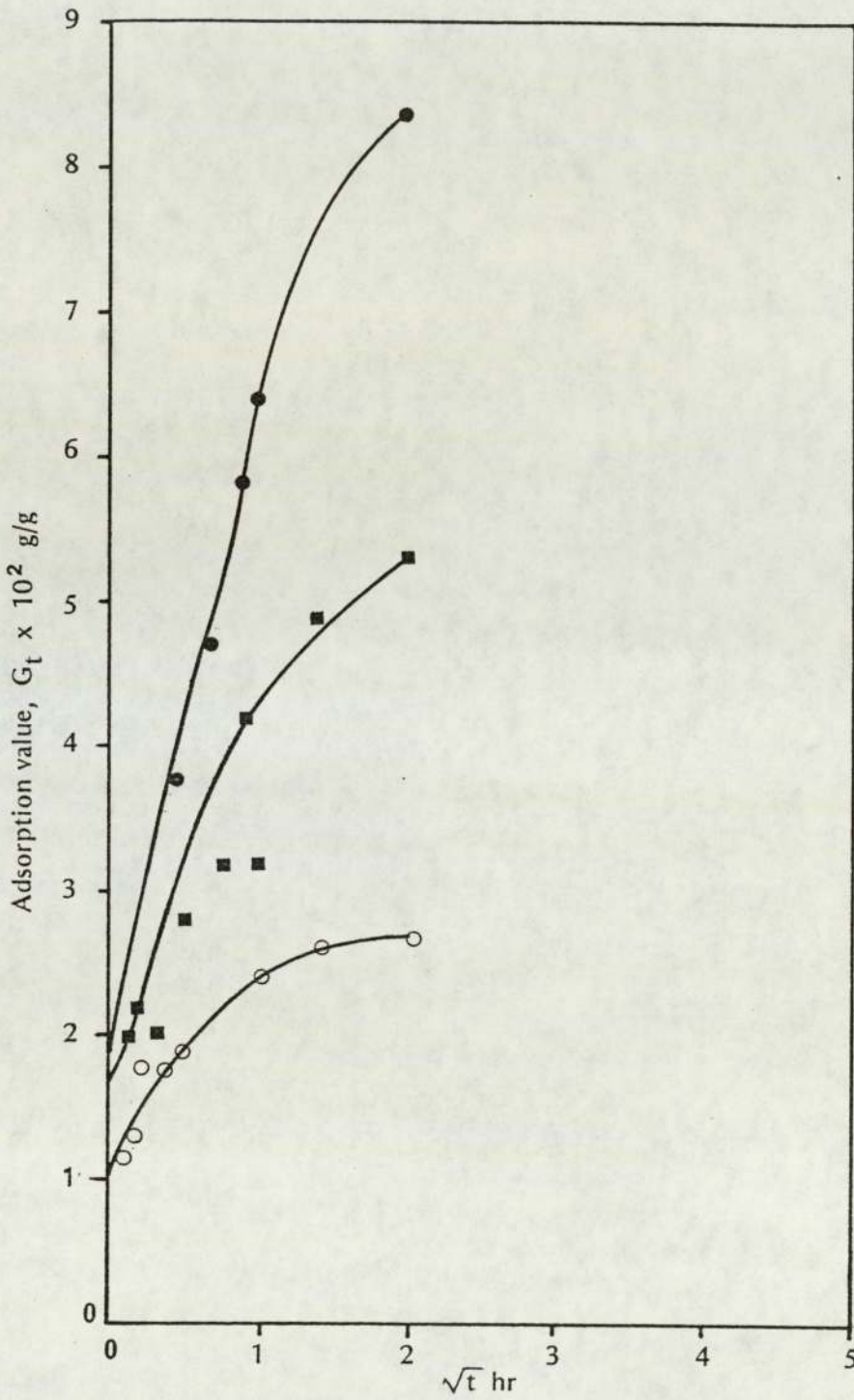
Figure 8.4   Kinetic Curve for
            Adsorption G_t g/g
            for ● Extract
            fraction 1, ■
            Extract fraction 2,
            and O Extract
            fraction 3 from
            Isooctane at 343 K
            on NaX Zeolite
               Pellets.
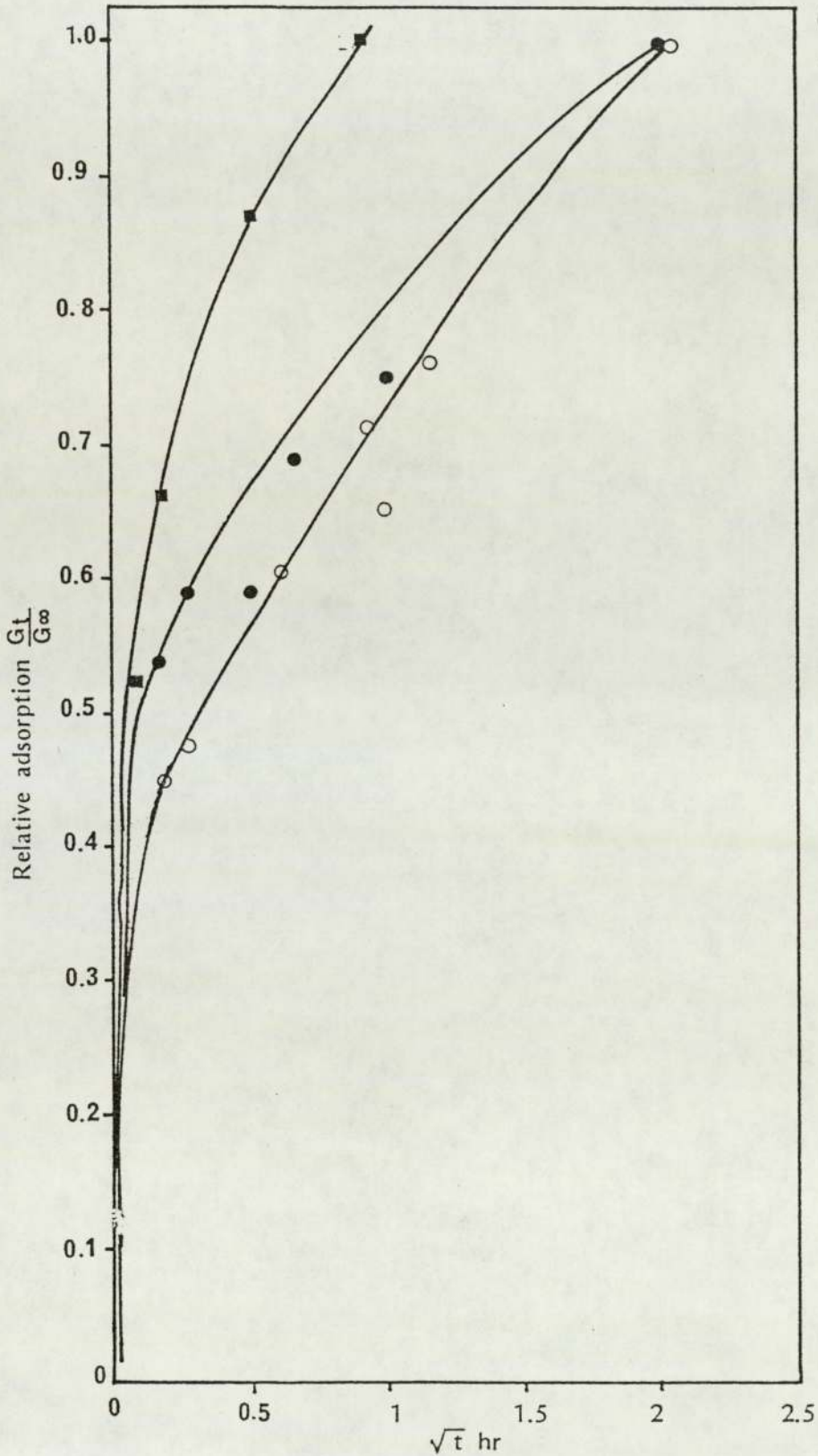
Figure 8.5   Kinetics of Relative Adsorption $\frac{Gt}{G_\infty}$ of ● Extract fraction 1, ■ Extract fraction 2, and ○ Extract fraction 3 from Iso-octane at 303 K on NaX Zeolite Pellets.
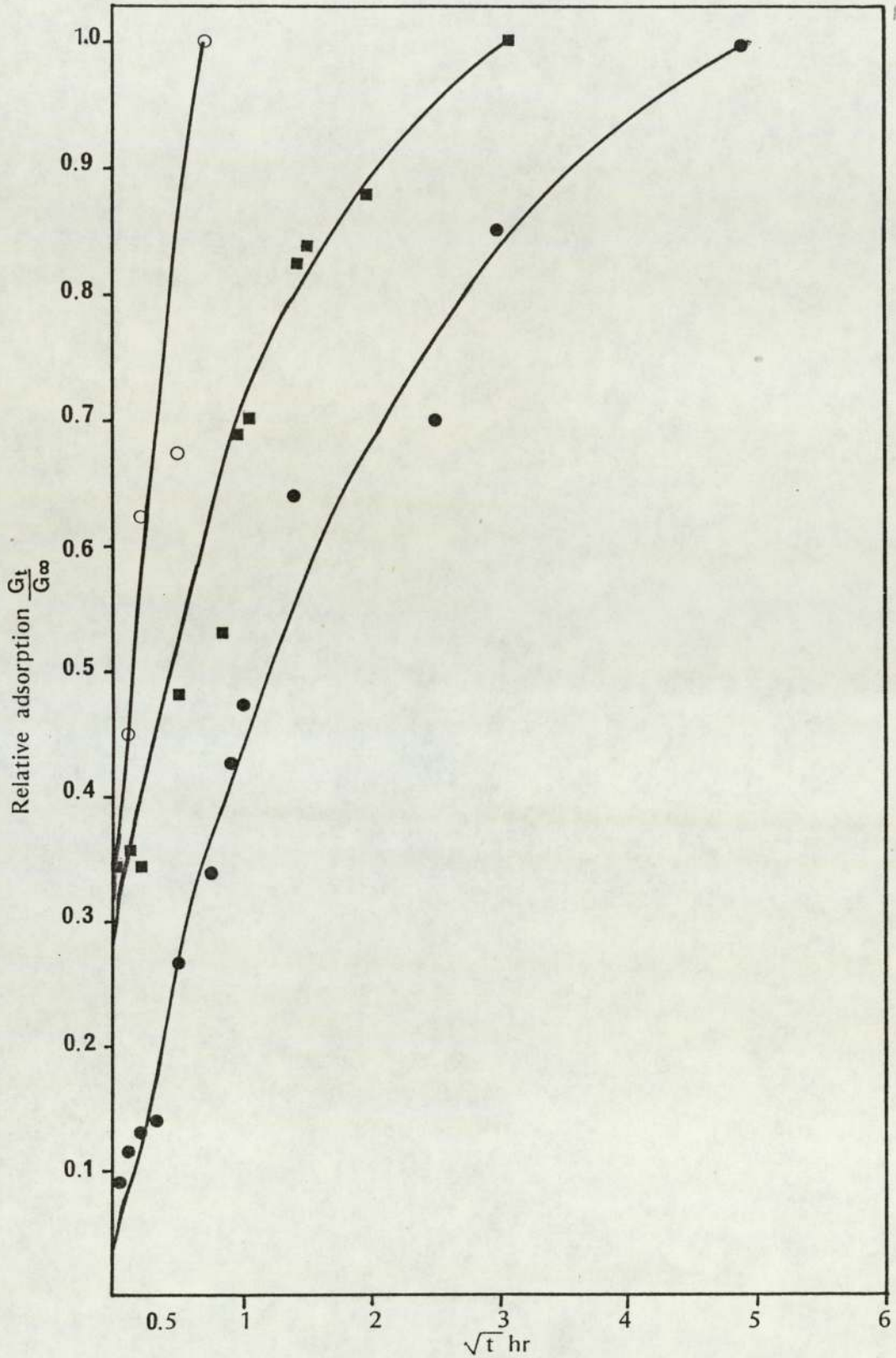
Figure 8.6 Kinetics of Relative Adsorption
$\frac{G_t}{G_\infty}$ of ● Extract fraction 1,
■ Extract fraction 2 and O
Extract fraction 3 from Iso-
octane at 343 K on NaX
Zeolite Pellets.
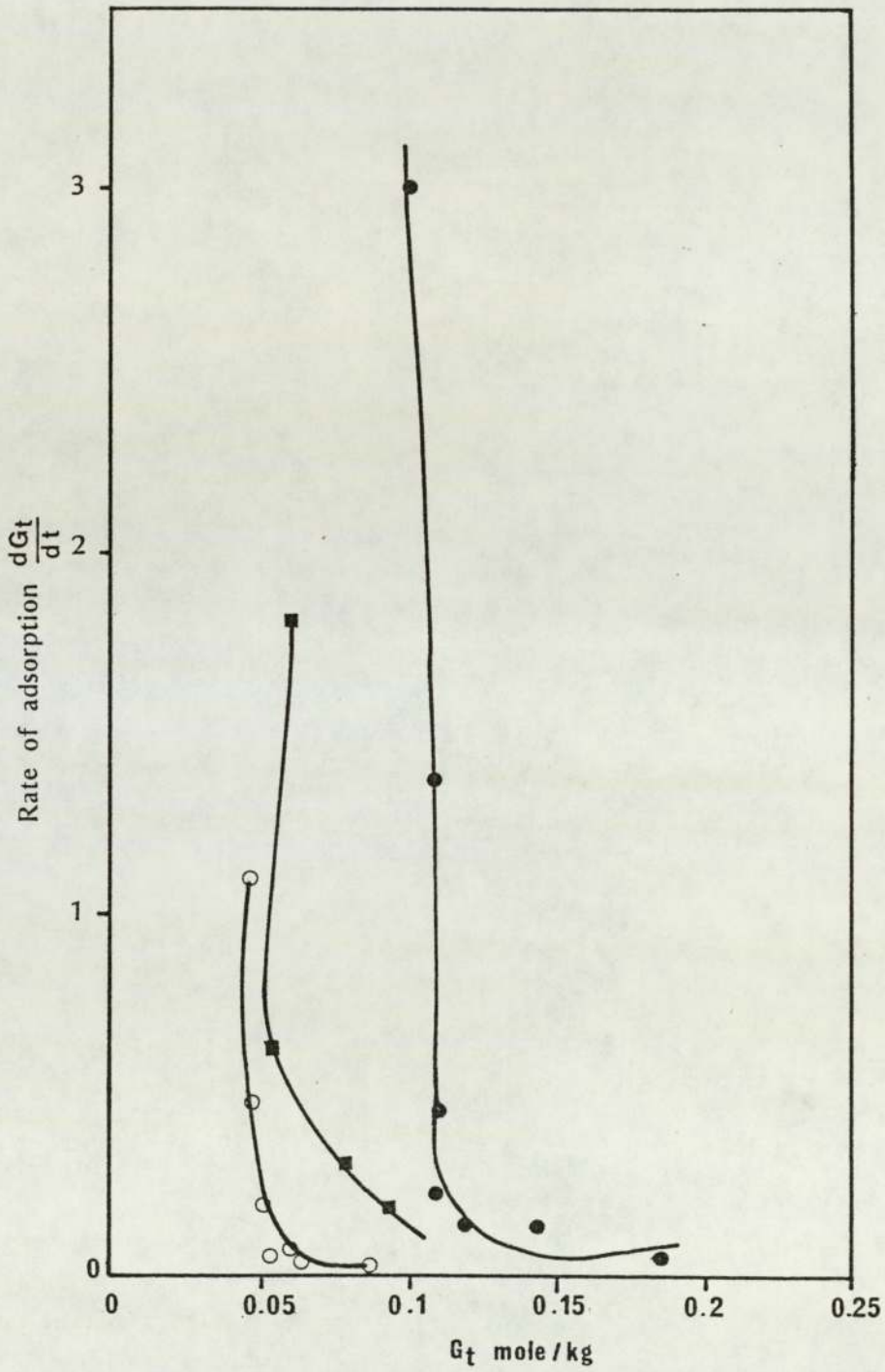
Figure 8.7   Rate of Adsorption $\frac{dG_t}{dt}$
              of ● Extract fraction 1,
              ■ Extract fraction 2 and
              ○ Extract fraction 3 at
              303 K on NaX Zeolite
                    Pellets.
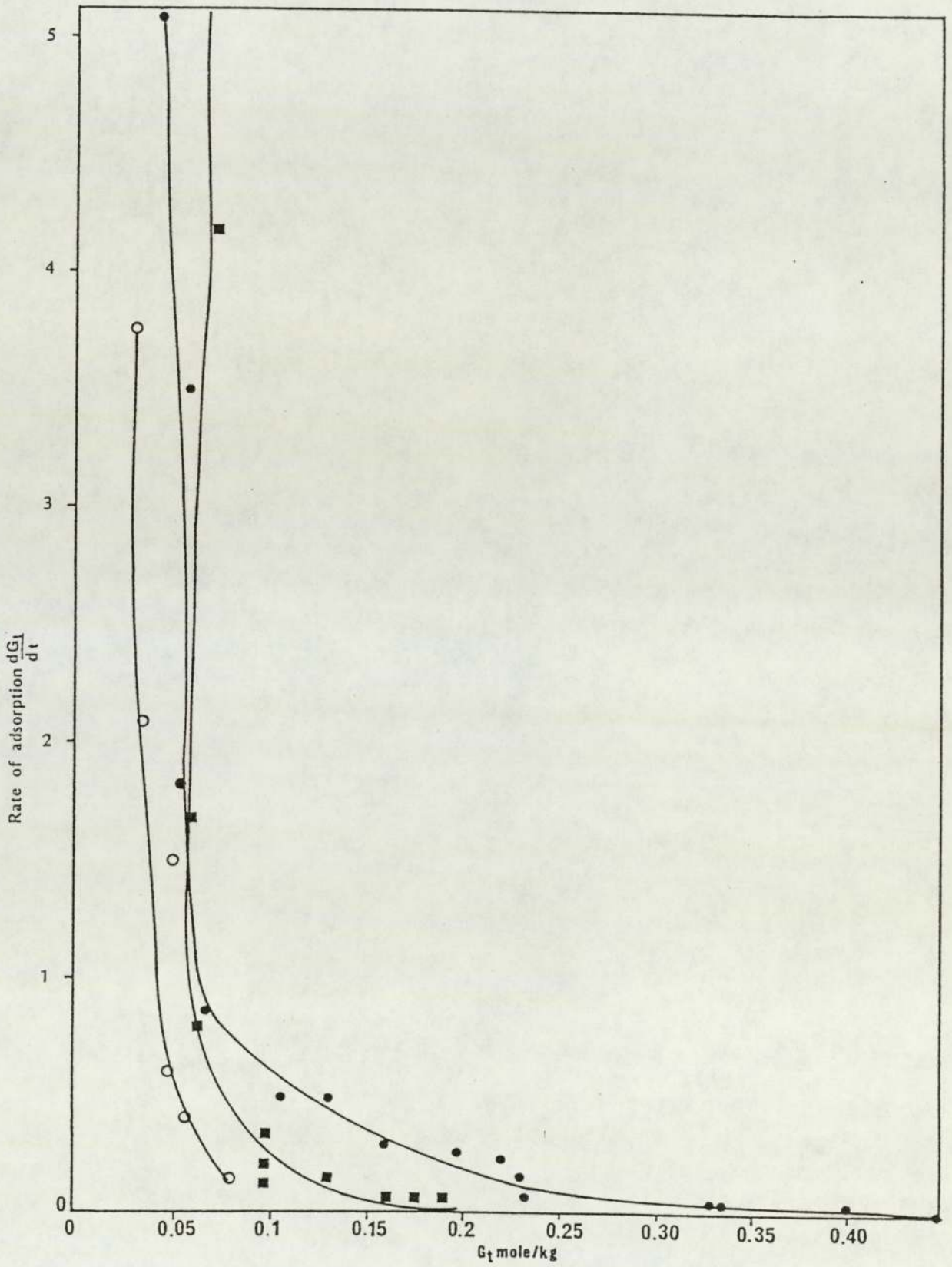
Figure 8.8   Rate of Adsorption $\frac{dG_t}{dt}$ of ● Extract fraction 1, ■ Extract fraction 2 and ○ Extract fraction 3 at 343 K on Nax Zeolite Pellets.

As the adsorption value increases so the rate of adsorption decreases; this can be explained as follows: As the absorbate-molecules occlude in the cavities of the molecular sieves, the polar compounds in the extract will firstly interact very strongly with the cations of the active sites. This will result in multi-component adsorption which tends to block the pores of the molecular sieve and the aperture diameter will be decreased. Adsorbate molecules which follow will not be allowed to penetrate through the channel of the cavities and the rate of adsorption will diminish.

At the lower temperature the rate of adsorption for the strongly polar compounds in extract fraction 3 was slow both because of the high percent of resins present and its high molecular weight. The rate of adsorption was much higher for the first extract fraction due to the reduced resin content and lower molecular weight. An increase in temperature increased the rate of adsorption. At higher temperatures the molecules would tend to be occluded more, but as the adsorption value increases the rate of adsorption decreases.

Measurements of the kinetics of adsorption were conducted by the volumetric method, under both constant concentration ($\approx$ mole fraction) and constant volume conditions. Under these conditions the diffusion coefficients of the three extract fractions were determined taking into consideration the value of adsorption at a certain time t, versus the total volume of the pore, and the external surface area of the crystallites. The results of the calculated effective diffusion coefficient are illustrated in Figures 8.9 and 8.10, where they are plotted against the coverage rate of the molecular sieves $\frac{G_t}{G_\infty}$ at temperatures of 303 and 343 K. These indicate that, at 343 K, as the polarity increased and the sorption coverage rate increased the diffusivity decreased in the order:

extract 3 < extract 2 < extract 1

As shown above, the polarity of the sorbate molecules contribute substantially to the energy barriers to diffusion along the interstitial channels.

At the lower temperature of 303 K extract 2 had a higher diffusion coefficient. This was due to the easy transition of the adsorbate molecule from one pore to another, because the interactions were weak and
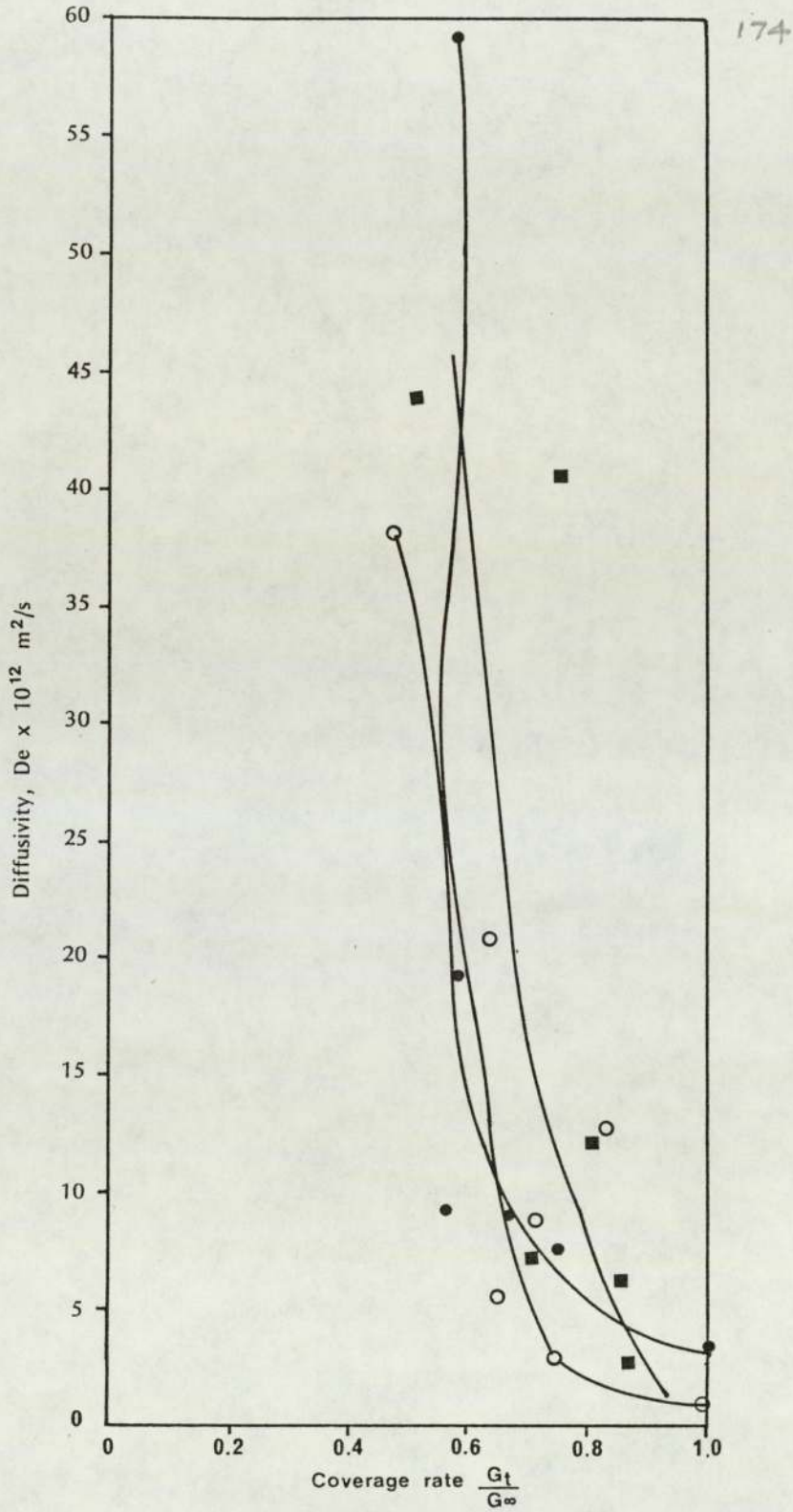
Fgiure 8.9 Effective Diffusion
Coefficient De of
● Extract fraction 1,
■ Extract fraction 2
and o Extract fraction
3 as a Function of Degree
of Coverage Rate $\frac{G_t}{G_\infty}$ at
303 K on NaX Zeolite
Pellets.
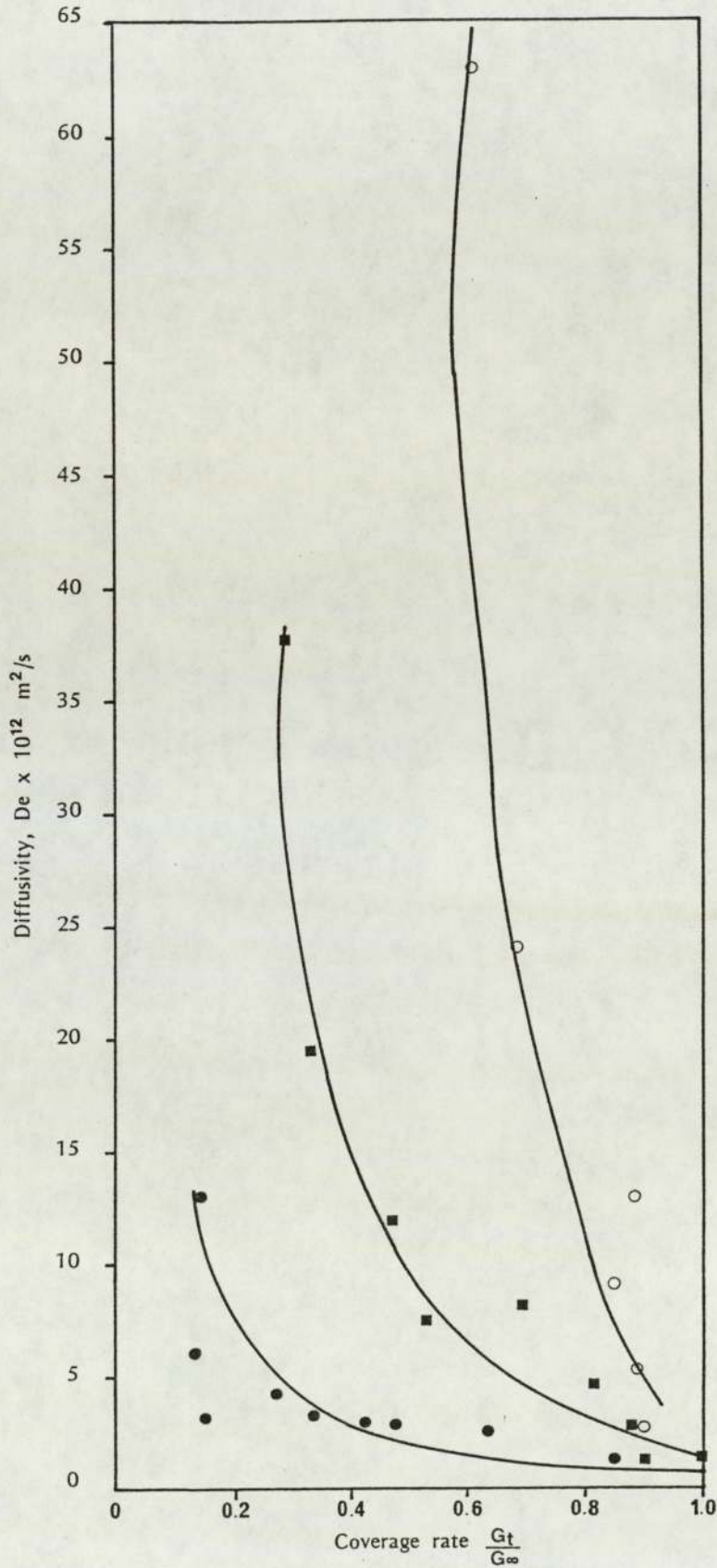
Figure 8.10   Effective Diffusion
Coefficient De of
● Extract fraction 1,
■ Extract fraction 2
and ○ Extract fraction
3 as a Function of Degree
of Coverage Rate $\frac{G_t}{G_\infty}$ at
343 K on NaX Zeolite
Pellets.

allowed the adsorbate molecules of extract fraction 2 to jump to the next equilibrium position in the cavity of the molecular sieve crystal. Figures 8.9 and 8.10 show that an increase in the coverage rate resulted in a decrease in the diffusion coefficient.

Table 8.1 presents calculated values of the activation energy for the three extract fractions at different coverage rates. The activation energy increased considerably as the molecular weight of the extract fractions decreased. Extract fraction 1 contained aromatic molecules which are attracted more energetically to the cations in the active site of the molecular sieve. Consequently these molecules which exhibit positive interactions, require a higher activation energy to break-away, and to allow the adsorbate molecules to jump to the next pore with a higher equilibrium level. Activation energies for the three extract fractions were calculated had the following order:

extract 1 > extract 2 > extract 3

8.2 Conclusions

To separate traces of aromatic compounds from the wax fractions, it is preferable to start with a low molecular weight and sulphur-free lube-oil fraction. This will yield a better, higher quality of purified wax fraction.

TABLE 8.1

AVERAGE DIFFUSION COEFFICIENTS AND ENERGIES OF ACTIVATION
FOR EXTRACT FRACTIONS IN MOLECULAR SIEVES TYPE 13X (NaX)

$\dfrac{G_t}{G_\infty}$	$De \times 10^{12}$ m^2/s 303 K	$De \times 10^{12}$ m^2/s 343 K	Log De 303 K	Log De 343 K	Log De 343	Log De 303	E_A Kcal /mol	E_A kJ/ mole
	Extract 1							
0.6	21	1.5	-6.67	-7.82	1.15		13.09	54.7
0.7	8.5	1	-7.07	-8	0.93		10.58	44.22
0.8	5.25	1	-7.28	-8	0.72		8.19	34.26
	Extract 2							
0.6	33.5	7	-6.47	-7.15	0.68		7.74	32.36
0.7	17.5	4.5	-6.45	-7.34	0.59		6.71	28.07
0.8	8	3	-7.09	-7.52	0.43		4.89	20.46
	Extract 3							
0.6	19	45	-6.72	-6.34	0.38		4.32	18.08
0.7	5.5	22	-7.25	-6.65	0.6		6.831	28.5

9.0 THE DYNAMIC ADSORPTION OF AROMATIC COMPOUNDS FROM BINARY SOLUTION IN ISOOCTANE AND N-ALKANES

9.1 Introduction

Establishment of the basic criteria for isothermal dynamic adsorption in a fixed bed of adsorbent is based upon the equilibrium isotherm and the kinetics of adsorption which characterize the external and internal mass transfer. The dynamic adsorption characteristics can usually be determined from the breakthrough curves, which identify the change in concentrations of gases or solution of the adsorbate molecules after passing through the fixed bed of the adsorbent, versus time or volume.

Consideration of the technical feasibility of the dearomatization of the waxes or n-paraffins using adsorption generally requires a study of the dynamic process of adsorption using fixed adsorbent beds and a wide concentration range. In this investigation, however, a narrow concentration range, < 5 wt%, was used since the objective was to study the adsorption dynamics of low aromatic compounds from waxes or n-paraffins.

9.2 Theoretical Background

The basic theory of dynamic adsorption was given by Michaels (55). He studied the dynamic adsorption of sodium ions from solution with sodium chloride over a packed bed of acid-form cation exchanger particles at a constant flow rate.

Michaels found that if the concentration of metallic cation in the effluent from a fixed-bed ion exchange column is plotted as a function of the total volume of effluent collected, a characteristic S-curve (Figure 9.1) is obtained. The 5% exit concentration is designated the breakthrough point of the bed. If operation of the column is continued, the concentration of metallic ion in the effluent rises until it reaches 95% of the effluent value; this point is termed the exhaustion point, at which the exchange zone has moved out of the bed and the exchanger is, for all practical purposes, exhausted. Rates of adsorption in fixed bed dynamic systems may be described by using the mass transfer zone concept. The Mass Transfer Zone (MTZ) is the volume of the efficiency in which the concentration of adsorption in the bed increases from nominally 5% to 95%. This is useful since it characterizes the behaviour of adsorbate in the bed in terms of flux and concentration gradient.

Michaels theories are now applied to the analysis of large scale commercial adsorption and ion-exchange processes.

For the dearomatization of waxes or n-paraffins using a fixed bed of molecular sieves type X, Michaels theory can be applied if the following requirements are satisfied,

o   The fixed bed should be uniformly packed.

o   The velocity, the temperature and the composition of the influent should be constant.

o   There should be no radial gradient of temperature, concentration or velocity.

o   The initial temperature of the adsorbent and the influent should be approximately equal.

o   There should be no phase change and no chemical reaction.

o   Adsorption heat effects are negligible.

Under these conditions the effluent volume versus concentration S-curve will give a true picture of the concentration variations through the packed bed of molecular sieves (Figure 9.1). When the concentration of the aromatic in the effluent waxes or n-paraffins reaches 95% of the total concentration X_O, the influent flow would be stopped.

The time, θ_z, required for the exchange zone to move its own height up through the bed under steady-state conditions is proportional to the volume of effluent, V_z (Figure 9.1):

Hence

$$\theta_z = V_z / \left(U_f \right) \left(A_{cs} \right) \tag{9.1}$$

Similarly, the time, θ_T, required for the zone to reach at the top of the bed is proportional to the total volume of effluent collected; V_T:

$$\theta_T = V_T/U_f \ A_{cs} \tag{9.2}$$

Except for the period of time during, which it is being formed at the beginning of the process θ_f, the velocity of the zone through the bed at a constant rate is determined by:
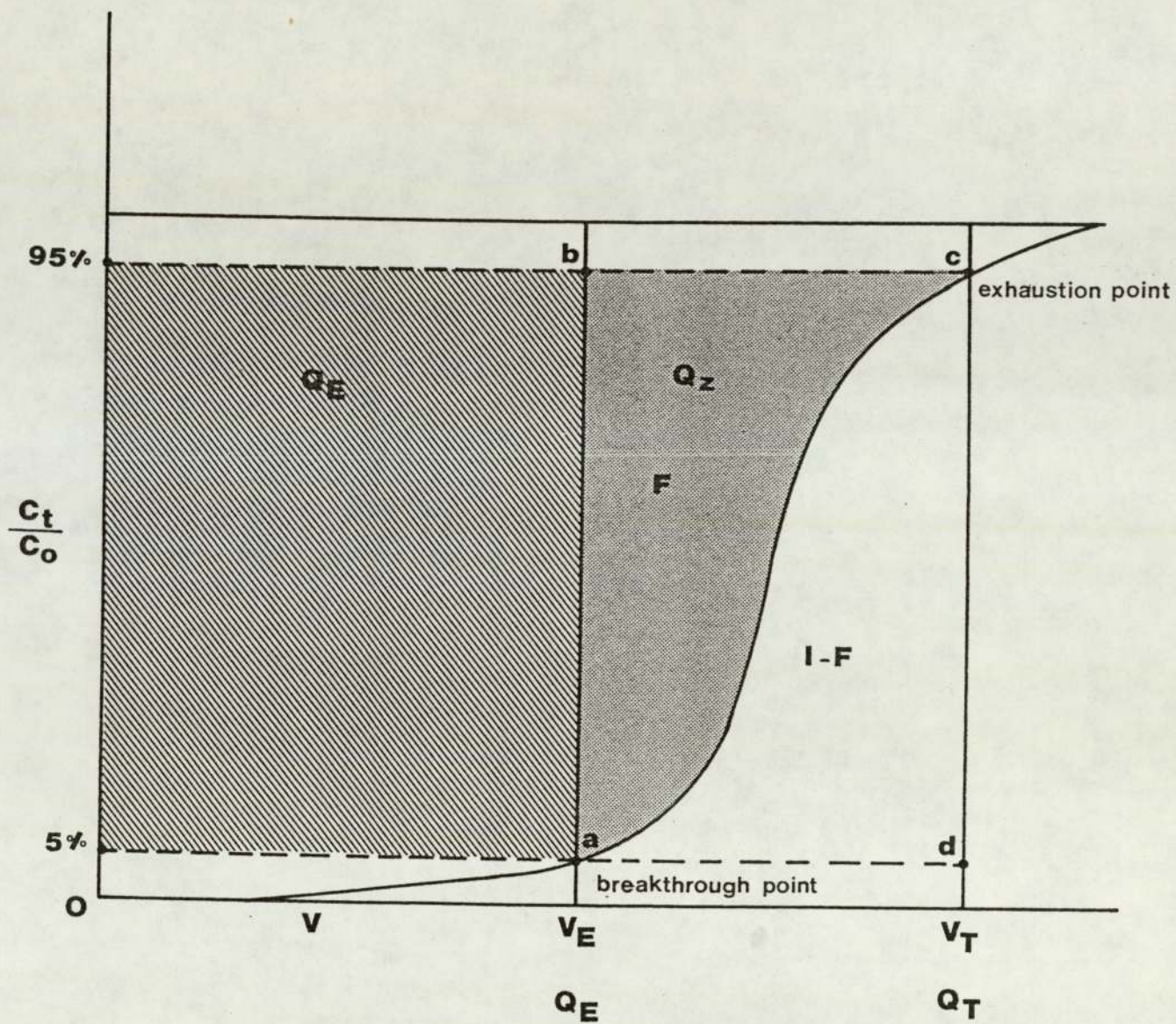
Figure 9.1. Breakthrough Curve Using Packed
Bed of the Molecular Sieves.

$$U_z = \frac{h_T}{\theta_T - \theta_f} \tag{9.3}$$

The height of the mass transfer zone (MTZ) can be determined from,

$$h_z = U_z \theta_z = h_T \left(\frac{\theta_z}{\theta_T - \theta_f} \right) \tag{9.4}$$

The only unknown in equation (9.4) is the zone formation time, θ_f. This can be estimated as follows: The quantity of aromatics removed by the bed from the breakthrough point to exhaustion may be determined graphically (Figure 9.1) from:

$$Q_z = \int_{V_E}^{V_T} \left(c_o - c \right) dv \tag{9.5}$$

If, however, the bed was completely occupied by the aromatic hydrocarbons then the full capacity of the packed bed would be approximately equal to:

$$Q_{z_{max}} = C_o V_z \tag{9.6}$$

Then the symmetricity factor (F) will be equal to:

$$F = \frac{Q_z}{Q_{z\,max}} = \frac{\int_{V_E}^{V_T} \left(c_o - c \right) dv}{C_o V_z} \tag{9.7}$$

where from Figure 9.1 the total Q_z is equal to the area of abc; and Q_z max. is equal to area abcd.

If F=0 (i.e., if the packed bed is fully-saturated by the aromatics within the zone at steady state), the time of formation of the zone at the bottom of the bed would be expected to be nearly equal to the time

required for the zone to descend a distance equal to its own height, θ_z, after steady-state is reached. Conversely, if F=1.0 (i.e., if the packed bed within the zone at steady state is essentially free of the aromatics being removed), the time of formation θ_f would be very short.

A simple relation for estimating zone formation time which satisfies the limiting conditions is,

$$\theta_f = \left(1-F\right)\theta_z \qquad (9.8)$$

In many cases the S-curves are found to be symmetrical, so that F=0.50, and θ_f=0.5 θ_z.

Based on these assumptions, the height of the mass transfer zone can be calculated from the S-curve using equations (9.4) and (9.8):

$$h_z = h_T \left(\frac{\theta_z}{\theta_T - \left(1-F\right)\theta_z}\right) = h_T \left(\frac{V_z}{V_T - \left(1-F\right)V_z}\right) \qquad (9.9)$$

or for symmetrical curves

$$h_z = h_T \left(\frac{V_z}{V_T - 0.5\, V_z}\right) \qquad (9.10)$$

For any fixed bed unit operating at constant feed flow rate for which the S-curve has been determined, the total capacity of the bed can be calculated by graphical integration of the relation:

$$C_T = \int_o^{V_T} \frac{\left(C_o - C\right)\, dv}{V_a} \qquad (9.11)$$

Similarly the effective, or working, capacity of the molecular sieves can be determined by calculating the area above the S-curve up to the breakthrough point.

$$C_E = \frac{\int_o^{V_E} \left(C_o - C\right) dv}{V_a} \tag{9.12}$$

The breakthrough capacity of the bed may be determined from,

$$C_E = C_T \left(\frac{h_T - \left(1-F\right) h_z}{h_T}\right) \tag{9.13}$$

The adsorption efficiency γ is a relationship between C_E and C_T which can be determined by:

$$\gamma = \frac{C_E}{C_T} = \frac{\left(h_T - \left(1-F\right) h_z\right)}{h_T} \tag{9.14}$$

Hence the efficiency of the packed bed can be determined by calculation of the dynamic properties such as height of mass transfer zone h_z, dynamic effective capacity A_d and adsorption efficiency γ.

9.3 Literature Survey

Ahmetovic and Sevel-Cerovecki (56) studied the possibility of preparing low aromatic solvents by passing refinery fractions of gasoline, white spirit and kerosene over molecular sieve 13X. The experiments were carried out in a glass column of 25 mm diameter and 400 mm height for gasoline and 700 mm height for kerosene and white spirit.

Dynamic equilibrium capacity was calculated and the height of mass transfer zone and height of unused mass transfer zone were calculated from S-curves.

They concluded from their results that molecular sieve 13X can be used for dearomatization of such refinery streams and the optimal conditions of velocity and temperature for laboratory experiments were for gasoline 0.26 cm/min and temperature 293 K, and for white spirit and kerosene 0.4 to 0.6 cm/min and temperature 310 K. Within the range of rates from 0.2 to 0.8 cm/min the heights of mass transfer zone were:

for gasoline at 293 K h_z = 173 mm

for white spirit at 310 K h_z = 174 mm

for kerosene at 310 K h_z = 270 mm

Bolotov et al. (57) developed a method for calculating the quantity of displacing agent exchanged on the zeolite in the cyclic release of n-paraffins. The method is based on traditional concepts of adsorption technology (saturation capacity of the zeolite, exit curve for adsorption of n-paraffins, isotherms of ammonia adsorption by the zeolite) and also a mechanism of n-paraffins adsorption by zeolite under dynamic conditions that takes into account the formation of three zones in the zeolite bed: a saturated zone, a mass transfer zone (in this zone, the concentration of n-paraffins changes from the original concentration to the breakthrough concentration), and an unoccupied zone.

The method of calculation was tested on commercial units for the adsorptive recovery of paraffins on CaA zeolites. The mean temperatures of the zeolite bed at the ends of the adsorption and desorption stages were found to be 640 K and 660 K, respectively. The calculated quantity of exchanged ammonia, was found to be 14,661 kg/hr in comparison with a value of 14,628 kg/hr measured in the unit. So the calculated results were in satisfactory agreement with the actual data.

Michaels (55) and Collins (58) studied the factors affecting the mass transfer zone such as temperature, molecular sieves type, particle size, feed concentration and feed flow rate.

Rasmuson (59) studied the influence of adsorbent particle shape on the dynamics of fixed beds in general. Calculations showed that if the area-to-volume ratio of the slabs, cylinders or spheres is the same, identical breakthrough curves are produced for short and long contact times. In the intermediate range the first breakthrough times are in the order, spheres < cylinders < slabs which indicates a greater number of macropores in slabs compared with spheres and cylinders.

Dorogochinski et al. (16) studied the influence of the mass transfer zone on the dynamic adsorption of aromatics from a kerosene cut in a packed bed column, of length 370 mm and diameter 30 mm, using binder-free

molecular sieves NaX at 573 K. The mass transfer zone h_z was found to equal 150 mm indicating that the efficiency of adsorption was very high. Fominykh et al. (8) studied the dynamic adsorption efficiency of separation of aromatic hydrocarbons from mixtures with paraffins or naphthenes over molecular sieves type NaX and CaX. The synthetic zeolites NaX and CaX were found to possess high dynamic activity and selectivity with respect to benzene. The dynamic activity of the zeolite decreased with increase in the feed flow rate.

Fominykh found that an increase in the aromatic concentration in the feed resulted in a reduction in the dynamic activity of NaX zeolite.

Kehat and Rosenkranz (60) studied separation of n-hexane from a solution in benzene using molecular sieve type 5A. They utilised a single, coiled copper, column 3.68 m long and 7.2 mm i.d., packed with 110 g of molecular sieve 5A in the form of 1-2 mm granules. Heating was provided by coils and the temperature could reach 673 K. All runs were made with one feed concentration, 6 mole % n-hexane in benzene, and one adsorbent bed. The same adsorbent gave results reproducible within 5% after > 720 ks of operation. Runs were made at 423 K, 473 K, and 523 K and pressures of 266, 466, 666 and 999 kN/m^2. The maximum sieve capacity of 11 kg of n-hexane per 100 kg of adsorbent was achieved at the higher temperatures and higher pressures. Increased flow rate reduced the time of adsorption more than it reduced the capacity of the adsorbent. For example, at 523 K, doubling the flow rate reduced the breakthrough time by 4, and the adsorption capacity by 2.

Epperly et al (61) claimed a process for the separation of aromatics (1-3 weight percent) and/or nonhydrocarbons from saturated hydrocarbon and/or olefins and for the separation of olefins from saturated hydrocarbons. The process was particularly related to the purification of saturated hydrocarbons and/or olefins, especially n-paraffins, utilizing a zeolite adsorbent and a displacing agent. The process comprises two steps, i.e. adsorption and desorption, both preferably carried out in the vapour phase in a fixed bed at about atmospheric pressure. The process can also be operated in the liquid phase. Suitable displacing agents for the process include SO_2, NH_3, CO_2, C_1 to C_5 alcohols, glycols, halogenated compounds, and nitrated compounds. The adsorbent included any zeolitic adsorbent having pore sizes of 6.5 to 13 A$^\circ$; molecular sieve of type 13X

or 10X of mono or divalent cations were preferred. In general the amount of feed per cycle was 0.02 to 2; for C_{10} to C_{25} hydrocarbons the preferred amount per cycle was 0.03 to 0.7 wt./wt. The time of adsorption was 900 to 10 s;the time for desorption was from 20 to 1 s. Five examples are given of varying operating conditions and the purity of the products obtained. The aromatic content which was varied from one cycle to another ranged within 0.1 to 0.02% by weight, and the preferred temperature ranged between 495 and 720 K.

Roger and Macnab (62) described a process for separating straight-chain hydrocarbons from mixtures with branched-chain and/or cyclic hydrocarbons. These mixtures had boiling points within the range 400 - 720 K. The mixture was contacted with a fixed bed of 0.9-2.4 m length of 5A molecular sieve. In a first stage the straight chain hydrocarbons were selectively adsorbed. The sieve bed was purged in a second stage to remove surface-adsorbed and interstitially-held hydrocarbons from the sieve. In the last stage, the adsorbed straight chain hydrocarbons were desorbed. The experiments were conducted isothermally in the vapour phase and process temperature was within the range 598-648 K for gasoline feedstock, 623-673 K for kerosene and 653-693 K for gas oil. The preferred pressure varied with the feedstock, i.e. for gasoline it was 266-666 kN/m^2, for kerosene 100-230 kN/m^2 and for gas oil 30-200 kN/m^2. The feed rate to the adsorption stage was 1.0-2.0 volume of feed/volume of molecular sieve/60 s. The n-paraffin yield was 3.0% sieve weight/3.6 ks with a purity of 97.5% weight and a carbon number distribution substantially similar to the feed. By desorbing from both ends of the bed simultaneously, the n-paraffin yield was increased to 3.5% sieve weight/3.6 ks

Epperly et al (63) presented a process for removing cyclic constituents such as cyclic paraffins and aromatics from fuels. The fuels were first subjected to dehydrogenation to convert the naphthenes into aromatics. It was then contacted with a molecular sieve adapted to selectively adsorb the aromatic compounds. Ammonia was employed both to reactivate the catalyst and to desorb the molecular sieve. The fuels obtained by this process exhibit improved luminometer numbers and are useful as supersonic jet fuels. In their first invention the feedstock was kerosene boiling between 440 and 520 K. The feed was initially dearomatized by adsorption in a type X molecular sieve, and then passed into the dehydro-

genation zone over an alumina catalyst. Two beds of catalyst were utilized each containing 40 g of catalysts. Ammonia was utilized as desorbent agent; it was fed at the same temperature and a rate of 1.8 wt/60s/wt, and pressure was maintained at 100 kN/m^2. Significant amounts of aromatics were produced in the bed, demonstrated by an increase in refractive index of the product from 1.4230 to 1.4271.

After 2 wt/wt of feed had been passed over the bed a product with an aromatic content of about 1.8% by weight was collected. Deactivation had occurred, but appreciable activity was maintained. Adsorption removed about 60% to 99% of cycloparaffins and aromatics from the original cyclic compounds, and the product constituted a fuel with a luminometer number of about 75 to 130 compared to an original value of about 50.

Mahto et al. (64) studied the separation of n-paraffins from kerosene and gas oil using adsorption on molecular sieves. A 0.65 m long, 2.5 mm diameter stainless steel column containing 5 A molecular sieve as 1.5 mm pellets was used in this study. Recovery under equilibrium loading, and efficiency of the column, were studied as a function of temperature. It was found that the time for equilibrium loading continuously decreased with increasing temperature. Although the total volume of normal paraffins adsorbed on the sieves decreased, the percent volume recovery increased up to a certain temperature after which it started to decrease. The maximum loading was found to be 20 g and 26 g per 100 g of dry molecular sieves for kerosene and gas oil respectively at 293 K (room temperature). They compared the results obtained from this adsorption process with those from the urea process; the amount of n-paraffins recovered were 7 and 12 per 100 g of urea for kerosene and gasoline respectively. Hence the former was more efficient and more economic. An optimum adsorption temperature existed for each petroleum fraction.

Denisenko et al. (65) reported certain aspects of the quantitative determination of naphthenic, n-paraffinic, and isoparaffinic hydrocarbons in mixtures of naphtha and gasoline by using molecular sieves type 13X. It was concluded that there was essentially no irreversible adsorption for C_5-C_{10} hydrocarbons on 13X molecular sieves in gas chromatography.

Lauder and Rolfe (66) invented a cyclic vapour-phase, pressure swing process for the separation of n-paraffins from a mixture with non straight-chain hydrocarbons, for example, aromatics, cycloparaffins and

isoparaffins. The steps in the process were adsorption, purging, and desorption using 5A molecular sieve.

The feed stocks which they recommended were gasoline, kerosene or gas oil fractions, i.e. fractions which boiled within the ranges 350-473 K, 423-573 K and 473-723 K. The preferred operating temperatures for different feedstocks were 573-650 K for gasoline, 623-673 K for kerosene and 650-710 K for gas oil. Preferred adsorption pressures also varied with the feed stock i.e. from 33-2000 kN/m^2 for gasoline to 33-330 kN/m^2 for kerosene and gas oil. The preferred feed rate to the adsorption stage was 1.5-3.0 v/v/60 s. The durations of the adsorption, purge and desorption stages were 60-300 s, < 180 s and 120-600 s, respectively.

Al-Ameeri and Owaysi (67) studied the separation of n-paraffins from petroleum fractions such as straight-run kerosene, and naphtha-kerosene blend by adsorption on 5A molecular sieves. They compared the efficiency of the adsorption process with the efficiency of urea adduct formation as an alternative separation technique. The purity of the isolated n-paraffins was 96.6% by adsorption and ranged between 85-91% using the urea adduct process. The dynamic capacity of the molecular sieves was found to be 21.35 g of paraffins/100 g of adsorbent when straight run kerosene was used and 14.61 when naphtha kerosene blend was used. The pour point of the denormalized kerosene was reduced by 32% to 92% which is a large improvement and tenders the fuel suitable for cold climatic applications.

Schirmer et al (68) studied the measurements of the equilibrium adsorption of n-paraffins of medium chain length such as n-decane, n-dodecane, n-tridecane, n-tetradecane, n-hexadecane and n-octadecane on synthetic zeolites 5A in the range of temperature from 550-700 K. The heats of adsorption of all n-paraffins investigated showed a distinct dependence on the degree of pore filling. The heats of adsorption of the n-paraffins of medium chain length increased linearly with increasing number of carbon atoms.

Hedge (30) achieved a practical method for separating 2, 6 dimethynaphthalene (DMN) from 2, 7 dimethylnaphthalene in a dimethylnaphthalene concentrate mixture using sodium type Y molecular sieve. Selective adsorption of 2, 7 dimethylnaphthalene was accomplished in a column 20 mm i.d. and 0.9 m in length. The mixture of 2, 6-DMN and 2, 7 DMN was pumped

into the bottom of the column. At the end of the DMN charge, the desor-
bent benzene, O-xylene or toluene was pumped into the bottom of the column
to desorb the 2, 7 DMN adsorbate. Effluent from the column was taken in
small cuts and analyzed by gas chromatography. The adsorbent column was
held at a temperature just below the boiling point of the desorbent to
speed diffusion into the sieve particles. A study of the breakthrough
curves for the 3 desorbents showed that benzene allowed a rapid break-
through of 2, 7 DMN. Toluene allowed a faster equilibrium to be reached
than O-xylene; thus it was superior at higher flow rate and the best
desorbent.

Epperly et al. (22) developed a novel process for removing benzene,
olefins and sulfur compounds from feed streams by adsorption with 13X
molecular sieve. The resulting feed can then be used for isomerization
and paraffin alkylation, since these aromatic and olefin compounds tend to
retard the isomerization reaction. Naphtha feed was preheated to a pre-
ferred temperature of about 380-470 K, i.e. it was a vapour phase process.
The pressure was 100-400 kN/m^2 and the flow rate 0.5-3.0 w/w/60 s. The
feed entered the contacting zone where aromatics were stripped-off by
fresh 13X molecular sieve. The dearomatized hydrocarbon stream then
passed into a condenser, where it was cooled down; and then to the isomer-
ization reactor. At, or just before, breakthrough the adsorption step was
terminated and the heat purge stage commenced at 570-630 K, to desorb the
aromatic mixtures which might be used as high grade gasoline. The occur-
rence of breakthrough was identified by refractive index measurements or
ultraviolet absorption analysis of the effluent stream.

Fominykh et al. (8) studied the adsorption of benzene from mixtures
of benzene and n-heptane. Experiments were conducted in both the liquid
and vapour phase and the adsorbents used were synthetic zeolites of type
NaX or CaX of 1.5-2 mm size which were activated at 623 K for 10.8 ks.
The adsorbers comprised glass tubes of 22 mm diameter and 200 mm height;
the charge of zeolite was 10 g. In experiments carried out in the liquid
phase, the stream of the feedstock was directed upward from below; in the
vapour phase experiments flow was in the reverse direction. Samples of
the dearomatized product were withdrawn in 1 ml lots and analyzed for ben-
zene by refractive index n_D^{20}. Breakthrough was observed when the refrac-
tive index of the filtrate became > 1.388. The liquid phase process was

conducted at room temperature and the vapour phase process at 418-423 K. At a given height of adsorbent layer, its dynamic activity changed appreciably with an increase in the feed rate. From the data obtained the dynamic activity of NaX zeolite was found to be somewhat greater than that of CaX zeolite under similar conditions. The dynamic efficiency of zeolite decreased with an increase in benzene concentration from 4-20 vol.%. Also, the higher the concentration of the component being adsorbed the more rapidly breakthrough occurred. Multiple-cycle operations were used, and for desorption heating the adsorbent at 573 K and applying vacuum of 98 kN/m^2 for 10.8 ks allowed the zeolites to be used repeatedly.

9.4 Experimental Investigation

Methodology.

A pre-weighed quantity of molecular sieve was activated by calcination in a muffle furnace at 720 K for 14.5 ks (See 3.2.2). The equipment for dynamic studies, shown in Figure 9.2, comprised

Identifying Number	Item
1.	A receiver of 500 cm^3 capacity with a heating jacket. This was used for the n-alkane and the wax to be purified from the aromatic content
2.	Preheater of capacity 20 cm^3.
3.	660 mm long, 16 mm diameter column.
4.	Collectors.
5.	Pulsation pump, RBF 0.09/4.71 RPM 1400 MPL SS 8c ex Bauknecht, U.K.
6.	Vacuum pump, BS 2511/12 RPM 1425 ex Edwards, U.K.

The pump was pre-calibrated by using a burette. Its outlet was connected to one neck of the preheater.

The adsorption column comprised a glass tube; the desired temperature was maintained by means of an electrically-heated coil wrapped around it and insulated by a glass tube of 17-18 mm i.d. covered with insulation material. The column temperature was measured with thermocouples connected to an electrical controller-regulator to maintain the temperature at the desired level.

9.4.1 Experimental Procedure

1. The column was filled with freshly-activated, molecular sieve and the temperature was maintained at 473 K under vacuum to avoid any air or moisture adsorption.

2. The vacuum pump was replaced by the pulsation pump, and the column was cooled, or heated up, to the desired temperature. The mixture was then passed through the preheater to the column at a linear velocity of 0.21 cm/min. When the mixture contacted the adsorbent, the time t_1 was recorded.

3. The mixture was run through the layers of adsorbent and when it reached the top layer of the column (near the exit) time t_2 was recorded.

4. The exit valve was connected to the automatic collector with all sample tubes numbered.

5. The collector was switched on. When the first drop had been collected into the first tube, it was regulated to move to the second tube after a set time, e.g. 600 s.

6. The samples collected were analyzed for aromatics content using ultraviolet spectroscopy.

7. The run was continued until the UV analysis showed the aromatics content in the sample was the same as the original content, i.e. equilibrium was established. The run was then stopped.

9.4.2 Calculation of Design Parameters

The efficiency of the adsorption column was measured by the length of working layer (h_z),

$$h_z = h_T \frac{\theta_T - \theta_n}{\theta_T - \left(1-F\right)\left(\theta_T - \theta_n\right)} = h_T \frac{\theta_z}{\theta_T - \left(1-F\right)\left(\theta_z\right)}$$

Dynamic capacity A_d was determined from the equation:

$$A_d = \sum \left(w_1 c_o - w_2 c\right)$$

The effective coefficient of utilized layer (γ) was determined according to the equation:
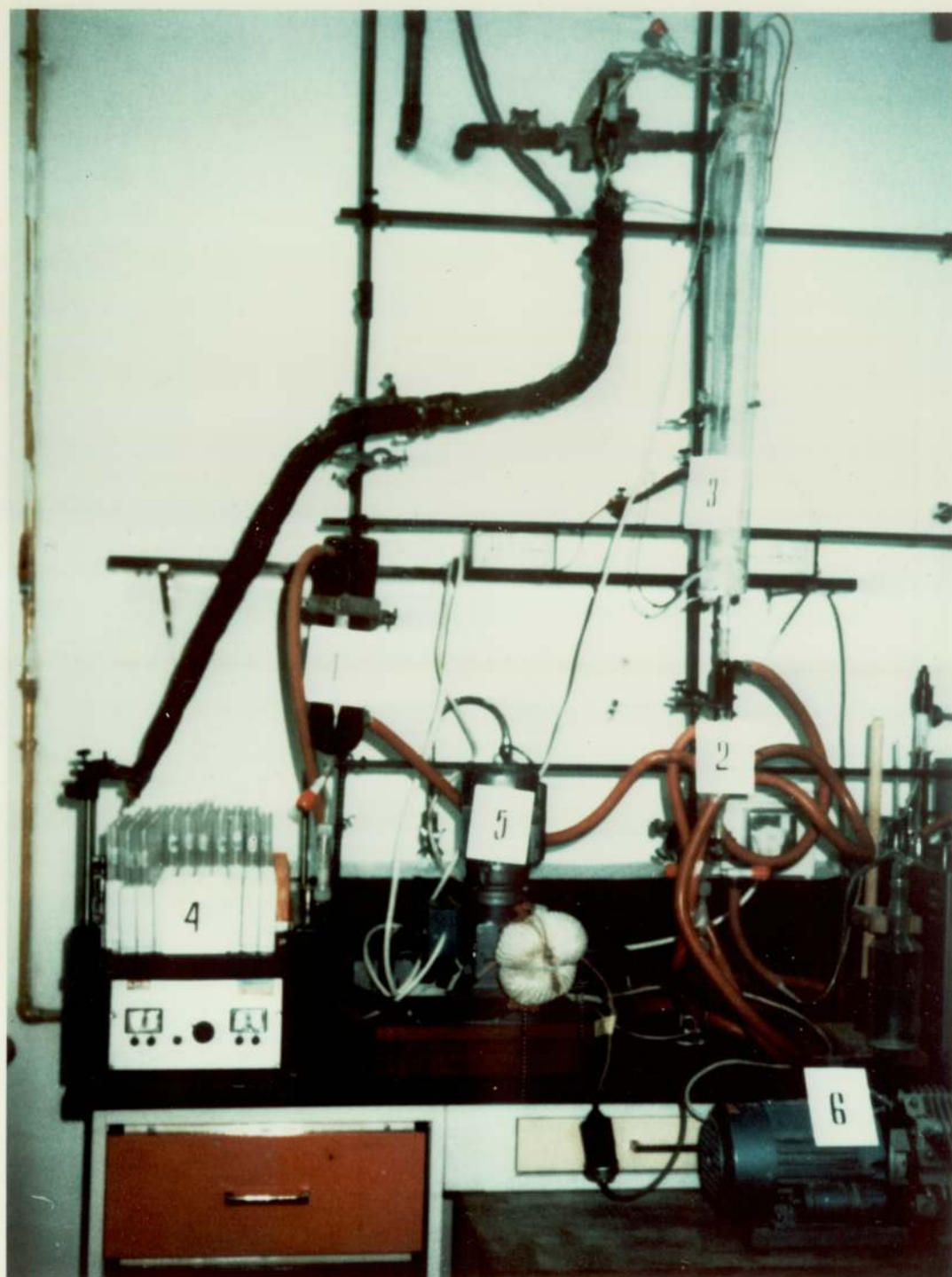
Figure 9.2   Plant for Purification of Waxes
From Aromatic Contents.

$$\gamma = \frac{h_T - (1-F)h_z}{h_T}$$

9.5 Results and Discussion

9.5.1 Effect of Aromaticity on Dynamic Adsorption Process

The solution of dynamic adsorption problems is related basically to the motion of the mass transfer front of the adsorbate molecules among the fixed bed of the adsorbent in the column. This mass transfer exhibits a variation of adsorbate concentration with the coverage rate of adsorbate molecules in the void volumes of the adsorbent, i.e. the dynamic adsorption is associated with a breakthrough curve which describes the behaviour of the adsorption activity of the adsorbate and its saturation point (equilibrium point).

The dynamic adsorption of the aromatic compounds from solution with isooctane varied with process temperature, adsorbent type and particle size, height of the adsorbent bed, feed flow rate, type of the solvent, the adsorbate structure and adsorbate concentration in the solution.

The dynamic adsorption from solution in isooctane was studied for three types of aromatics; mononuclear aromatic hydrocarbon such as dodecylbenzene, dinuclear aromatic hydrocarbon such as naphthalene and trinuclear organic compound such as dibenzothiophene. The process conditions were:

o   adsorbent particle size 1-2 mm
o   height of the adsorbent bed 660 mm
o   diameter of the adsorbent bed 16 mm
o   feed flow rate 0.42 cm^3/60s
o   adsorption temperature 343 K
o   the concentration of the aromatic compound (the adsorbate) in the solution isooctane ranged between 3-4 weight percent

Since the objective was to identify the effect of aromaticity, operation at a range of temperatures and flow rates was not justified.

Breakthrough curves were determined for the three aromatic compounds and are illustrated in Figure 9.3. The length of the working or utilized layer h_z, dynamic capacity A_d and the effective coefficient of utilized layers γ were calculated and are presented in Table 9.1.
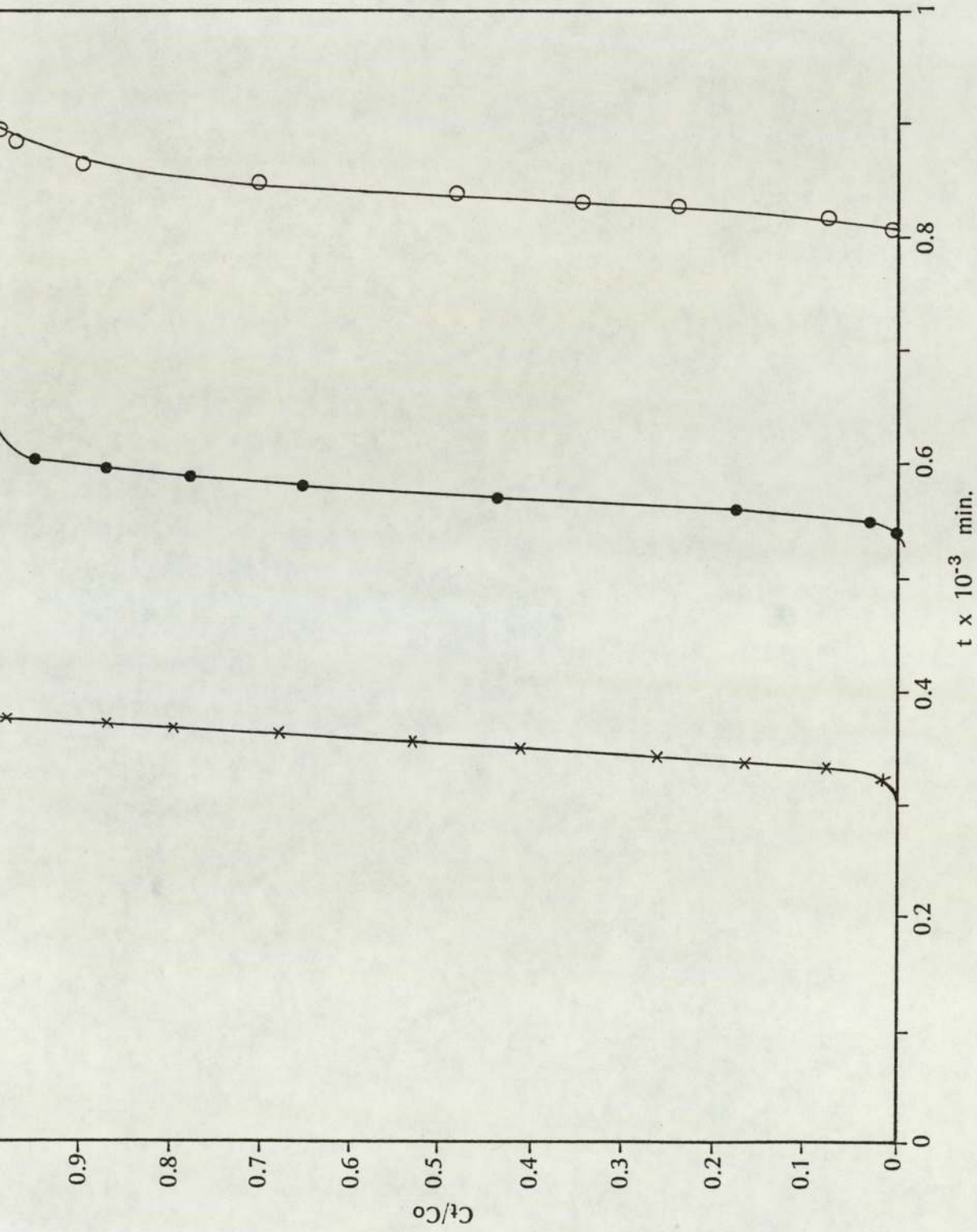
Figure 9.3 Breakthrough Curves of Liquid Phase
Adsorption of Different Types of
Aromatic Compounds From Solution
with Isooctane: x Dodecylbenzene,
● Dibenzothiophene and O Naphthalene.

TABLE 9.1

DYNAMIC PROPERTIES FOR ADSORPTION OF DODECYLBENZENE, NAPH-
THALENE, AND DIBENZOTHIOPHENE FROM ISOOCTANE AT 343 K

Parameters	Dodecylbenzene	Naphthalene	Dibenzothiophene
h_z (mm)	111	47	58
γ	90	95.7	94.7
A_d	4.5	12.9	6.6

From the kinetics of adsorption (Chapter 7) it was concluded that adsorption is controlled by internal diffusion, i.e. the rate of fluid adsorption is related to transport of the adsorbate molecules in the cavities of the zeolite particles. Therefore any increase, or decrease, in the height of the working layer of the adsorbent bed and changes in the adsorption efficiency of the packed bed are attributable to the type of adsorbate molecules.

It is clear from Table 9.1 that at 343 K, naphthalene possessed the best dynamic adsorption properties, followed by dibenzothiophene and with dodecylbenzene last.

Comparison of these data for the behaviour of these compounds undergoing dynamic adsorption with the data obtained on adsorption isotherms (Chapter 4), indicates similar trends. For example, the numbers of molecules captured per unit cell of adsorbent in adsorption isotherm studies were 5.1, 11.4 and 10.5 for dodecylbenzene, naphthalene and dibenzothiophene respectively at 343 K; the dynamic efficiency shows the same trend i.e. the dynamic adsorption efficiency was highest for naphthalene and lowest for dodecylbenzene.

From Table 9.1, an increase in the polarity of the adsorbate molecules resulted in an increase in the dynamic adsorption efficiency. This is attributable to the strong interactions between π bonds of the aromatic compound and the electrostatic charge of the cations present in the adsorbent. With adsorbate molecules of dodecyl benzene the alkyl chain attached to the benzene ring shields the aromatic ring and thus weakens

the interaction between the aromatic ring of the adsorbate material and the cations present in the adsorbent. Therefore it has the lowest dynamic capacity. In the case of dibenzothiophene the sulfur atom, which possesses two pairs of electrons, results in high dipole moments and hence strong interactions between the cations of the adsorbent and the dibenzothiophene molecules. However, it has a negative effect in continuous adsorption because such a sulfur compound will block the surface of the pore cavities. This phenomena of pore blockage leads to a lower dynamic capacity (6.6 g/100g of adsorbent at saturation point), compared with naphthalene which has the highest dyanmic capacity (12.9 g/100g of adsorbent). As a result, the heights of the working layers for dynamic adsorption of dodecylbenzene, naphthalene, and dibenzothiophene were 111 mm, 47 mm and 58 mm respectively. Due to the higher affinity of molecular sieve type 13X to adsorb polar aromatic compounds, the adsorption efficiency of naphthalene was 95.7% whilst for dibenzothiophene and dodecylbenzene it was 94.7% and 90% respectively.

9.5.2 Effect of Solvent on Dynamic Adsorption Process:

This study covering adsorption of naphthalene molecules from solutions using different types of solvents such as isooctane and n-alkanes (n-decane, n-dodecane, n-tetradecane) confirmed that the solvent has a significant effect on the adsorption of aromatic compounds. The feed flow rate was maintained constant at 0.42 cm^3/60 s, the height of the packed bed was 660 mm, and the concentration of napthalene in each solvent was 3 weight percent.

The breakthrough curves for the dynamic adsorption of naphthalene from solutions using the different types of solvents are presented in Figure 9.4. Table 9.2 illustrates the working or utilized layer h_z, the adsorption efficiency γ and the dynamic capacity A_d for the adsorption of naphthalene from each type of solvent.

TABLE 9.2

DYNAMIC PROPERTIES FOR NAPHTHALENE ADSORPTION
FROM DIFFERENT TYPES OF SOLVENT AT 343 K

Parameters	Naph/ Isooct.	Naph/ Decane	Naph/ Dodecane	Naph/ Tetradecane
h_z (mm)	47	166	168	179
γ	95.7	84	82	83
A_d	12.9	8.3	7.2	5.1

Kiselev and Lopatkin (69), found during adsorption of different
n-alkanes such as n-hexane and n-pentane over molecular sieve type X, that
an increase in the number of carbon atoms of the n-alkanes resulted in an
increase in the heat of adsorption. Hence the cations on the surface of
the molecular sieve were concluded to have non-specific interactions with
the heavier n-alkanes. It was also found that the heat of adsorption
increased with coverage and reaches a maximum near saturation.

The adsorption of naphthalene molecules from different types of sol-
vent increased with decreasing molecular weight of the solvent. The ease
of mass transfer of the naphthalene molecules through the pores of the
molecular sieve will depend on the type of solvent. The rate of leaching
out of naphthalene molecules from the solvent differed; increase in molec-
ular weight, i.e. number of carbon atoms, of the solvent resulted in dif-
ficulty in leaching-out naphthalene molecules.

The working layer, or utilized layer, increased with an increase in
the carbon number of the solvent. Conversely the dynamic capacity and
adsorption efficiency decreased with an increase in the carbon number of
the solvent (see Table 9.2).
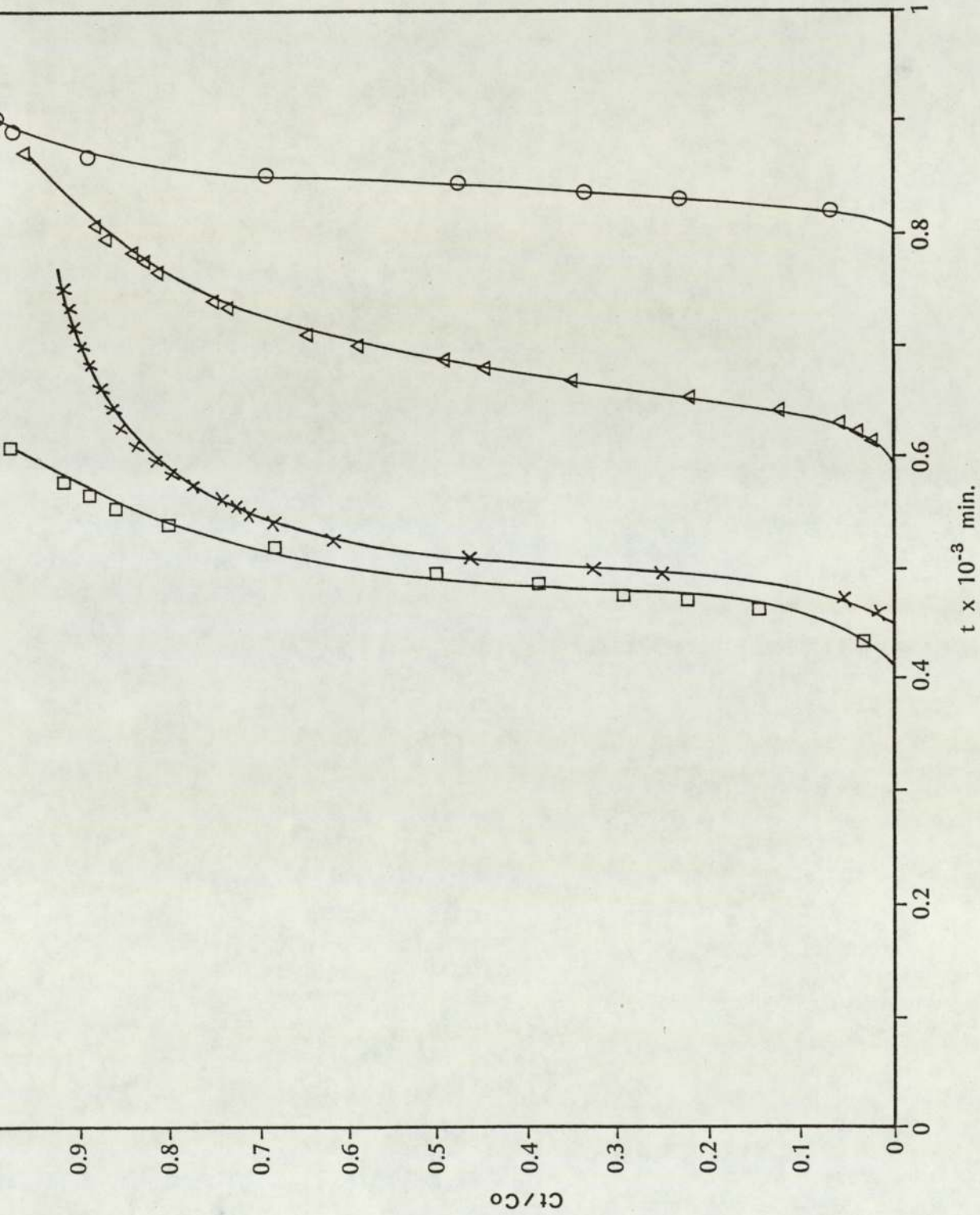
Figure 9.4 Breakthrough Curves of Liquid Phase
Adsorption of Naphthalene From
Different Types of Solvents:
O Isooctane, Δ Decane
× Dodecane and □ Tetradecane,

9.5.3 Purification of Paraffin Waxes from Aromatic Compounds:

As explained earlier, the purity of paraffin waxes is an important aspect in their grading. The required purity depends upon the field of application. For example, paraffin waxes for use in food conservation and packing, must be odourless and be free from compounds damaging the human organism, particularly mono, di, and polycyclic aromatic substances. Similar, but even more stringent, specifications apply to paraffin products for medical purposes.

As mentioned in Chapter 1.3, the slack waxes produced from heavy petroleum fractions using a dewaxing process normally require further treatment for reduction of aromatics, olefins, or sulfur compounds. Finishing usually employs sulfuric acid treatment, hydrogenation, or a combination of both. However, the levels of purity achievable are generally unsatisfactory. The increasing demand for high purity waxes has made it necessary to seek economic methods of purification of waxes from aromatic hydrocarbons.

The results of the equilibrium isotherms, the kinetic adsorption, and the dynamic adsorption studies of different types of aromatic compounds from solution with iso-octane and n-alkanes have shown the high affinity of molecular sieves type NaX to adsorb the aromatic compounds within a limited range of aromatic concentration (3-5 wt. percent). Thus slack waxes with an aromatic content ≤ 5 wt. percent can be purified from these aromatic hydrocarbons using molecular sieves type NaX.

9.5.3.1 Effect of Temperature on Dynamic Adsorption Process

The dynamic adsorption of aromatic compounds from slack waxes, to produce highly purified waxy materials, was studied under the following conditions:

o   adsorbent particle size 1-2 mm

o   height of packed column 660 mm

o   diameter of the packed column 16 mm

o   flow rate 0.42 cm^3/60 s

o   concentration of aromatics in the slack waxes 4.8 wt %.

To reduce the viscosity of the liquid paraffin (wax) and to increase its fluidity, and hence rate of the migration of aromatic compounds in the internal cavities of the molecular sieve crystals, adsorption was conducted at high temperature in the range 363 - 583 K.

Figure 9.5 illustrates the breakthrough curves for the adsorption of aromatic compounds at temperatures of, 363, 383, 423, 443, 543 and 583 K, respectively. The dynamic properties of adsorption were determined according to the symmetry of the breakthrough curves, at different temperatures and at a different coverage rates of adsorption, at $C_t/C_o = 1$ and at $C_t/C_o = 0.5$. Table 9.3 and 9.4 illustrate the dynamic properties of adsorption of aromatics from slack waxes at $C_t/C_o = 1$ and $C_t/C_o = 0.5$.

TABLE 9.3

DYNAMIC PROPERTIES OF LIQUID PHASE ADSORPTION OF AROMATIC COMPOUNDS FROM SLACK WAX AT DIFFERENT TEMPERATURES AND AT $C_t/C_o = 1$

Parameters	363 K	383 K	423 K	443 K	543 K	583 K
h_z,mm	822	783.9	714	497.8	477	504.6
γ,%	9	28.7	38.3	57.8	57.3	64.0
A_d at $\frac{C_t}{C_o} = 1$	4.8	8.2	8.4	9.2	12.9	10.4

TABLE 9.4

DYNAMIC PROPERTIES OF LIQUID PHASE ADSORPTION OF AROMATIC COMPOUNDS FROM SLACK WAX AT DIFFERENT TEMPERATURES AND AT $C_t/C_o = 0.5$

Parameters	363 K	383 K	423 K	443 K	543 K	583 K
h_z,mm	252	364.5	410	283	203.5	220
γ,%	80	72.4	68.9	88	92.9	89.7
A_d at $\frac{C_t}{C_o} = 0.5$	0.9	2.0	2.0	3.0	3.7	2.9

When the molten waxes were brought into contact with molecular sieve type 13X, the aromatic compounds were adsorbed. Figure 9.5 shows the breakthrough curves at different temperatures. These demonstrate the increase in concentration of the aromatics after a certain time; it rises slowly to reach a saturation point following which no more adsorption of aromatics occurs. The saturation value corresponds to complete filling of the internal voids of the molecular sieves crystals, and this point depends on several variables including temperature.
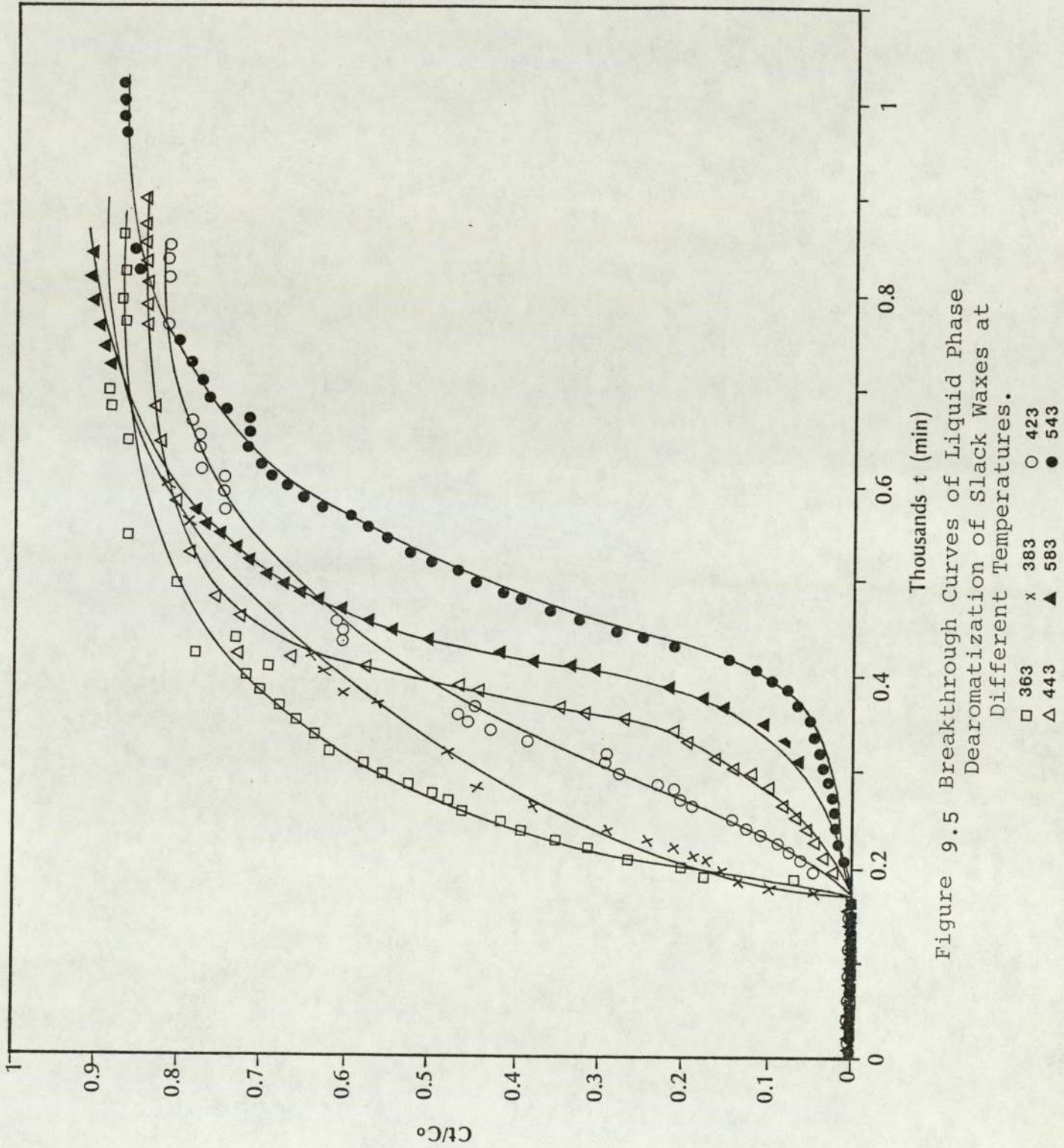
Figure 9.5 Breakthrough Curves of Liquid Phase
Dearomatization of Slack Waxes at
Different Temperatures.

□ 363   x 383   ○ 423
△ 443   ▲ 583   ● 543

Clearly from Figure 9.5 up to a temperature of 543 K the time to breakthrough increased as the temperature increased; however the breakthrough time was longer at 543 K than at 583 K. An increase in the process temperature resulted in slower adsorption of aromatics from liquid wax and hence approach to the saturation point required a longer time. Packing of the bed is therefore more efficient at the higher temperatures. However, diffusivity of the adsorbate molecules of aromatics in the molecular sieves cavities increases with increasing temperature, thus there was a decrease in the rate of adsorption as shown in Figure 9.5 for temperature 583 K.

As shown in Table 9.3 the adsorption of aromatic compounds from waxes at low temperatures has no positive effect on dynamic adsorption and the mass transfer zone exceeds the column length 660 mm, which means that the separation process is not efficient. This may be due to the difficulty of leaching out the high molecular weight n-alkanes (waxes) by the aromatics. An increase in the number of carbon atoms in the n-alkanes results in a decrease in the rate of adsorption of the aromatic compounds as explained in 9.5.2. In the case of dearomatization of waxes the existing n-alkanes in the waxes act as solvent for compounds in the range C_{19}-C_{32}; this has a negative effect on dynamic adsorption at low temperatures, because these long chain n-alkanes cause blockage of the pore cavities thus hindering entry of the aromatics and greatly decreasing the rate of adsorption.

From Tables 9.3 and 9.4 the efficiency of the adsorbent at low filling rate, C_t/C_o = 0.5, was apparently higher than the efficiency at saturation point C_t/C_o = 1. This can be explained since during the initial filling of the voids, the interactions between the aromatic compounds and the cations present in the molecular sieve cavities is very strong. After accumulation of multilayers of adsorbate molecules, the physical interactions are reduced until saturation point is approached; the effluent will then have a similar aromatic content to the original feed and no more adsorption occurs.

Due to the diffusion mechanism described earlier, increase in the adsorption temperature to 583 K will tend to increase the transition of aromatic molecules between the two adjacent cavities. The value of adsorption would therefore be expected to be lower and this is shown in Table 9.3. The dynamic capacity at 583 K was 10.4 g/100g of molecular sieves, and 12.9/100g at 543K.

9.5.3.2 Effect of Concentration On Dynamic Adsorption Process:

The effect of aromatic concentration in the slack waxes on the dearomatization process was studied for the following conditions:

o   adsorbent particle size 1-2 mm

o   height of the adsorbent bed 660 mm

o   diameter of the adsorbent bed 16 mm

o   feed flow rate 0.42 cm^3/60 s

o   Adsorption temperature 543 K

Breakthrough curves for dearomatization of the waxes at initial aromatic concentrations of 4.8 and 1.8 wt % are illustrated in Figure 9.6. This indicates that at low concentration of aromatics (up to 0.01), the volume of purified waxes collected was 300 mls, while at aromatic concentration of 4.8 wt % the volume was 190 mls, i.e., the dynamic capacity of adsorption of aromatic hydrocarbons from waxes was higher at lower aromatic concentrations.

The breakthrough time with low aromatic contents was longer than for waxes of high aromatic contents. The reason is that the packing density of aromatics in the pores of the molecular sieves for waxes with low aromatic content (1.8 wt %) is better than that for waxes with high aromatic content (4.8 wt %).

Because of the limitations of the molecular sieves for adsorption of aromatic hydrocarbons to produce a high purity effluent from waxes containing a high percent aromatics, a longer column or multistages (multicycles) of dearomatization i.e. a series of packed beds would be required.

9.6 Conclusions

1.   Of the three individual aromatic compounds studied dodocylbenzene exhibited the lowest effective coefficient and dynamic capacity together with the highest utilized layer. Dibenzothiophene was more readily adsorbed. Naphthalene exhibited the best dynamic adsorption properties (Table 9.1).

2.   Of the four solvents investigated the best adsorption properties were associated with the lowest number of C atoms, ie. isooctane (Table 9.2).

3.   In wax purification the dynamic properties involved with an increase in temperature up to an optimum at 543K. (Tables 9.3 & 9.4). The dynamic capacity decreased with an increase in feed concentration.
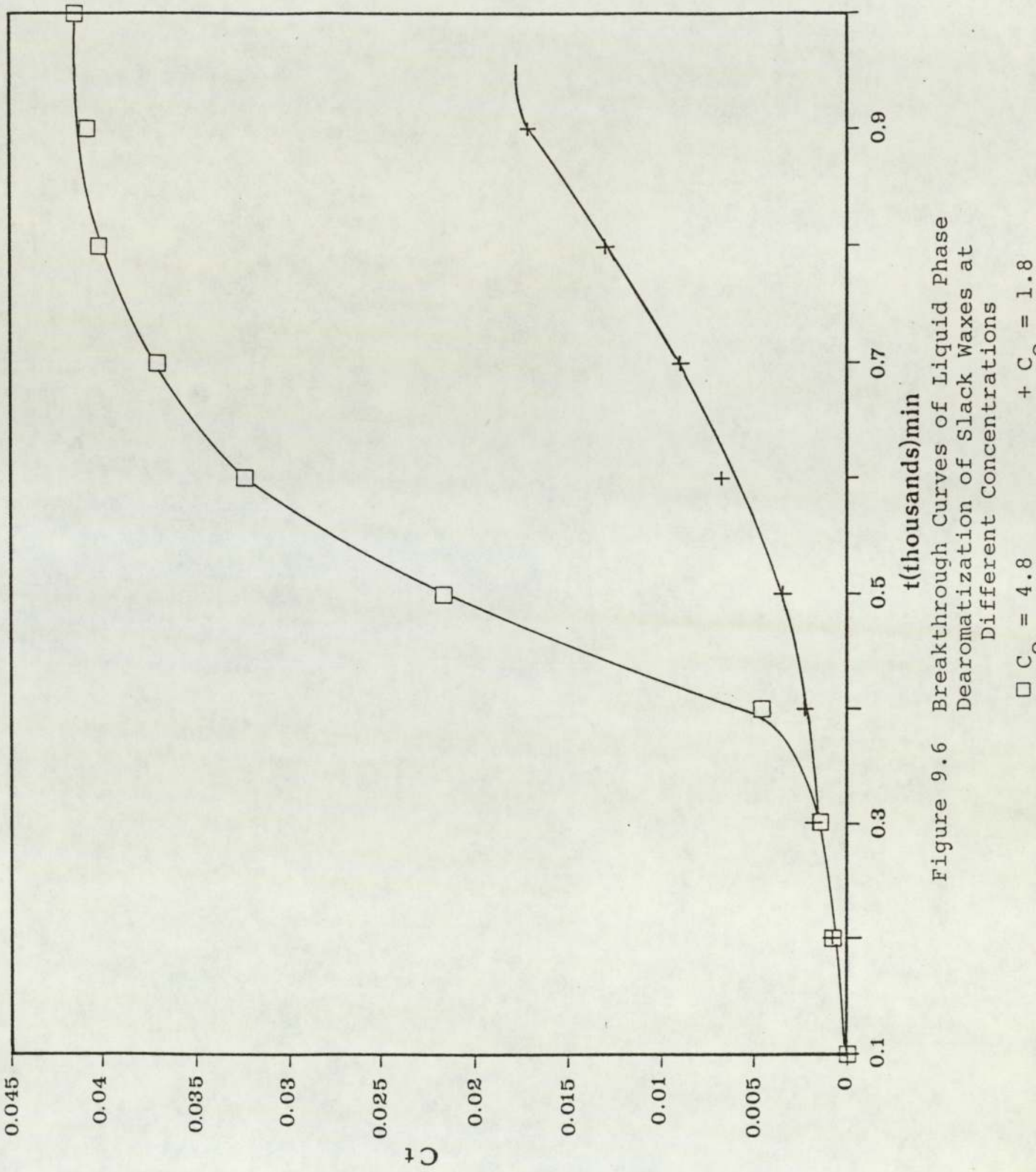
Figure 9.6 Breakthrough Curves of Liquid Phase
Dearomatization of Slack Waxes at
Different Concentrations

□ C_0 = 4.8   + C_0 = 1.8

10.0 A MATHEMATICAL MODEL FOR FIXED BED ADSORPTION SYSTEMS

10.1 Development of a General Model for the Dynamic Behaviour of a Fixed Bed Adsorber

The mathematical modelling of adsorption of solutes from liquids, or gases, on solid beds is complicated since each of the numerous mechanisms which can be postulated has some practical basis. Certain problems have been solved completely whilst others, in which more complex mechanisms are assumed, have been solved only partially by either linearizing approximations or numerical methods (70).

Assume a typical adsorption system comprising a column or bed filled with a packed material. A fluid is passed through the column and a component is transferred from the fluid phase to the solid phase. Since the solid is static, the composition of the fluid changes with time in the solid phase and with time and space in the bulk. Therefore, conditions in the column are unsteady-state in character.

Consider the adsorption column shown in Figure 10.1, in which,

Voidage	$= \varepsilon$	
Interstitial Velocity	$= V$	
Solute Concentration	$= c$	moles/unit volume of fluid

Let bed cross section = 1.0.

Let n moles of solute be adsorbed in unit volume of packing.
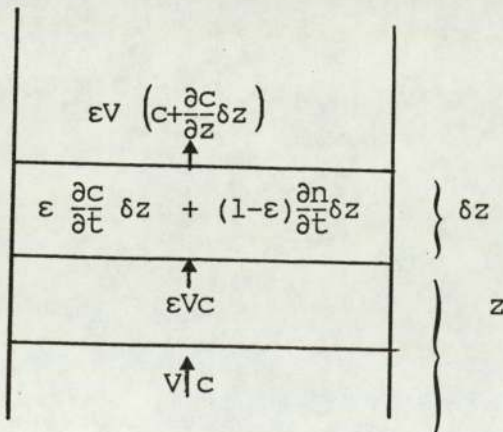
Figure 10.1. Fixed Bed Adsorption Column.

Then a material balance on the fluid phase contained in an element of unit cross-section and height, δz, in time interval, δt, gives,

Rate of input $\qquad = \varepsilon Vc \, \delta t$

Rate of output $\qquad = \varepsilon V \left(c + \dfrac{\partial c}{\partial z} \, \delta z \right) \delta t$

Rate of accumulation in time interval δt

   In fluid voids $\qquad = \varepsilon \, \delta z \, \dfrac{\partial c}{\partial t} \, \delta t$

   Adsorbed on zeolite $\qquad = (1-\varepsilon) \, \delta z \, \dfrac{\partial n}{\partial t} \, \delta t$

The partial differential equation for the material balance is:

$$\varepsilon Vc \, \delta t - \varepsilon V \left(c + \dfrac{\partial c}{\partial z} \, \delta z \right) \delta t = \varepsilon \, \delta z \, \dfrac{\partial c}{\partial t} \, \delta t + (1-\varepsilon) \, \delta z \, \dfrac{\partial n}{\partial t} \cdot \delta t$$

where $\dfrac{\partial n}{\partial t}$ is the rate of adsorption on the packing

$$- \varepsilon V \, \dfrac{\partial c}{\partial z} = \varepsilon \, \dfrac{\partial c}{\partial t} + (1-\varepsilon) \, \dfrac{\partial n}{\partial t}$$

or $\qquad \varepsilon V \, \dfrac{\partial c}{\partial z} + \varepsilon \, \dfrac{\partial c}{\partial t} + (1-\varepsilon) \, \dfrac{\partial n}{\partial t} = 0$

Rearranging

$$V \, \dfrac{\partial c}{\partial z} + \dfrac{\partial c}{\partial t} + \dfrac{1-\varepsilon}{\varepsilon} \, \dfrac{\partial n}{\partial t} = 0 \tag{10.1}$$

Equation (10.1) is the conservation equation.

Now let the following variables be defined as:

$$Y = \left(t - z \right) \tag{10.2}$$

where $Z = \dfrac{z}{V}$ and Y is the time after the feed

reaches the plane at z.

Now

$$\left(\frac{\partial}{\partial \bar{z}} \right)_t = \left(\frac{\partial}{\partial \bar{Y}} \right)_Z \left(\frac{\partial Y}{\partial \bar{z}} \right)_t + \left(\frac{\partial}{\partial \bar{Z}} \right)_Y \left(\frac{\partial Z}{\partial \bar{z} t} \right) \tag{10.3}$$

From Equation 10.2

$$\left(\frac{\partial Y}{\partial \bar{z}} \right)_t = -\frac{1}{V} \qquad \text{and} \qquad \left(\frac{\partial Z}{\partial \bar{z}} \right)_t = \frac{1}{V} \tag{10.4}$$

$$\therefore \ \left(\frac{\partial}{\partial \bar{z}} \right)_t = -\frac{1}{V} \left(\frac{\partial}{\partial \bar{Y}} \right)_Z + \frac{1}{V} \left(\frac{\partial}{\partial \bar{Z}} \right)_Y \tag{10.5}$$

or

$$V \ \frac{\partial}{\partial \bar{z}} = \left(\frac{\partial}{\partial \bar{Z}} \right)_Y - \left(\frac{\partial}{\partial \bar{Y}} \right)_Z \tag{10.6a}$$

and from Equation 10.2

$$\left(\frac{\partial}{\partial \bar{t}} \right)_z = \left(\frac{\partial}{\partial \bar{Y}} \right)_Z \tag{10.6b}$$

Combining both parts of Equation 10.6 gives, on insertion into Equation 10.1;

$$\frac{\partial c}{\partial \bar{Z}} - \frac{\partial c}{\partial \bar{Y}} + \frac{\partial c}{\partial \bar{Y}} + \left(\frac{1-\varepsilon}{\varepsilon} \right) \frac{\partial n}{\partial \bar{Y}} = 0$$

or

$$\frac{\partial c}{\partial \bar{Z}} + \alpha \ \frac{\partial n}{\partial \bar{Y}} = 0 \tag{10.7}$$

where $\alpha = \frac{1-\varepsilon}{\varepsilon}$

Equation 10.7 is linear with two dependent variables.
From the Figure 10.1,

$$\frac{\partial n}{\partial Y} = K \, a \, (x-x^*) = -\frac{1}{\alpha} \frac{\partial c}{\partial Z}$$

where   a = adsorbent area per unit volume of packing

   K = overall mass transfer coefficient.

   x = mole fraction of solute in the liquid phase.

   x* = mole fraction of solute at the liquid-solid interface.

Then

By definition

$$C = \rho \frac{x}{M}$$

where

   ρ = liquid density

   M = molecular weight

and so

$$Ka \left(x - x^* \right) = -\frac{\rho}{\alpha M} \cdot \frac{\partial x}{\partial Z} \tag{10.8}$$

Assuming that the interphase equilibrium distribution takes the form

$$x^* = mn + b \tag{10.9}$$

where n = the moles of adsorbed component per
         unit volume of the solid phase

and m and b are empirical constants

$$\left(\frac{1}{Ka \, m} \right) \frac{\partial x^*}{\partial Y} = \left(x - x^* \right) = -\left(\frac{\rho}{Ka.\alpha M} \right) \frac{\partial x}{\partial Z} \tag{10.10}$$

Define

$$\theta \quad = \quad Ka \, m.Y \tag{10.11}$$

$$N \quad = \quad \left(\frac{Ka\alpha \, M}{\rho} \right) Z \tag{10.12}$$

$$w \quad = \quad \frac{x}{x_o} \tag{10.13}$$

$$w^* \quad = \quad \frac{x^*}{x_o} \tag{10.14}$$

where x_o is the feed concentration.

In terms of these variables, the differential equations and boundary conditions become

$$\frac{\partial w^*}{\partial \theta} \quad = \quad w - w^* \tag{10.15}$$

$$-\frac{\partial w}{\partial N} \quad = \quad w - w^* \tag{10.16}$$

with

$$w^* \quad = \quad 0 \qquad \text{at } \theta = 0 \quad \text{for all } N \tag{10.17}$$

and

$$w \quad = \quad 1 \qquad \text{at } N = 0 \quad \text{for all } \theta \tag{10.18}$$

The boundary conditions provide for the introduction of a step into a bed initially free of the adsorbable component.

Using the Laplace transformation:

$$-\frac{d\bar{w}}{dN} = \bar{w} - \bar{w}* \tag{10.19}$$

$$s\bar{w}* = \bar{w} - \bar{w}* \tag{10.20}$$

using the initial condition presented as Equation (10.17).

From Equation (10.20)

$$\bar{w}* = \frac{\bar{w}}{(s+1)} \tag{10.21}$$

Using Equation (10.21) in (10.19)

$$-\frac{d\bar{w}}{dN} = \left(\frac{s}{s+1}\right)\bar{w} \tag{10.22}$$

and the boundary condition, presented as Equation (10.18), in the form

$$\bar{w} = \frac{1}{s} \quad \text{at} \quad N = 0 \tag{10.23}$$

leads to

$$\bar{w} = \frac{1}{s} \cdot e^{-\left(\frac{s}{s+1}\right)N} \tag{10.24}$$

Inversion of Equation (10.24) can be achieved by, first, replacing

$\left(\frac{s}{s+1}\right)$ by $1 - \left(\frac{1}{s+1}\right)$ in Equation (10.24)

leading to

$$\bar{w} = \frac{1}{s} \cdot e^{-N} \cdot e^{+\left(\frac{N}{s+1}\right)} \tag{10.25}$$

Then using Equations (10.21) and (10.25)

$$\bar{w}* = \frac{e^{-N}}{s} \cdot \frac{e^{\left(\frac{N}{s+1}\right)}}{(s+1)} \tag{10.26}$$

From Tables of Transform Relations, reference (71), (72)

$$L^{-1} \quad \frac{e^{\frac{N}{s}}}{s} \quad \text{----}> \quad I_o (2\sqrt{N\theta}) \tag{10.27}$$

Invoking the translational properties of the Transform:

$$L^{-1} \quad \frac{e^{\left(\frac{N}{s+1}\right)}}{(s+1)} \quad \text{----}> \quad e^{-\theta} I_o(2\sqrt{N\theta}) \tag{10.28}$$

The Inverse Transform of Equation (10.26) is then obtained by convolution:

$$w* = e^{-N} \int_o^\theta e^{-\theta} \cdot I_o (2\sqrt{N\theta}) \cdot d\theta \tag{10.29}$$

Now

$$\left(\frac{\partial w*}{\partial \theta}\right)_N = e^{-N} \cdot e^{-\theta} \cdot I_o (2\sqrt{N\theta}) \tag{10.30}$$

and so using Equations (10.15), (10.16) and (10.18)

$$-\left(\frac{\partial w}{\partial N}\right)_\theta = \left(\frac{\partial w*}{\partial \theta}\right)_N \tag{10.31}$$

$$w = 1 - \int_{0}^{N} e^{-(N*+\theta)} \; I_{0} \, (2 \sqrt{N*\theta}) \, . \, dN* \qquad (10.32)$$

in which $N*$ is a dummy variable.

Equation 10.32 enables estimates to be made of the change in concentration with time of adsorbate leaving a specific fixed bed, of known height and voidage, at any given throughput. Hence, a breakthrough curve may be predictable using equilibrium isotherm and kinetic data.

The limitations are,

1.   Equation 10.9 relates to linear equilibrium data, whereas, as discussed in Chapter 5, in reality this was not the case.

2.   Since 1 mm particles were used it may be assumed that external diffusion was controlling. (The case for pellets may be different). In the laminer flow regime the correlation of K_f data is imprecise; therefore predictions may be inexact pending the availability of more data.

Nevertheless this model is a starting point for further detailed analysis.

As an example of the approach to be used, the adsorption of naphthalene from isooctane is considered in Appendix J.

11.0

11.1 Overall Conclusions

The conclusions arising from each separate experimental, or modelling, study were given earlier. Therefore only the overall conclusions and significance will be discussed.

It has been demonstrated that the dearomatization of slack wax using NaX zeolite can, within the parameters investigated, yield wax containing < 0.01 % aromatics. Thus the process merits further investigation for high purity wax applications (Chapter 9).

The study of equilibrium isotherms for adsorption of pure individual aromatic compounds showed that those of lower molecular weight and more compact structure were preferentially adsorbed, and the number of adsorbate molecules captured by one cage or unit cell of the molecular sieve decreased as the molecular weight of the adsorbate molecules increased. An increase in the adsorption temperature resulted in a decrease in the value of adsorption, indicative of a decrease in the number of adsorbate molecules captured by one unit cell (Chapter 3).

In the kinetic studies using different aromatic compounds the diffusivity tended to decrease considerably when a long alkyl chain was attached to a benzene ring such as in dodecylbenzene. Molecules of small cross-sectional diameter, e.g. cumene, were taken up at a high diffusion rate. The sorption rate was increased by a rise in temperature. Apparent energies of activation increased as the polarity increased (Chapter 7).

Separation of multicomponent aromatic compounds (extract fractions) was successfully conducted in spite of the low adsorption values compared with pure individual aromatic compounds. These lower values were due to the complexity of the components in the extract fractions (Chapter 5).

The concentration of aromatics in the feed had a very significant effect on the achievable wax purity; therefore any commercial process should commence with a feed containing low molecular weight aromatics and with a low sulphur content.

11.2 Recommendations for Future Work

Clearly the dynamic studies on the purification of liquid paraffins or slack waxes to get liquid paraffins or waxes of high purity, i.e < 0.01 wt % aromatics, are incomplete and a great deal of work needs to be done. However, the process is sufficiently promising to justify further

research. The following future work is recommended, using the apparatus and techniques already tested.

1.   Determine the optimum conditions for dearomatization of wax. This will involve studying the effects of,

    a.   Varying temperature of operation and velocity , the most important parameters. The preferred temperature will be in the range of 473 to 573 K.

    b.   Change in flowrate which should be within 0.5 - 4 volume of feed/volume of adsorbate/hr.

    c.   Particle size within the range 0.5 to 2 mm.

    d.   Change in column height which should be varied up to 1 m.

2.   Investigate multicyle adsorption with, and without, intermediate reactivation of the adsorbent particles. Attempt to find the optimum desorption agent, consisting of a polar or polarizable material having an appreciable affinity for the zeolite adsorbent compared with the material desired to be desorbed. The possible desorption agents for the process include NH_3, N_2, CO_2, C_1 to C_5 alcohols such as methanol and propanol.

Following completion of 1 and 2 the preferred process should be tested on the existing KISR, dual-tower, adsorption pilot plant.

APPENDICES

A. CHEMICAL ANALYSIS

The determination of small quantities of aromatic hydrocarbons in highly-refined waxes and oils on the basis of UV absorption spectra was established by Siryuk et al (10). Using the recommended methods aromatic contents can be determined down to 0.01% with a relative accuracy of 10%.

The method (Gost 9437-60) by Siryuk et al., can be used to determine aromatic contents from 0.2 to 2%. A rapid method (Method No. 1) also enables the composition of aromatic hydrocarbons to be determined by means of ultraviolet absorption spectra. This method gave estimates of the contents of benzene, naphthalene and phenanthrene hydrocarbons when present in amounts from 0.01 to 100%.

The calculation of such aromatic hydrocarbons uses a system of equations set up on the basis of average coefficients:

$$C_{ab} = 0.152 \ K_{200} - 0.029 \ K_{230} - 0.045 \ K_{255}$$

$$C_{an} = 0.008 \ K_{200} + 0.163 \ K_{230} - 0.042 \ K_{255}$$

$$C_{ap} = 0.001 \ K_{200} - 0.008 \ K_{230} + 0.331 \ K_{255}$$

where C_{ab}, C_{an}, C_{ap}, are the contents of benzene, naphthalene, and phenanthrene nuclei, in % by weight; K_{200}, K_{230}, and K_{255} are the specific extinction coefficients of the sample with analytical wave lengths of 200, 230, and 255 nm (K=D/C.d.) where D is the optical density; C is the concentration of the sample in g/L; and d is thickness of the layer in mm.

The contents of benzene, naphthalene and phenanthrene hydrocarbons (C_b, C_n, C_p) are determined in accordance with the formulae:

$$C_b = \frac{C_{ab}\ M\ 0.87}{72} \cdot 100\%$$

$$C_n = \frac{C_{an}\ M\ 0.87}{120} \cdot 100\%$$

$$C_p = \frac{C_{ap}\ M\ 0.87}{168} \cdot 100\%$$

where M is the molecular weight of the sample; 72, 120 and 168 are the total weights of the carbon atoms present in benzene, naphthalene and phenanthrene nuclei; 0.87 is a fraction representing the total weight of carbon in relation of the average molecular weight of the sample.

B. CALIBRATION OF INDIVIDUAL AROMATIC COMPOUNDS

For determination of concentration of individual aromatic compounds, calibration curves were plotted by weighing different known quantities of each aromatic compound and dissolving it in solvent (isooctane). The absorbance was measured by UV, with a cell path length of 0.1 cm, e.g. Cumene

1.   1 ml/25 ml = 34.2 µg/ml
2.   1 ml/10 ml = 85.5 µg/ml
3.   2 ml/10 ml = 171.0 µg/ml
4.   3 ml/10 ml = 256.5 µg/ml
5.   4 ml/10 ml = 342.0 µg/ml and so on.

Their absorbance were:

at 208 nm   0.318

0.771

1.505

2.255

3.025

The calibration curve was made by plotting the absorbance (values from UV) versus the concentrations µg/ml. A straight line passing through the zero point was obtained.

Accordingly any unknown concentration of cumene was determineable according to the calibrated curve. This was repeated for each of the individual aromatic compounds. Example calibration curve for cumene.
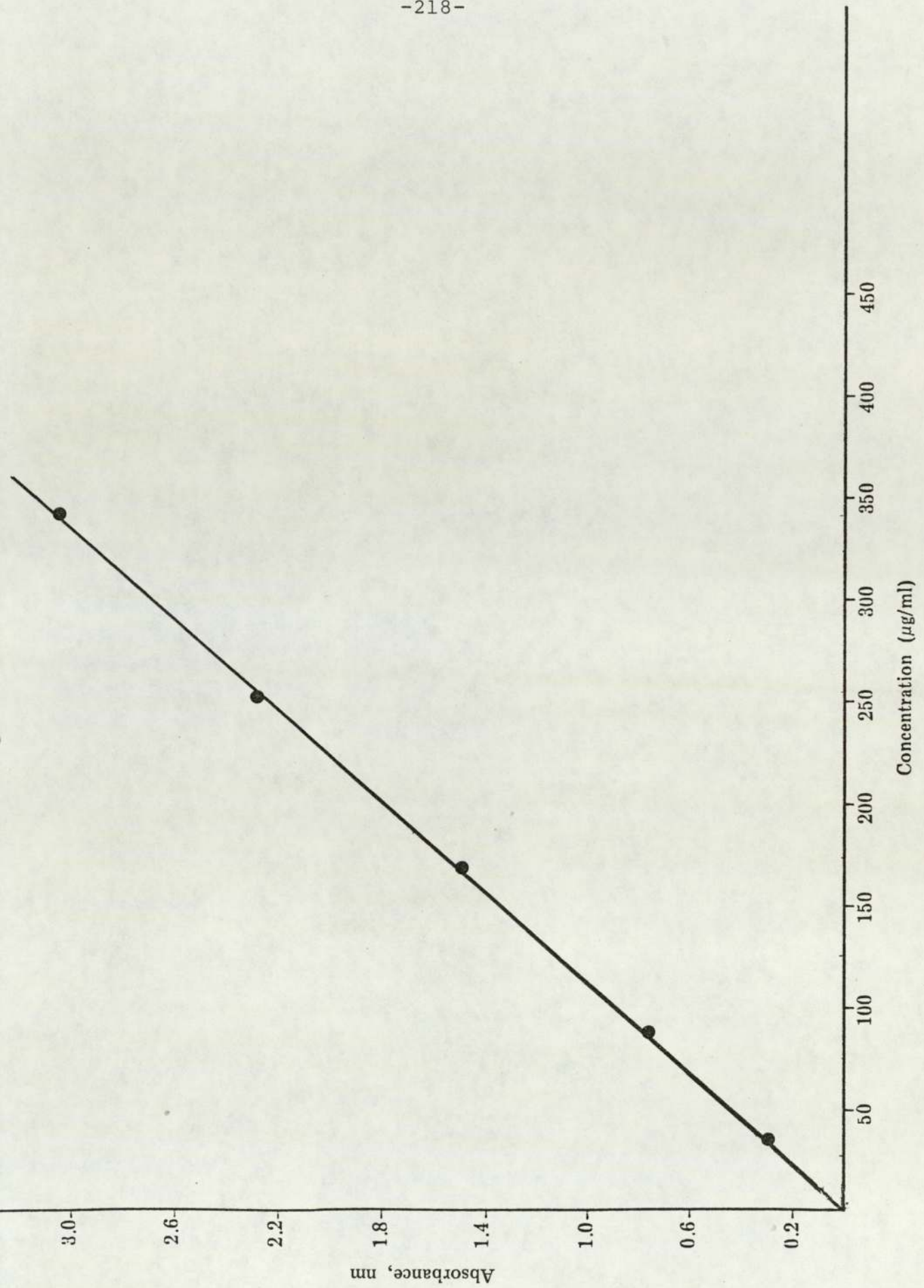
Fig. B.1. Calibration curve for cumene.

C. DETERMINATION OF EXPERIMENTAL VALUE OF ADSORPTION FOR INDIVIDUAL AROMATIC COMPOUNDS

C.1 Preparation

Different concentrations for each aromatic were prepared by dissolving a specific weight of the aromatic in isooctane solvent. Example, Dodecylbenzene:-

Flask (1)

      2.3005 g/50 ml   i.e. = 0.04601 g/ml --->

  i.e. 46.010 µg/ml   --->   i.e. = 46.01 g/L

Flask (2)

      1.5880 g/50 ml --->   0.03176 g/ml --->

      31.760 µg/ml   --->   31.76 g/L

Flask (3)

      1.2875 g/50 ml --->   0.02575 g/ml --->

      25.750 µg/ml   --->   25.75 g/L

Flask (4)

      0.7213 g/50 ml --->   0.014426 g/ml -->

      14426 µg/ml   --->   14.426 g/L

Flask (5)

      0.5561 g/50 ml   i.e. = 0.011122 g/ml -->

      11.122 µg/ml   i.e.   11.12 g/L

Flask (6)

        0.3999 g/50 ml   i.e. = 0.007998 g/ml -->

        7.998 μg/ml   i.e.   7.998 g/L

Flask (7)

        0.2404 g/50 ml   i.e. = 0.004808 g/ml -->

        4.808 μg/ml   i.e.   4.8 g/L

Flask (8)

        0.2068 g/50 ml   i.e. = 0.004136 g/ml -->

        4.136 μg/ml   i.e. = 4.136 g/L

C.2 Experimental Results

The concentration in each flask was determined by UV spectroscopy and the results are shown in Table C.1.

Column No. 1 is weight of molecular sieve in each autoclave for each concentration. Column No. 2 is original concentration of individual aromatic in isooctane g/L. Column 3. Original concentration of individual aromatic in isooctane C_o mmole/L. i.e. for dodecylbenzene, molecular weight is 246.

$$\therefore \qquad \frac{46.00}{246} = 0.19166 \text{ mole/L}$$

$$= 187 \text{ m.mole/L}$$

Column 4. Concentration of the aromatic in isooctane after adsorption. g/L (by UV).

Column 5. Concentration of the aromatic compound in isooctane after adsorption C m.mole/L.

Column 6. Mole fraction before adsorption can be determined by the equation:-

Table C.1

Type of Expt.   : Equilibrium isotherm   Mol. Wt. Isooctane : 114.22
Type of Arom. H.C: Dodecylbenzene in Isooctane   Density   : 0.6829
Mol. Wt. dodecyl benzene : 246   Temperature   : 303 K
Density : 8495 g/L   Time   : 4 days
Volume : 10

Mass of Mol.sieve	Conc. of org. soln. mg/ml g/L Co	Conc. of org. soln. mmole/L Co/246×1000	Conc. of soln. after adsorption g/L	Conc. after adsorption C1 m mole/L	Mole Frac-tion Xo 10^3	Mole Frac-tion X1 10^3	Mole (HCl) n1	Mole (Iso-octane) n2	Σ n1,n2	G ad-sorption m mole/g
1.1409	46.00	187.06	30.810	125.2	31.5	21.2	0.0019	0.0566	0.0585	0.52
0.8795	31.69	128.8	22.216	90.3	22.17	15.4	0.0013	0.0579	0.0592	0.46
1.0305	25.82	104.9	12.788	51.9	18.0	8.7	0.001	0.0584	0.0595	0.53
1.1571	14.805	60.2	3.800	10.2	10.2	2.6	0.0006	0.0594	0.0600	0.44
1.0976	11.050	44.9	2.700	10.9	7.6	1.84	0.00046	0.05973	0.0602	0.32
1.2517	8.272	33.6	0.248	1.0	5.7	0.169	0.00034	0.0599	0.0602	0.26
1.2872	4.800	19.5	0.245	0.995	3.3	0.167	0.0002	0.06028	0.0604	0.14
1.1582	4.158	16.9	0.203	0.825	2.8	0.14	0.00017	0.06033	0.06040	0.13

221

$$X_o = \frac{0.001 \cdot C_o \text{ (m.mole)}}{0.001\, C_o + \left(\dfrac{1000 - (\text{Mol. wt. arom}) (C_o)}{\rho \text{ arom}}\right)\left(\dfrac{\rho \text{ isooctane}}{\text{Mol. wt. isooctane}}\right)}$$

e.g.

$$X_o = \frac{(0.001) \times (187)}{0.001\,(187) + \left(1000 - \dfrac{(246)\,(187)}{849.5}\right)\left(\dfrac{0.6829}{114.2}\right)}$$

$$X_o = \frac{0.187}{0.187 + 5.6557} = .0315$$

$$= 31.5 \times 10^{-3}$$

Column 7   Mole fraction after adsorption

$$X_1 = \frac{0.001 \times 125.2}{0.001 \times 125.2 + \left(1000 - \dfrac{(246)\,(125.2)}{849.5}\right)\left(\dfrac{0.6829}{114.2}\right)}$$

$$= \frac{0.1252}{0.1252 + 5.7622} = 0.02126$$

$$= 21.2 \times 10^{-3}$$

Column 8   Number of moles of aromatic compounds n_1

$$n_1 = \frac{\text{Weight (g)}}{\text{Mol. Wt.}} = \frac{0.046 \times 10 \text{ ml}}{246} = 0.0019$$

Column 9   Number of moles of solvent (isooctane) n_2

$$n_2 = \frac{(10 \text{ mls} \times \rho\text{iso } 0.692) - 0.46}{114.2} = 0.0566$$

Column 10 is the summation of number of moles

$$\sum n_1 n_2 = 0.0019 + 0.0566 = 0.0585$$

Column 11 is value of adsorption G in mmole/g according to Gibb's equation

$$G = \frac{\left(x_o - x_1 \right) \sum n_1 n_2}{m}$$

$$G = \frac{(31.5 - 21.2)\ 0.0585}{1.1409} = \frac{0.6025}{1.1409} = 0.528 \text{ mmole/g}$$

A similar calculation was used for all other concentrations to determine equilibrium values of adsorption.

D. DETERMINATION OF THEORETICAL VALUE OF ADSORPTION FOR
INDIVIDUAL AROMATIC COMPOUNDS

Theoretical value of adsorption was determined by modified B.E.T. equation, by plotting values of $\dfrac{X_1(1-X_1)}{G}$ versus (X_1) mole fraction after adsorption to give a straight line: (see Figure D.1).

$$\text{Example for one point} = \frac{X_1(1-X_1)}{G} = \frac{0.0212\,(1-.0212)}{0.528} = 0.0393$$

$$= 39.3 \times 10^{-3}$$

From the straight line $\tan \alpha$, A_m, b, β, f, log f were calculated:

$$\tan \alpha = \frac{4}{2} = 2$$

$$\tan \alpha = \frac{1}{A_m}$$

$$2 = \frac{1}{A_m}$$

$$\therefore\ A_m = \frac{1}{2} = 0.5$$

Theoretical value of adsorption is = 0.5 mmole/g

b (intercept) = 1.0×10^{-3}

$$\beta = \frac{\text{Molar volume of the aromatic}}{\text{Molar volume of the solvent}}$$

$$= \left(\frac{\text{(Mol. wt.) aromatic}}{\rho \text{ aromatic}}\right)\left(\frac{\rho \text{ isooctane}}{\text{(Mol.wt.) isooctane}}\right)$$

$$= \left(\frac{246}{0.8495}\right)\left(\frac{0.6829}{114.2}\right)$$

$$= 1.7$$

$\therefore$ Separation Coefficient f =

$$f = \frac{\tan \alpha}{\beta b} + 1$$

$$= \frac{2}{1.7 \times 0.001} + 1 = 1177.4$$

$$\log f = 3.07$$

Consequently, G (theoretical values of adsorption) were determined, according to B.E.T. formula:

$$G = \frac{\beta A_m (f-1) X(1-X)}{1 + (\beta f - 1) X}$$

First assumption for X were established and values for G were calculated.

X	G
0.0001	0.12
0.0005	0.3
0.001	0.38
0.005	0.46
0.008	0.478
0.02	0.48
0.025	0.48
0.03	0.48

Then theoretical equilibrium isotherm curve for dodecylbenzene at 303 K was plotted and experimental adsorption values were placed on the curve (See Figure D.2). The same method of calculation was applied for all aromatic components at 303, 323 and 343 K, respectively.
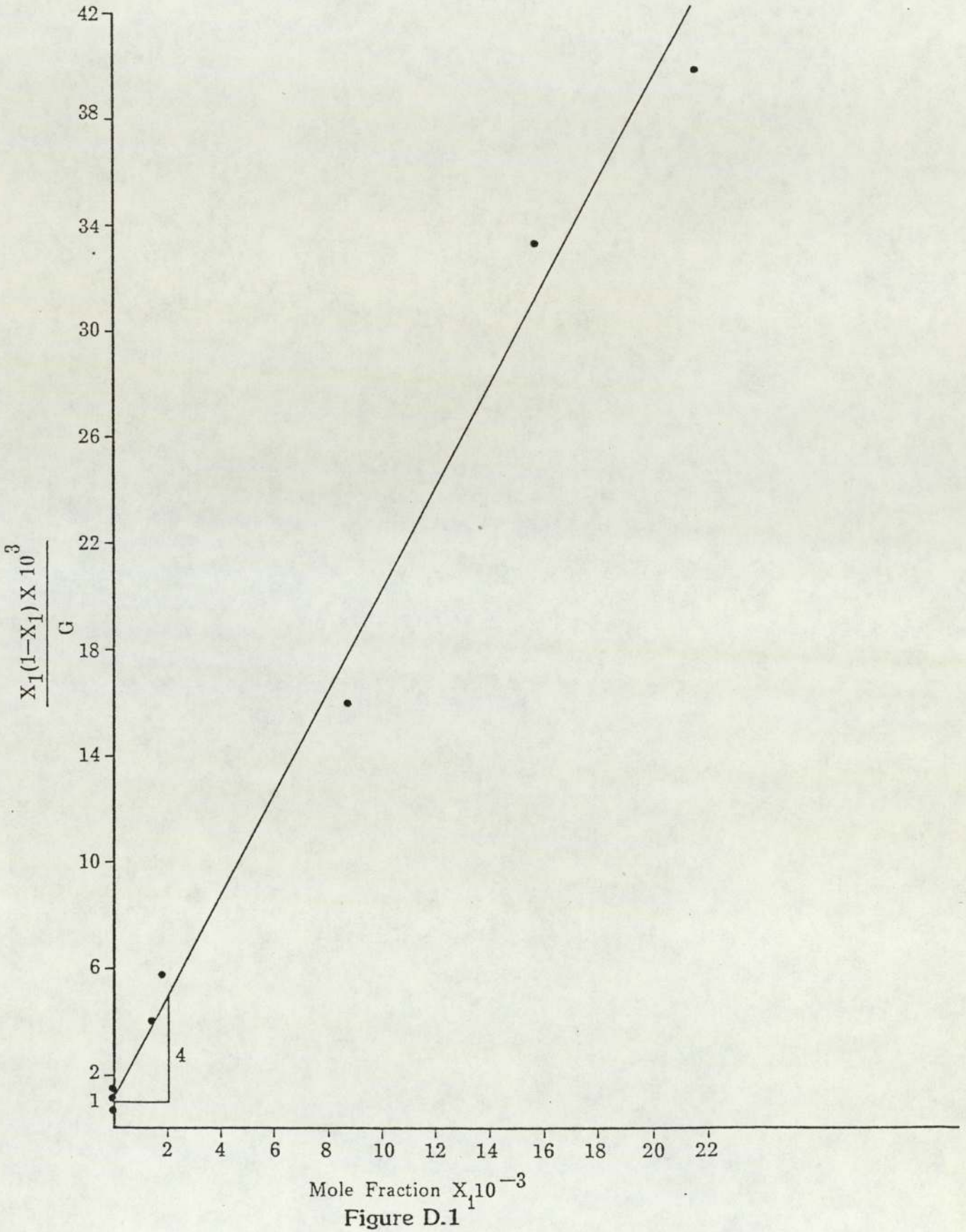
Figure D.1
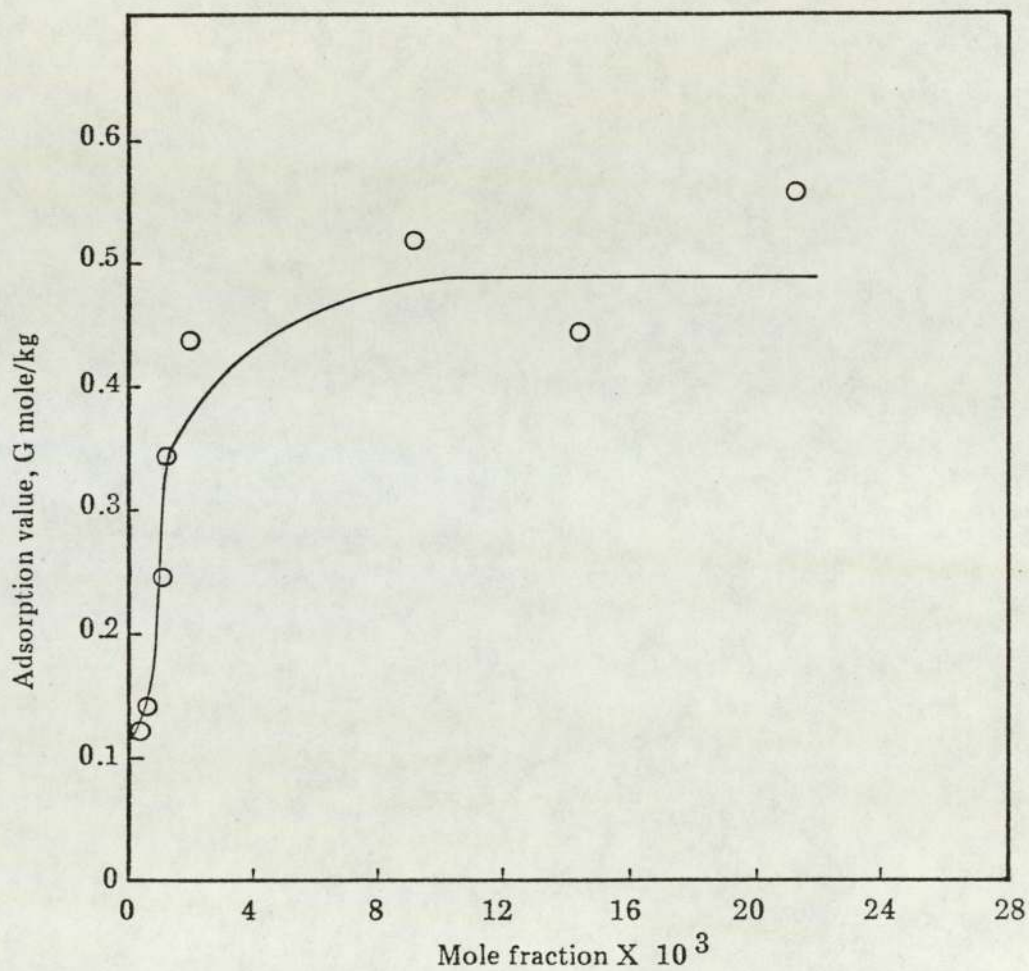
Fig. D.2. Adsorption isotherms of dodecylbenzene on pellets of
zeolite NaX (13X) at 303 K.

   ○   Experimental G value
Solid line : Theoretical G value

The following equations were used for determining the number of molecules occupied by 1 unit cell. For example for dodecylbenzene at 303 K:-

Molar volume μ $= \dfrac{\text{Mol. Wt.}}{\rho \text{ aromatic}}$

$= \dfrac{246}{0.8495} = 289.5 \text{ cm}^3/\text{mole}$

$G\mu = 0.528 \times 289.5$

$\dfrac{\text{m.mole}}{g} \cdot \dfrac{\text{cm}^3}{\text{mole}}$

$= \dfrac{\text{mole}}{1000 \text{ g}} \cdot \dfrac{\text{cm}^3}{\text{mole}} = 0.1528 \text{ cm}^3/\text{g}$

Coverage $\dfrac{G\mu}{V_p} = \dfrac{0.528 \times 289.5}{1000 \times 0.296} = 51.6\%$

Number of molecules adsorbed by one gram GN =

$= \dfrac{0.528 \times 6.023 \times 10^{23}}{1000} = 3.18 \times 10^{20}$

Number of molecules adsorbed by one unit cell $\dfrac{GN}{n} =$

$= \dfrac{0.528}{1000} \times \dfrac{6.023 \times 10^{23}}{.45 \times 10^{20}} = 7.1$

E. CALCULATION OF HEATS OF ADSORPTION

To determine the isosteric heat of adsorption the following calculations were applied:-

Example: Dodecylbenzene

Value of Adsorption, G m.mole/g   = 0.528

ρ at 303 K   = 0.8495

Mol. Wt.   = 246

$$G = \frac{0.528}{1000} \times 246 = 0.1298 \text{ g/g}$$

$$\text{Coverage,} \quad a = \frac{0.1298}{0.8495} = 0.1528 \text{ cm}^3/\text{g}$$

$$= 15.3 \times 10^{-2} \text{ cm}^3/\text{g}$$

The same calculation was applied for all G mmole/g values to get coverages, a cm^3/g at 303 and 343 K, see Figure E.1.

Thus q^a heat of adsorption at certain coverage (a) were calculated by applying:

$$q_{iso}^{a} = R \left(\frac{\partial \ln X}{\partial \frac{1}{T}} \right)$$

$$= \frac{1.987 \times 2.303 \log \Delta X}{\frac{1}{303} - \frac{1}{343}}$$

$$= \frac{4.58}{0.0004} \log \Delta X$$

$$= 11450 \left(\log X_{303} - \log X_{343} \right)$$

Example from Figure E.1 at: $a = 11 \times 10^{-2} \text{ cm}^3/\text{g}$.
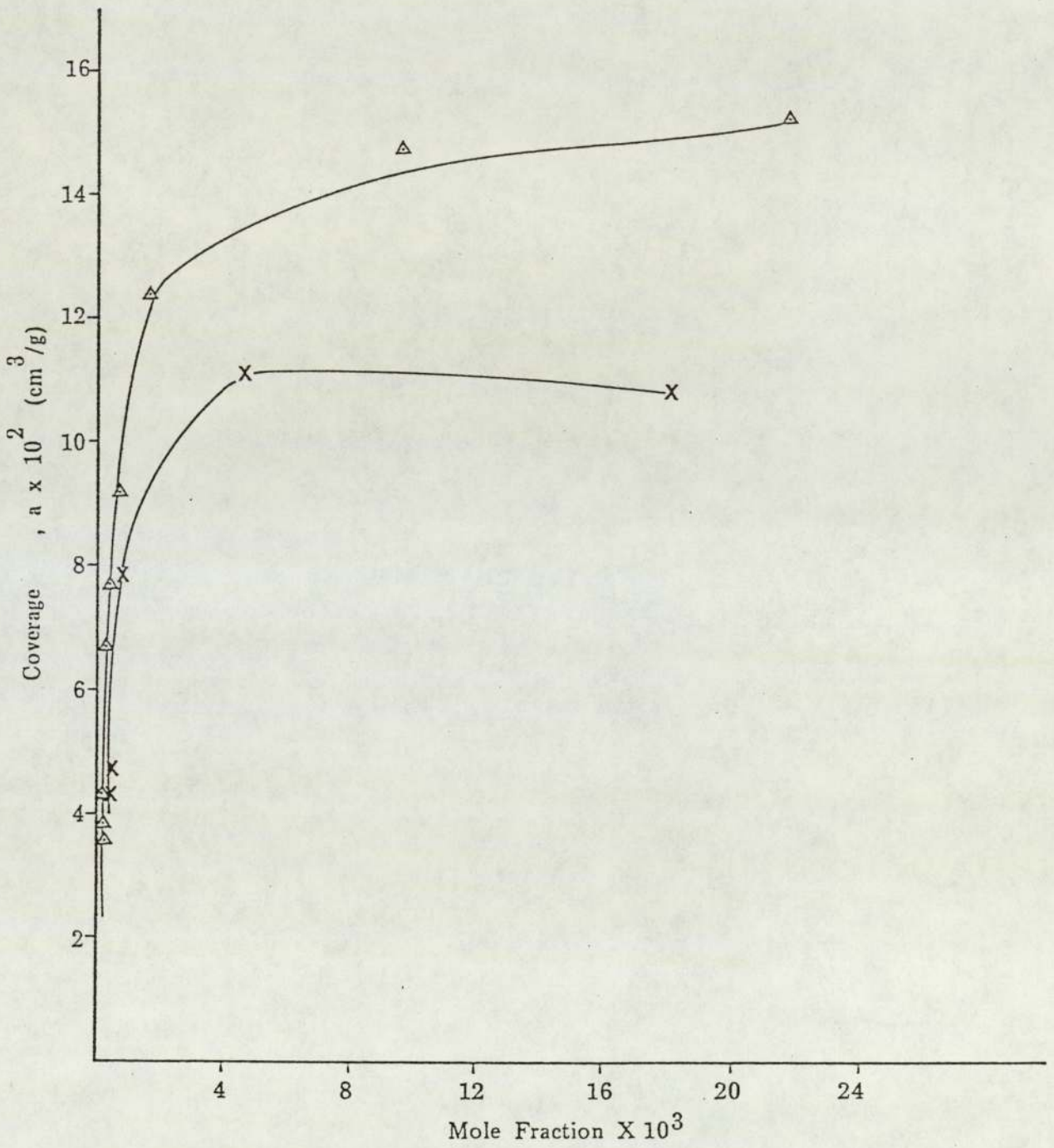
Fig. E.1. Adsorption isotherms for dodecylbenzene on pellets of zeolite NaX (13X) at △ 303 K and X 343 K.

$$q = -11455 \, (\log 0.001 - \log 0.004)$$
$$= -11455 \, (-3 - (-2.39))$$
$$= -11455 \, (.6)$$
$$= -6986 \quad cal/mole$$
$$= -6.98 \quad Kcal/mole = 4.18 \times 6.98 = 29.2 \, kJ/mole$$

For other coverage values see Table E.1.

TABLE E.1

CALCULATED HEAT OF ADSORPTION VALUES AT DIFFERENT COVERAGES
FOR DODECYLBENZENE ON MOLECULAR SIEVE (NaX)

a cm^3/g 10^{-2}	X.10^3 303 K	X.10^3 343 K	Log X 303 K	Log X 343 K	q kJ/mole iso
11	1.0	4.0	-3.0	-2.39	29.2
10	0.9	2.5	-3.0	-2.6	19.2
9	0.8	1.5	-3.1	-2.8	14.2
8	0.6	0.8	-3.2	-3.01	9.2
7	0.3	0.4	-3.5	-3.4	4.8
6	0.2	0.3	-3.6	-3.5	4.8

F. CALCULATION OF N-D-M. METHOD
Van Ness and Van Westen Methods

Extract 1

Measurements at 20°C

η = 1.5682   S% = 3.83
d = 1.0042   Mol. Wt. = 293

ν = 2.51 (1.5682 − 1.4750) − (1.0042 − .8510)
         2.51 (.0932)   −   .1532
    = 0.2339   − .1532
    = 0.0807

ω = (1.0042 − 0.8510)   − 1.11(1.5682 − 1.4750)
    =   0.1532   −   0.1034
    = 0.0498

If ν is +ve
    $\%C_A$ = 430 (.0807) + 3660/293

              34.7 + 12.49
                  47.19

Percentage of aromatic carbon C_A = 47.19

If ω is +ve
    $\% C_R$ = 820 x ω − 35 + 10000/M
       = 820 x .0498 − 3x3.83 + 10000/293
       =   40.836 − 11.49 + 34.129
       = 63.475

Percentage of carbon in total (Aromatic and Naphthenic rings)
Naphthenic rings) structures

    $\% C_R$ = 63.475
    $\% C_N$ = $\% C_R$ − $\% C_A$
        = 63.475 − 47.19
        = 16.285

Percentage of naphthenic carbon = 16.285
    $\% C_P$ = 100 − $\% C_R$
        = 100 − 63.475
        = 36.525

Percentage of parraffinic carbon = 36.525
    R_A = 0.44 + 0.55 Mν

        = .44 + .055 x 293 x .0807
        = 1.74

Average No. of aromatic rings/molecule

R_A = 1.74

R_T = 1.33 + .146 M (ω - .005 S)

= 1.33 + .146 x 293 $\left(.0498 - .005 (3.83)\right)$

= 1.33 + 42.778 (.03065)

= 2.64

Average total No. of rings/molecule

R_T = 2.64

R_N = R_T - R_N

= 2.64 - 1.74

= 0.90

Average No. of Naphthenic ring/molecule

R_N = 0.9

G. CALCULATION OF PARAMETERS OF KINETICS OF ADSORPTION

1. Values of adsorption for different individual aromatic compounds were determined at different times for the maximum concentration by applying Gibbs equation. Example for dodecylbenzene at 303 K is shown in Table G.1.

    Column No. 1 is weight of molecular sieves in each autoclave for certain period of time.

    Column No. 2 is concentration of dodecylbenzene in isooctane after adsorption for certain time in g/L.

    Column No. 3 is concentration of dodecylbenzene in isooctane after adsorption for certain time in mmole/g.

    Column No. 4 is the time period for adsorption in hr.

    Column No. 5 is square roots for the time period for adsorption in hr.

    Column No. 6 is the original mole fraction.

    Column No. 7 is mole fraction at certain period of time.

    Column No. 8 is summation of the number of moles.

    Column No. 9 is value of adsorption in mole/kg at certain period of time G_t.

    Column No. 10 is value of adsorption in g/g at certain period of time G_t.

    Column No. 11 is rate of adsorption $\frac{dG_t}{dt}$ where each value of adsorption was divided by the period of time e.g. $\frac{0.11}{0.05} = 2.2$.

    Column No. 12 is the relative adsorption $\frac{G_t}{G_\infty}$ where each value of adsorption was divided by the maximum value of adsorption (0.52), e.g. $\frac{0.11}{0.52} = 0.21$.

    Column No. 13 is Diffusivity De and it was calculated according to the following equation

Table G.1

Type of Expt. : Kinetics adsorption   Mol. Wt. HC.: 246   Co m.mole/L : 123.9   Dens. of
Type of Arom. H.C: Dodecylbenzene   Density : .8495   n1 : .00127   Isooctane:.6829
Temperature : 303 K   Co g/L : 30.5   n2 : .05802   Mol.wt. :114

C1 g/L	C1 mmole/L	t min	t hr	√t hr	Xo X 10³	X X 10³	Σn₁+n₂	Gt mole/kg	Gt g/g	dGt/dt	Gt/G∞	D cm²/s
28.0	113.8	3	.05	.22	21.3	19.13	0.05929	0.11	.024	2.2	.21	1.2x10⁻⁷
25.5	103.6	5	.083	.288	-	17.7	-	0.19	.046	2.29	.37	2.2x10⁻⁷
24.8	100.8	15	.25	.5	-	17.3	-	0.23	.055	.92	.44	1.1x10⁻⁷
24.8	97.5	21	.35	.59	-	16.7	-	0.25	.055	.66	.44	7.5x10⁻⁸
22.2	90.2	30	.5	.707	-	15.45	-	0.35	.084	.7	.67	1.2x10⁻⁷
22.0	89.4	45	.75	.866	-	15.3	-	0.37	.089	.49	.71	9.1x10⁻⁸
20.7	84.1	60	1.0	1.0	-	14.4	-	0.39	.094	.39	.75	7.65x10⁻⁸
21.2	86.2	90	1.30	1.242	-	14.8	-	0.40	.098	.27	.79	5.65x10⁻⁸
19.7	80.0	120	2.0	1.414	-	13.7	-	0.45	.108	.23	.87	5.1x10⁻⁸
21.7	88.2	135	2.25	1.5	-	15.1	-	0.36	.086	.16	.69	2.87x10⁻⁸
19.7	80.0	141.6	2.36	1.511	-	13.7	-	0.48	.115	.19	.92	4.6x10⁻⁸
18.7	76.0	147	2.45	1.565	-	13.0	-	0.46	.110	.17	.88	3.8x10⁻⁸
20.7	84.1	180	3.0	1.73	-	14.4	-	0.39	.095	.13	.76	2.6x10⁻⁸
20.0	81.3	198	3.30	1.81	-	13.9	-	0.42	.101	.12	.81	2.5x10⁻⁸
19.5	79.26	240	4.0	2.0	-	13.6	-	0.46	.11	.12	.88	2.6x10⁻⁸
19.3	78.4	300	5.0	2.236	-	13.4	-	0.46	.11	.09	.88	2.1x10⁻⁸
20.5	83.3	360	6.0	2.45	-	14.3	-	0.41	.101	.07	.81	1.48x10⁻⁸
16.7	67.8	540	9.0	3.0	-	11.6	-	0.48	.115	.05	.92	1.2x10⁻⁸
17.0	69.1	810	13.5	3.67	-	11.8	Max.	0.52	.125	.04	1.0	1.0x10⁻⁸
17.7	71.9	1440	24.0	4.9	-	12.3	-	0.51	.123	.02	.99	5.5x10⁻⁹

$$D = -\frac{\pi}{4t} \left(\frac{Q_t}{Q_\infty} \right)^2 \left(\frac{v}{A} \right)^2$$

where

$$\frac{v}{A} = 0.025$$

since

$$\frac{2A}{v} = \frac{6}{r_o}$$

$$\frac{A}{v} = \frac{3}{r_o}$$

$$\frac{A}{3v} = \frac{1}{r_o}$$

$\therefore$ particle size $r_o = 1-2$ mm, i.e. ~ 1.5 mm $= 0.075$ cm

$$\therefore \quad \frac{A}{3v} = \frac{1}{0.075}$$

$$\frac{A}{v} = \frac{1}{0.025}$$

at t 3 minutes

$$De = \frac{3.14}{4 \times 3 \times 60} \ (0.21)^2 \ (0.025)^2$$

$$= 1.2 \times 10^{-7} \ cm^2/s$$

$$= 1.2 \times 10^{-11} \ m^2/s$$

H. CALCULATION OF ACTIVATION ENERGY

Activation energy was determined for each aromatic compound
by applying the equation:-

$$E_A = R \frac{\partial \ln De}{\partial \frac{1}{T}}$$

$$E_A = 1.98 \times 2.3 \left(\frac{\log De_{343} - \log De_{303}}{\frac{1}{303} - \frac{1}{343}} \right)$$

$$E_A = \frac{4.58}{0.0004} \log \Delta De$$

$$E_A = 11450 \left(\log De_{343} - \log De_{303} \right)$$

Example from Figure H.1 at $\frac{G_t}{G_\infty} = 0.3$

$$E_A = 11450 (-6.4723 + 6.9706)$$

$$= 11450 \times 0.4982$$

$$= 5705.5 \quad Kcal/mole$$

$$E_A = 5705.5 \times 4.186 = 23.8 \ kJ/mole$$

See Table H.1.

TABLE H.1

ENERGIES OF ACTIVATION FOR DIFFUSION OF DODECYLBENZENE
IN MOLECULAR SIEVES TYPE 13 X (NaX)

$\frac{G_t}{G_\infty}$	$De.10^8$ 303K cm^2/s	$De.10^8$ 343 K cm^2/s	Log De 303 K	Log De 343 K	Log De-Log De 343 303	E_A kJ/mole
0.3	10.75	33.75	-6.9706	-6.4723	0.4982	23.748
0.5	10.5	33.5	-6.9788	-6.4749	0.5038	24.01
0.7	8.0	31.0	-7.0969	-6.5086	0.5883	28.039
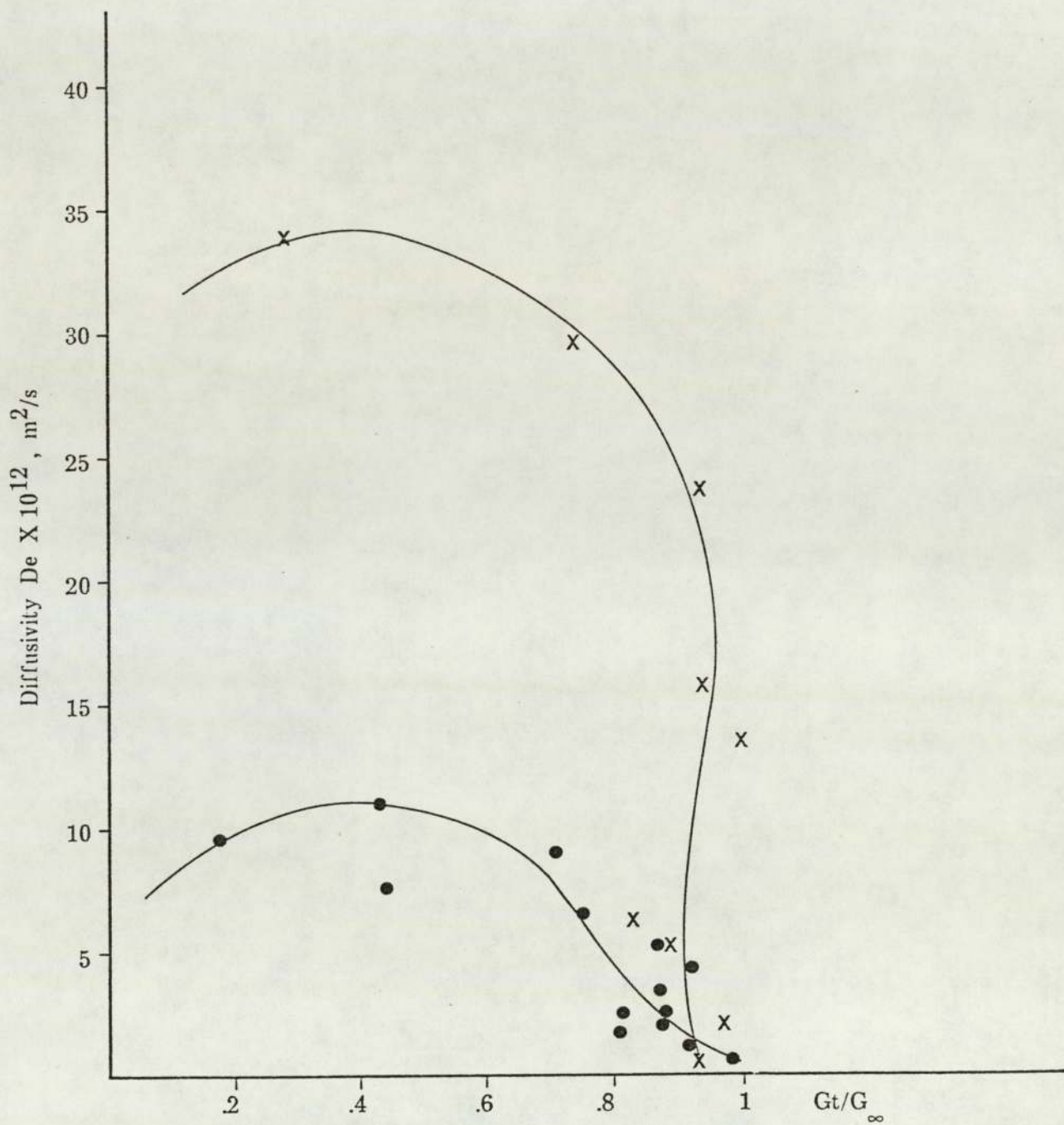
Fig. H.1. Effective diffusion coefficient D_e of dodecylbenzene
as a function of degree of coverage rate of NaX zeolite
pores. At ● 303 K and X 343 K.

I. EXPERIMENTAL CHARACTERIZATION OF MOLECULAR SIEVE*

I.1 Pore Volume and Surface Area

The surface area was determined by B.E.T. method using a Micromeritics Surface Area Analyser (model-Digisorb 2500). Pore volume was measured by adsorption and condensation of nitrogen at liquid nitrogen temperature using the same adsorption unit.

I.2 X-Ray Defraction

X-ray defraction, which indicates, the crystal structure and chemical composition of the material was used. The instrument used was a Phillips X-Ray Defraction type PW 1050.

---

* The methods and procedures are fully described in Catalyst Characterization Handbook, 1984. KISR Publication No. 1464 (Edited by A. Stanislaus and M. Absi-Halabi).

J. APPLICATION OF MODEL PROPOSED IN CHAPTER 10

Adsorption of naphthalene from isooctane solution in a fixed bed of NaX molecular sieves with a height of 66 cm at a temperature of 343 K. Flowrate = 0.42 cm^3/min.

Equation 10.32 in the form,

$$w = 1 - e^{-\theta} \int_0^N e^{-N} I_0 (2 \sqrt{N\theta}).dN$$

could be used to estimate the change in concentration of the adsorbed component in the liquid phase with time at any plane by reference to the graphical solutions, provided as plots of x/x_0 versus time, in Figs. 216 and 216a by Hougen and Watson (73).

Using the Nomenclature of Chapter 10,

$$Y = t - \frac{z}{V}$$

$$\alpha = \frac{1 - \varepsilon}{\varepsilon} = \frac{0.6}{0.4} = 1.5$$

$$\theta = Ka.m.Y$$

$$N = \frac{Ka.\alpha.M}{\rho} z$$

K = overall mass transfer coefficient $\left(\frac{mol}{area \times time} \right)$

$K' = \frac{KM}{\rho} \left(\frac{length}{time} \right)$

$z = 66$ cm

$V = $ intersticial velocity $= \dfrac{0.42}{\dfrac{\pi}{4} \times (1.6)^2 \times 0.6 \times 60}$

$= 0.0058$ cm/s

$= 0.35$ cm/min

$\therefore \ Z = \dfrac{z}{V} = 189$ min.

$a = $ interfacial area per unit volume of packing $= \dfrac{6}{d_p} = \dfrac{6}{0.15} = 40 \ \dfrac{cm^2}{cm^3}$

$M = 114$ g/mol

$\rho = 0.66$ g/cm^3

$c = \dfrac{\rho . x}{M}$

$x = $ mole fraction of solute in liquid

$n = $ moles adsorbate per unit volume of packing

$x^* = m.n + b$

The requirement is therefore to evaluate K (or K'), m and b.

Evaluation of K (or K')

Assuming that external diffusion is rate controlling, k_f for this case may be estimated from published correlations.

Now $\quad Re_p = \dfrac{d_p . \rho . v'}{\mu}$

where $\mu = 0.35$ cp $= 0.35 \times 10^{-2}$ g/cm

Particle diameter d_p is between 0.1-0.2 = 0.15 cm

Density of the mixture ρ = 0.04 x 0.993 + 0.960 x 0.647

$$= 0.04 + 0.621 = 0.661 \text{ gm/cm}^3$$

v' = superficial velocity

$$= \frac{0.42}{\frac{\pi}{4} \times (1.6)^2 \times 60} = 3.48 \times 10^{-3} \text{ cm/s}$$

Hence $Re_p = \dfrac{0.15 \times 0.66 \times 3.48 \times 10^{-3}}{0.35 \times 10^{-2}}$

$$= 9.8 \times 10^{-2}$$

So that operation is in the laminar flow regime.

i) Using the correlation

$$Sh = 3.45 \ Pe^{0.5}$$

For this purpose,

D = diffusivity of solute in the solvent.

$$= 7.4 \times 10^{-8} \left[\left(\sigma_B \times M_B \right)^{1/2} \frac{343}{\mu_B \times (V_A)^{0.6}} \right]$$

where M_B is molecular weight

σ_B is surface tension for solvent = 1.0

μ_B is viscosity in cP.

$$\therefore \ D \ = \ 7.4 \times 10^{-8} \left[(1.0 \times 114)^{1/2} \ \frac{343}{0.35 \times (147.6)^{0.6}} \right]$$

$$= \ 3.8 \times 10^{-5} \ cm^2/s$$

Superficial velocity $v' = 3.48 \times 10^{-3} \ cm/s$

Hence $Pe = \dfrac{d_p \cdot v'}{D} = \dfrac{0.15 \times 3.48 \times 10^{-3}}{3.8 \times 10^{-5}} = 13.7$

And $Sh = 3.45 \ (13.7)^{0.5} = 12.8$

$$\therefore \ k_f \ = \ \frac{12.8 \times 3.8 \times 10^{-5}}{0.15} \ = \ 3.24 \times 10^{-3} \ cm/s$$

Alternatively use may be made of,

ii)
$$\left[\frac{k_f + \varepsilon}{v'} \right] \ Sc^{2/3} \ = \ 0.81 \ Re_p^{-0.5}$$

so,
$$k_f \ = \ \left[\frac{0.81}{Re^{0.5} \ Sc^{2/3}} \right] \frac{v'}{\varepsilon}$$

Since $\varepsilon \sim 0.4$

and $Sc = \dfrac{\mu}{\rho \cdot D} = \dfrac{0.35 \times 10^{-2}}{0.66 \times 3.8 \times 10^{-5}} = 140$

$$k_f \ = \ \left[\frac{0.81}{(9.8 \times 10^{-2})^{0.5} \ \times \ (140)^{2/3}} \right] \frac{3.48 \times 10^{-3}}{0.4}$$

$$= \ 8.34 \times 10^{-4} \ cm/s.$$

Alternatively,

iii) $\qquad \dfrac{k_f d_p}{D} = \dfrac{1}{6 (1 - \varepsilon) \xi} \cdot Pe$

ξ is a channelling factor which may vary from 1 to 10.

$\therefore \quad \dfrac{k_f d_p}{D} = \dfrac{1 \times 13.7}{6 \times 0.6 \, \xi}$

Assuming

$$k_f = \dfrac{13.7 \times 3.8 \times 10^{-5}}{3.6 \, \xi \times 0.15} = \dfrac{9.6 \times 10^{-4}}{\xi} \text{ cm/s}$$

Finally

$$K = \dfrac{k_f \, \rho}{M} = \dfrac{k_f \, 0.66}{144} \left[\dfrac{gmol}{cm^2.s} \right]$$

but wide variations are apparent in the predictions of k_f from existing correlations (i.e. by a factor of 10 or more).

Approximation of Equilibrium Data

Assume $x^* = m'n'$ provides an approximate description of the equilibrium data.

From Figure 3.6, $x^* \sim 5 \times 10^{-3}$ at $n^1 \sim 0.8 \times 10^{-3} \dfrac{gmole}{g \text{ adsorbent}}$

$\therefore \quad m' = \dfrac{x^*}{n'} = \dfrac{5 \times 10^{-3}}{0.8 \times 10^{-3}}$

Bulk density of powdered adsorbent $= 0.770 \text{ g/cm}^3$

Assuming the voidage, $\varepsilon \qquad\qquad = 0.4,$

Catalyst density, $\rho \qquad\qquad = \dfrac{0.770}{(1 - 0.4)}$

$\qquad\qquad\qquad\qquad\qquad\qquad\quad = 1.28 \text{ g/cm}^3$

$$\therefore \quad m' = m \, \rho \text{ adsorbent}$$

$$\text{or} \quad m = \frac{m'}{\rho \text{ adsorbent}} = \frac{5 \times 10^{-3}}{0.8 \times 10^{-3} \times 1.28}$$

$$= 4.9 \ \frac{cm^3}{gmole}$$

Calculation of N and θ

$$\theta = Ka \, m \, Y$$

For example

$$K = 3.24 \times 10^{-3} \times \frac{0.66}{144} \qquad \frac{gmole}{cm^2 s}$$

$$a = 40 \ \frac{cm^2}{cm^3}$$

$$m = 4.9 \ \frac{cm^3}{gmole}$$

$$\theta = 3.68 \times 10^{-3} \ Y \ (sec) = 0.221 \ Y \ (min)$$

where the time-scale is from 0 --> 100 min

after breakthrough is detected.

$$N = k_f a \, \alpha \, \frac{M}{\rho} \cdot Z = k_f a \, \alpha \cdot Z$$

$$k_f = 3.24 \times 10^{-3} \ \frac{cm}{s}$$

$$a = 40 \ \frac{cm^2}{cm^3}$$

$$\propto = \left(\frac{1 - 0.4}{0.4} \right) = 1.5$$

$$Z = \frac{z}{V} = \frac{66}{0.0058} \text{ s}$$

$$N = 3.24 \times 10^{-3} \times 40 \times 1.5 \ Z \ (s)$$

$$= 0.194 \ Z \ (sec) = 11.7 \ Z \ (min)$$

Discussion

Because of the difficulties in predicting k and hence K, the use of the graphical solution in reference (73) is not justified. Moreover internal diffusion, and the fact that not all the entire superficial surface will be available, are likely to be important. For example if

$$k_s = \frac{10.D}{d_p (1 - \varepsilon)}$$

$$k_s = \frac{10 \times 3.8 \times 10^{-5}}{0.15 \times 0.6} = 4.2 \times 10^{-3} \text{cm/s}$$

for the case of naphthalene (which exhibited the best dynamic properties) However, some relevant deductions can be made from the analysis.

Firstly, it can be shown that N is equivalent to the Number of Transfer Units, i.e.

$$N = \left(\frac{Ka \ \alpha \ M}{\rho} \right) Z = \left(\frac{Ka \ \alpha \ M}{\rho V} \right) z$$

$$= \left[\frac{1}{H.T.U.} \right] \times \text{packed height}$$

In the example chosen therefore the Number of Transfer Units was of the order of 100 to 1000.

Secondly, the relationship between 'active' operating time of the bed and the period for breakthrough can be examined.

$$Y = 0 \quad \text{when} \quad t = \frac{Z}{V} \quad = \quad 189 \text{ min}$$

N is large, as is the adsorptive capacity of the bed, so that a relatively long time will elapse before the adsorbate concentration at the exist > 0. The period of breakthrough will be comparatively short relative to the 'active' life of the bed. (In fact reference to Figure 9.3 shows that the breakthrough period was of the order of 100 minutes).

NOMENCLATURE

a   Adsorbate loading, m^3/kg

A   Total surface area, m^2

A_{cs} Column cross-sectional area, mm^2

A_d Dynamic capacity g of the adsorbate/100 g of the adsorbent

A_m The maximum quantity of the adsorption capacity of aromatic compounds covering 1.0 g of molecular sieves

β Coefficient of mutual displacement, = the ratio between molar volumes of aromatic compound and the solvent (iso-octane)

C   Adsorbate concentration, g/cm^3

c   Adsorbate concentration in moving phase g/cm^3

C_E Effective, or working, capacity of the molecular sieves

C_o Original concentration of aromatics in the feed, g/cm^3

C_T Specific total capacity of the packed bed

C_t Adsorbate concentration at time t, g/cm^3

% C_A Percent of aromatic carbon

% C_R Percent of carbon in total aromatic and naphthenic rings structures

% C_N Percent of naphthenic carbon

% C_P Percent of paraffinic carbon

D, De	Diffusivity or diffusion constant, m^2/s
D_o	Limiting diffusivity at zero sorbate concentration, m^2/s
D_k	Knudson diffusion coefficient, m^2/S
D_s	Surface diffusion coefficient, m^2/S
$\frac{\partial c}{\partial x}$	Concentration gradient
E	Energy of adsorbate molecules in the pores
E_A	Activation Energy needed for a jump
E_1	Potential energy of adsorbate molecules at the boundary of one pore
E_2	Potential energy of adsorbate molecules at the boundary of an adjacent pore
F	Symmetricity factor
f	Separation coefficient, a function characterizing collective interactions occurring in the zeolite solution system
G	Adsorption value, mole/kg
G_t	Adsorption value at time t, mole/kg
G_∞	Maximum adsorption value, mole/kg
ΔG	Free energy change
H	Energy of adsorbate molecules in gas phase
ΔH	Change in enthalpy

h_T Total height of the packed bed, mm

h_z Height of mass transfer zone (utilized zone), mm

J Rate of transfer of molecules per unit area

K Boltzman's constant

K' Factor depends on diffusion constant

K Mass transfer coefficient cm/sec. in Chapter 10

m Mass of zeolite used in the adsorption, g

M Molecular weight, g/mole

Mol.wt.   Molecular weight, g/mole

N Avogadro's number $= 6.023 \times 10^{23}$ molecules/mole

n Number of unit cells/g of molecular sieves
              0.45×10^{20}

n_1 Number of moles of solute in solution

n_2 Number of moles of solvent in solution

q Heat of adsorption

q_{iso} Isosteric heat of adsorption, kJ/kg K

Q_o Quantity occluded at time zero

Q_t Quantity occluded at time t

Q_z	Total aromatic compounds occupied by the molecular sieve, g
Q_∞	Quantity occluded at time infinity
r	Pore radius, mm
r_o	Radius of spherical particles, mm
R	Gas constant
R_A	Average number of aromatic rings per molecule
R_N	Average number of naphthenic rings per molecule
R_T	Average total number of rings per molecule
% S	Percent sulphur
ΔS	Change in entropy
t	Time of the effluent passing through the packed bed, hr
T	Absolute temperature
U_f	Feed flow rate, cm^3/s
U_z	Rate of descent of exchange zone, cm/s
v	Total pore volume, cm^3
V	Velocity of fluid through the interstices of the bed in cm/s.
V_a	Average volume occupied by molecular sieve
V_E	Total volume of effluent collected up to break-through point, cm^3

V_T	Total volume of effluent collected up to equilibrium point, cm^3
V_z	Volume of effluent, collected from mass transfer zone, cm^3
W_1	Weight of the mixture passed through the adsorbent, g
W_2	Weight of the mixture leaving the adsorbent, g
X_o	Mole fraction in solution before adsorption
X_1, X	Mole fraction in solution after adsorption
z	Bed height, in Chapter 10
Z	Time required to displace fluid hold up in the column, in Chapter 10
δ	Distance moved in a single jump
$\sum$	Summation symbol
ρ	Density, g/cm^3
θ	Fraction of adsorbent surface covered by adsorbate, in Chapter 7.
θ_f	Time of formation of zone

θ_n Time until the break-through point

θ_T Time to the equilibrium point

θ_z Time for the exchange zone to move from break-through to equilibrium point

γ Adsorption efficiency

τ Average time a site is occupied by a molecule between jumps or, a specific time period

τ_o Period of vibration

μ Molar volume

ε Porosity

REFERENCES

1. Breck, D. W., Zeolite Molecular Sieves Structure Chemistry and Use, John Wiley Interscience (1974). New York, U.S.A.

2. Barrer, R. M., and Ibbitson, D. A., Occlusion of Hydrocarbons by Chabazite and Analcite. Tran. Faraday Soc., 40, 195-206 (1944),U.K.

3. Clark, E. L., Molecular Sieves Perform Well in Sweetening Light Hydrocarbon Liquids. Oil and Gas Journal, 60, 46, 178-179 (1962), Canada.

4. Mair, B. J., Hwang, P. T. R., and Ruberto, R. G., Separation of Petroleum Hydrocarbons by Selective Adsorption with Sephadex LH-20. Anal. Chem., 39, 7, 838-840 (1967), Washington, D.C., U.S.A.

5. Mair, B. J., and Shamaiengar, M., Fractionation of Certain Aromatic Hydrocarbons with Molecular Sieve Adsorbents. Anal. Chem., 30, 2, 276-279 (1958), Washington, D.C., U.S.A.

6. Satterfield, C. N., and Cheng, C. S., Liquid Counterdiffusion of Selected Aromatic and Naphthenic Hydrocarbons in Type Y Zeolites. A.I.Ch.E.J., 18, 4, 724-728 (1972), New York, U.S.A.

7. Gupta, R. K., Kunzru, D., and Saraf, D. N., Liquid-Phase Adsorption of Binary and Ternary Systems of n-Paraffins on LMS-5A. Ind. Eng. Chem. Fundam, 20, 1, 28-34 (1981), Washington, D.C., U.S.A.

8. Fominykh, L. F., Samoilov, N. A., Stekol's-hehikov, M. N., and Komlev, G. K., Extraction of Benzene from Hydrocarbon Mixtures with Synthetic Zeolites, Chem. and Tech. of Fuels and Oils, 3, 4, 230-233 (1967), New York, U.S.A.

9. Satterfield, C. N., and Smeets, J. K., Liquid Sorption Equilibria of Selected Binary Paraffin Systems in NaY Zeolite, A.I.Ch.E.J., 20, 3, 618-619 (1974), New York, U.S.A.

10. Siryuk, A. G., and Barabadze, Sh. Sh., Selection of Method for Determination of the Composition of Aromatic Hydrocarbons in High-Boiling Petroleum Cuts, Chem. and Tech. of Gas and Oils, 10, 746-748 (1977), New York, U.S.A.

11. Cherednichenko, V. P., Fadeev, V. S., and Garbalinskii, V. A., Composition of Aromatic Hydrocarbons Present as Impurities in Liquid

Paraffins, Chem. and Tech. of Fuels and Oils, 14, 5, 328-331 (1978), New York, U.S.A.

12. Epperly, R. W., and Pramuk, F. S., Process for Improving Stability, United States Patent, No. 3, 278, 422 (1966).

13. Dielacher, M., and Hanseen, U., Process for the Separation of Unsaturated Compounds from Liquid Hydrocarbon Mixtures, United States Patent 4, 290, 881 (1981).

14. Aveisi, F., Gureev, A. A., El'tekov, Yu. A., Fal'kovich, M. I., and Solodovnikova, V. T., Adsorption of Aromatic Hydrocarbons and Organic Sulphur Compounds by NaX Zeolite, Chemistry and Technology of Fuels and Oils, 17, 2, 85-88 (1981), New York, U.S.A.

15. Sundstrom, D. W., and Krautz, F. G., Equilibrium Adsorption of Liquid Phase Normal Paraffins on Type 5A Molecular Sieves, J. of Chem. and Eng. Data, 13, 2, 223-226 (1968).

16. Dorogochinskii A. Z., Frid, M. N., Borisova, L. V., Breshchenko, V. Ya., and Shutova, T. L., Thorough Dearomatization of Kerosine Cut on Zeolite, Chem. and Tech. of Fuels and Oil, 9, 8, 577-579 (1973), New York, U.S.A.

17. Neuzil, R. W., Grove, D., Aromatic Hydrocarbon Separation by Adsorption, United States Patent, 3, 686, 342 (1972).

18. Fal'kovich M. L., El'tekov, Yu., A., and Chernozhukov, N. I., Kinetics of the Adsorption of C_{10} - C_{17} Normal Alkanes from Isooctane Solutions by Granules of CaA Zeolite, Chem. and Tech. of Fuels and Oils, 12, 868-871 (1968), New York, U.S.A.

19. Avgul N. N., Bezus, A. G., and Dzhigit, O. M., Heats of Adsorption on X-Type Zeolites Containing Different Alkali Metal Cations, Molecular Sieve Zeolites - II. The Second International Conference, Co-sponsored by Am. Chem. Soc. and Worcester Polytechnic Institute, Sept. 8-11, 1970, U.S.A. 184-192 (1971), Washington, D.C., U.S.A.

20. Gel'ms, I. E., Krymov, P. V., Yudinson, R. N., Kel'tsev, N. V., Yuzefovich, V. I., and Bliguras, A. P., Purification of Propylene from Isopropyl Alcohol and Water with NaX Zeolite During the Process of Producing Polypropylene, Chem. and Tech. of Fuels and Oils, 1, 17-20 (1971), New York, U.S.A.

21. Hansjoerg, H., Einicke, W. D., Messow, U., Quitzsch, K., and Schoellner, R., Liquid Phase Adsorption of n-Olefins and n-Paraffins

on X and Y zeolites, Wiss. Z. Karl Marx Univ. Leipzig Math - Natur-
wiss. Reihe 30, 4, 411-420. (1981). Ger.

22. Epperly, W. R., Feldbausr, G. F., Tuttle, J. R., and Tyson, C. W.,
Removal of Aromatics, Olefins and Sulphur from Naphtha Feed, United
States Patent No. 3, 063, 934 (1962).

23. Rosback, D.H., and Newzil, R.W., Olefin Separation Process, United
States Patent No. 3,969,233 (1976).

24. Jean, G.; Chantal, P.; Ahmed, S.; and Sawatzky, H. The Competitive
Adsorption of Fuel-Type Compounds on Zeolite 13X. Prepr. Pap. - Am.
Chem. Soc., 31(3), 262-265 (1986), Washington, D.C., U.S.A.

25. Casellato, F., Selectivity of Adsorption of Dimethylnaphthalenes on
Zeolites, Riv. Combust., 38(5), 126-30 (1984), Italy.

26. Barrer, R. M., Intracrystalline Diffusion, Molecular Sieve Zeolites
- II, The Second International Conference. Co-sponsored by Am.
Chem. Soc. and Worchester Polytechnic Institute, Sept. 8-11, 1970,
U.S.A., 1-36 (1971), Washington, D.C., U.S.A.

27. Owaysi, F., Adsorption Isotherms of Individual Aromatic Compounds
Using Molecular Sieves, Ph.D. Thesis, Moscow Petroleum Institute
(1978).

28. Newman, S. A., Correlations Evaluated for Coal-Tar Liquid Solutions,
Hydrocarbon Processing, 60, 12, 133-142 (1981), Houston, Texas,
U.S.A.

29. Eltekov, Yu. A., and Kiselev, A. V., Adsorption by Zeolites from
Liquid Solutions, Molecular Sieves Series, 4th-6th April 1967, Uni-
versity of London, 267-273 (1967), London, U.K.

30. Hedge, J. A., Separation of 2,7 Dimethylnaphthalene from 2,6 Dime-
thylnaphthalene with Molecular Sieves, Molecular Sieve Zeolites -
II, The Second International Conference, Co-sponsored by Am. Chem.
Soc. and Worcester Polytechnic Institute, Sept. 8-11, 1970, U.S.A.,
238-246 (1971), Washington, D.C., U.S.A.

31. Hattori, T., Akizuki, I., Kamogawa, K., and Murakami, Y., Adsorption
of Aromatic Hydrocarbons on Zeolites as Examined by Pulse-Technique,
Edited by Rees, L.V., Proceedings of the Fifth International Confer-
ence on Zeolite, Naples, Italy, 2-6 June, 1980, Sponsored by (SCI),
(SIMP), (CNR), (IZA), (ICNZ) and University of Napoli, Department of
Synthetic Chemistry, Faculty of Engineering, Nagoya University, Chi-
kusa, Nagoya 464, Japan, 449-457 (1980).

32. Masuda, T., Tsutsumi, K., and Takahashi, H., Calometric Evidence for Non-specific and Specific Interactions of Several Gases with Surfaces of NaA and CaNaA Zeolites, Edited by Dr. L.V.C. Rees, Proceedings of the Fifth International Conference on Zeolite, Naples, Italy, 2-6 June, 1980, Sponsored by (SCI), (SIMP), (CNR), (IZA), (ICNZ) and University of Napoli, Institute of Industrial Science, The University of Tokyo, Japan, 483-489 (1980).

33. Kiselev, A. V., Vapor Adsorption on Zeolites Considered as Crystalline Specific Adsorbents, Molecular Sieve Zeolites - II, The Second International Conference, Co-sponsored by Am. Chem. Soc. and Worcester Polytechnic Institute, Sept. 8-11, 1970, U.S.A., 37-55 (1971), Washington, D.C., U.S.A.

34. Dubinin, M. M., and Astakhov, V. A., Description of Adsorption Equilibria of Vapors on Zeolites over Wide Range of Temperature and Pressure, Molecular Sieve Zeolites - II, The Second International Conference, Co-sponsored by Am. Chem. Soc. and Worcester Polytechnic Institute, Sept. 8-11, 1970, U.S.A., 69-85 (1971), Washington, D.C., U.S.A.

35. Khudieve, A. T.; Klyachko-Gurvich, A. L.; Brueva, T. R.; Isakov, Ya. I.; and Rubinshtein, A. M., Heat of Adsorption of Benzene on Synthetic Faujasites, Chem. and Tech. of Fuels and Oils, 4, 717-720 (1968), New York, U.S.A.

36. Barrer, R. M., Structure of Faujasite and Properties of its Inclusion Complexes with Hydrocarbons, Tran. Farad Soc., 53, 1111 (1957), U.K.

37. Joubert, J. I., and Zwiebel, I., Multicomponent Adsorption Isotherms on Hydrogen Mordenite, Molecular Sieve Zeolites - II, The Second International Conference, Co-sponsored by Am. Chem. Soc. and Worcester Polytechnic Institute, Sept. 8-11, 1970, U.S.A., 209-216 (1971), Washington, D.C., U.S.A.

38. Van Ness and Van Westen, Calculation of Carbon Distribution and Structural Group Analysis of Petroleum Oils by the n-d-M Method, ASTM D 3238-74 (1954), U.S.A.

39. Barrer, R. M., and Ibbitson, Kinetics of Formulation of Zeolitic Solid Solutions, D. A., Trans. Frad. Soc., 40, 206-216 (1944), U.K.

40. Barrer, R. M., and Brook, D. W., Molecular Diffusion in Chabazite, Mordenite and Levynite, Trans. Faraday Soc., 49, 1049-1059 (1953), U.K.

41. Eberly, P. E., Zeolite Chemistry and Catalysis, ACS Monograph 171, Diffusion in Zeolites, American Chemical Society, (1976), Washington, D.C., U.S.A.

42. Satterfield, C. N., and Cheng, C. S., Single-Component Difffusion of Selected Organic Liquids in Type Y Zeolites, A.I.Ch.E, 67, 117, 43-50 (1972), New York, U.S.A.

43. Loughlin, K. F., Derrah, R. I., and Ruthven, D. M., On the Measurement of Zeolitic Diffusion Coefficients, Canad. J. of Chem. Eng., 49, 66-70 (1971), Canada.

44. Ruthven, D. M., Derrah, R. I., and Loughlin, K. F., Diffusion of Light Hydrocarbons in 5A Zeolites, Canad. J. of Chem., 51, 3514-3519 (1973), Canada.

45. Doetsch, I. H., Ruthven, D. M., and Loughlin, K. F., Sorption and Diffusion of n-Heptane in 5A Zeolite, Canad. J. of Chem., 52, 2717-2724 (1974), Canada.

46. Caro J., Bulow, M., and Karger, J., Sorption Kinetics of n-Decane on 5A Zeolites from a Nonadsorbing Liquid Solvent, A.I.Ch.E.J. 26, 6, 1044-1046 (1980), New York, U.S.A.

47. Ruthven, D. M., and Doetsch, I. H., Diffusion of Hydrocarbons in 13 X Zeolite, A.I.Ch.E.J., 22, 5, 882-886 (1976), New York, U.S.A.

48. Ruthven, D. M., and Derrah, R. I., Transition State Theory of Zeolitic Diffusion of CH_4 and CF_4 in 5A Zeolite, J. of Chem. Soc. Farad. Trans., 68, 2332-2343 (1972), U.K.

49. Vavlitis, A. P., Ruthven, D. M., and Loughlin, K. F., Sorption of N-Pentane, N-Octane, and N-Decane in 5A Zeolite Crystals, Journal of Colloid and Interface Science, 84, 2, 526-531 (1981), New York, U.S.A.

50. Fal'kovich, M. I., Gureev, A. A., Aveisi, F., El'tekov, Yu. A., and Solodovnikova, V. T., Kinetics of Adsorption of Aromatic Hydrocarbons and Organic Sulphur Compounds by Zeolite, Chem. and Tech. of Fuels and Oils, 17, 8, 446-449 (1981), New York, U.S.A.

51. Amerik, M.B. and Novikov, V.A., Study of the Kinetics of High-Temperature Sorption of C_{10}-C_{19} n-alkanes on 5A Zeolites.

52. Timofeev, D. P., Diffusion in Granular Zeolites, Molecular Sieve Zeolites - II, The Second International Conference, Co-sponsored by Am. Chem. Soc. and Worcester Polytechnic Institute, Sept. 8-11, 1970, U.S.A., 247-259 (1971).

53. Ruthven, D. M., Loughlin, K. F., and Derrah, R. I., Sorption and Diffusion of Light Hydrocarbons and Other Simple Nonpolar Molecules in Type A Zeolites, Molecular Sieve Zeolites - II, The Second International Conference, Co-sponsored by Am. Chem. Soc. and Worcester Polytechnic Institute, Sept. 8-11, 1970, U.S.A., 330-344 (1971).

54. Novoselova, L.A., Rakhlevskaya, M.N., and Zolotova, T.P., High-Temperature Adsorption of 2-ethylthiophene on Zolites of X type, Zh. Fiz. Khim, 58, 11, 2856-2858 (1984), USSR.

55. Michaels, A. S., Simplified Method of Interpreting Kinetic Data in Fixed-Bed Ion Exchange, Ind. and Eng. Chem., 44, 8, 1922-1930 (1952), Washington, D.C., U.S.A.

56. Ahmetovic, D., and Sevel-Cerovecki, S., Low Aroma tic Solvents Through Dearomatization and Molecular Sieve 13X Zeolites: Synth., Struct., Technol., 24, 683-690 (1985), Yugoslavia.

57. Bolotov, L.T., Borisova, L. V., Volyanyuk, Bi.I., and Lipert, Yu. I., Method for the Calculation of the Quantity of Displacing Agent Sorbed by Zeolite in the Production of Liquid Paraffins, Chem. and Tech. of Fuels and Oils, 21, 2, 66-69 (1985), New York, U.S.A.

58. Collins, J. J., The LUB/Equilibrium Section Concept for Fixed-Bed Adsorption, Chemical Engineering Progress Symposium Series, 74, 63, 31-35 (1967), New York, U.S.A.

59. Rasmuson, A., The Influence of Particle Shape on the Dynamics of Fixed Beds, Chem. Eng. Science, 40, 7, 1115-1122 (1985), U.K.

60. Kehat, E., and Rosenkranz, Z., Separation of n-Hexane from a Solution in Benzene by Adsorption on Molecular Sieve SA, I&EC Process Design and Development, 4, 2, 217-220 (1965), U.S.A.

61. Epperly, W. R., Hill, M. and McCall, P. P., Separation Process, United States Patent No. 3,228,995 (1966).

62. Roger, H. A., and Macnab, R. M., Hydrocarbon Separation Process, United States Patent No. 1,026,116, (1966).

63. Epperly, W. R., and Tyson, C. W., Converting Naphthalenes to Aromatics and Separating the Aromatics, United States Patent No. 3,372,108 (1968).

64. Mahto, J. N., Saraf, D. N., and Singhal, A. K., Recovery of Normal Paraffins from Petroleum Fractions, Petroleum and Hydrocarbons, 7, 4, 257-261 (1973).

65. Denisenko, A. N., Sidorov, R. I., Petrova, V. I., and Gamayunova, P. B., Quantitative Determination of Naphthenic, n-Paraffinic, and Iso-paraffinic Hydrocarbons in Mixtures by the Use of 13X Molecular Sieves in Adsorption Gas Chromatography, Chem. and Tech. of Fuels and Oils, 8, 643-647 (1976), New York, U.S.A.

66. Lauder, B. T., and Rolfe, J. R. K., Hydrocarbon Separating Process, United States Patent No. 4,069,142, (1978).

67. Al-Ameeri, R. S., and Owaysi, F. A., Separation of n-Paraffins from Petroleum Fractions by Adsorption on 5A Molecular Sieves, Ind. Eng. Chem. Prod. Res. Dev., 23, 4, 634-638 (1984), U.S.A.

68. Schirmer, W., Fiedrich G., Grossmann, A. and Stach, H., Adsorption Behaviour of Pure and Mixed n-Alkanes of Medium Chain Length on Zeolites, Molecular Sieves Series, 4th-6th April, 1967, University of London, 276-290 (1967).

69. Kiselev, A.V. and Lopatkin, A.A., Energy of Adsorption by Zeolites of Molecules of Different Structure, Molecular Sieves Series, 4th-6th April, 1967, University of London, 252-266 (1967).

70. Amundson, N. R., A Note on the Mathematics of Adsorption in Beds, The Mathematical Understanding of Chemical Engineering Systems (1980), Selected Papers of Amundson, N. R., p. 133-138 (1980).

71. Johnson, D. E. and Johnson, J. R., Solving the Mathematical Models for Dynamic Systems, Mathematical Methods in Engineering and Physics, Englewood Cliffs, NJ: Prentice-Hall (1981), U.S.A.

72. Mickley, H. S., Sherwood, T. K. and Reed, C. E., Applied Mathematics in Chemical Engineering. McGraw Hill (1957), New York, U.S.A.

73. Hougen, O. A., and Watson, K. M., Chemical Process Principles - Part 3 Kinetics and Catalysis, John Wiley & Sons Inc (1947), New York, U.S.A. to Chemical Engineering Problems. University of Delaware (1947).